The role of PTEN in cardioprotection against ischaemia-reperfusion injury

Thesis submitted by

Hilary Kathleen Siddall

BSc (Hons)

For the degree of

Doctor of Philosophy

Faculty of Biomedical Sciences, Division of Medicine

University College London

The Hatter Cardiovascular Institute

University College London Hospital and Medical School
67 Chenies Mews, UCL
London, WC1E 6HX

April 2009

Dedicated to health and well-being

Declaration

I, Hilary Kathleen Siddall, confirm that the work presented in this thesis is my own. Where information has been derived from other sources, I confirm that this has been indicated in the thesis.

Miss Hilary Kathleen Siddall

Abstract

Activation of the PI3K/AKT pathway protects the heart from ischaemia-reperfusion injury. Phosphatase and Tensin Homolog deleted on Chromosome10 (PTEN) is a negative regulator of this pathway. The hypothesis on which this thesis was based stated that inhibition of PTEN would confer protection against ischaemia-reperfusion injury. PTEN was reduced using: 1) a PTEN inhibitor, bpV(HOpic), 2) a mouse model of PTEN haploinsufficiency and 3) PTEN siRNA. The effects of PTEN reduction on ischaemia-reperfusion injury were investigated by using: 1) an isolated perfused heart model of ischaemia-reperfusion injury, 2) an isolated cardiomyocyte model of ROS induced mitochondria damage and 3) a cellular model of hypoxia-reoxygenation injury. No protection against ischaemia-reperfusion was observed in isolated perfused myocardium from C57BL/J6 mice, which were perfused with bpV(HOpic), or from $PTEN^{+/-}$mice. Likewise, no protection against ROS induced mitochondrial damage was observed in isolated cardiomyocytes from the $PTEN^{+/-}$ mice. In these models an increase in AKT activity was recorded, however, this was not sufficient to confer cardioprotection. Similarly, H9c2 rat myoblast cells, silenced for PTEN expression using siRNA, were not protected against hypoxia-reoxygenation injury. Nevertheless, in isolated C57BL/J6 hearts perfused with bpV(HOpic) and in myocardium from $PTEN^{+/-}$ mice, when the PI3K/AKT pathway was stimulated by the cardioprotective intervention of ischaemic preconditioning a reduced threshold for protection was achieved. To conclude, the level of PTEN inhibition achieved in this study was not sufficient to bestow protection against simulated ischaemia-reperfusion injury. However, it appears that reductions in PTEN can increase the sensitivity towards cardioprotection.

Acknowledgments

I would like to express my sincere gratitude to my supervisors Professor Derek Yellon and Dr Mihaela Mocanu for giving me this opportunity and for all their time and support throughout this project.

I would like to acknowledge the British Heart Foundation for funding the research at the Hatter Cardiovascular Institute.

Additionally, I would like to express my appreciation to all the members of the Hatter Institute who have supported me throughout this study; with special gratitude to Dr Derek Hausenloy, Dr Christopher Smith, Dr Sean Davidson, Dr Shiang Yong (Max) Lim, Mr Sang Bing Ong, Ms Abigail Wynne and Ms Linda Dutton. I am especially grateful to Ms Marta Pavia whose genuine passion for science was an inspiration, for which I will always be grateful.

Essentially, I would like to thank my friends and family for their support during my studies. In particular Malcolm Begg (the key and rock) whose patience, understanding and voice of reason was an essential component for my PhD survival and my personal sanity.

Table of contents

List of figures and tables

Abbreviations

A.U	Arbitrary units
AIP	Apoptosis inhibitory factor
AKT	AKT/protein kinase B
APAF-3	Apoptotic protease activating factor 3
APS	Ammonium persulfate
ASK	Apoptosis signal regulated kinase
ATP	Adenosine triphosphate
β (B) actin	Beta actin
b.p	Base pairs
BAD	Bcl-2 associated death promotor
BAX	Bcl-2-associated x protein
BDM	Butanedione monoxime
BID	BH3 interacting domain death agonist
BIM	BCl2 like 11
bpV(HOpic)	Bisperoxo(5-hyroxypyridine-2carboxy) oxovanadate
BSA	Bovine serum albumin
Cx43	Connexin 43
Ca^{2+}	Calcium ion
Caspase	Cystein aspartate specific proteases
CBF1	CBF1 also known as recombination signal binding protein for immunoglobulin kappa J region (RBBJ)
CENP-C	Centromere protein C
cGMP	Cyclic guanosine monophosphate
CK	Creatine kinase
CK2	Casein kinase II
CMV	Cytomegalovirus
CO2	Carbon dioxide
CsA	Cyclosporine A
CVD	Cardiovascular disease
DAPI	4,6,diamidino-2-phenylindole
DMSO	Dimethyl sulfoxide
DNA	Deoxyribonucleic acid
DTT	Dithiothreitol

ECG	Electrocardiogram
ECL	Electrochemiluminescence
EGF	Epidermal growth factor
EGFR	Epidermal growth factor receptor
ELISA	Enzyme linked immunosorbant assay
eNOS	Endothelial nitric oxide synthase
ERK	Extra signal-regulated MAPK
ERM	Ezrin-radixin-meosin
FADD	Fas – associated protein with death domain
FasL	Fas ligand
FBS	Foetal bovine serum
G	Grams
GAPDH	Glyceraldehyde 3-phosphate dehydrogenase
GPCR	G coupled protein receptor
GLUT4	Glucose transporter 4
GSK3b	Glycogen synthase kinase 3b
H+	Hydrogen ion/proton
H_2O_2	Hydrogen peroxide
H_2SO_4	Sulfuric acid
$^{\cdot}HO_2$	Hydroperoxyl radical
HDL	High density lipoprotein
HEPES	hydroxyethylpiperazine N- 2 ethanesulfonic acid
HES1	Hairy and enhancer of split 1
HIF1a	Hypoxia inducible factor 1a
HR	Heart rate
HRP	Horse radish peroxidase
HSP	Heat shock protein
HtrA2	HtrA serine peptidase 2
i.p	Intra peritoneal
I/R%	Percentage of infarction to risk area
IAP	Inhibitor of apoptosis
IGF1	Insulin like growth factor 1
IKK	IκB kinase
IPC	Ischaemic preconditioning
IRS	Insulin receptor substrate
JNK	c-Jun N-terminal kinase

K^+	Potassium ion
K_{ATP}	ATP sensitive potassium channel
KDa	Kilodaltons
LDH	Lactic dehydrogenase
LDL	Low density lipoprotein
LVEDP	Left ventricular end diastolic pressure
LVPP	Left ventricular perfusion pressure
MAGI3	Membrane-associated guanylate kinase with inverted orientation
MAPK	Mitogen activated protein kinase
Mdm2	Murine double minute 2
Mg^{2+}	Magnesium ion
mK_{ATP}	Mitochondrial adenosine triphosphate sensitive potassium channels
MI	Myocardial infarction
mPKCε	Mitochondrial protein kinase C epsilon
mPTP	Mitochondrial membrane permeability transition pore
mRNA	Messenger ribonucleic acid
mTOR	Murine target of rapamycin
NADPH	Nicotinamide adenine dinucleotide phosphate
NEDD4-1	Neural precurser cell expressed developmental down Regulated 4-1
NFκB	Nuclear factor kappa light chain enhancer of activated B cells
NGF	Nerve growth factor
NHE1	Sodium/hydrogen exchange protein 1
NO	Nitric oxide
NOS	Nitric oxide synthase
O2	Oxygen
O_2^-	Superoxide
%	Percentage
p	Phosphorylation (p) / phospo
p42/p44 (MAPK)	Protein 42/ protein 44 mitogen activated kinase
p70S6K	70 kDa ribosomal protein S6 kinase
PCAF	p300/CBP associated factor

PARP	Poly (ADP-ribose) polymerase
PDGF	Platelet derived growth factor
PDK1	3-phosphoinositide dependent protein kinase1
PDZ	Post synaptic density protein, Drosophila disc large tumour suppressor and Zonula occludens-1 protein
PFTα	Pifithrin alpha
PHLPP	PH domain leucine rich repeat protein phosphatase
PI	Propidium iodide
PINK1	PTEN induced kinase 1
PIP2	Phosphatidylinositol 2 phosphate
PIP3	Phosphatidylinositol 3 phosphate
PI3K	Phosphatidylinositol 3 kinase
PKC	Protein kinase C
PKG	Protein kinase G
PP2A	Protein phosphatase 2A
PPAR	Peroxisome proliferators-activated receptors
PP	Perfusion pressure
RPP	Rate pressure product
Prdx1	Peroxidase peroxiedoxin
PTEN	Phosphatase and tensin homolog deleted on chromosome 10
PTP	Protein tyrosine phosphatases
PUMA	p53 upregulated modulator of apoptosis
RCF	Relative centrifugal force
RISK	Reperfusion injury salvage kinase pathway
RISC	RNA induced silencing complex
RNA	Ribonucleic acid
ROCK	Rho associated kinase 1
ROS	Reactive oxygen species
Na^+	Sodium ion
$SarcK_{ATP}$	Sarcolemmal adenosine triphosphate sensitive potassium channels
SDS PAGE	Sodium disulphide poly acrylamide gel electrophoresis
SGK1	Serum and glucocorticoid regulated kinase1
SHIP	SRC homology 2 containing inositol 5 phosphatase
SHP1	The Src homology domain 2 (SH2) containing tyrosine phosphtase 1

SHP2	The Src homology domain 2 (SH2) containing tyrosine phosphtase 2
siRNA	Small interfering ribonucleic acid
Smac/DIABLO	Second mitochondria-derived activator of caspase/ Diablo homolog
t	Total levels
TBS	Tris buffered saline
TEMED	Tetramethylethlenediamine
TK	Tyrosine kinase
TMB	Tetra methyl benzidine
TMRM	Tetra methyl rhodamine methyl
TNFα	Tumour necrosis factor alpha
TPIP	TPTE and PTEN homolog inositol lipid phosphatase
TPTE	Transmembrane phosphatase with tensin homology
TRAP	TNF receptor activated protein
TTC	Triphenyltetrazolium chloride
Tunel	Terminal deoxynucleotidyl transferase dUTP nick end labelling
U	Units
Ub	Ubiquitination
WHO	World health organisation

1 Chapter 1 – General Introduction

1.1 Cardiovascular disease

In 2004 the World Health Organization (WHO) updated a study investigating the global burden of disease. It states that cardiovascular disease (CVD) is the leading cause of mortality worldwide. Astonishingly, 12% of all deaths can be attributed to ischaemic heart disease. Moreover, these figures are estimated to increase by 2015 [i](WHO). In addition to fatalities, possibly the most shocking information relates to heart disease as the leading cause of global burden. Therefore, medical and financial costs associated with CVD are also predicted to increase. Quality of life can be dramatically reduced, thus having a substantial impact on patient lifestyle (Allender et al., 2007) [i](WHO).

The number of known risk factors associated with the development of CVD are ever increasing and currently include: hypertension, hypercholesterolemia, increased low density lipoprotein (LDL), decreased high density lipoproteins (HDL), obesity, diabetes mellitus, smoking and physical inactivity (Smith and Kampine, 1990; Fuller et al., 2001; Allender et al., 2007)[i](WHO). To limit the prevalence of CVD and these risk factors, personal accountability and prevention must be promoted. Furthermore, hereditary factors influence the development of CVD (Marion et al., 2002; Ishihara et al., 2003; Ferdinandy et al., 2007), some of which will be highlighted in the following chapters. Nonetheless, clinicians and scientists alike are striving to reduce this disease burden, in order to increase the quality of life and ultimately, to reduce the mortality subsequent to CVD.

[i] The world health organization. The global burden of disease. 2004 update. Geneva, World health organization, 2008 accessed on 24.11.2008 http://www.who.int/healthinfo/global_burden_disease/2004_report_update

1.2 Myocardial infarction

Severe abrogation of blood supply (ischaemia) to a region of the heart can cause cell death, which is known as myocardial infarction (MI). This is detrimental and can induce tissue damage and consequentially the initiation of ischaemic heart disease (Smith and Kampine, 1990). Periods of reduced blood supply to the heart can result in an energy demand that outweighs supply; thereby effecting function. Clinicians often observed this condition in patients who develop angina, which can be caused by the narrowing or obstruction of coronary arteries due to debris, such as a thrombus and/or atherosclerotic plaque formation, as illustrated in Figure 1.1. Ultimately, this ischaemic period initiates the process of tissue damage that is associated with MI. Reperfusion of the ischaemic area is required to prevent further tissue damage however, paradoxically, the act of reperfusing the ischaemic area can itself induce additional damage and can affect cardiac function thereafter (Smith and Kampine, 1990; Argaud et al., 2005a; Hausenloy et al., 2005; Ferdinandy et al., 2007). This damage is referred to as ischaemia-reperfusion or reperfusion-induced injury.

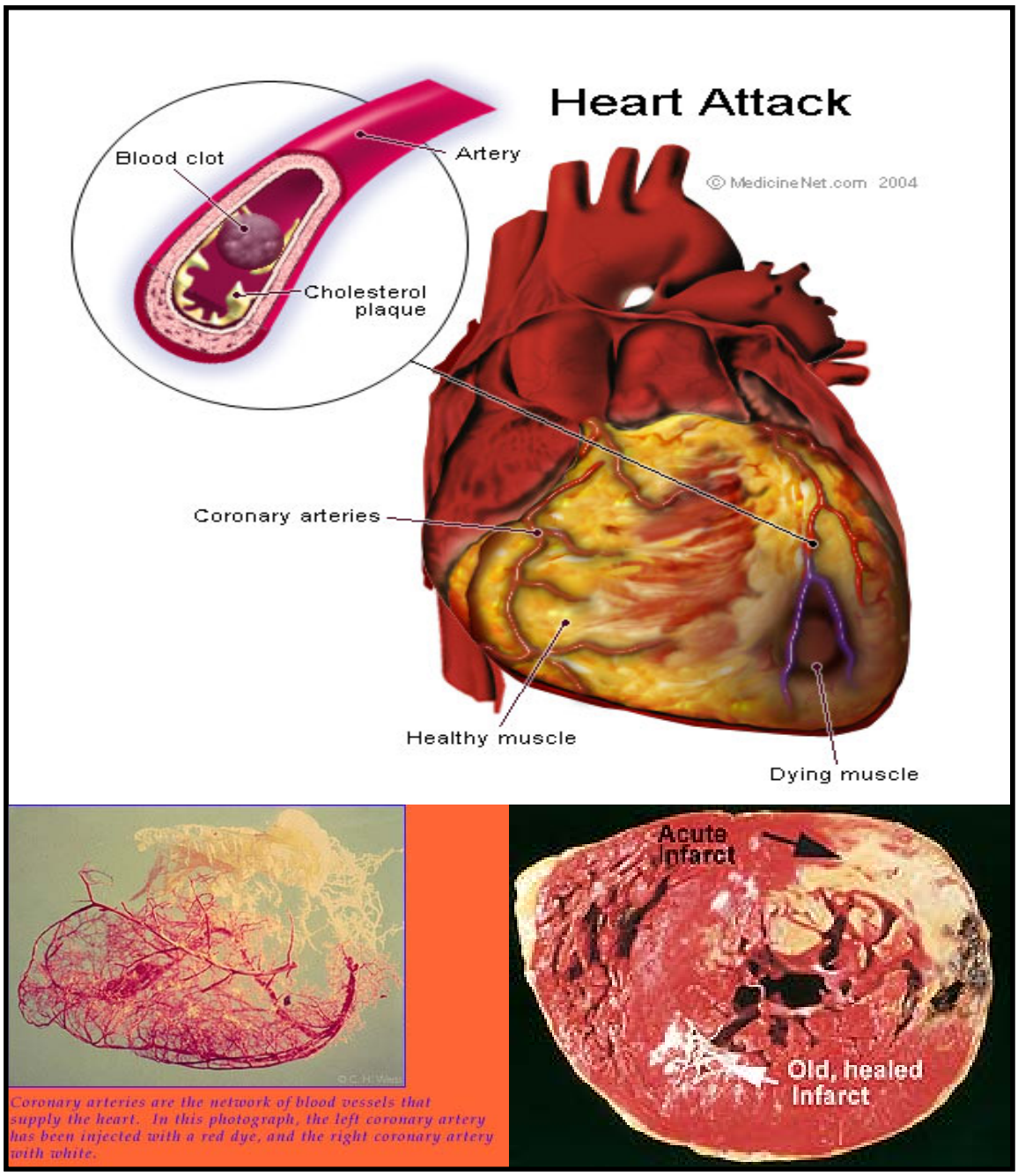

<u>Figure 1.1:</u> The effects of myocardial infarction and the consequence of ischaemia-reperfusion injury, on the myocardium and coronary system.

Top = http://images.medicinenet.com/images/illustrations/heart_attack.jpg,

Bottom left = http://www.pbs.org/wgbh/nova/heart/troubled.html

Bottom right = http://www.opt.indiana.edu/v543/labs/images/myo_infar1.jpg

Ischaemia-reperfusion injury can trigger cardiac stunning, arrhythmias, endothelial dysfunction and cell death (Smith and Kampine, 1990; Maddock et al., 2002; Ferdinandy et al., 2007). Further to promoting changes in life style, therapies for MI aim to decrease cardiac work load and minimise ischaemia-reperfusion injury. Current best practice for the treatment of patients suffering with a MI is to restore blood flow using thrombolytic therapy or to use surgical interventions, such as balloon catheter angioplasty or coronary artery bypass surgery (Smith and Kampine, 1990; Dauterman and Topol, 2002). While these interventions have proven successful, some are invasive and may result in further tissue damage and reoccurrence of MI later in life. Therefore, alternative strategies to enhance tissue viability post MI are required to help address this unmet clinical need (Dauterman and Topol, 2002; Ferdinandy et al., 2007). Much research is directed at investigating the cellular pathways involved in ischaemia-reperfusion injury and the cell death resulting in the formation of infarcted tissue. The period of ischaemia and the reperfusion of an ischaemic area, together, contribute to cell death and to the severity of myocardial injury (Headrick et al., 2001).

1.2.1 Ischaemic injury

The myocardium is highly dependent on mitochondrial oxidative phosphorylation, also known as aerobic metabolism, for the production of ATP. With the onset of anoxia this form of metabolism cannot be sustained (Murry et al., 1986; Smith and Kampine, 1990; Ferdinandy et al., 2007). The remaining stores of ATP can only supply a few minutes of ventricular function. Consequentially, a switch to anaerobic glycolysis follows and lactate accumulates in the cardiomyocytes, resulting in low pH and acidic conditions (Smith and Kampine, 1990; Halestrap et al., 2004).

The low pH alters metabolic signalling further; and also activates the sodium/hydrogen (Na^{+}/H^{+}) ion pump which acts to restore normal pH. Sodium (Na^{+}) accumulates in the cell

because the Na^+/K^+ ATPase is inactive, due to the lack of ATP, and thus Na^+ is no longer pumped out of the cell. Additionally, the Na^+/Ca^{2+} exchanger ceases to function normally and fails to pump calcium out of the cell. This is due to the high intracellular Na^{2+} levels which causes the exchanger to switch into a reverse exchange mode, permitting the entry of calcium (Ca^{2+}) into the cell (Yellon and Baxter, 2000; Ferdinandy et al., 2007). Collectively, this overload of intracellular ions promotes swelling of the sarcoplasmic reticulum and the mitochondria (Halestrap et al., 2004). A proportion of cells become damaged, their membranes become permeable and as a result cellular enzymes are released. Lactate dehydrogenase (LDH) and creatine kinase (CK) are examples of such enzymes, they are predominantly cytoplasmic and their releases can be used as an indicator of necrotic cell death (van Nieuwenhoven et al., 1996). This type of cell death is described in section 1.3. Once such a chain of events occurs, signals for cell death in the affected area and the initiation of ischaemic injury commence, as described below in more detail (Smith and Kampine, 1990). To salvage remaining viable tissue, it is imperative to reperfuse the ischaemic myocardium as quickly as possible.

1.2.2 Reperfusion injury

Rapid reperfusion of the ischaemic area is required to limit tissue damage and is necessary to reoxygenate and salvage remaining viable tissue. Conversely, reperfusion itself can cause additional damage; this phenomenon is termed lethal reperfusion-induced injury (Hausenloy et al., 2005; Argaud et al., 2005a; Ferdinandy et al., 2007). Such damage promotes further cell death, which contributes to an increase in irreversible tissue damage in the reperfused myocardium.

Reperfusion of the ischaemic myocardium causes an enhanced generation of reactive oxygenation species (ROS), which induces cellular damage. Within the mitochondria, under

normoxic conditions, oxidative phosphorylation occurs freely. At the inner mitochondrial membrane a number of redox-reduction reactions occur along the electron transport chain to produce ATP (Gao et al., 2008a). This form of respiration will result in the low level generation of ROS, such as superoxide (O_2^-) and hydrogen peroxide (H_2O_2) (Gao et al., 2008a). Nevertheless, the cell is equipped with antioxidants, such as superoxide dismutase, glutathione peroxidase and catalase which can quickly convert the free radicals into H_20 (Becker, 2004; Zhao, 2004). However, during ischaemia these antioxidants cease to function due to restrictions in the levels of ATP and the level of free radicals intensifies. At reperfusion, the abrupt increase of oxygen in the ischaemic and acidic myocardium favours the production of the highly reactive, hydroperoxyl radical ($^{\cdot}HO_2$). Such elevated levels of ROS generation causes oxidative stress and induces severe cellular damage to lipids, proteins, deoxyribonucleic acid (DNA) and can cause apoptosis (Becker, 2004; Zhao, 2004). Moreover, reperfusion promotes a sudden increase in ATP synthesis which restores the level of ATP and reactivates the ion pumps, permitting further influxes of Na^+ and Ca^{2+} into the cell. When mitochondria are overloaded with Ca^{2+} ions the non specific mitochondrial permeability transition pore (mPTP) is thought to open, causing organelle disruption (Argaud et al., 2004). Consequently, further changes occur to the mitochondria, such as additional swelling, membrane instability and release of cytochrome c from the intramembrane space which contributes to mitochondrial membrane depolarisation. This makes the organelle unstable and initiates signalling for cell death (Halestrap et al., 2004), which are highlighted below.

1.3 Cell death and myocardial ischaemia-reperfusion injury

There are two well-defined mechanisms of cell death, known as apoptosis and necrosis, which are distinct from each other and are compared in Table 1.1. Intermediate forms can exist, bearing a mixture of features from each one (Kajstura et al., 1996; Crompton, 1999).

Table 1.1: Markers of necrosis and apoptosis induced cell death (Kajstura et al., 1996; Crompton, 1999). Adenosine triphosphate = ATP.

Necrosis	Apoptosis
No ATP required.	ATP dependent.
Influx of water, causing mitochondrial and cell swelling.	Efflux of water, causing dehydration and cell shrinkage.
Small nuclear structural changes.	Nuclear break down, condensation and fragmentation.
Membrane rupture.	Membrane integrity maintained.
Non functioning organelles released.	Formation of apoptotic bodies containing functional organelles.

1.3.1 Necrosis

Membrane disintegration causes the absorption of water, membrane rupture, release and destruction of cellular organelles. Subsequently, this attracts inflammatory cells to the area of necrosis which initiates inflammation and further damage to surrounding tissue (Kajstura et al., 1996; Crompton, 1999). For example, in canine hearts, neutrophil accumulation occurs following ischaemia-reperfusion injury, which can be detected by the presence of myeloperoxidase activity (Corvera et al., 2003). Necrosis does not require energy and because of this it has been proposed that necrosis is the predominant type of cell death occurring during ischaemia, and that apoptosis occurs mainly during reperfusion when the energy supply is restored (Kajstura et al., 1996; Jeremias et al., 2000; Hamacher-Brady et al., 2006b). This makes apoptosis a key research area in investigating novel therapies post ischaemia-reperfusion.

1.3.2 Apoptosis

In contrast to necrosis, apoptosis is considered a mechanism of programmed cell death, for which energy is required. Cells undergoing apoptosis release water, shrink and undergo changes to membrane integrity. Thereafter, apoptotic bodies and membrane blebs form which engulf and preserve functional organelles. As described below, in section 1.3.4 other cells and mechanisms can preserve cellular organelles. In addition apoptosis can be identified by the presence of DNA condensation, fragmentation and breakdown of the nucleus (Kajstura et al., 1996; Crompton, 1999; Arbustini et al., 2008).

The main effectors of apoptosis are a group of enzymes called caspases; which are cysteine containing proteases that specifically cleave proteins after aspartate residues. They are synthesised in a dormant prozymogen formation, but once stimulated, mature active fragments are generated (Nicholson et al., 1995). Importantly, a basal level of apoptosis is required for tissue development and cellular homeostasis (Kerr et al., 1972; Danial and Korsmeyer, 2004). However, enhanced apoptosis is observed in ischaemia-reperfusion injury and during cardiac remodelling (Hamacher-Brady et al., 2006b; Arbustini et al., 2008). Apoptotic cell death was first identified by Kerr, Wyllie and Currie early in the 1970s and can be initiated by two main mechanisms which are referred to as extrinsic and intrinsic pathways of cell death (Kerr et al., 1972; Wyllie et al., 1980).

1.3.2.1 Extrinsic cell death pathways

The extrinsic cell death pathway is activated by ‘death receptor’ ligands such as tumour necrosis factor alpha (TNFα) and Fas ligand (FasL), which bind to specific death receptors (Jeremias et al., 2000; Lee et al., 2003). Down stream stimulation of such receptors results in a number of proteolytic cleavages which activate initiator caspases, such as caspase 8 and 10 (Kothakota et al., 1997; Li et al., 1998; Luo et al., 1998). The initiator caspases 8 and 10

activate the executioner caspase 3. Caspase inhibition using z-VAD-fmk can prevent TNFα induced apoptosis (Li et al., 1998; Luo et al., 1998).

TNFα and FasL- stimulated apoptosis can induce cleavage of structural proteins such as gelsolin, which can affect the actin cytoskeleton. This has been attributed to functional caspase 3, which also necessitates cleavage for function (Kothakota et al., 1997). The release of an active caspase 3 fragment can cleave Poly(ADP-ribose) polymerase (PARP); this cleavage prevents DNA repair and increases the level of apoptosis (Kothakota et al., 1997). Following an apoptotic stimuli, the cleavage of PARP prevents DNA repair, which can be recorded by measuring DNA fragmentation (Nicholson et al., 1995; Li et al., 1997b; Communal et al., 2002). The incubation of purified myocyte microfilament proteins with caspase 3 can induce cleavage of structural proteins such as alpha actin and troponin c, and also of PARP. Over expression of the Fas receptor or addition of FasL to neonatal cardiomyocytes causes cell shrinkage and nuclear condensation, ultimately leading to apoptosis. This phenomenon can be assessed by positive staining for 4,6,diamidino-2-phenylindole (DAPI), a nuclear morphology stain and terminal deoxynucleotidyl transferase dUTP nick end labelling (Tunel), a DNA cleavage marker (Jeremias et al., 2000; Lee et al., 2003). Furthermore, compared to control hearts, mouse myocardium lacking functional Fas receptors showed a reduction in Tunel staining and a reduction in infarct size, following ischaemia-reperfusion (Lee et al., 2003). However, this observation is not unanimous (Tekin et al., 2006), highlighting the discrepancy in this area of study.

1.3.2.2 Intrinsic cell death pathways

Activation of intrinsic cell death pathways is usually independent of death receptors. The process can be regulated directly at the mitochondrial level involving a balanced interaction of many pro death and pro survival factors. Such factors include the Bcl family of proteins, which

contain a BH_3 domain and are classified as either pro apoptotic (BH_3 interacting domain death agonist (BID), BIM, Bcl-2-associated x protein (BAX) and Bcl-2 associated death promotor (BAD)) or anti apoptotic (Bcl2,$Bclx_L$) (Luo et al., 1998; Li et al., 1998; Chen et al., 2001; Kuwana et al., 2002). Their level of activity can depend on interactions from another protein family member; for example, the cleaved form of the pro apoptotic factor BID can activate BAX resulting in the formation of channels in the mitochondria membrane. These pores facilitate the release of large mitochondrial proteins up to 1500 Daltons, including cytochrome c (Luo et al., 1998; Kuwana et al., 2002). These proteins are up regulated in ischaemia-reperfusion injury. Subsequent to simulated ischaemia-reperfusion injury in the HL-1 myocardial cell line the expression of BAX is increased, causing cell death (Hamacher-Brady et al., 2006a). Consequentially, BID/BAX interactions at the mitochondrial membrane level can initiate apoptosis (Kuwana et al., 2002). Counteracting these events are the Bcl2/$Bclx_L$ proteins which are anti apoptotic; over expression of $Bclx_L$ protein at the mitochondrial membrane level can prevent BID/BAX induced apoptosis by sequestering these pro apoptotic proteins (Kuwana et al., 2002; Chipuk et al., 2004). The change in balance between pro survival and pro death proteins at the level of the mitochondria depends also on the type of apoptotic stimuli such as free radicals, UV light or DNA damage. UV light can induce the tumour suppressor, p53, which is involved in cell cycle arrest and apoptosis (Chipuk et al., 2004; Wang et al., 2005).

The tumour suppressor p53 plays a role in apoptosis. During renal ischaemia and reperfusion p53 expression is increased and this is associated with activation of p21 and BAX induced cell death (Kelly et al., 2003). The proteins p21 and p53 promote G1 cell cycle arrest, halting the progression of the cell cycle (Katayose et al., 1995; Kelly et al., 2003). In the heart p53, has a role in the damage induced by ischaemia-reperfusion injury. Its contribution to cell death can be both due to its promotor dependent and independent activity (Chipuk et al., 2004; Kelly et al., 2003; Zhao et al., 2001). As stated above, p53 stimulates cell cycle arrest

by up regulating cell cycle factors such as p21. In addition p53 can activate the apoptotic proteins BAX and indirectly effect caspase activity (Kelly et al., 2003; Ashkenazi, 2002). Pifithrin alpha (PFTα), a p53 inhibitor, can inhibit the apoptosis associated with ischaemia-reperfusion injury (Kelly et al., 2003). Induction of cell death in the presence of nuclear import inhibition demonstrates that p53 can directly activate BAX, changing membrane permeability independent of its p53 promoter activity (Chipuk et al., 2004). Myocardium from p53 heterozygous knockout mice exhibit less apoptosis and have a higher survival rate post MI (Matsusaka et al., 2006). Collectively, this implicates p53-induced apoptosis to ischaemia-reperfusion injury and indicates that a reduction in apoptotic factors, such as p53, can facilitate survival.

Moreover, once the mitochondrial membrane integrity has been compromised, cytochrome c is released where it can interact with Apaf3 and procaspase 9 forming a pro apoptotic complex. Procaspase 9 is activated in this complex and acts as an initiator caspase of the intrinsic death pathway, which can cleave (therefore activate) procaspase 3 (Kothakota et al., 1997; Li et al., 1997b).

1.3.2.3 Crosstalk between extrinsic and intrinsic death pathways

Irrespective of the apoptotic trigger, the down stream signalling factors can converge. For example the activation of caspase 8 can initiate cleavage of BID. The over expression of BID in HeLa cells can cause an increase in apoptosis stimulated by TNFα. Furthermore, the cleaved form of BID can translocate from the cytosol to the mitochondrial membrane. This has been associated with the loss of mitochondrial membrane potential, cytochrome c release and consequentially cell shrinkage and nuclear fragmentation (Li et al., 1998; Luo et al., 1998). In contrast, some BH_3 containing Bcl2 related proteins such as the pro survival protein Bcl2, can prevent such apoptosis. This shows that although activation of the extrinsic

pathway does not directly act in the mitochondria; it can activate the mechanisms within the intrinsic pathway (Arbustini et al., 2008). As shown in Figure 1.2.

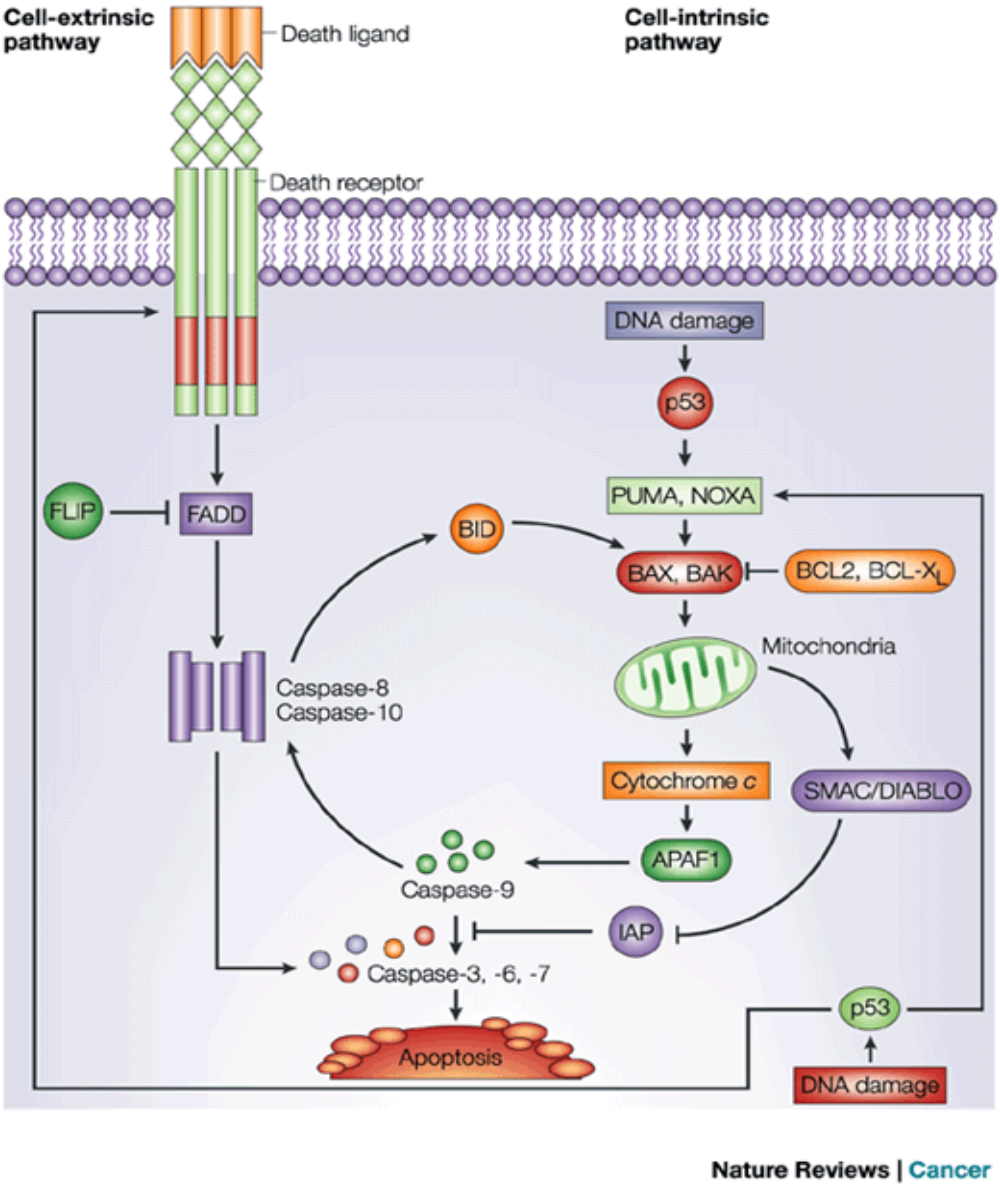

Figure 1.2: Intrinsic and extrinsic mechanisms of apoptosis and the cross talk that can occur between these pathways (Ashkenazi, 2002) including apoptotic protease activating factor 3 (APAF-1), Bcl-2 – associated x protein (BAX), BH_3 interacting domain death agonist (BID), BCL, Fas – associated protein with death domain (FADD), FLIP, inhibitor of apoptosis (IAP), Second mitochondria-derived activator of caspase/ Diablo homolog (SMAC/DIABLO).

1.3.3 The Mitochondria and cell death

Mitochondria are pivotal generators of cellular energy. Structurally they consist of an inner and an outer membrane that envelops an inter-membrane space. The inner membrane forms many folds known as cristae, which protrude into the mitochondrial matrix. In addition to generating ATP, mitochondria play a crucial role in maintaining a balance between cell survival and death (Crompton, 1999; Duchen et al., 2008).

During apoptosis the mitochondrial structure is altered and its contents are released which executes the signalling involved in cell death. As described above the release of cytochrome c occurs. In addition second mitochondria-derived activator of caspase/ Diablo homolog (Smac/DIABLO), an apoptotic mitochondrial protein, is released from the mitochondrial inner membrane space where it inactivates inhibitors of apoptosis (IAP) (Adrain et al., 2001; Du et al., 2000). Such inhibitors include XIAP (X-linked inhibitor of apoptosis), which is highly expressed in cardiomyocytes and functions to prevent the activation of caspases (Potts et al., 2005; Hamacher-Brady et al., 2006b). Smac/DIABLO release amplifies the signal for cell death. Furthermore, apoptosis inducing factors (AIF) and endonucleases released from the mitochondria can locate at the level of the nucleus to promote chromatin condensation and DNA fragmentation (Hamacher-Brady et al., 2006a; Hamacher-Brady et al., 2006b).

Table 1.2 highlights some of the contributing factors crucial to cell survival. Pro death and pro survival signals contribute to mitochondrial stability by altering mitochondrial permeability, release of cytochrome c and mitochondrial membrane depolarisation (Kajstura et al., 1996; Crompton, 1999). The change in mitochondrial permeability has been attributed to the formation and opening of a non specific mitochondrial permeability transition pore (mPTP); which is a central factor in the disruption of mitochondria homeostasis (Hunter and Haworth, 1979; Crompton et al., 1987).

Table 1.2: Contributors to the cellular pro and anti apoptotic status (Kajstura et al., 1996; Crompton, 1999; Davidson et al., 2006). Bcl-2 associated death promoter (BAD), Bcl-2 associated x protein (BAX), BH3 interacting domain death agonist (BID), BCl2 like 11 (BIM), mitochondrial permeability transition pore (mPTP) and p53 upregulated modulator of apoptosis (PUMA).

Pro apoptosis	Anti apoptosis
Pro death Bcl family proteins BID, BAD, BAX, BIM, PUMA	Bcl pro survival protein; sequestered Pro death factors
Caspase activation	Caspase inactivation
Opening of mPTP and release of cytochrome c	Delay to opening of mPTP and prevention of the release of cytochrome c
Presence and/or activation of detrimental pathways transcription factors p53, p21	Prevention of nuclear condensation and DNA fragmentation.

Opening of the mPTP is involved in cell death. Once the pore is formed the mitochondria are permeable to molecules up to 1500 Daltons. Solutes and water enter causing the organelle to swell, initiating damage (Hunter and Haworth, 1979; Crompton et al., 1987; Halestrap et al., 1997; Hamacher-Brady et al., 2006b). Mitochondrial cristae projections unfold and, to an extent, can withstand some changes to the inner membrane. However, the outer membrane cannot adapt to such changes and quickly ruptures (Halestrap et al., 2004). Furthermore, the inner membrane becomes damaged, and oxidative phosphorylation becomes uncoupled. Consequentially, the normal activity of the mitochondria ceases; ATP is no longer produced and instead, becomes exhausted (Halestrap et al., 2004; Hamacher-Brady et al., 2006b).

The structure of the mPTP

The precise structure and mechanism of mPTP transition has not been completely elucidated (Halestrap, 2009). Previously, it was proposed that two adjacent adenine nucleotide translocase (ANT) proteins spanned the mitochondrial membrane and in the presence of ATP

and ADP they were capable of maintaining an impermeable barrier (Halestrap et al., 1997). It has also been suggested that a voltage dependent anion channel (VDAC), a mitochondrial outer membrane protein, is involved (Halestrap et al., 2004). Since these suggestions, the production of knockout models have demonstrated that these components are not essential for the formation of the mPTP (Kokoszka et al., 2004; Krauskopf et al., 2006; Baines et al., 2007). However, the role of ANT is still debated, which may have a regulatory role in mPTP formation (Woodfield et al., 1998; Halestrap, 2009).

Knockout models have implicated cyclophilin D, an inner membrane mitochondrial protein, in the formation of the mPTP (Woodfield et al., 1998; Baines et al., 2005). Interestingly, studies have indicated that cyclophilin D can bind to ANT proteins, which can change protein conformation to create a membrane channel (Woodfield et al., 1998). The binding of cyclophilin D is thought to be calcium dependent, however, exceptionally high levels of calcium open the pore independent of cyclophilin D (Halestrap et al., 1997). In addition, members of the Bcl2 family have been associated with the regulation of the mPTP (Halestrap et al., 2004). More recently, it has been proposed by Leung *et al.,* 2008 that the mitochondrial phosphate carrier may be involved in the formation of the mPTP, where it can bind to cyclophilin D and ANT to promote pore opening (Leung et al., 2008; Halestrap, 2009).

Opening of the mPTP

The mPTP opening is enhanced by oxidative stress, Ca^{2+} overload in the mitochondrial matrix, adenosine nucleotide reduction, increased phosphate and increased pH (Halestrap et al., 1997; Halestrap et al., 2004; Kim et al., 2006a). Atractyloside, which opens the mPTP causes the release of cytochrome c and induces cell death (Gao et al., 2006; Wang et al., 2007a).

Pore opening is inhibited by binding of ATP, this has been associated with magnesium, low pH and adenine nucleotides (Halestrap et al., 1997). Pharmacological agents such as the immunosuppressant cyclosporine A (CsA) and sangliferin A can inhibit pore opening by preventing cyclophilin D binding to ANT (Halestrap et al., 1997; Woodfield et al., 1998). Additionally, the increase in mPTP opening and cell death associated with calcium overload can be prevented by cyclosporine A (CsA) (Argaud et al., 2005a; Baines et al., 2005; Wang et al., 2007a).

Myocardial cell death has been associated with opening of the mPTP, for example CsA and sangliferin A can prevent myocardial LDH release following ischaemia-reperfusion injury (Clarke et al., 2002; Halestrap et al., 2004). During ischaemic conditions the mPTP remains closed, however, the conditions following reperfusion favour mPTP opening (Clarke et al., 2002; Halestrap et al., 2004). Inhibition of the mPTP opening subsequent to ischaemia-reperfusion injury has a role in myocardial protection (Clarke et al., 2002; Argaud et al., 2005a). In isolated rat hearts subjected to ischaemia-reperfusion, inhibition of the mPTP opening with CsA at reperfusion, conferred protection (Argaud et al., 2005a). Investigating mechanisms that prevent mPTP opening may lead to the development of drugs that can prevent cell death and ischaemia-reperfusion injury.

1.3.4 Autophagy

Recently, another form of cell death (autophagy) has been described. Similar to apoptosis, this pathway is associated with programmed cell death, however, it produces energy instead of utilising it (Hamacher-Brady et al., 2006b; Gurusamy et al., 2009).

Broadly speaking, autophagy is executed when non-specific cytosolic proteins or organelles are engulfed in a membrane envelope. This forms an autophagosome which can fuse with

cellular lysosomes to create an autophagolysosome (Hamacher-Brady et al., 2007). The contents within this complex can be degraded by lysosmal hydrolases and in the process can produce ATP (Hamacher-Brady et al., 2006b; Hamacher-Brady et al., 2006a; Gurusamy et al., 2009). Cells subjected to stress, such as ischaemia and reperfusion, respond by increasing the number of autophagosomes, which, when it occurs to a limited degree, is thought to be a pro survival response (Gurusamy et al., 2009; Yitzhaki et al., 2009). In the HL-1 myocardial cell line, for example, over expression of Beclin1 (a component of the autophagesome) causes an increase in the volume and number of autophagosomes following simulated ischaemia-reperfusion. The authors of this work linked this to a reduction in the activation of BAX, conferring protection against ischaemia-reperfusion injury (Hamacher-Brady et al., 2006a).

The mechanisms of cell death are diverse and include necrosis, apoptosis and autophagy (Lemasters et al., 1998). The role and the importance of each of these processes in ischaemia-reperfusion injury are still debated. There are suggestion that apoptosis, which requires energy, may not occur during ischaemia. Consequentially, it has been postulated that in ischaemia-reperfusion injury apoptosis predominantly occurs during reperfusion, when ATP has been restored (Kajstura et al., 1996; Jeremias et al., 2000; Toth et al., 2006). In contrast it has been proposed that apoptosis is not important in cardiomyocytes. For example, Taimor et al., 1999 preposed that isolated rat cardiomyocytes subjected to 18hr simulated hypoxia followed by 4hr reoxygenation undergo necrosis, however, this form of injury is not sufficient to cause apoptosis. In this study cells were considered necrotic if they fulfilled the criteria of 1) dual staining for annexinV and propidium iodide (PI), 2) LDH release and 3) non specific DNA degradation. Cells were considered apoptotic following the criteria of 1) annexinV staining, 2) tunel staining and 3) DNA laddering. Importantly, the authors of this work were able to induced apoptosis in ischaemic cells by using an additional stress stimulus such as UV light or H_20_2 (Taimor et al., 1999). Potts *et al.,* 2005, showed that differentiated

cardiomyocytes are resistant to cytochrome c injections due to high levels of XIAP that prevent the activation of caspases (Potts et al., 2005). Collectively, this highlights the controversy surrounding the contribution of apoptosis to ischaemia-reperfusion injury. Interestingly, there appears to be some cross talk between the signalling pathways involved in cell death (Li et al., 1998; Luo et al., 1998; Arbustini et al., 2008). It has been proposed that following ischaemia-reperfusion injury, necrosis and apoptosis occur and share a common end target to elicit cell death, by opening of the mPTP; the authors of this concept have termed such convergence of cell death as necrapoptosis (Kim et al., 2003). Nevertheless, whatever the form of cell death, strategies that focus on minimising such death may be important in reducing ischaemia-reperfusion injury.

1.4 Cardioprotection

The balance of pro survival and pro apoptotic cellular factors contributes to homeostasis. Therefore, survival from a cellular insult, such as ischaemia-reperfusion injury may be achieved by modulating these pathways in order to confer cardioprotection.

1.4.1 Known survival pathways

A network of cellular pathways contribute to cell growth and survival. Amongst these, the PI3K/AKT, ERK 1/2 , JAK/STAT, PKC, and p38 MAPK pathways are shown to promote survival in different models of myocardial ischaemia-reperfusion injury (Ping et al., 1999b; Ping et al., 1999a; Kuwahara et al., 2000; Gross et al., 2006). For example the cytokine, cardiotrophin-1 activates the PI3K/AKT pathway in ventricular cardiomyocytes and increases survival, which can be abolished in the presence of the PI3K/AKT inhibitor LY294008 (Kuwahara et al., 2000). Furthermore, in isolated rat hearts subjected to ischaemia-reperfusion, the presence of morphine conferred protection which has been attributed to an

increase in JAK/STAT3 phosphorylation and activation (Gross et al., 2006). Protection caused by the activation of this pathway can be abolished with the JAK/STAT inhibitor AG490, highlighting the role of STAT3 in survival (Gross et al., 2006). Additionally, inhibitors of p38 MAPK (SB203580), PKC (chelerythrine) and ERK1/2 (PD98059) used in models of survival can abolish cardioprotection (Mocanu et al., 2000; Hausenloy et al., 2004b).

Conversely, other cellular pathways can promote cell death. Activation of angiotensin II type 1 receptor, JNK, p53 and ROCK can be detrimental and can mediate ischaemia-reperfusion injury (Kelly et al., 2003; Ferrandi et al., 2004; Lange et al., 2007; Hamid et al., 2007). For example, phosphorylation and activation of the Rho kinase 1 (ROCK) substrate ezrin-radixin-meosin (ERM) has been associated with myocardial ischaemia-reperfusion injury (Bao et al., 2004; Hamid et al., 2007) and ROCK inhibitors, Fasudil and Y-27632 can protect against this injury (Bao et al., 2004; Hamid et al., 2007). Such inhibition in a mouse model of ischaemia-reperfusion injury can decrease neutrophil accumulation and maintain the level of the pro survival factor Bcl2 (Bao et al., 2004). The PI3K inhibitor, wortmanin can abolish this protection, indicating that ROCK inhibits the PI3K/AKT pathway. Furthermore, in the presence of the nitric oxide synthase (NOS) inhibitor, nitro L-arginine methyl ester (L-NAME), the protective effects of ROCK inhibition were abolished (Hamid et al., 2007). This work indicates that the activity of NOS is important in cardioprotection and that ROCK is a reperfusion injury kinase which acts to down regulate PI3K/AKT and the down stream survival factor nitric oxide (NO) (Hamid et al., 2007). In addition, inhibitors of angiotensin receptor activation (ARB), JNK (AS601245) and p53 (pifithrin alpha) can confer cardioprotection against ischaemia-reperfusion injury (Mocanu and Yellon, 2003; Ferrandi et al., 2004; Liu et al., 2006; Lange et al., 2007).

Reperfusion induced salvage kinase (RISK) pathway

The reperfusion injury salvage kinase (RISK) pathway encompasses PI3K/AKT and ERK 1/2 signalling, and is considered an important signalling system involved in cardioprotection (Hausenloy and Yellon, 2004a). As shown in Figure 1.3 activation of either pathway can affect a number of the same substrates (Hausenloy and Yellon, 2004a; Hausenloy and Yellon, 2004b; Zhang et al., 2007). These two parallel pathways are not independent of each other; on the contrary there is a crosstalk between them. In isolated rat hearts perfusion with the PI3K inhibitor LY294008 can enhance phosphorylation and activation of ERK1/2. Similarly, perfusion with the ERK1/2 inhibitor PD98059 can enhance the phosphorylation and activation of AKT (Hausenloy et al., 2004b).

Activation of the RISK pathway upon reperfusion of an ischaemic myocardium, can alter the balance of pro apoptotic and pro survival molecules, to promote cell survival. It is believed that protection is conferred down stream of the RISK pathway at the mitochondria and nuclear level. Survival is promoted when the activity of apoptotic proteins such as p53, caspases and members of the Bcl family, BIM, BAD, BAX are decreased (Gross and Gross, 2006). In addition activation of RISK pathway activates pro survival factors such as AKT, murine double minute 2 (Mdm2), Bcl survival protein Bcl2/$Bclx_L$, endothelial nitric oxide synthase (eNOS), and 70 kDa ribosomal protein S6 kinase (p70S6K) to confer protection (Mocanu and Yellon, 2003; Hausenloy et al., 2004b; Gross and Gross, 2006). p70S6K activation plays a role in protein translation, cell cycle progression and has anti apoptotic effects (Jonassen et al., 2001; Jonassen et al., 2004). Inhibitors of these RISK associated survival factors can influence cardioprotection.

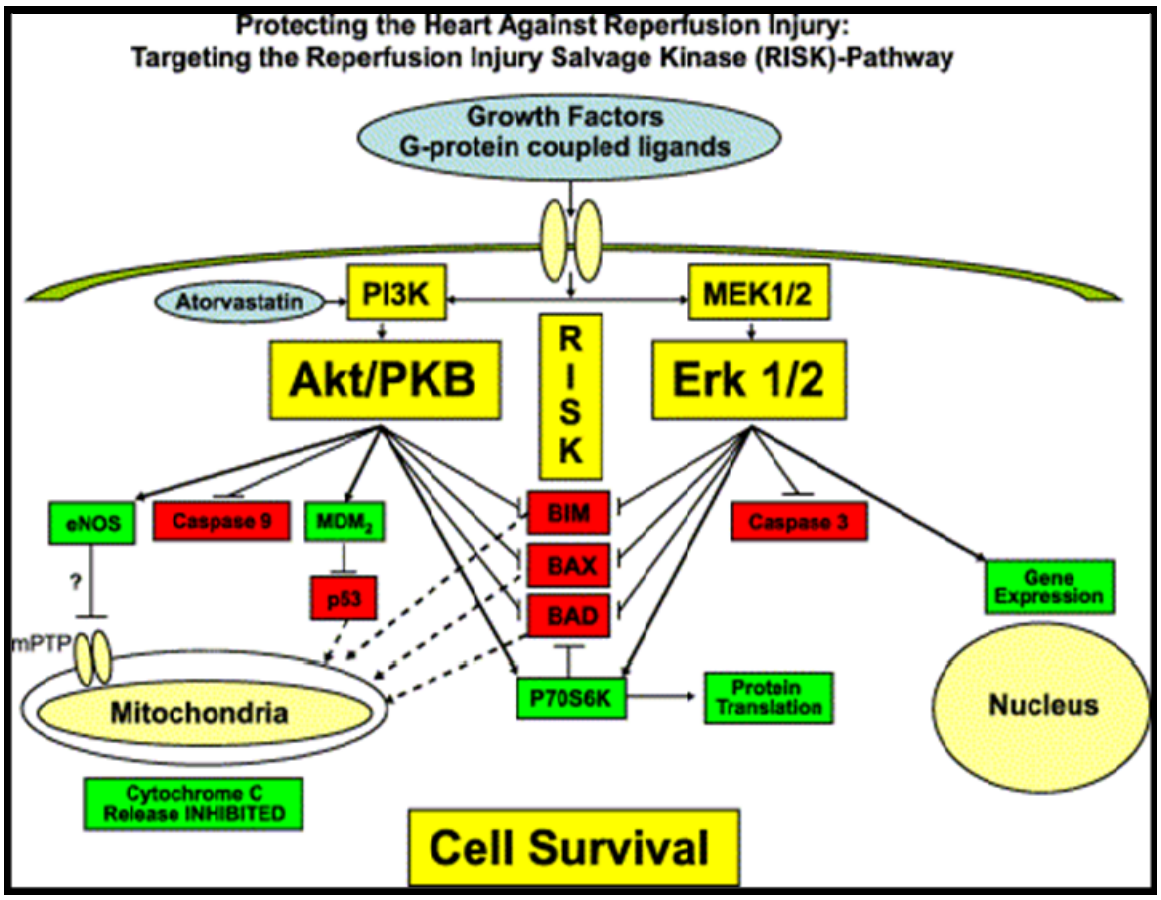

Figure 1.3: Reperfusion induced salvage kinase (RISK) pathway and the cell survival targets activated by PI3K/AKT and MEK/ERK. Red encodes pro apoptotic factors and green encodes pro survival factors (Hausenloy and Yellon, 2004b). Including Bcl-2 associated death promoter (BAD), BCl-2-associated x protein (BAX), endothelial nitric oxide synthase (eNOS), murine double minute 2 (MDM2), extra signal-regulated MAPK (MEK/ERK), 70 kDa ribosomal protein S6 kinase (p70S6K), Phosphatidylinositol 3 kinase (PI3K).

For example the p70S6K inhibitor, rapamycin abolished protection in the presence of RISK activation, suggesting that both PI3K/AKT and ERK1/2 can confer protection by activating 70S6K (Hausenloy et al., 2004b). Perfusion of the NO donor SNAP, in isolated mouse hearts, conferred protection against ischaemia-reperfusion injury which additionally activates and opens mitochondrial K_{ATP} channels (Bell et al., 2003). The presence of the mitochondrial K_{ATP}

channel blocker, 5HD can prevent the cardioprotection associated with SNAP (Bell et al., 2003; Hausenloy and Yellon, 2004a).

Activation of the RISK pathway prior or subsequent to a lethal period of ischaemia promotes protection from ischaemia-reperfusion injury (Hausenloy et al., 2005). Cardioprotective agents such as bradykinin and insulin can activate the RISK pathway to promote cardioprotection (Jonassen et al., 2001; Bell and Yellon, 2003; Davidson et al., 2006). As described, the protective effects of the RISK pathway are attributed to many signalling molecules. However, research suggests that the end target of this pathway may be the mPTP (Hausenloy et al., 2004a; Davidson et al., 2006). Activation of the RISK pathway using insulin, delays the time to mPTP opening and has been coupled with protection. The PI3K inhibitor, LY294008 blocked this delay, highlighting the role of the RISK pathway and the inhibition of the mPTP, to the survival of cardiomyocytes (Davidson et al., 2006). Interestingly, the activation of the RISK pathway is associated with protection in other tissues, such as the brain, kidneys lung and liver (Kelly et al., 2003; Banga et al., 2005; Wu et al., 2006).

1.4.1.1 PI3K/AKT pathway

Phosphatidylinositol 3,4,5 phosphate kinase

Phosphatidylinositol 3,4,5 phosphate kinase (PI3K) is a lipid kinase functioning down stream of G coupled protein receptors (GCPRs) and protein tyrosine/growth factor receptors (Stephens et al., 1993; Oudit et al., 2004). There are 3 classes of PI3K, known as class I,II and III (Kok et al., 2009). PI3K is important for cell growth, proliferation and survival. The majority of the research to date mainly focuses on type I, which in a heterodimeric enzyme and compromises an 110kDa catalytic domain and a 85kDa regulatory enzyme domain (Kok et al., 2009). Class 1A are classified according to the types of catalytic units and includes PI3Kα,β andδ and are coupled to protein tyrosine kinase/growth factor receptors. They are

thought to be involved in determining myocardial cell size. Class 1B includes catalytic unit γ (PI3Kγ), which is associated with GCPR and has a role in myocardial contractility (Stephens et al., 1993; Crackower et al., 2002; Hawkins and Stephens, 2007). In addition to the regulatory and a catalytic subunits PI3K class I contain a PH domain which localises the kinase to the membrane where it is active and has the capability to phosphorylate phosphatidylinositol 4,5 phosphate (PIP2) (Hennessy et al., 2005; Hawkins and Stephens, 2007). It is important to mention that the phosphorylation or dephosphorylation at different positions of the PIP2 inositol ring can influence cell signalling (Oudit et al., 2004).

The product of PI3K is phosphatidylinositol 3,4,5 phosphate (PIP3) which acts as a lipid second messenger and is responsible for recruiting signalling kinases to the membrane (Kane and Weiss, 2003). PIP3 can attract and bind proteins containing PH domains. For example, PIP3 causes phosphoinositide-dependent kinase 1 (PDK1) phosphorylation and translocation to the membrane where in turn it is anchored, activated and can phosphorylate the pro survival protein AKT (Seo et al., 2005). Similarly, PDK2 can phosphorylate and activate AKT at the membrane level (Mao et al., 2008). Subsequently, phosphorylated AKT facilitates the activation of many additional pro survival factors, as described below.

AKT

The activation of the PI3K/AKT pathway results in the membrane recruitment of AKT which is central to controlling survival. AKT is a 57kDa ser/thr kinase. There are 3 isoforms including AKT1(α), AKT2(β) and AKT3(γ) (Sasaoka et al., 2004; Brognard et al., 2007). As shown in Figure 1.4, once AKT is phosphorylated, it becomes active influencing many factors that regulate growth, proliferation and survival (Vanhaesebroeck and Alessi, 2000). These include serum and glucocorticoid regulated kinase (SGK1) and p70S6K (Nakashima et al., 2000), p44/p42 mitogen activate protein kinase (p42/p44 MAPK), eNOS, Mdm2, IκB kinase (IKK), murine target of rapamycin / p70S6K (mTOR/p70S6K) (Kane and Weiss, 2003; Ijuin and

Takenawa, 2003; Jonassen et al., 2004; Zito et al., 2007). In addition activated AKT can phosphorylate and inactivate pro apoptotic targets such as apoptosis signal regulated kinase (ASK1) and glycogen synthase kinase 3 beta (GSK3β) (Al Khouri et al., 2005). Inhibition of GSK3β induces translocation of glucose transporter 4 (GLUT4) vesicles to the membrane. Primarily these responses have a role in glucose homoeostasis, however, they are also connected to a pro survival status (Mosser et al., 2001).

There are 2 regulatory phosphorylation sites, one at amino acid threonine 308 (Thr308 – in the activation domain) and the second at serine 473 (Ser473 – in the regulatory domain) (Ma et al., 2008; Manning and Cantley, 2007). Prior phosphorylation at Thr308 is thought to be a requisite for Ser473 phosphorylation and it has been proposed that the phosphorylation of both Thr308 and Ser473 are required for maximal activation (Vanhaesebroeck and Alessi, 2000; Carpten et al., 2007). However, the full mechanism of AKT activation is not completely elucidated. PIP levels can influence the activity of AKT for example D-3 phosphoinositides such as PI(3,4)P2 and PI(3,4,5)P3 can recruit and activate AKT at the membrane level (Vanhaesebroeck and Alessi, 2000; Kane and Weiss, 2003; Ma et al., 2008).

The end effector of the PI3K/AKT pathway may be at the level of the mitochondria. Phosphorylated and activated AKT inhibits pro apoptotic factors such as caspases, BAD, BIM, BAX, and p53 (Li and Sato, 2001). In addition, it can increase the activity of the pro survival protein Bcl2, which sequesters and inhibits pro apoptotic signals (Luo et al., 1998; Chen et al., 2001). Furthermore, insulin activation by the PI3K/AKT pathway has been shown to delay the time to mPTP opening and reducing cell death in an eNOS dependent manner (Davidson et al., 2006).

Biological roles of the PI3K/AKT pathway

The PI3K/AKT pathway is responsible for development, growth, proliferation, cell cycle progression, migration and survival, as shown in Figure 1.4. This pathway is activated by numerous factors that stimulate membrane receptors. For example, agents such as insulin, okadaic acid and Epidermal growth factor (EGF) activate the PI3K/AKT pathway resulting in phosphorylation of AKT at Thr308 and Ser473 which enhances AKT activity (Sasaoka et al., 2004; Gao et al., 2005b; Brognard et al., 2007). Furthermore, PI3K/AKT is involved in vascular homeostasis and is important for glucose uptake (Ijuin and Takenawa, 2003). Insulin strongly activates the PI3K/AKT pathway, increasing the level of phosphorylated AKT and phosphorylated p70S6K, which induce GLUT4 translocation and 2-deoxyglucose uptake (Nakashima et al., 2000). In endothelial cells, incubation with HDL can activate the PI3K/AKT pathway increasing PIP3, phosphorylation of AKT and reducing caspase 3 activity and cell death (DeKroon et al., 2006), indicating that activation of AKT can prevent cell death.

Numerous studies have demonstrated that the pharmacological activation of the PI3K/AKT pathway can promote myocardial protection and tissue salvage following periods of injury. Bell and Yellon, 2003, showed that mouse hearts were protected from ischaemia-reperfusion injury in the presence of bradykinin. This protection was attributed to the increase in phosphorylation and activation of AKT and eNOS because the effects were abolished in the presence of the PI3K inhibitor wortmanin (Bell and Yellon, 2003). In contrast, bradykinin failed to protect myocardium from eNOS knockout mice, even though phosphorylation of AKT was enhanced. This indicates that eNOS is required to confer protection downstream of the PI3K/AKT pathway (Bell and Yellon, 2003). There are numerous studies demonstrating that a large number of pharmacological agents which induce cardioprotection against ischaemia-reperfusion injury can activate the PI3K/AKT pathway (Jonassen et al., 2001; Li and Sato, 2001; Maddock et al., 2002; Clarke et al., 2002; Efthymiou et al., 2005).

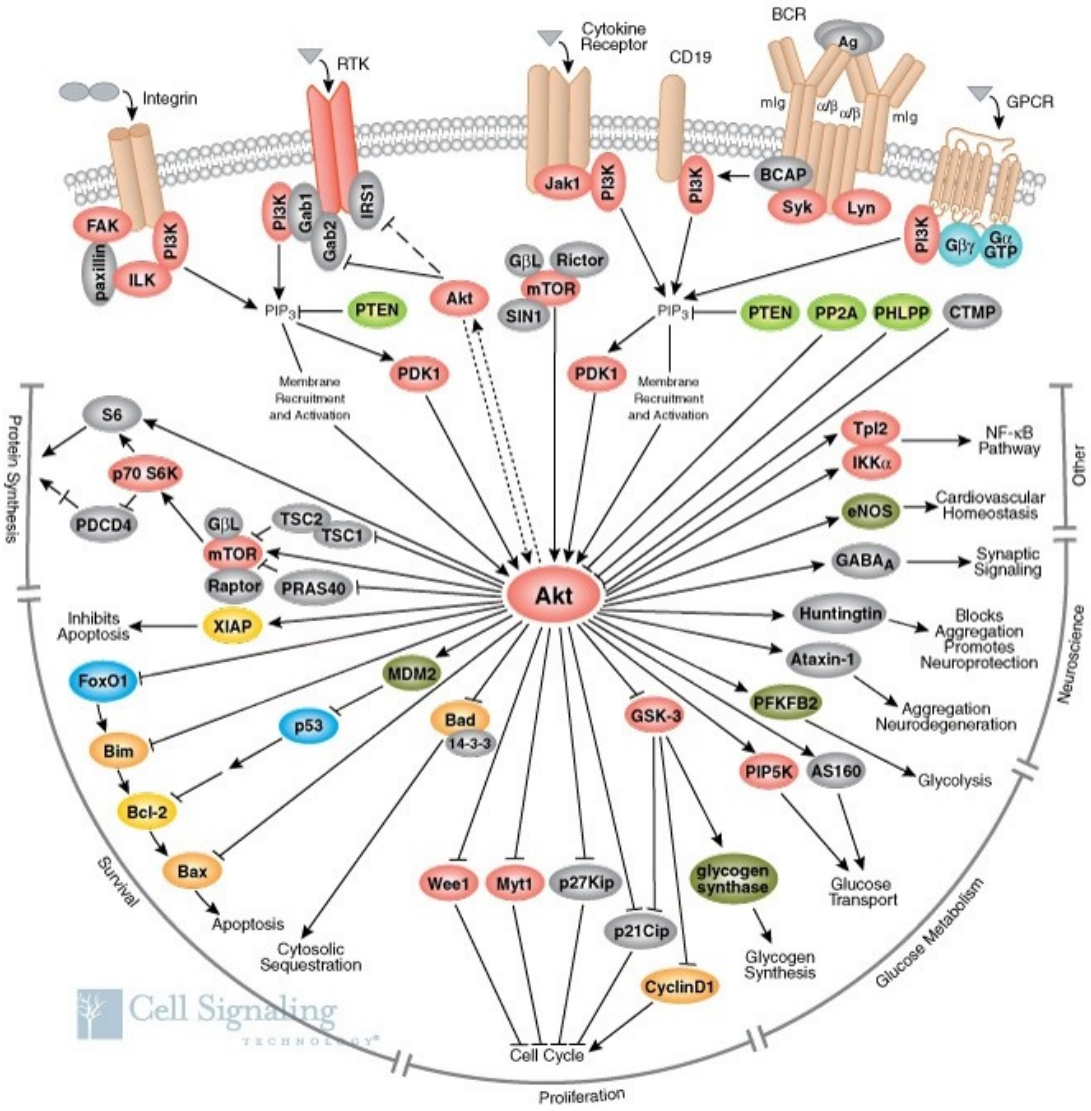

<u>Figure 1.4:</u> Downstream signalling factors of activated AKT.

http://www.cellsignal.com/reference/pathway/Akt_PKB.html on 17.03.2009

In summary, activation of the PI3K/AKT pathway signals for cell survival, as shown in Figure 1.4. This pathway is a central component of the RISK pathway and its enhanced activation can protect the myocardium from lethal ischaemia-reperfusion injury. This pro survival pathway can be activated by pharmacological agents and by ischaemic interventions such as pre and post conditioning, which is described in more detail below (Hausenloy et al., 2004b; Tsang et al., 2004).

1.4.2 Ischaemic preconditioning and cardioprotection

Research investigating ischaemia-reperfusion injury and cell death in the heart reached a turning point when the pioneering research of Murry et al, 1986 was first published. This work has been referenced in over 3000 publications as the first to discover the paradoxical phenomenon of ischaemic preconditioning (IPC). Murry *et al.,* 1986 discovered that four cycles of 5 minutes (min) ischaemia followed by 5 min of reperfusion conferred protection against a subsequent prolonged period of ischaemia; by significantly reducing infarct size in canine hearts (Murry et al., 1986). In 1997 the concept of IPC was validated in humans (Jenkins et al., 1997). Patients undergoing elective coronary artery bypass graft surgery for more than 3 vessels were included in an IPC study. Half the patients were subjected to 2 additional 3 min ischaemic episodes immediately prior to revascularisation of the first artery. 72h later the study was considered a success because these patients had significantly less serum troponin T (Jenkins et al., 1997).

1.4.2.1 Ischaemic preconditioning, cell signalling and cardioprotection

Over 5000 publications have investigated the mechanisms involved in IPC. Despite this, knowledge of the precise mechanisms involved in IPC induced protection remains incomplete. The signalling involved in IPC is complex, and implicates a number of known survival signalling pathways such as PI3K/AKT, ERK1/2, JAK/STAT, p38, and PKC. Classic ischaemic preconditioning, originally described by Murry *et al,* 1996 involves short sub lethal ischaemia-reperfusion periods prior to a lethal ischaemic injury. Paradoxically, this initiates redox signalling sufficient to generate ROS, which can act in combination with other effectors of IPC, to signalling survival (Baines et al., 1997). However, the ROS generated by this stimulus is not damaging unlike that generated by prolonged lethal ischaemia (Baines et al., 1997). The minimal stress of the IPC stimulus can trigger the release of ligands such as

adenosine, opioids and bradykinin (Gross and Gross, 2006; Cohen and Downey, 2008). When these ligands bind to their GCPR, a signal for survival is promoted. For example perfusion of adenosine or an adenosine receptor agonist prior to lethal ischaemia confers a level of protection equal to that of IPC (Liu et al., 1991). Furthermore, in isolated rabbit hearts perfusion with the adenosine receptor blocker, 8-sulfophenyl theophylline (8SPT) can abolish the protection conferred by IPC (Liu et al., 1991).

Down stream of GPCRs are cell signalling pathways such as JAK/STAT, p38, PKC, ERK and PI3K/AKT, activation of which have been associated with pro survival signalling and cardioprotection, as shown in Figure 1.5 (Ferdinandy et al., 2007). IPC has been associated with the activation of cell survival pathways, including the RISK pathway (Tsang et al., 2005; Hausenloy et al., 2005). The activation of the PI3K/AKT pathway is thought to be important for the protection obtained by IPC and increases in phosphorylated AKT levels can be detected in models of cell survival (Mocanu et al., 2002). Both PI3K and ERK pathways have been linked together and it has been shown that activation of these pathways is involved in the IPC protection (Hausenloy et al., 2004b; Tsang et al., 2005).

Enhanced PI3K/AKT in IPC can also activate Mdm2 which binds and sequesters p53 to inhibit p53 activity and cell death (Mocanu and Yellon, 2003). In preconditioned rat hearts the expression of p53 is reduced and the level of p53 bound to Mdm2 is enhanced. Furthermore, perfusion with the p53 inhibitor pifithrin alpha, conferred myocardial protection against ischaemia-reperfusion injury however, the protection was not as powerful as IPC induced protection (Mocanu and Yellon, 2003). This indicates that other signalling molecules are also important in IPC-PI3K/AKT protection. Additional signalling downstream of this is the activation of NOS and PKG, which have been implicated in the prevention of mPTP opening and calcium overload (Bell and Yellon, 2003; Ferdinandy et al., 2007).

Cardioprotection using IPC has been shown to trigger opening of the K_{ATP} channels (Auchampach et al., 1992; Yao et al., 1993; Hausenloy et al., 2002), however, their role in IPC is still debated (Ferdinandy et al., 2007). It has been hypothesised that opening of the K_{ATP} channels is associated with a delay to mPTP opening however, the precise mechanism is unknown (Gross et al., 2008).

Moreover, recently it has been observed that propagation of IPC signals between cells is required to convey protection throughout the heart; and gap junctions are thought to play a role in this signalling (Li et al., 2002). Connexin 43 is the major component of gap junction in the heart; IPC fails to protect the myocardium from connexin 43 knockout mice (Schwanke et al., 2002). Interestingly, connexin 43 has been located at the mitochondria, where it may have an additional role in cell survival (Rodriguez-Sinovas et al., 2006). In summary, this highlights the variety of signalling components and end effectors that have been associated with IPC.

Pharmacological preconditioning and cardioprotective interventions

Preconditioning can be induced pharmacologically without sub lethal ischaemia-reperfusion stimuli. The presence of pharmacological cardioprotective agents administered prior to lethal ischaemia or at the onset of the lethal reperfusion can confer protection against ischaemia-reperfusion injury. Such agents are known as preconditioning and postconditioning mimetics, respectively. The concept of postconditioning is described in more detail below.

As described above, activators of PI3K/AKT such as adenosine, bradykinin, opioids and also insulin (a tyrosine receptor ligand) confer protection against lethal ischaemia-reperfusion injury; mimicking IPC (Baines et al., 1999; Li and Sato, 2001; Maddock et al., 2002; Bell and Yellon, 2003; Gross and Gross, 2006). Other drugs targeting specific proteins can salvage tissue from ischaemia-reperfusion, for example, the presence of diazoxide, a mitochondrial K_{ATP} channel opener. In addition this cardioprotective agent can activate the PKC isoform

PKCε. Diazoxide is reported to instigate PKCε translocation from the cytosol to the mitochondria; where in the presence of hypoxia it can prevent Ca^{2+} accumulation, membrane depolarisation and cytochrome c release (Kim et al., 2006b). Such observations are not recorded when cells containing a dominant negative form of PKCε are incubated in diazoxide (Kim et al., 2006b).

1.4.2.2 Preconditioning and mitochondria

As described in section 1.3 prevention of the mPTP opening confers protection against ischaemia-reperfusion injury. IPC induces a delay in Ca^{2+} induced mPTP opening, mitochondrial rupture and cell death, as demonstrated in rabbit hearts and rat ventricular cardiomyocytes (Argaud et al., 2004; Davidson et al., 2006). Furthermore, a delay in the opening of the mPTP in rabbit hearts has been associated with the protection bestowed by IPC (Argaud et al., 2004; Argaud et al., 2008). In isolated rat hearts, perfusion with atractyloside, an mPTP opener, can abolish myocardial protection conferred with IPC and diazoxide (Hausenloy et al., 2002). Furthermore cyclophilin D (a component of the mPTP) knock out mice, are protected from lethal myocardial ischaemia-reperfusion injury. The mPTP is still able to form in these mice (Baines et al., 2005), however, IPC fails to protect the myocardium which already manifest small levels of infarction (Lim et al., 2007). Collectively, these observations suggest that IPC confers protection by inducing a delay in the mPTP opening and has a role in maintaining cell death and apoptosis. Additionally, autophagy has been shown to be important for IPC induced protection (Yitzhaki et al., 2009; Lemasters et al., 1998). Sub lethal periods of autophagy are proposed to be beneficial in maintaining ATP levels and preserving viable tissue, however, lethal periods of autophagy, as seen in lethal periods of ischaemia, can be detrimental (Sadoshima, 2008; Yitzhaki et al., 2009).

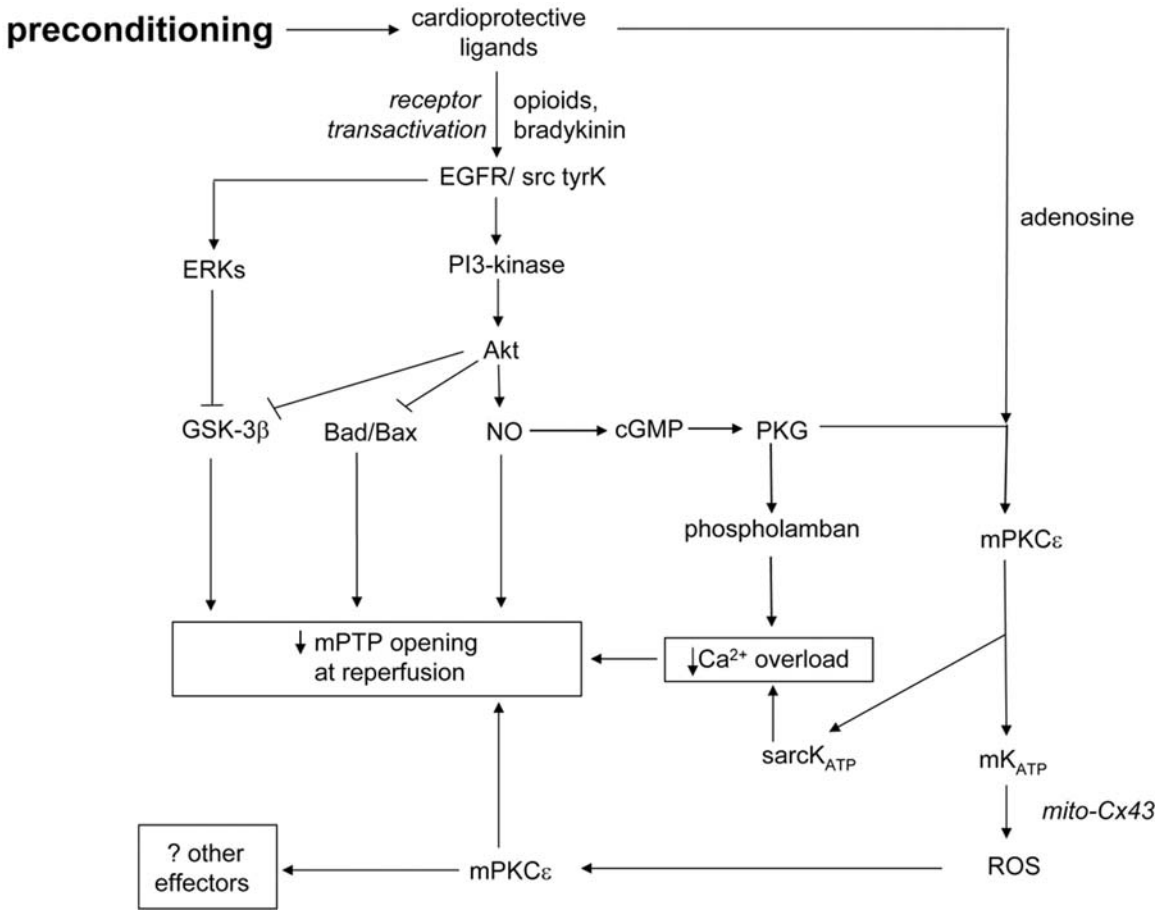

Figure 1.5: Signalling associated with ischaemic and pharmacological preconditioning (bradykinin is an example of a pharmacological preconditioning agent) (Ferdinandy et al., 2007). Including Bcl-2-associated death receptor (BAD), Bcl-2 associated x protein (BAX), cyclic guanosine monophosphate (cGMP), connexin 43 (cx43), epidermal growth factor receptor (EGFR), extracellular related kinase (ERK), glycogen synthase kinase 3 β (GSK3β), mitochondrial adenosine triphosphate sensitive potassium channels (mK_{ATP}), mitochondrial protein kinase C epsilon (mPKCε), mitochondrial permeability transition pore (mPTP), nitric oxide (NO), protein kinase G (PKG), reactive oxygen species (ROS), and sarcolemmal adenosine triphosphate sensitive potassium channels ($SarcK_{ATP}$).

1.4.3 Ischaemic postconditioning and cardioprotection

In 2003, the phenomenon of postconditioning was first defined. Zhao *et al.,* 2003 discovered that 3 cycles of 30 sec periods of ischaemia and reperfusion immediately following an extended period of ischaemia conferred cardioprotection against ischaemia-reperfusion injury (Zhao et al., 2003). This recent discovery has lead to much excitement. Clinically, it appears more practical and achievable to induce protection following an ischaemic episode due to the unpredictability of MI. Unlike IPC which would be limited to scheduled operations, post conditioning may be a more versatile therapy (Cleveland, Jr. et al., 1997; Loukogeorgakis et al., 2006). In 2005, postconditioning was successfully applied to human hearts (Staat et al., 2005). Patients with acute MI, undergoing coronary angioplasty were subjected to control or post conditioning stimuli. Postconditioning was induced by subjecting the myocardium to an additional number of angioplasty balloon inflations and deflations, immediately following the initial rescue angioplasty balloon inflation/deflation. This resulted in a decrease in circulating creatine kinase in the postconditioned patients (Staat et al., 2005). The mechanisms involved in postconditioning are not completely understood. However, pathways similar to those involved in IPC have been implicated, the RISK pathway is one of them (Tsang et al., 2004; Hausenloy et al., 2005; Lim et al., 2007). For example, in rat myocardium subjected to postconditioning an increase in PI3K/AKT, phosphorylated p70S6K and eNOS can be recorded. The protection can be abolished with the PI3K inhibitors LY294002 and wortmanin (Tsang et al., 2004). Furthermore, postconditioning in rabbit myocardium has been attributed to a delay in the opening of the mPTP (Argaud et al., 2004; Argaud et al., 2005b; Lim et al., 2007; Argaud et al., 2008).

In summary, it appears that the activation of the RISK pathway, either prior to ischaemia or at reperfusion, is important in cardioprotection and that the PI3K/AKT pathway is a fundamental member of this salvage pathway. The development of novel therapies that enhance

protection following ischaemia-reperfusion may include mechanisms that up regulate and maintain the PI3K/AKT pathway in an activated state.

1.4.4 Regulators of PI3K/AKT

Unfortunately, unregulated activation of the PI3K/AKT pathway can promote excessive growth and hypertrophy in the myocardium (Liaw et al., 1997; Latronico et al., 2004; Hennessy et al., 2005). To counterbalance this, the cells are equipped with a range of phosphatase enzymes which down regulate this pathway. The main negative regulator of this pathway is phosphatase and tensin homolog deleted on chromosome 10 (PTEN). Additionally phosphatases such as SRC homology 2 containing inositol 5 phosphatase 2 (SHIP2), PH domain leucine rich repeat protein phosphatase (PHLPP) and protein phosphatase 2A (PP2A) can down regulate AKT activity. Figure 1.6 displays some of the cellular mechanisms involved in negatively regulating PI3K and AKT activity.

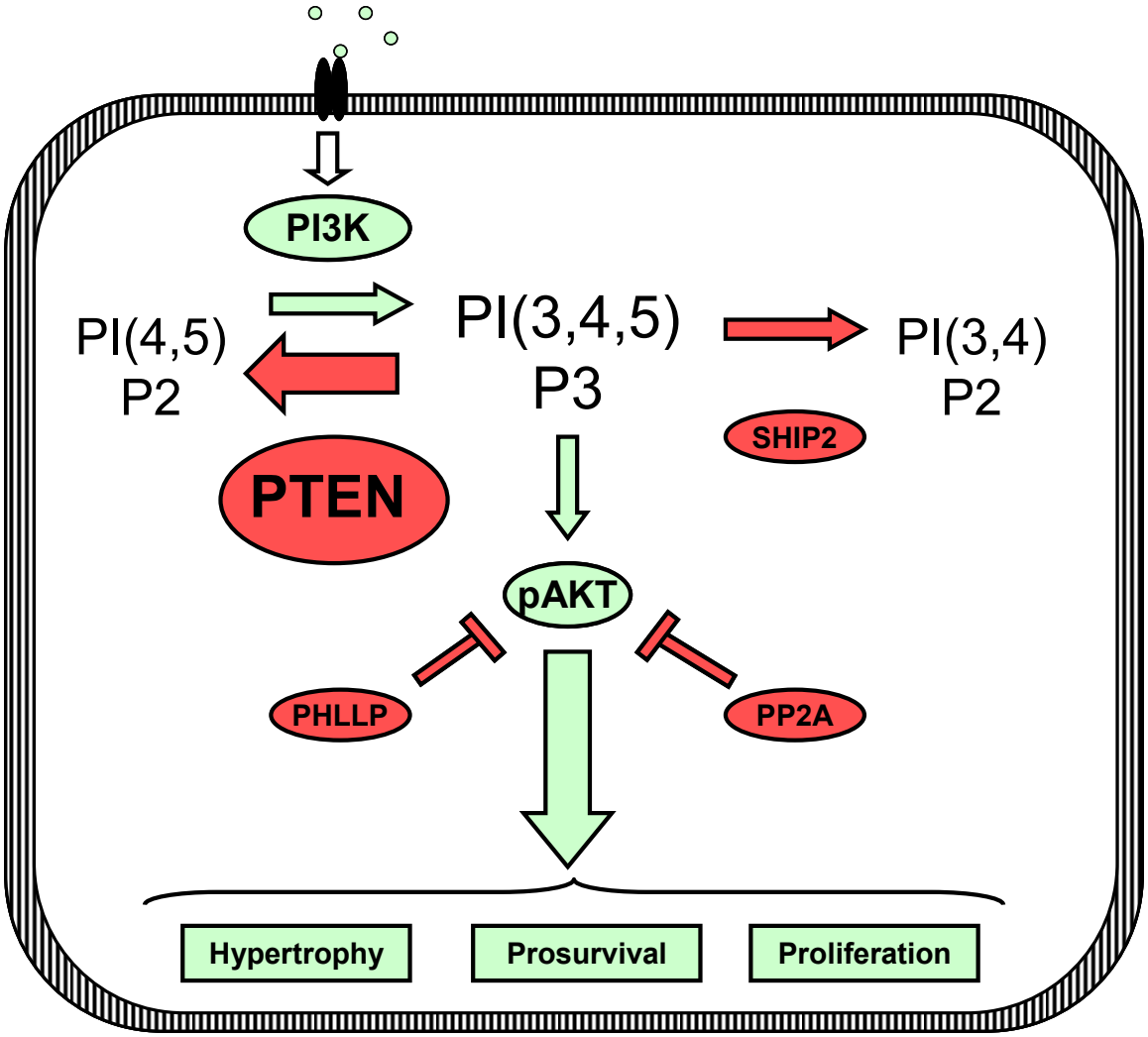

Figure 1.6: Phosphatases that negatively regulate the PI3K/AKT pathway: the main regulator is Phosphatase and tensin homolog deleted on chromosome 10 (PTEN). In addition, SH containing inositol phosphatase 2 (SHIP2), PH domain leucine rich repeat protein phosphatase (PHLPP) and protein phosphatase 2A (PP2A) may also regulate this pathway. Phosphorylated AKT (pAKT) levels are indicative of AKT activity. Including phosphatidylinositol 3 kinase (PI3K), Phosphatidylinositol 2 phosphate (PIP2), and Phosphatidylinositol 3 phosphate (PIP3).

1.5 PTEN

Phosphatase and tensin homolog deleted on chromosome 10 (PTEN) is a lipid and protein phosphatase that was first identified in 1997 (Li et al., 1997a; Steck et al., 1997). It is the main negative regulator of the PI3K/AKT pathway. It dephosphorylates PI(3,4,5)P3 to produce PI(4,5)P2 (Maehama and Dixon, 1998b; Lee et al., 1999). Its mutation is associated with the development of a hereditary disease called Cowden's syndrome (Liaw et al., 1997). PTEN is a tumour suppressor and patients with this disease are predisposed to the development of multiple sporadic haematomas (Liaw et al., 1997). Since this discovery, over 3700 research articles have been published with the aim to understand PTEN signalling and function.

1.5.1 PTEN structure

The PTEN protein, presented in Figure 1.7, consists of 403 amino acids and has a molecular weight of 54kDa (Lee et al., 1999). As the name suggests, PTEN contains a homology sequence to tensin, which is a focal adhesion protein capable of binding to actins and is involved in maintaining normal cell shape (Li et al., 1997a; Steck et al., 1997; Lee et al., 1999; Chen et al., 2000).

N terminus

The N terminus of PTEN contains 179 residues, 6-15 encompass a PIP2 binding motif and work by Maehama *et al.,* 2001 demonstrate that this is important for membrane binding (Maehama et al., 2001). Residues 15-185 contain what is known as the phosphatase catalytic domain which is pivotal for PTEN function (Lee et al., 1999). PTEN contains homology to general protein tyrosine phosphatases (PTP), but in contrast, the active site of PTEN is both wider and deeper than general PTP (Lee et al., 1999; Rosivatz et al., 2006). PTENs large active site facilitates sufficient binding to phosphatidylinositol 3,4,5 phosphate (PIP(3,4,5)P3)

(Myers et al., 1997; Maehama and Dixon, 1998b). Within this catalytic domain exists a cysteine (Cys124) residue fundamental for enzyme activity (Kwon et al., 2004).

C terminus

As described in more detail below, the core structure and activity of PTEN depend on its stability. This stability can be influenced by modifications to the C terminus, also termed the non catalytic domain of PTEN (Gil et al., 2006). The C terminus contains 166 residues, with a phospholipid C2 binding domain located at residues 185-350; and is critical for membrane binding (Lee et al., 1999). Within this region are loops that contain positive charges responsible for membrane binding independent of Ca^{2+}. This is different to PTPs which require Ca^{2+} to promote a positive charge and membrane binding (Lee et al., 1999). In addition, there are nuclear inclusion and exclusion sequences in the C terminal domain, important for PTEN localisation and function, which are described in more detail below (Chung et al., 2005). Residues 350-403 are known as the PTEN stability motif and phosphorylation at this site can result in proteasomal degradation (Torres and Pulido, 2001). Finally, at the tail end of the C terminus resides as post synaptic density protein, drosophila disc large tumour suppressor and zonula occludens-1 protein (PDZ) binding domain. This is also important in PTEN stability and activity and is required to anchor the protein to membranes (Wu et al., 2000b).

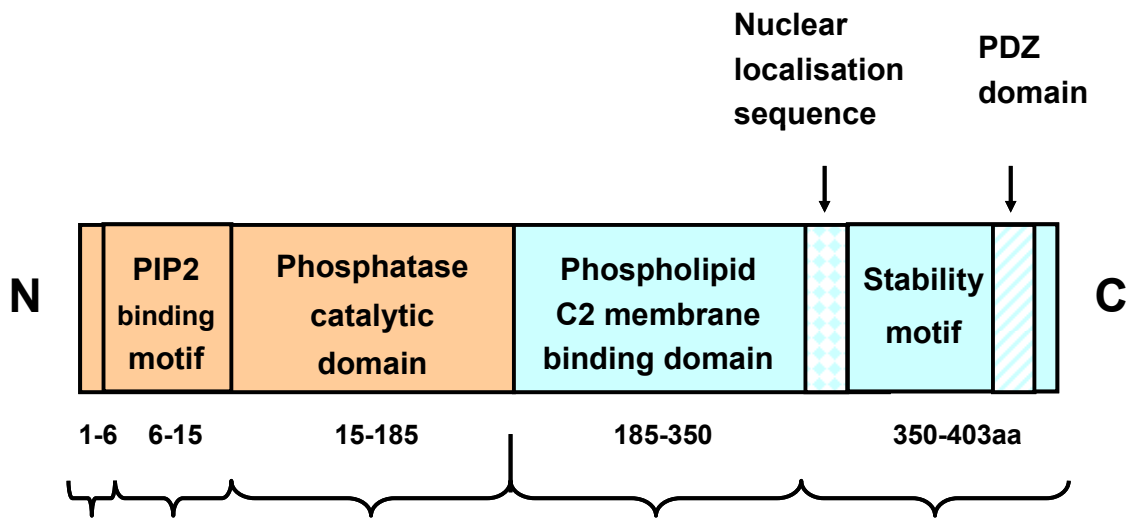

Figure 1.7: Structure of PTEN, a 403 amino acid (aa) protein: displaying the N terminal catalytic domain, non catalytic C terminus, Phosphatidylinositol 2 phosphate (PIP2) and the Post synaptic density protein, Drosophila disc large tumour suppressor and Zonula occludens-1 protein (PDZ) domain (Lee et al., 1999; Wu et al., 2000b; Maehama et al., 2001; Gil et al., 2006).

1.5.2 PTEN function

PTEN is an endogenous lipid and protein phosphatase (Lee et al., 1999). As a protein phosphatase, it is active at tyrosine, serine and threonine residues and as a lipid phosphatase it can dephosphorylate the second messenger phosphatidylinositol 3,4,5 phosphate (PIP(3,4,5)P3) into phosphatidylinositol 4,5, phosphate (PI(4,5)P2) (Myers et al., 1997; Maehama and Dixon, 1998a). PTEN is a 3' PIP phosphatase because it removes phosphate groups specifically from the 3' position of the inositol ring. In addition it can dephosphorylate phosphatidylinositol 3,4, phosphate (PI(3,4)P2), phosphatidylinositol 3,5, phosphate (PI(3,5)P2) and phosphatidylinositol 1,3,4,5 phosphate (PI(1,3,4,5)P4). However, in vivo these are secondary substrates to PI(3,4,5)P3 (Myers et al., 1997; Maehama and Dixon, 1998b; Lee et al., 1999; Campbell et al., 2003; Rosivatz et al., 2006). As shown in

Figure 1.8 PTEN negativity regulates the PI3K/AKT proliferation, growth and survival pathway, which is described further in section 1.5.5.

Additionally, PTEN is reported to have a role in cell migration, embryonic development, cell adhesion and cell cycle (Mise-Omata et al., 2005; Hamada et al., 2005). For example functional PTEN can enhance the number of cells in the G1 cell arrest phase of the cell cycle. Whereas, inhibition of PTEN in human embryonic kidney cells 293 and mouse embryonic cells has been shown to increase AKT activity and decrease the number of cells in the G1 phase (Okumura et al., 2006). Indicating that reduced PTEN can enhance the survival signalling. Functional PTEN can induce apoptosis and inhibition of PTEN can reduce the response to the apoptotic factor TNFα (Gil et al., 2006).

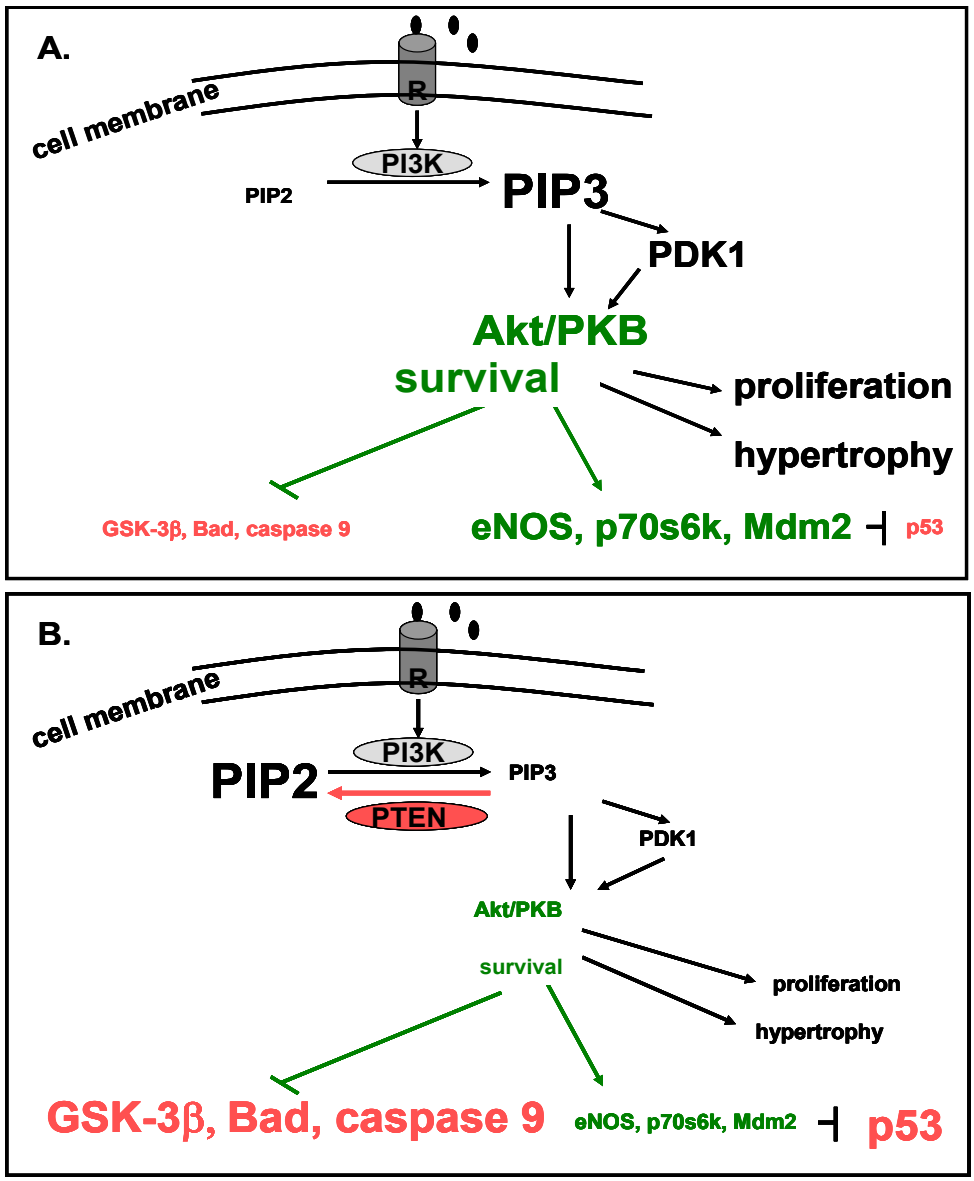

Figure 1.8: Hypothesised role of PTEN: Receptor stimulation of the PI3K/AKT pathway in the absence (A) and presence (B) of PTEN. Including BCL-2-associated death promoter (BAD), endothelial nitric oxide synthase (eNOS), glycogen synthase kinase 3β (GSK3β), murine double minute 2 (Mdm2), 70 kDa ribosomal protein S6 kinase (P70S6K), 3-phosphoinositide dependent protein kinase1 (PDK1), Phosphatidylinositol 3 kinase (PI3K), Phosphatidylinositol 2 phosphate (PIP2), and Phosphatidylinositol 3 phosphate (PIP3). Figure adapted from (Mocanu and Yellon, 2007).

1.5.3 PTEN localisation

PTEN is constitutively expressed and is located predominately in the cytosol. When active it can be found at the lipid membrane (Lee et al., 1999). In addition PTEN has been observed in the endoplasmic reticulum and the nucleus (Gil et al., 2006; Lindsay et al., 2006). The localisation of PTEN within compartments of the cell is important to its function.

1.5.3.1 PTEN localisation in the cytosol

PTEN is implicated in cell motility, for which the cellular location is important. In leukocytes and HEK cells, chemoattractant factors can activate and control PTEN activity and localisation (Li et al., 2005). In resting leukocytes PTEN has been located in the cytoplasm. In contrast, in migrating cells PTEN co-localises with RhoA, towards the posterior of the cell at the plasma membrane. This facilitates an increase in PTEN activity whereas in the lateral and leading edge of the migrating cell PTEN was not present and the levels of PIP(3,4,5) were free to promote cell motility. Moreover, this group demonstrated that PTEN can be phosphorylated in vitro by Rho associated kinase 1 (ROCK1) the downstream effector of RhoA, and this contributes towards increasing PTEN activity (Li et al., 2005).

1.5.3.2 PTEN localisation in the nucleus

PTEN appears to have a role in the nucleus and this may involve regulating cell cycle and apoptosis. A nuclear pool of PI(3,4,5)P3 and PTEN has been identified, and a nuclear localisation sequence in the C terminus of PTEN has been discovered (Gimm et al., 2000; Chung et al., 2005; Lindsay et al., 2006). Lindsay Y, *et al*., 2006 demonstrate that PTEN is capable of dephosphorylating PI(3,4,5)P3 in the cytosolic fraction of the cell however. a proportion of PTEN in the endoplasmic reticulum and nucleus was unable to dephosphorylate

PI(3,4,5)P3 (Lindsay et al., 2006). Therefore PTEN may have a role in the nucleus independent of the PI3K/AKT pathway.

In contrast, other groups have detected a nuclear pool of PTEN dependent on the expression of a PTEN nuclear localisation domain in the N terminus of the protein. In addition it has been suggested that a PTEN nuclear exclusion motif may be involved in its localisation. Normal expression of this motif appears to maintain cytosolic PTEN and mutations in this area have been associated with accumulation in the nucleus. Apoptotic stimuli such as doxorubicin or TNFα can induce PTEN accumulation in the nucleus (Gil et al., 2006). The authors of this work demonstrated that deletion of the PDZ membrane binding domain abolished the nuclear accumulation and PTEN protein remained in the cytoplasm (Gil et al., 2006). This may indicate that PTEN translocation to the nucleus may require membrane binding.

Furthermore, monoubiquitination of PTEN can also induce its localisation in the nucleus. PTEN can be ubiquitinated by the E3 ligase NEDD4-1 which is involved in its degradation (Wang et al., 2007b). The monoubiquitinated PTEN is reported to be stable and capable of maintaining its tumour suppressor functions. However, further ubiquitination of PTEN results in re-accumulation in the cytosol where the polyubiquitinated PTEN is degraded (Trotman et al., 2007).

An additional role for PTEN in the nucleus has been proposed, and this is to promote nuclear and chromosomal stability. Nuclear PTEN has been co-localised with the centromeres. Disruption of PTEN or mutations in the C terminal region can induce double stranded breaks of centromere and DNA. Therefore, the authors of this work suggested that nuclear PTEN plays a role in chromosomal integrity and DNA repair (Shen et al., 2007).

Nuclear PTEN level can be increased by depletion of ATP, while the restoration of ATP can reverse nuclear localisation of PTEN (Lobo et al., 2008). The complete mechanisms and consequence of PTEN nuclear accumulation remains unknown, however, it is evident that PTEN localisation can influence its role in the cell. The cellular localisation of PTEN is highlighted in Figure 1.9. To summarise, PTEN is abundant in the cytosol, however, it appears active when located at the membrane, and conditionally, in the nucleus.

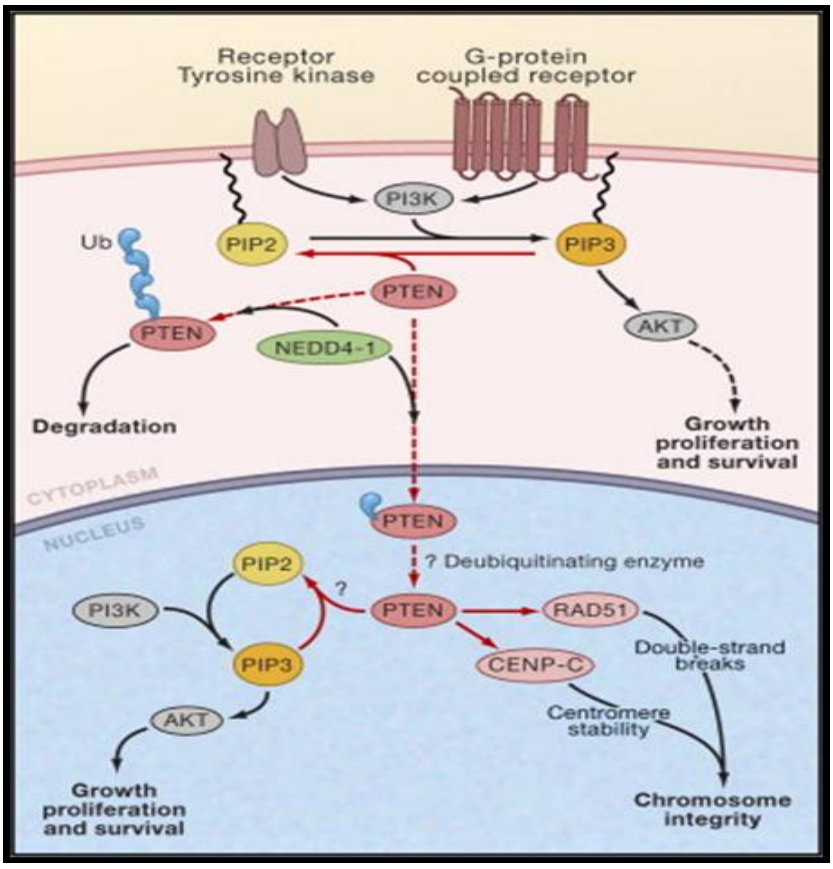

Figure 1.9: The role of PTEN in the nucleus and cytoplasm (Baker, 2007). Including centromere protein C (CENP-C), neural precurser cell expressed developmental down regulated (NEDD4-1), Phosphatidylinositol 3 kinase (PI3K), Phosphatidylinositol 2 phosphate (PIP2), and Phosphatidylinositol 3 phosphate (PIP3), phosphatase and tensin homolog deleted on chromosome 10 (PTEN) and ubiquitination (Ub) signalling.

1.5.4 PTEN regulation

Reversible inhibition of PTEN may have a major impact in the treatment for apoptotic related diseases, because inhibition of PTEN can enhance the signalling of the PIP3/PI3K/AKT survival pathway (Schmid et al., 2004; Wu et al., 2006). The potential methods for manipulating PTEN level and function are described below.

1.5.4.1 Transcriptional regulation of PTEN

As described below in more detail and displayed in Figure 1.10 changes in the transcription and translation of PTEN can regulate its expression.

1.5.4.1.1 Positive transcriptional regulators

Factors that positively regulate the transcription of PTEN can enhance PTEN protein expression such factors include agents such as dimethyl sulfoxide (DMSO) and cellular proteins such as peroxisome proliferators-activated receptors (PPARγ) and p53. In HL60 cells, the addition of 0.5 – 1.5% DMSO increased PTEN expression, in a dose dependent manner (Lee et al., 2005). Additionally, there is a proposed PPARγ binding site on the PTEN promoter. In the MCF-7 breast cancer cell line, rosiglitazone (a PPAR activator) and lovastatin (a HMG CoA reductase inhibitor) activate PPARγ and increase PTEN mRNA expression, in a time and dose dependent manner. This increase was associated with reduced phosphorylation of AKT and an increased number of cells in G1 cell cycle arrest (Teresi et al., 2006).

Mensah, *et al.,* 2005 were the first to demonstrate changes in PTEN whilst studying ischaemia-reperfusion injury. In a rat model of myocardial ischaemia-reperfusion injury acute atorvastatin treatment (1 and 3days) can induce protection. However, this protection was

abolished with chronic atorvastatin treatment (1 and 3 weeks) (Mensah et al., 2005). The authors of this work attributed the loss of protection in chronic atorvastatin treatment to an increase in PTEN protein expression. Such stimulation may be due to the up regulation of PPARγ however, the involvement of such mechanisms were not investigated in this study.

Furthermore, there is a p53 dependent binding element in the PTEN promoter region and p53 can cause the inducible activation of PTEN (Stambolic et al., 2001). PTEN regulation is sensitive to changes in p53 levels. In fibroblasts the presence of pifithrin alpha (PFTα), a p53 inhibitor, induces a decrease in the PTEN protein levels (Wang et al., 2005). Collectively, these studies are important and they imply that PTEN can be regulated acutely and manipulated pharmacologically.

1.5.4.1.2 Negative transcriptional regulation

Negative transcriptional regulation of PTEN results in a reduction of PTEN protein expression and/or function. The micro RNA 21 (MiRNA-21) has been linked to the degradation of PTEN. MiRNA's are endogenous oligonucleotides that are responsible for silencing protein expression, targeting specific mRNA sequences for degradation (Haghikia and Hilfiker-Kleiner, 2009). Interestingly, fibroblasts extracted from hearts subjected to ischaemia-reperfusion have enhanced distribution of MiRNA-21, which are thought to be responsible for reduction of PTEN protein level (Roy et al., 2009).

Mutations in the genetic coding of PTEN can also reduce expression and function. For example, PI(4,5)P2 can bind and activate PTEN. However, mutations in the N terminus which codes for PI(4,5)P2 binding site can disrupt PTEN activity (Campbell et al., 2003). Similarly, PTEN activity is highly influenced by membrane localisation. Over expression of PTEN can reduce insulin stimulated GLUT4 translocation. However, mutations in regions coding for

PTEN membrane binding can abolish this effect (Mosser et al., 2001). PTEN mutations have been associated with diverse human pathology; the physiological relevance of PTEN mutations and inhibition are described below, in section 1.6.

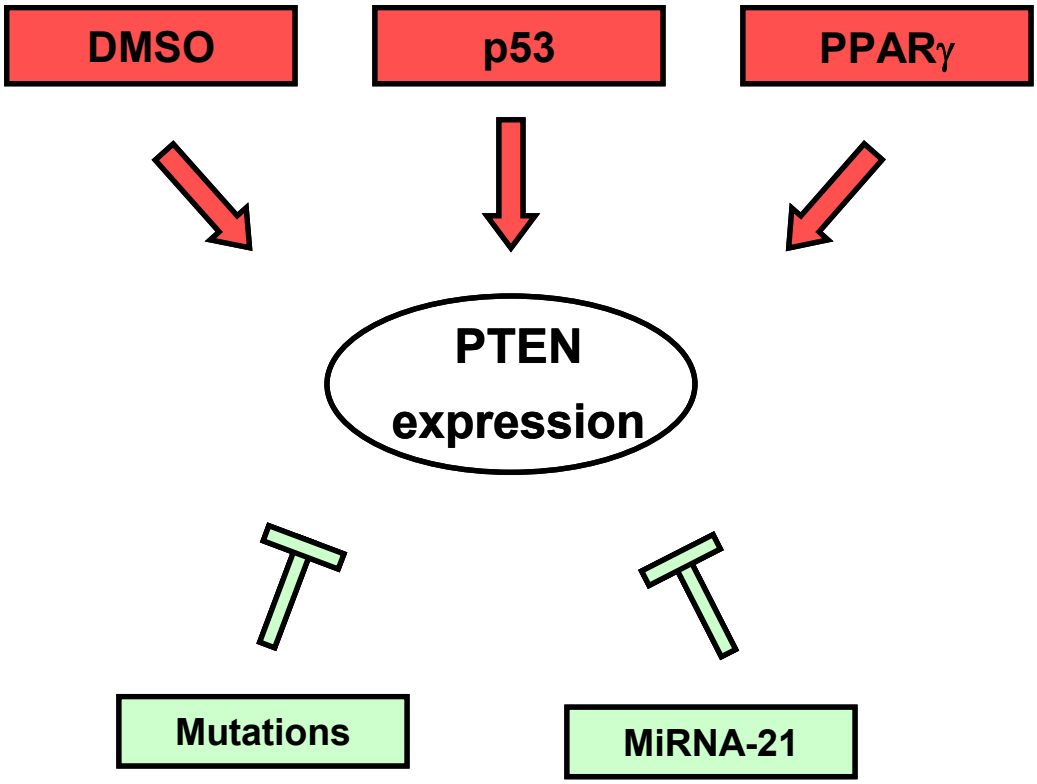

Figure 1.10: Factors that regulate the transcriptional activity of phosphatase and tensin homolog deleted on chromosome 10 (PTEN) and total PTEN expression. DMSO = dimethyl sulfoxide, PPAR = peroxisome proliferators-activated receptors, MiRNA-21 = Micro ribonucleic acid-21.

1.5.4.2 Post translational modifications of PTEN

The activity of PTEN can be altered by factors that modify translated PTEN protein. Factors effecting post translation modifications of PTEN are displayed in Figure 1.11 and described below.

1.5.4.2.1 Positive post translational modifications of PTEN

Factors that induce post translational regulators of PTEN induce modifications that enhance PTEN activity. As displayed in Figure 1.11 modifications increasing activity can include PTEN membrane binding and PTEN-ROCK1 interactions (Wu et al., 2000b; Li et al., 2005).

PTEN membrane binding

Wu Y, et al., 2000 have demonstrated that PTEN can bind to 'membrane-associated guanylate kinase with inverted orientation' (MAGI3). This interaction has been shown to facilitate PTEN binding and localisation at the membrane. It is thought that MAGI3, which contains a PDZ domain, binds to the PDZ binding domain in the C terminus of PTEN, acting as a scaffold for PTEN function. The author of this research demonstrated that PTEN-MAGI3-membrane binding is associated with a decrease in AKT activity and enhanced PTEN activity (Wu et al., 2000b). Mutations in the PDZ domain of PTEN prevents this effect, indicating that membrane binding is important for PTEN function (Wu et al., 2000b).

ROCK enhanced expression.

The kinase, ROCK1, can phosphorylate PTEN at Ser229-Thr223 and Thr319-Thr321, which increases PTEN activity. In leukocytes, RhoA and ROCK1 have been shown to up regulate PTEN activity. ROCK1 is involved in enhancing apoptosis and plays a role in ischaemia-reperfusion injury (Chang et al., 2006; Hamid et al., 2007). In patients with heart failure an increased expression of active ROCK1 has been observed in myocardial tissue. Similarly, in a mouse model of cardiomyopathy enhanced ROCK1 has been observed in parallel to an increase in PTEN activity and a decrease in AKT activity (Chang et al., 2006). Furthermore, ROCK1 has been attributed to the phosphorylation and activation of PTEN in migrating leuokocytes (Li et al., 2005).

Cytomegalovirus

Viral infections have also been shown to modify PTEN activity. For example incubation of human aortic endothelial cells with the human cytomegalovirus has been associated with activation of PTEN and endothelial dysfunction. This is indicated by a decreased activity of AKT and eNOS following insulin stimulation. Furthermore, human cytomegalovirus has been shown to increase PTEN mRNA and total protein levels. In addition PTEN dephosphorylation at Ser380 and Thr382/383 has been observed, and these effects were dependent on p38 MAPK. Therefore this study indicates that PTEN activity can be enhanced by dephosphorylation of PTEN at Ser380,Thr382/383 (Shen et al., 2006).

Additional regulators effecting the activity of PTEN

Recently, it has been communicated that components of the NOTCH signalling pathway can increase the activity and protein expression of PTEN. For example, transcription factor hairy and enhancer of split 1 (HES-1) and the promoter CBF-1 (also known as recombination signal binding protein for immunoglobulin kappa J region (RBBJ)) can enhance PTEN activity. (Palomero et al., 2008; Whelan et al., 2007; Chappell et al., 2005). An additional factor that positively influences PTEN is s-nitrosylation (Zhang et al., 2007; Pei et al., 2009). However, the precise effect of s-nitrosylation appears complex, as it is noted to cause either PTEN activation or PTEN inhibition. These opposite effects may be dependent on the order and position of the nitrosylation which may contribute to either activity or inactivity. See figure 6.24.

1.5.4.2.2 Negative post translational modifications of PTEN

Negative post translational regulators of PTEN induce changes that reduce PTEN activity. Such modifications include phosphorylation, oxidation, acetylation and ubiquitination

(protesomal degradation), as displayed in Figure 1.11 (Torres and Pulido, 2001; Wu et al., 2003; Meuillet et al., 2004).

Phosphorylation and endogenous inhibitors of PTEN

Initial experiments investigating PTEN phosphorylation indicate that Ser380, Thr382 and Thr383 phosphorylation reduces PTEN activity. In these original studies, active PTEN was readily degraded and unstable (Torres and Pulido, 2001; Valiente et al., 2005). Subsequently, a flourish of experiments investigating the phosphorylation and activity of PTEN have been published.

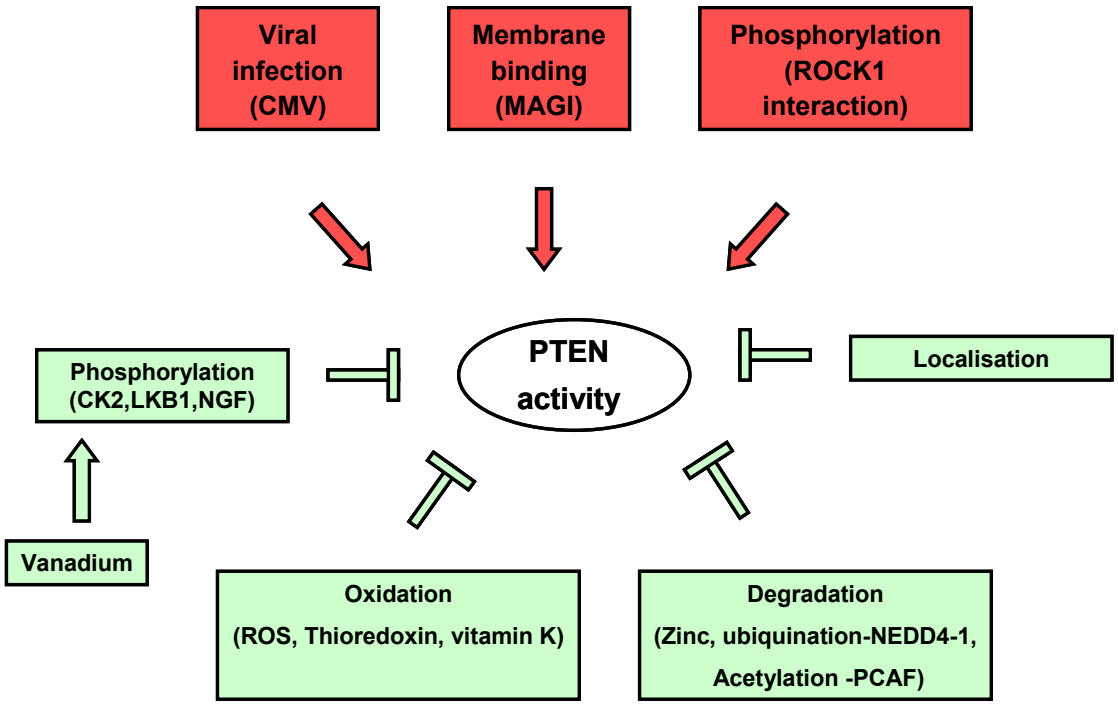

Figure 1.11: Post translational modifications that effect PTEN function. Casein kinase II (CK2), Cytomegalovirus (CMV), membrane-associated guanylate kinase with inverted orientation (MAGI), neural precursor cell expressed developmental down regulated (NEDD4-1), nerve growth factor (NGF), p300/CBP associated factor (PCAF), phosphatase and tensin homolog deleted on chromosome 10 (PTEN), and reactive oxygen species (ROS).

A number of endogenous intracellular factors and enzymes such as casein kinase II (CK2), caspase 3, nerve growth factor (NGF), the tumour suppressor LKB1 and the mitochondrial protein DJ-1 have been shown to regulate PTEN: some of which are described below.

Casein kinase II

Casein kinase II (CK2) can phosphorylate the C terminus of PTEN, decreasing PTEN stability and increasing its protesomal degradation (Torres and Pulido, 2001). Similarly, in pancreatic

and hypothalamic cells stimulated with the cardioprotective adipocytokine leptin, the level of CK2 activity is increased and is associated with reduced PTEN function (Ning et al., 2006; Smith et al., 2006). This finding was attributed to the activation of CK2 by leptin which, in turn phosphorylated and destabilised PTEN (Ning et al., 2006).

Furthermore, in HEK293 cells casein kinase I (CKI), CK2 and GSK3B were shown to phosphorylate the C terminus of PTEN in the presence of insulin like growth factor 1 (IGF1) (Al Khouri et al., 2005). The authors of this work demonstrate that CKI and CK2 can phosphorylate PTEN at Ser385 and Ser370, whereas GSK3β only phosphorylated Ser362 and Thr366 (Al Khouri et al., 2005). Moreover a synergistic effect between these enzymes was demonstrated. The physiological relevance of these phosphorylation events were explained as a decrease in PTEN activity, measured by an increase in phosphorylated AKT at Ser473 and consequentially a decrease in GSK3β phosphorylation at Ser21/9. These phenomena appear to be dependent on Thr366 phosphorylation, as IGFα, in cells null for Thr366 phosphorylation, was unable to stimulate the increase in AKT phosphorylation (Al Khouri et al., 2005).

Additionally, in gliblastoma cells, phosphorylation of PTEN at Thr366 has been associated with protein destabilisation. Mutations in this region prevented the phosphorylation of Thr366 and enhanced PTEN stability, the phosphatase activity remained unaffected (Maccario et al., 2007).

Caspase 3

The apoptotic factor, caspase 3 can negatively regulate PTEN. In HEK293 cells the apoptotic ligand, TNFα causes caspase 3 binding to PTEN which facilitates caspases 3 cleavage at the C terminal domain of PTEN. This cleavage can abolish PTEN binding to MAGI, which is important for PTEN activity (Wu et al., 2000a; Wu et al., 2000b; Torres et al., 2003). Torres J,

et al., 2003 indicate that the cleaved PTEN is non functional, unstable and is rapidly degraded (Torres et al., 2003). Conversely, PTEN phosphorylation by CK2 protects PTEN from caspase 3 cleavage (Torres et al., 2003). Nonetheless, as described above CK2 phosphorylation of PTEN promotes the occurrence of ubiqitination and proteosomal degradation of PTEN (Torres and Pulido, 2001).

Nerve growth factor

Nerve growth factor (NGF) reduces PTEN level in hippocampal neurons. This PTEN inhibition was attributed to the activation of CK2 (by NGF) which in turn was shown to phosphorylate PTEN at Ser380. This phosphorylation was associated with a decrease in PTEN activity as indicated by an increase in phosphorylation of AKT (at Ser473 phosphorylation site), phosphorylation of GSK3β and axon elongation (Arevalo and Rodriguez-Tebar, 2006).

LKB1

LKB1 is a protein kinase, up regulated in many cancers, which can regulate PTEN activity (Shaw et al., 2005). A study looking at the activity of LKB1 showed that this kinase binds to PTEN. In addition LKB1, normally located in the nucleus, translocates to the cytoplasm where it interacts with PTEN. LKB1 can phosphorylate PTEN at the C terminal, between phosphorylation sites Ser360-Ser385, leading to the onset of tumours (Mehenni et al., 2005).

Mitochondrial proteins

A mitochondrial protein called DJ-1 can negatively regulate PTEN. Mutations of this protein are associated with the early onset of Parkinson's disease. It is thought to act as a sensor of oxidative stress. Reduced expression of DJ in NIH-3T3 cells results in decreased AKT phosphorylation. Furthermore the over expression of DJ-1 can enhance AKT activity and cell viability (Kim et al., 2005).The precise mechanism of this negative regulation is unknown.

Oxidation and inhibition of PTEN

Oxidation of PTEN has been associated with loss of activity. A cysteine (Cys124) residue within the phosphatase catalytic domain is fundamental for PTEN activity. Cys124 can be oxidised by H_2O_2 forming a disulfide bridge with Cys71 and rendering the enzyme inactive however, this effect is reversible (Lee et al., 2002).

In a redox engineered cell line expressing increased levels of mitochondrial manganese superoxide dismutase, enhanced levels of H_2O_2 was produced, which increased PTEN oxidation. Consequentially, it was demonstrated that PTEN activity was decreased and AKT activity increased. This effect was abolished when PTEN was over expressed (Connor et al., 2005). Moreover, peptide growth factors such as platelet derived growth factor (PDGF) or EGF can inhibit PTEN by producing H_2O_2 which reversibly oxidises PTEN at Cys124. The over expression of nicotinamide adenine dinucleotide phosphate (NADPH) oxidase 1 amplified PIP3 levels and further enhanced the increase in AKT activity (Kwon et al., 2004). In addition, insulin stimulation in neuroblastoma cells was shown to induce ROS formation which inhibited PTEN activity. The PI3K activity in these cells remained the same however, the level of phosphorylated AKT was enhanced in the presence of insulin. The authors of this work attributed this effect to the production of ROS and the inhibition of PTEN, because no increase in phosphorylated AKT using insulin was observed in cells that lacked the ability to generate ROS (Seo et al., 2005).

Redox reduced PTEN has been associated with normal regulation of PTEN function (Lee et al., 2002). Thioredoxin-1, a redox protein and electron donor, can affect PTEN activity. Peptide growth factors can stimulate H_2O_2 production and subsequently, oxidise PTEN. Mutagenesis studies reveal that thioredoxin 1 can form a disulfide bond at the Cys32 in the active site of PTEN, Moreover, thioredoxin 1 can bind to PTEN at the C2 domain where it can abolish membrane binding and prevent lipid phosphatase activity (Meuillet et al., 2004).

Interestingly, peroxidase peroxiedoxin (Prdx1) can bind to PTEN and protect it from becoming oxidised and inhibited, thereby maintaining PTEN stability (Cao et al., 2009).

The synthetic analogue of vitamin K, menadione (2-methyl-1,4-nahthoquinone), can inhibit protein tyrosine phosphatases and has been reported to affect PTEN. Menadione can induce oxidative stress. In CHO cells it reduces PTEN phosphatase activity and increases phosphorylation of AKT at Ser473 and Thr308 (Yoshikawa et al., 2007).

Acetylation and inhibition of PTEN

Lysine residues (Lys125 and Lys128) located in the PTEN phosphatase catalytic domain can be acetylated and in turn, can affect PTEN function. The presence of EGF in HEK293 cells that over express the histone acetyltransferase, (p300/CBP associated factor (PCAF)) can induce PCAF-PTEN binding and PTEN acetylation (Okumura et al., 2006). PTEN acetylation has been associated with a reduction in lipid phosphatase activity, an increase in AKT phosphorylation (Ser473) and a reduction in the number of cells in G1 phase of cell cycle (Okumura et al., 2006).

Ubiquitination and inhibition of PTEN

PTEN can be ubiquitinated by the E3 ligase NEDD4-1. This ubiquitination is involved in PTEN degradation and causes tumourgenosis. Deletion of NEDD4-1 increases PTEN protein level and activity (Wang et al., 2007b). Monoubiquitination of PTEN can induce localisation in the nucleus where it retains activity as a stable tumour suppressor (Wang et al., 2007b). It has been suggested that mutations in a lysine residue prevent monoubiquitination and nuclear localisation. In patients suffering with Cowden syndrome mutations in a PTEN lysine residue have been observed. These patients have catalytically active PTEN, whilst expressing reduced nuclear PTEN content, although they still develop tumours (Trotman et al., 2007). These data underline that nuclear PTEN is important for function and that monoubiquitination

of PTEN is required for this activity. In contrast polyubiquitinated PTEN induces PTEN instability and degradation (Baker, 2007; Trotman et al., 2007). Recently, it has been shown that in mouse fibroblasts XIAP, an antiapoptotic factor, can associate with PTEN. This association was shown to cause polyubiquitination, nuclear exclusion, and protein reduction of PTEN, mirrored by an increase in AKT activity (Van Themsche et al., 2009). The authors of this work propose that XIAP is an E3 ubiquitin ligase for PTEN, which acts to inhibit and reduce PTEN activity.

Chemical inhibitors of PTEN

Vanadium compounds, which are tyrosine phosphatase inhibitors, are reported to affect PTEN phosphatase activity (Schmid et al., 2004). Incubation with bisperoxo(5-hyroxypyridine-2carboxy) oxovanadate (bpV(HOpic), in NIH3T3 cells, can increase AKT phosphorylation. This compound was demonstrated to have 100 fold specificity for PTEN inhibition compared to general tyrosine phosphatase inhibition (Schmid et al., 2004). Additionally, in Sprague-Dawley rats i.p injections of orthovanadate conferred protection in the brain following ischaemia-reperfusion injury in addition to down regulating PTEN activity. PTEN and AKT phosphorylation were increased and the activity of ASK1, a pro apoptotic substrate of AKT, was decreased (Wu et al., 2006). However, the mechanism by which PTEN phosphorylation is induced by the vanadium compounds is unclear.

Zinc can also inhibit PTEN, by signalling for its inactivation and protesomal degradation. In human airway epithelial cells, zinc can decrease PTEN activity in a dose and time dependent manner. This effect is abolished in the presence of a proteasome inhibitor. The authors of this work assessed the decrease in PTEN phosphatase activity by measuring changes in phosphorylated AKT levels (Wu et al., 2003).

Additional factors that appear to inhibit PTEN activity, include the activation of the c-Jun N terminal kinases (JNK) and NFκB (Zhang et al., 2007; Kim et al., 2004). In summary, PTEN function can be modified by altering synthesis, catabolism or activity. Processes by which PTEN function can be altered include protein localisation, membrane binding, phosphorylation, oxidation, acetylation, nitrosylation and ubiquitination (protesomal degradation) (Torres and Pulido, 2001; Wu et al., 2003; Meuillet et al., 2004). The following sections highlight why a reversible inhibition of PTEN may be clinically desirable when targeting ischaemia-reperfusion injury.

1.5.5 PTEN/PI3K/AKT pathway and cell survival

PTEN knockout models and conditional tissue specific PTEN deletion models have been produced. The published data relating to these models is described over the next sections. Figure 1.9 represents the role of PTEN when the PI3K/AKT pathway is stimulated. PTEN is thoroughly researched as a tumour suppressor; mutations have been associated with proliferative diseases such as Cowden syndrome. In this disease patients suffer multiple sporadic haematomas (Pilarski and Eng, 2004). Mice with PTEN deletions (PTEN haploinsufficient mice heterozygous for $PTEN^{+/-}$) exhibit multiple organ neoplasms, enhanced cell proliferation and defective apoptotic abilities. Homozygous littermates ($PTEN^{-/-}$) do not survive gestation further than embryonic day E6.5 (Podsypanina et al., 1999).

PTEN is negatively involved in growth and development. For example PTEN can regulate axon cell growth. In hippocampal neurons the presence of nerve growth factor (NGF) can induce cell elongation and growth. The authors of this work attributed this to the activation of CK2, which phosphorylates PTEN at Ser380 and decreases PTEN activity; as indicated by increased phosphorylation of AKT and GSK3β (Arevalo and Rodriguez-Tebar, 2006). Moreover the authors demonstrate that the presence of 0.2μM dipotassium bisperoxo

(pyridine-2-carboxyl) oxovanadate (bpV(pic)), a PTEN inhibitor, can increase phosphorylation of AKT and GSK3β to promote axon elongation and growth (Arevalo and Rodriguez-Tebar, 2006).

PTEN can delay proliferation and wound repair. In lung epithelial cells PTEN inhibitors bpV(pic) and dipotassium bisperoxo (1,10-phenanthroline) oxovanadate, (bpV(phen)), increased phosphorylation of AKT and promoted time to wound healing (Lai et al., 2007). Similarly PTEN siRNA and dominant negative PTEN transfection, used to limit PTEN activity, also decreased the time to wound healing (Lai et al., 2007). Interestingly, PTEN inhibition can be used as a tool to study survival, proliferation and growth. The pharmaceutical company, Semafore Pharmaceuticals are currently investigating PTEN inhibition as a way of targeting the side effects of chemo therapy (Hennessy et al., 2005).

However, recently PTEN has been associated with pro survival. For example the localisation of nuclear PTEN has been associated with chromosomal stability and PTEN inhibition has been associated with double stranded DNA breaks (Puc and Parsons, 2005; Shen et al., 2007). Similarly, PTEN has also been associated with mitochondrial pro survival proteins such the Ser/Thr kinase PTEN induced kinase 1 (PINK1). This kinase is highly expressed in heart, skeletal muscle and testis (Unoki and Nakamura, 2001).

1.5.5.1 PTEN Induced Kinase 1 (PINK1)

PINK1 was originally discovered in PTEN deficient cancer cells as a gene transcriptionally activated by the re-expression of PTEN protein (Unoki and Nakamura, 2001). Therefore, PINK1 was hypothesised to be a potential tumour suppressor linked to the PTEN pathway. However, when the authors of this work expressed PINK1 in tumour cells surprisingly, tumour cell growth was not inhibited (Unoki and Nakamura, 2001).

Disruption of PINK1 has been associated with degenerative diseases and cell death. Mutations in this kinase have been discovered in patients suffering with autosomal recessive, early onset Parkinson's disease (Valente et al., 2004; Wang et al., 2007a). Silencing PINK1 using siRNA induces apoptosis in dopaminergic cells and incubation with pesticide rotenone, a complex I inhibitor, further increased cell death (Deng et al., 2005).

PINK1 is reported to have a molecular weight of 65Kda and to contain a mitochondrial targeting motif (Wang et al., 2007a). It is mainly observed in the mitochondria where it is rapidly processed, however a proportion of total PINK1 is also found in the cytosol (Valente et al., 2004; Wang et al., 2007a; Lin and Kang, 2008a). PINK1 has been associated with protection against neuronal oxidative stress (Deng et al., 2005; Pridgeon et al., 2007) and apoptosis (Valente et al., 2004). In HEK293 cells the effects of inducing apoptosis, using the proteosome inhibitor MG132, was prevented by over expressing PINK1. In these cells the release of cytochrome c and caspase 3 cleavage were minimal. (Wang et al., 2007a). Additionally, these cells were protected from atractyloside-induced mPTP opening and cell death. These phenomena were abolished in cells transfected with mitochondrial resistant PINK1. Therefore, the authors of this work suggested that the protective effects of PINK1 were dependent on PINK1 localisation in the mitochondria (Wang et al., 2007a).

Additionally, PINK1 has a role in the survival of neurons: reduced levels can lead to enhanced oxidative stress and changes in mitochondria morphology which can decrease neuronal viability (Wood-Kaczmar et al., 2008). Collectively, as shown in Figure 1.12 it appears that PINK1 is required for mitochondrial function and morphology, in addition to cellular survival post oxidative stress.

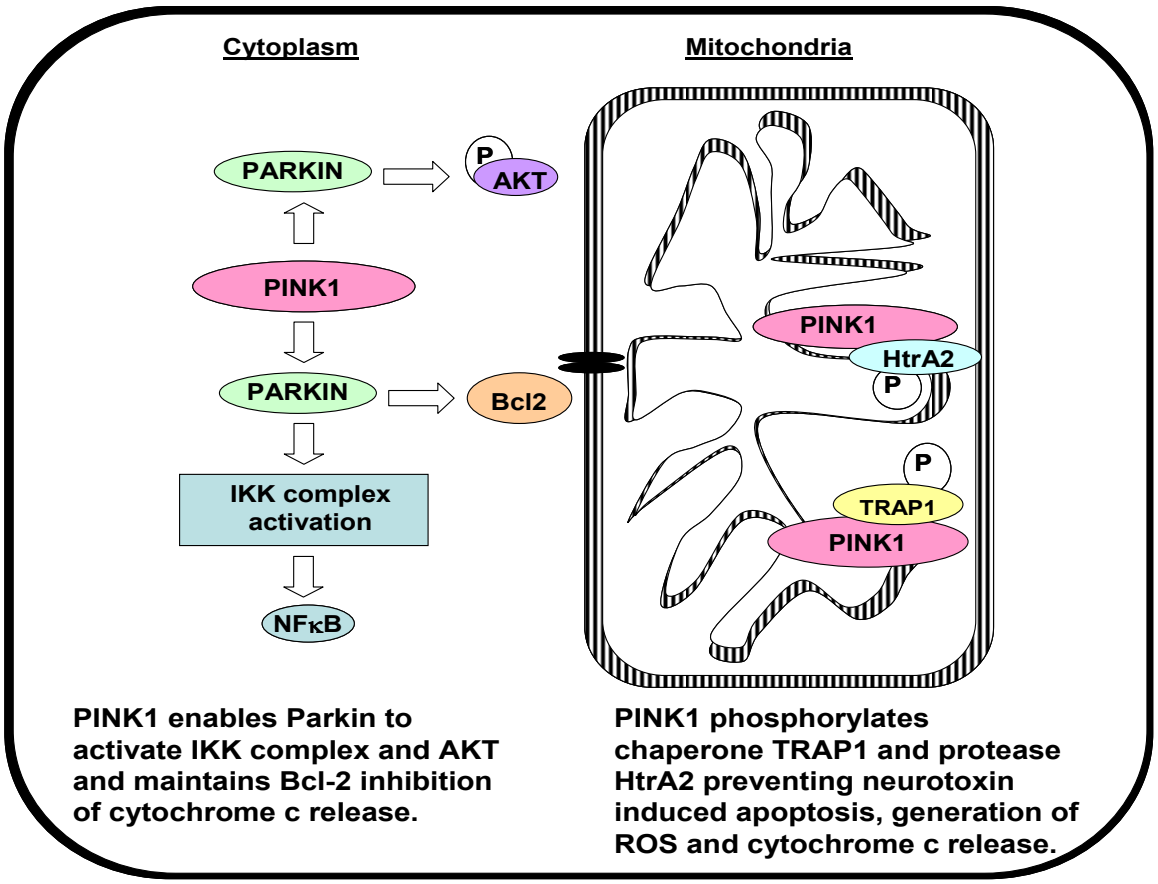

Figure 1.12: Suggested neuroprotective mechanisms of PINK1, adapted by Mills et al., 2008; p=phophorylated protein. Including, HtrA serine peptidase 2 (HtrA2), IκB kinase (IKK), nuclear factor kappa light chain enhancer of activated B cells (NFκβ), PTEN induced kinase 1 (PINK1), reactive oxygen species (ROS) and TNF – related activated protein (TRAP).

1.5.6 PTEN/PI3K/AKT pathway and the role in cardiovascular system

1.5.6.1 PTEN and cardiovascular physiology

PTEN is an important regulator of cell homeostasis and indeed plays a role in controlling vascular cell function, growth and development. In mice with endothelial specific knock down of PTEN (Tie2CrePten$^{flox/+}$) an increase in tumourgenesis can be observed. When stimulated with growth factors, VEGF release is enhanced and an increased rate of proliferation,

migration and angiogenesis is observed (Hamada et al., 2005). These mice do not survive past embryonic day 11.5 and die due to cardiac failure and bleeding. The authors of this work suggest that this is due to impaired recruitment of cardiomyocytes into the endocardium, and smooth muscles cells into the vasculature, during development (Hamada et al., 2005). Therefore PTEN is important in controlling vascular development and is involved in regulating cell migration and angiogenesis.

Furthermore, PTEN is important in the normal physiology of the heart, as shown in Figure 1.13. Characterisation of mice with targeted deletions of PTEN in smooth muscle cells, reveals the importance of PTEN in the vasculature and cardiac cells. In these mice an increase in phosphorylated AKT is recorded in the heart and blood vessels: moreover, hyperplasia (an increase in smooth muscle cell number) and vascular remodelling was documented. Furthermore, an increase in heart weight and right ventricular hypertrophy was observed in the myocardium from these mice (Nemenoff et al., 2008). Similarly, mice with targeted PTEN deletions in cardiomyocytes develop cardiac hypertrophy and exhibit reduced cardiac contractility. Myocardial phosphorylated AKT and phosphorylated GSKβ levels were increased (Crackower et al., 2002).

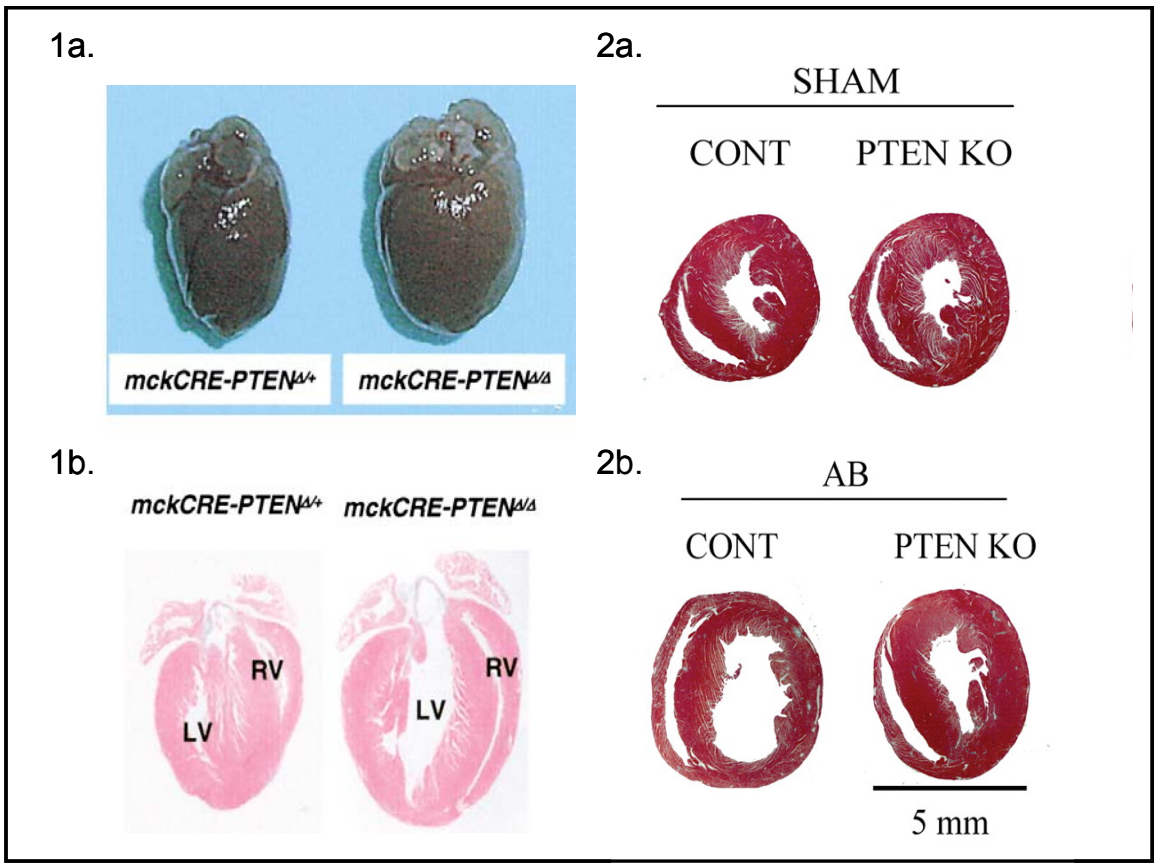

Figure 1.13: The effects of PTEN deletion on cardiac physiology in mouse myocardium. 1) Heart size (a) and heart sections (stained with trichrome for the detection of interstitial fibrosis) (b) from mckCRE-PTEN$^{\Delta/+}$ heterozygous littermates and mckCRE-PTEN$^{\Delta/\Delta}$ homozygous mutants (LV = left ventricle and RV = right ventricle). Hypertrophy is recorded when compared to control (Crackower et al., 2002). 2) Cross sections from control (mckCRE-PTEN$^{+/+}$) and PTEN knockout (mckCRE-PTEN$^{flox/flox}$) myocardium subjected to sham (a) or aortic banding (AB), to achieve pressure overload (b). Paradoxically, reduced ventricular distortion in response to pressure overload is observed in the PTEN mutants (Oudit et al., 2008).

PTEN can maintain normal cardiac contractility. In mice with targeted deletion of PTEN in skeletal muscle, an increase in cardiac L-Type calcium currents has been observed. Blockers of these channel are used as anti arrhythmic drugs, indicating that PTEN has a role in

regulating normal cardiac contraction (Sun et al., 2006). The evidence from these studies suggests that growth and survival pathways are enhanced when PTEN is inhibited and that PTEN functions to control normal cell development, growth and function of the myocardium and vasculature.

1.5.6.2 Diabetes

PTEN is linked to CVD, diabetes and cardiovascular metabolic syndrome. In diabetes suppression of the PI3K/AKT pathway can be observed (Kushner et al., 2005). As described, PTEN can negatively regulate the PI3K/AKT pathway and plays a role in glucose uptake. Over expression of PTEN can reduce insulin stimulated GLUT4 translocation and phosphorylation of AKT and p70S6K (Mosser et al., 2001; Nakashima et al., 2000).

In isolated diabetic Goto Kakazaki rat hearts the expression of PTEN protein is higher than in the non diabetic control (Mocanu et al., 2006). This indicates that Goto Kakazaki rats have desensitised insulin signalling pathway in conjunction with increased PTEN level. In addition, they display a higher threshold to IPC and consequentially are more difficult to protect against ischaemia-reperfusion injury (Tsang et al., 2005). Moreover, a Japanese study of patients with type 2 diabetes detected 3 different mutations in the PTEN gene (Ishihara et al., 2003).

Interestingly, muscle specific deletion of PTEN in mice on a high fat diet evade the development of diabetes and insulin resistance (Wijesekara et al., 2005). Similar prevention studies were performed in diabetic db/db and ob/ob mice with intra peritoneal injections (i.p) of PTEN antisense, which reduced PTEN mRNA and protein expression in liver and fat cells. Consequentially, these mice displayed normalised blood glucose levels with an increased sensitivity to insulin and increased levels of phosphorylated AKT (Butler et al., 2002).

Collectively, these experiments indicate that PTEN prevents glucose uptake and implicates PTEN in the patho-physiology of diabetes.

1.5.6.3 The physiological relevance of PTEN inhibition

As described above, PI3K/AKT is one of the most important intracellular signalling pathways responsible for increasing cell survival and repair (Manning and Cantley, 2007) Activation of this pathway is associated with reduced myocardial infarction following ischaemia-reperfusion injury (Hausenloy et al., 2005). However, if activated chronically, PI3K/AKT has pro hypertrophic and pro oncogenic consequences and therefore this signalling kinase cascade is tightly controlled. The most important down regulator of this pathway is PTEN, which dephosphorylates PI(3,4,5)P3 preventing AKT activation (Maehama and Dixon, 1998b). Potentially, this may have a negative impact upon myocardial survival following an ischaemic episode (Mocanu et al., 2006; Mocanu and Yellon, 2007).

PTEN targeted deletions in muscle have been generated (mckCRE-PTEN$^{flox/flox}$) and have been used to study the effects of PTEN reduction on the myocardium. As described, these hearts exhibit reduced contractility and increased heart size (Crackower et al., 2002). However, supplementary studies in these animals demonstrate a reduction in detrimental vascular cell remodelling subsequent to aortic banding. Such salvage was associated with a reduction in pathological hypertrophy, fibrosis, and apoptosis and was attributed to reduced phosphorylated JNK and p38 levels. Conversely, no difference in the detrimental remodelling effects of angiotensin II were observed in this model (Oudit et al., 2008). Collectively, this indicates that enhanced PI3K/AKT (as a consequence of PTEN inhibition) can be beneficial in a biomechanical model of cell stress and that PTEN may have a role on vascular remodelling and long term heart failure.

PTEN is involved in apoptosis (Stambolic et al., 1998) and its inhibition may have a role in IPC. Recently work by Cai and Semenza, has implicated PTEN inhibition to IPC induced myocardial protection. The group demonstrated that PTEN is oxidised and inhibited, as a consequence of IPC (Cai and Semenza, 2005). Hypoxia inducible factor 1alpha (HIF1α) signalling may be involved in the oxidation and inhibition of PTEN. In mice hearts with HIF1α targeted deletions, IPC induced protection was abolished, and is thought to be due to the lack of ROS and PTEN oxidisation (Cai et al., 2008a). Interestingly the presence of the GPCR agonist adenosine, used as an IPC mimetic, was sufficient to confer protection in these mice (Cai et al., 2008a). This may implicate that divergent mechanisms are involved in cardioprotection induced by IPC compared to protection induced pharmacologically. PTEN inhibition may have a protective function in CVD and ischaemia-reperfusion injury.

1.6 Additional negative regulators of the PI3K/AKT pathway

As outlined above and shown in Figure 1.6 PTEN is the main regulator of the PI3K/AKT pathway. However there are other phosphatases that negatively regulate this pathway, such negative regulators are described in more detail below.

1.6.1 SH containing inositol phosphatase 2 (SHIP2)

The SH containing inositol phosphatase 2 (SHIP2) protein is a lipid phosphatase that negatively regulates the PI3K/AKT pathway (Chi et al., 2004). It has a predicted molecular weight of 142kDa and is highly expressed in heart, skeletal, placental and insulin sensitive tissues (Pesesse et al., 1997).

SHIP2 appears to have an important role in the PI3K/AKT signalling by regulating the PI(3,4,5)P3 to PI(3,4)P2 ratio. Over expression of SHIP2 can result in a decrease of

phosphorylation of AKT (Sasaoka et al., 2004). Increased SHIP2 activity is associated with enhanced plasma membrane localisation facilitating a decrease in PIP3 production and reduced phosphorylation of AKT (DeKroon et al., 2006). SHIP2 has a role in proliferation and growth (Pesesse et al., 1997). The activity of this phosphatase is to convert PI(3,4.5)P3 into PI(3,4)P2 (Chi et al., 2004). Insulin stimulation in cells over expressing SHIP2 indicates that this phosphatase has a role negatively regulating PI3K/AKT activity (Marion et al., 2002). Unlike PTEN, the inhibition of SHIP2 has not been associated with formation of cancers, however the reason for this is unknown (Lazar and Saltiel, 2006).

SHIP2 appears to have an important role in regulating insulin signalling. In patients with type 2 diabetes genetic mutations have been observed and correlated with enhanced SHIP2 mRNA and protein expression (Marion et al., 2002). In diabetic Goto-Katizaki rats, mutations in the SHIP2 gene have been recorded (Marion et al., 2002). Additionally, the development of insulin resistance in C57BL/J6 mice subjected to a high fat diet provokes increases in SHIP2 protein expression in skeletal and fat tissue (Hori et al., 2002). Furthermore, db/db diabetic mice develop an increase in SHIP2 protein expression in skeletal and fat tissue. There is a diminished response to insulin treatment in these mice and less PI3K/AKT and PKC activity is recorded compared to control mice (Hori et al., 2002).

1.6.2 PH domain leucine rich repeat protein phosphatase (PHLPP)

PH domain leucine rich repeat protein phosphatase (PHLPP) is a ubiquitously expressed phosphatase, with the highest levels detected in the brain. It has a molecular weight of 140Kda and contains a PH domain, leucine rich repeat motif, PP2C domain and PDZ binding region (Gao et al., 2005b).

PHLPP functions as negative regulator of the PI3K/AKT pathway and it can directly bind to AKT. Over expression studies demonstrate that PHLPP dephosphorylates AKT at Ser473 but

not the Thr308, consequentially increasing apoptosis (Gao et al., 2005b). This data suggests that PHLPP is a key protein phosphatase acting at the AKT Ser473 phosphorylation site. The above authors showed that, by deleting the PDZ domain of PHLPP, the dephosphorylation of AKT is abolished, indicating that PHLPP is active at the plasma membrane (Gao et al., 2005b). In addition PHLPP can dephosphorylate PKC, for which the PHLPP PH domain is required, indicating the structure of PHLPP can influence its activity (Gao et al., 2008b).

In tumour cell lines, a reduction in PHLPP protein expression and increased AKT activity can be observed. Over expression of PHLPP in mice exhibiting tumour formation display a 68% reduction in tumour size (Gao et al., 2005b). Collectively, this indicates that PHLPP is a protein phosphatase involved in dephosphorylating AKT, suppressing tumour growth and inducing apoptosis (Gao et al., 2005b).

1.6.3 Protein phosphatase 2A

Protein phosphatase 2A (PP2A) is involved in regulating AKT, functioning as a negative regulator of the PI3K/AKT pathway. This phosphatase directly inactivates AKT in the cytosolic and membrane fractions of the cell and is involved in cell death and apoptosis. The PP2A inhibitor okadaic acid can reduce phosphatase activity and consequentially increase phosphorylation of AKT at Ser473 and Thr308 and reduce cell death (Resjo et al., 2002; Liu et al., 2003).

In addition PP2A can bind and dephosphorylate the pro survival protein Bcl2, preventing its anti apoptotic activity. (for a review on PP2A and apoptosis see Garcia et al, 2003). There is evidence to suggest that PP2A inhibition is protective against ischaemia-reperfusion injury. In an isolated rat heart model of ischaemia-reperfusion injury the presence of the PP2A inhibitor okadaic acid reduced PP2A activity to bestow cardioprotection. In addition, the authors of this work demonstrate that, in the ageing rat heart (which are not protected by IPC), there is

enhanced PP2A activity (Fenton et al., 2005). This indicates that PP2A has a role in cell death, negatively regulating PI3K/AKT signalling.

1.7 Summary

Activation of the prosurvival PI3K/AKT pathway can reduce apoptosis and protect against myocardial ischaemia-reperfusion injury (Hausenloy et al., 2005; Davidson et al., 2006). The main regulator of this pathway is PTEN, a lipid phosphatase that dephosphorylates PI(3,4,5)P3 into PI(4,5)P2 and limits AKT activation (Maehama and Dixon, 1998b; Lee et al., 1999). Inhibition of this phosphatase can enhance the PI3K/AKT pathway (Butler et al., 2002; Arevalo and Rodriguez-Tebar, 2006). Reduction of PTEN function may have a role in tissue salvage following an acute injury such as that observed in myocardial ischaemia-reperfusion injury. However, studying the reversible inactivation of PTEN would be required in order to avoid chronic PI3K/AKT activation. In this thesis methods to decrease myocardial PTEN were investigated to explore the effects of reduced PTEN on ischaemia-reperfusion injury.

1.8 Hypothesis

That PTEN reduction would be cardioprotective against ischaemia-reperfusion injury; by enhancing the PI3K/AKT prosurvival pathways and decreasing the extent of cell death. Aim: To investigate the role of PTEN down regulation in cardioprotection.

In order to investigate the hypothesis above the following methods were used:

1) Chemical inhibition of PTEN (bpV(HOpic
2)) and SF1773).
3) Biochemical modulators of p53 (pifithrin alpha).
4) Genetic modifications of PTEN (congenital haploinsufficient $PTEN^{+/-}$ mouse).
5) Genetic modifications of PTEN (small interfering RNA induced PTEN knockdown in H9c2 cells).

The experimental models used were:

1) An isolated perfused mouse heart model of global ischaemia-reperfusion injury.
2) A cellular model of reactive oxygen species induced mitochondrial damage.
3) A cellular model of hypoxia-reoxygenation injury.

The end points measured were:

1) Cell death, measuring infarct size developed in the ischaemic-reperfused myocardium, and time to mPTP opening and caspase 3 cleavage in the cellular models of simulated ischaemia-reperfusion injury.
2) The myocardial protein expression of kinases and phosphatases implicated in ischaemia-reperfusion injury, using Western blot technique.

2 Chapter 2 – General methods

2.1 Overview of experimental Models

We investigated the consequence of reducing PTEN level upon myocardial ischaemia-reperfusion injury. We used a variety of experimental models, which are outlined in this section and are described in more detail in the remaining sections of this chapter. Within each experimental chapter we described the specific protocols used, relevant to the investigation. All chemicals and reagents were purchased from Sigma Aldrich, UK unless otherwise stated.

2.1.1 Animal strains

All investigations using animals were carried out under the Home Office guidelines for the Animals (Scientific Procedure) Act 1986. Male NIH-Swiss White mice (10-15 weeks, 20-30g) (Charles River, UK) and male C57BL/J6 mice (10-15 weeks, 20-30g) (Charles River, UK) were used. In addition PTEN haploinsufficient mice ($PTEN^{+/-}$), donated by Dr D Alessi (Dundee University) with the permission of Raymon Parson (the original producer of these mice as described by Podsypanina et al., 1999), were bred in house.

2.1.2 Whole organ models used to investigate the effect of reduced PTEN level on myocardial ischaemia-reperfusion injury

We used a Langendorff model of isolated perfused mouse hearts to investigate infarct size resulting from ischaemia-reperfusion injury. In parallel with infarct measurements, Western blot techniques were used to monitor levels of pro and anti apoptotic markers. In these studies we used myocardium (perfused with chemical inhibitors of PTEN) from C57BL/J6 and isolated hearts from the $PTEN^{+/-}$ mouse strain.

We attempted to reduce PTEN levels using pharmacological and molecular mechanisms. Targeting the molecular reduction of PTEN, we aimed to inhibit the transcription of PTEN by reducing p53 levels, as described in chapter 5. The p53 inhibition studies were performed in NIH-Swiss White mice.

2.1.3 Cell models used to investigate the effects of reduced PTEN level on simulated ischaemia-reperfusion injury

We used two cellular models of simulated ischaemia-reperfusion injury, outlined below, to study the effects of reduced PTEN on myocardial cell damage.

1) Isolated primary myocytes from $PTEN^{+/-}$ mice and their littermate controls were used to investigate their sensitivity to ROS induced mitochondrial damage. This was done by measuring the time to mitochondrial permeability transition pore opening, using confocal microscopy.

2) H9c2 rat myoblast cells were subjected to simulated ischaemia-reperfusion injury using a model of hypoxia-reoxygenation. PTEN protein expression was silenced using siRNA. Western blot analysis was used to investigate changes in caspase 3 cleavage subsequent to simulated ischaemia-reperfusion to assess the cell damage.

2.2 Langendorff model of isolated perfused hearts

2.2.1 The concept of the isolated perfused heart

In the early 1900s Oscar Langendorff was one of the first to study and develop the model of isolated retrograde perfused myocardium (Zimmer, 1998; Skrzypiec-Spring et al., 2007). A simplified representation of the equipment and principle of the model is shown in Figure 2.1. This technique maintains cardiac activity and permits analysis of isolated hearts. Perfusion buffer flows to the heart, through a cannula placed in the ascending aorta. The pressure of the retrograde perfusion causes the aortic valves to close, forcing perfusion buffer into the coronary system, mimicking the conditions during diastole. The cardiac chambers are mainly empty through out perfusion whilst the buffer finally flows off the coronary sinus in the right atrium. This method can be used to maintain the cardiac activity for several hours. In this study we used a standard Langendorff ML870B2 perfusion apparatus (AD Instruments, UK) modified for perfusion of mouse hearts. We used a system of constant perfusion pressure where, changes in flow rate indicated changes in coronary vessel resistance. This measurement can be used as an indicator of vasoconstriction or vasodilatation. Haemodynamic recordings were converted to electronic data through a PowerLab system and monitored using MacLab Chart 4.3 software. (AD Instruments, UK) Figure 2.2 and Figure 2.3 show the apparatus set up and Figure 2.4 represents a typical Chart 4.3 tracing, when perfusing an isolated murine myocardium. More importantly, this method can be used to study the effects of ischaemia-reperfusion injury on isolated functional whole hearts. The details of the methods used to study this are described below. We performed optimisation experiments for the Langendorff perfusion of mouse hearts, which are described in chapter 3.

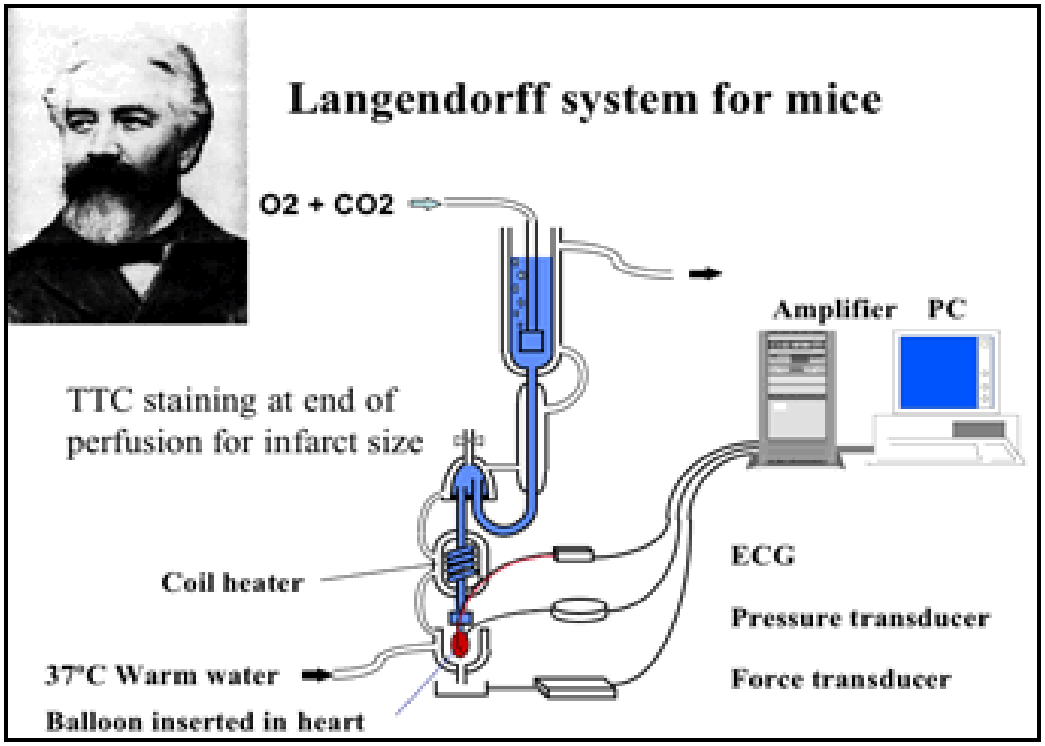

Figure 2.1: Schematic representation of a Langendorff experimental system used to study isolated perfused heart preperations, including a photo of Oscar Langendorff. O2 (oxygen), CO2 (carbon dioxide) and ECG (electrocardiogram).

http://www.med.uio.no/imb/fysiol/valen/pictures/Langendorff.gif

2.2.2 Preparation of hearts for isolated Langendorff perfusion

Mice were injected with 500U of heparin, i.p, 10 min prior to culling by cervical dislocation. The hearts were then removed and placed in ice cold perfusion buffer. As a consequence of the low temperature, hearts stopped beating. This temporary hypoxia eased the cannulation process but also, more importantly, reduced the metabolic processes and the amount of protease activity, and therefore, minimised cell damage. The myocardium was trimmed to expose the aorta which was cannulated with a 22 gauge murine cannula (ADinstruments,UK), secured with a 5/0 silk tie (Syneture,USA) and attached to the Langendorff apparatus, making sure to avoid air bubbles. Hearts were then retrogradedly perfused at a constant perfusion

pressure of 80-100 mmHg which matches the physiological pressures required to adequately supply the mouse coronary arteries. The perfusion buffer used was an oxygenated (bubbled with 95%O_2/5% CO_2 to pH 7.3-7.4) Krebs-Henseleit buffer containing 118mM NaCl, 25mM $NaHCO_3$, 11mM Glucose, 4.7mM KCl, 1.22mM $MgSO_4.7H_2O$,1.21mM KH_2PO_4 and 1.84mM $CaCl_2.2H_2O$.

<u>Figure 2.2:</u> The perfusion system used for studying isolated mouse hearts: A) dissection area, B) cannulation area, C) perfusion apparatus, D) PowerLab electronics and E) computer used for data acquisition.

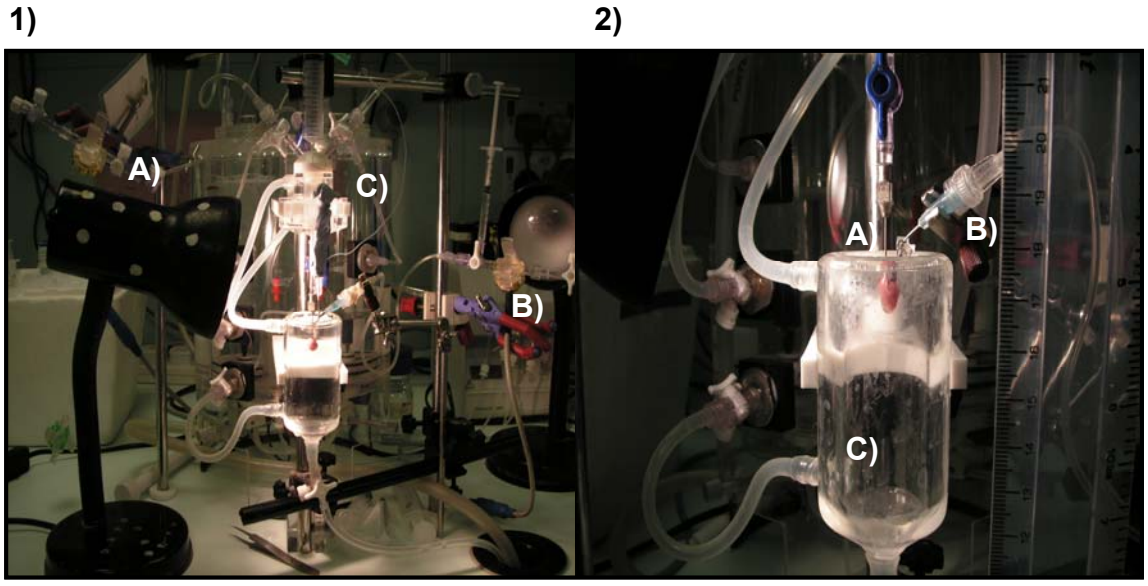

Figure 2.3: 1) Isolated mouse heart, mounted on the perfusion apparatus: pressure transducer used to measure A) perfusion pressure and B) left ventricular pressure and C) the heated water reservoir used to warm the perfusion buffer. 2) Closer image of the isolated mouse heart on the perfusion apparatus: A) cannulated heart, B) balloon inserted into the left ventricle of the heart to measure ventricular pressure and C) heated glass water jacket to surround the heart.

2.2.3 Measuring heart function in the Langendorff perfused myocardium

Haemodynamic parameters were measured to ensure fully functional hearts were used in all experiments and only healthy hearts were included. To minimise experimental error and to eliminate false positive or negative results, strict inclusion/exclusion criteria were set and adhered to, shown in Table 2.1.

Coronary flow was recorded by measuring the volume of perfusion buffer per minute required to maintain the set perfusion pressure. This closed circuit included a pressure transducer, attached to a fluid filled tube which was connected to the Langendorff apparatus (just above

the heart attachment point), which provided a feedback into a pump controller (ADInstruments,UK). This adjusts flow of perfusion buffer to achieve the fixed perfusion pressure, which was set between 80-100mmHg.

The status of the heart, was measured using a pressure transducer connected to a water filled balloon (roughly 4 mm x 3mm) inserted in the left ventricle and inflated to 5 –10 mmHg. The balloon detects the left ventricular end diastolic pressure (LVEDP) and left ventricular peak pressure (LVPP, the maximum pressure in systole). Left ventricular developed pressure (LVDP) is a measure of the force of contraction which was calculated by subtracting LVEDP from LVPP. Heart rate (HR) was calculated based on the number of systole-diastole cycles per minute. The rate pressure product (RPP) is an arbitrary measurement of heart function, which was obtained by multiplying HR by LVEP.

The temperature of the circulating perfusion buffer was adjusted in order to maintain the myocardium at 37±0.5°C. A desk lamp and a heated glass water jacket were additionally used to assist in controlling any smaller temperature fluctuations of the heart. The temperature was measured by placing a thermometer probe (T type) connected to a thermo pod and coupler (AD Instruments,UK) at the heart.

These haemodynamic parameters were recorded during a stabilisation period to ensure the hearts were functioning well. Any hearts with parameters which did not fit within the inclusion criteria, listed in Table 2.1 were excluded. A representation of a Chart 4.3 tracing during stabilisation is shown in Figure 2.4.

Table 2.1: Inclusion criteria for isolated hearts undergoing Langendorff perfusion. (BPM = beats per minute).

Measurement	Inclusion criteria
Time from extracting the heart to perfusion	≤ 5 min
Coronary flow	1.0 - 6.0 ml/min
Heart rate	≥ 300 BPM
Temperature	37.0 ± 0.5 °C

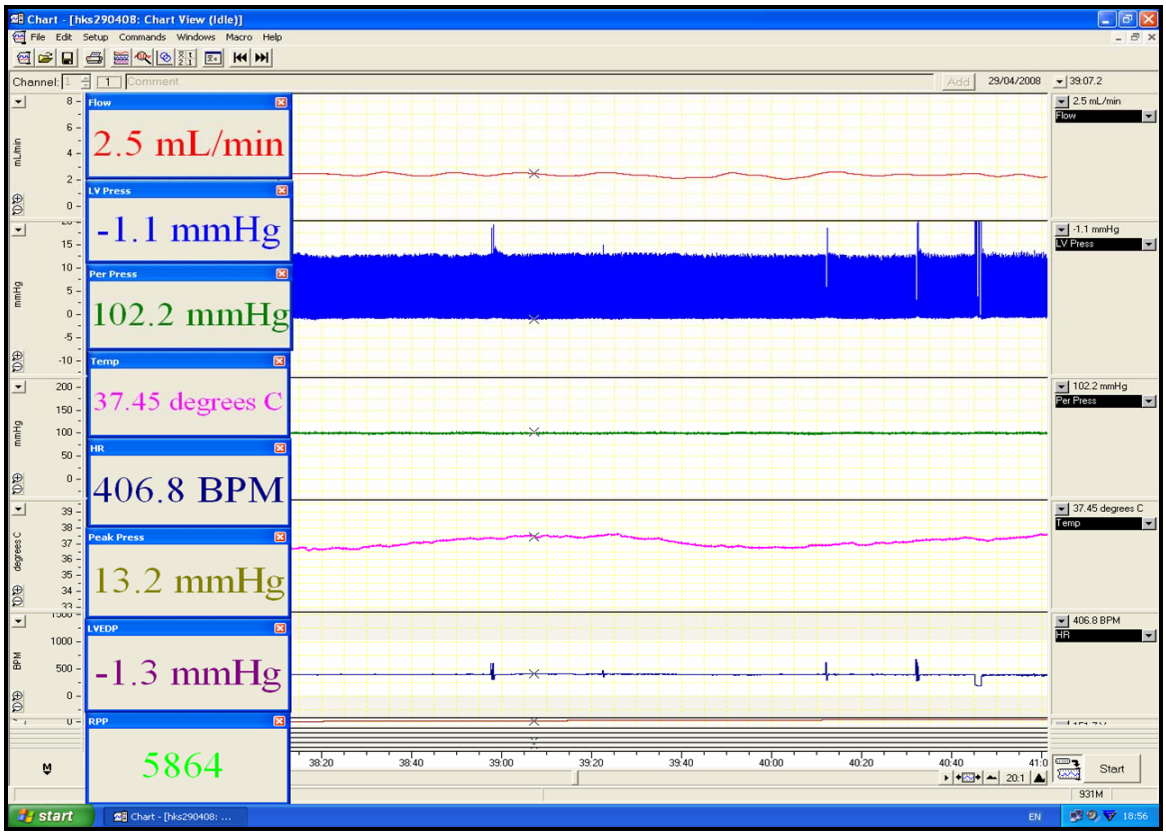

Figure 2.4 Typical Chart 4.3 tracing obtained during the stabilisation period of an isolated perfused mouse heart. BPM = beats per minute.

2.2.4 Ischaemia-reperfusion protocols in the isolated heart.

The standard protocol used for studying ischaemia-reperfusion injury in isolated perfused hearts is shown below and described in more detail in the following respective chapters. Myocardial injury was determined at the end of the protocol by measuring infarct size which is described below.

The control ischaemia-reperfusion protocol consisted of 30 min stabilisation followed by 35 min global ischaemia and 30 min reperfusion, as shown in Figure 2.5. Global ischaemia was achieved by interrupting the flow of perfusion of buffer, which was completely switched off. Sudden cooling of the heart during this time was avoided by submerging the heart in perfusion buffer (submersion buffer) at 37±0.5^{o}C.

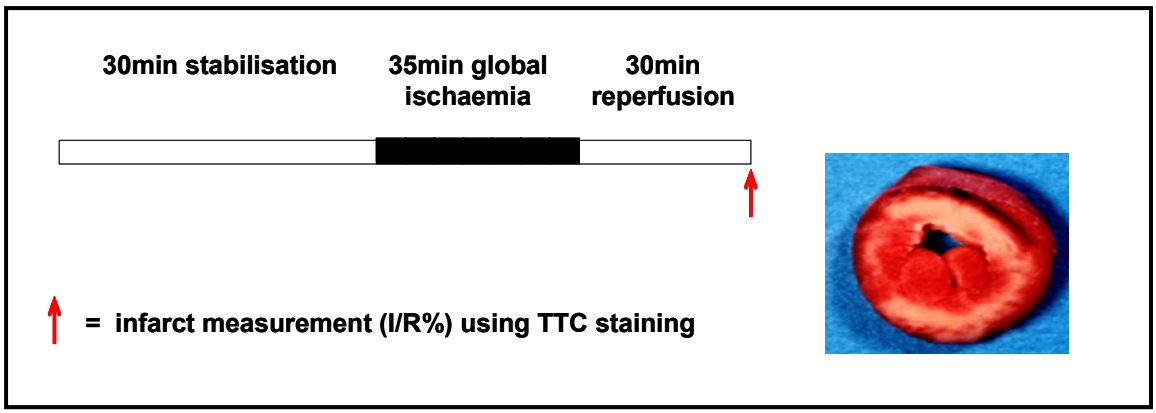

Figure 2.5: Langendorff control ischaemia-reperfusion protocol. Infarct size was measured as the percentage of infarction to risk area (I/R%), at the end of the reperfusion period, using triphenyltetrazolium chloride (TTC) (white areas represents the infarct and red areas the viable myocardium).

2.2.5 Ischaemia-reperfusion injury: analysis of infarct size

At the end of the reperfusion period, hearts were taken off the perfusion apparatus and perfused, through the aortic cannula, with 1% pre-warmed triphenyltetrazolium chloride (TTC) which acts as a viability dye. Hearts were subsequently immersed in TTC and incubated at 37^{o}C for 10 min, after which they were weighed and frozen at -20^{o}C for 24h. Whilst still frozen, hearts were sliced from base to apex at a thickness of ≈1mm. The slices were fixed in 10% formalin for 12h to define the stain borders.

The TTC is a redox indicator and can stain areas of viable myocardium red. This is because viable cells (with intact membranes) retain the dye where it can react with dehydrogenases and NADPH. In the presence of oxygen these enzymes can reduce TTC, causing a conversion into a red colour (Klein et al., 1981). Areas of tissue containing non viable/infarcted cells have lost their dehydrogenases, due to wash out in reperfusion, and are unable to retain or convert the dye and therefore emerge unstained and white in appearance. Examples of a mouse myocardium subjected to ischaemia-reperfusion and stained for infarction with TTC is shown in Figure 2.5 and 2.6.

Heart slices were then photographed on a perspex mounting block using a digital EsKape (Eskape, NY, USA) fixed camera. NIH Image 1.63 software was used to calculate the infarcted areas and the results were expressed as a % of the whole heart at risk of damage induced by ischaemia-reperfusion injury (I/R%) and presented as means ± standard error of the mean (SEM). A t-test or a one way ANOVA test were used to assess the differences between groups, as described in the statistics section further in this chapter. The results were considered significantly different when $p \leq 0.05$.

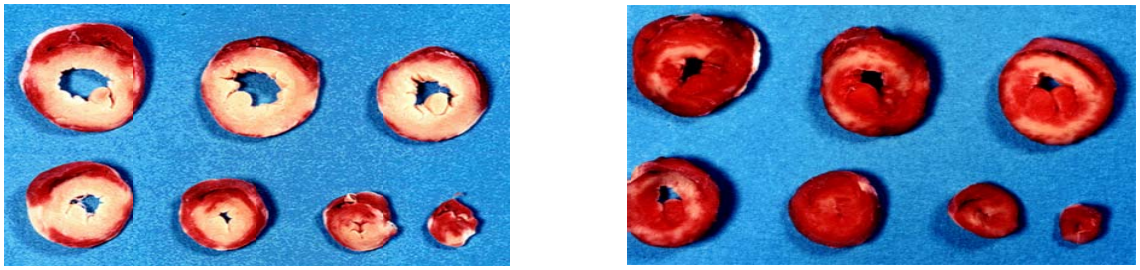

A: Ischaemia-Reperfusion injury **B: Myocardial protection**

Figure 2.6: Mouse myocardium subjected to: A) global ischaemia-reperfusion only and B) global ischaemia-reperfusion with ischaemic preconditioning as a cardioprotective stimulus, following triphenyltetrazolium chloride staining. Viable myocardium was stained red however; the infarcted tissue does not retain the dye and remains white.

2.3 Ischaemia-reperfusion injury and pharmacological inhibitors of PTEN

We used the PTEN inhibitors bisperoxo(5-hyroxypyridine-2carboxy) oxovanadate (bpV(HOpic)) and SF1773, a small peptide donated from Semafore Pharmacuticals, USA to reduce PTEN function. Secondly, we aimed to inhibit p53, using pifithrin alpha (PFTα) a p53 inhibitor purchased from Calbiochem, UK, as a potential tool to down regulate PTEN; as described in Chapter 5. The PTEN inhibitors bpV(HOpic) and SF1773 were diluted in water, the p53 inhibitor PFTα was diluted in 0.1%DMSO/0.9%saline and the pharmacological cardioprotective positive control (orthovanadate) was diluted in water. The chemical structures of these molecules are shown below in Figure 2.7.

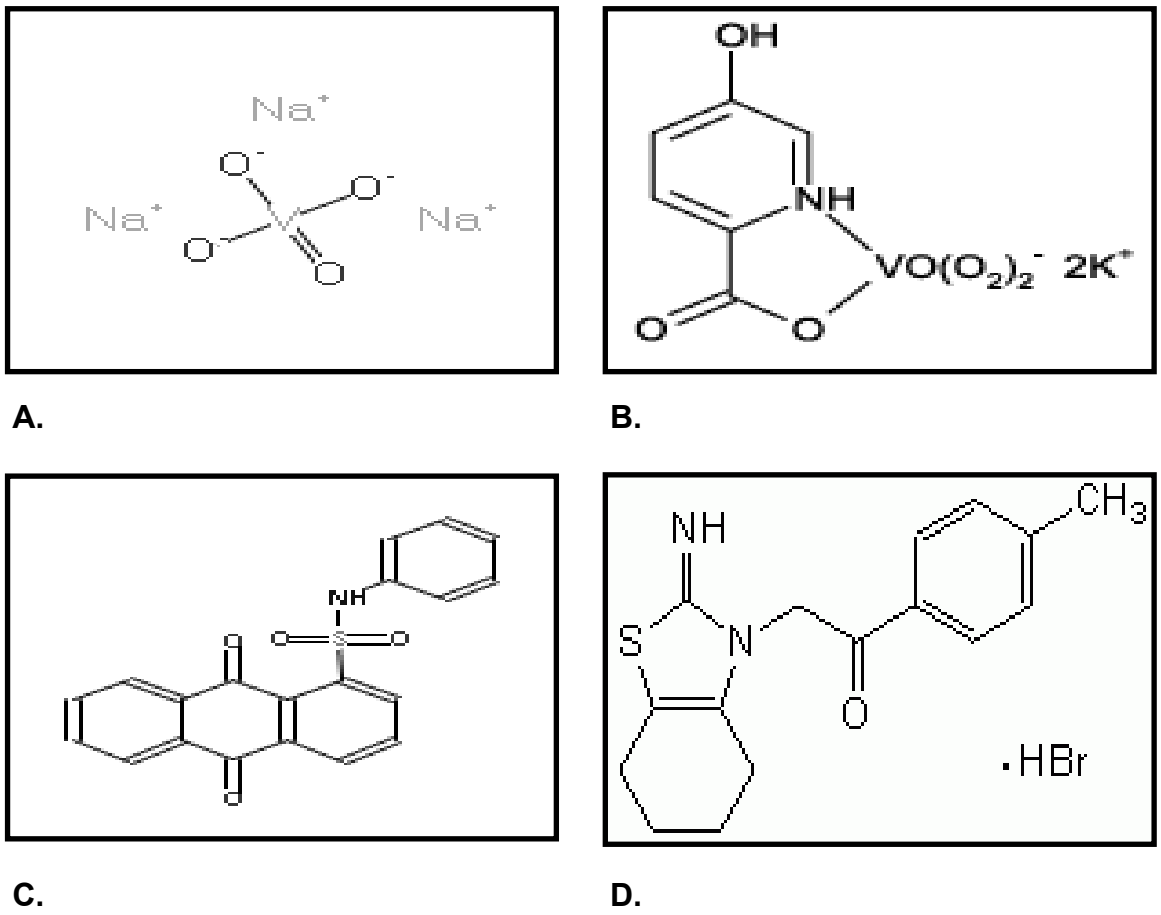

Figure 2.7: Chemical structure of: A) orthovanadate (Na_3VO_4), B) the PTEN inhibitor bpV(HOpic) ($K_2[VO(O_2)_2)C_6H_4NO_3]$, C) the PTEN inhibitor SF1773 ($C_{20}H_{13}NO_4S$) and D) the p53 inhibitor pifithrin alpha ($C_{16}H_{18}N_2OS.HBr$).

2.4 PTEN: haploinsufficient mice

2.4.1 Breeding

A breeding rota within UCL Biological Services was established; PTEN $^{+/+}$ and PTEN $^{+/-}$ mice were crossed, using male PTEN$^{+/-}$ as the preferred haploinsufficient carrier. Female PTEN $^{+/-}$ can breed but only for a few months as they suffer endometrial tumours, and each litter contains fewer pups until they cease producing litters. The PTEN$^{-/-}$ pups are not recorded alive beyond embryonic day 6.5; the PTEN$^{+/-}$ survive gestation, although they develop early

onset of sporadic tumours (Podsypanina et al., 1999). Male animals are used in investigations between the ages of 10-15 weeks, unless otherwise stated.

2.4.2 Genotyping PTEN haploinsufficient mice

2.4.2.1 DNA extraction

DNA was extracted from mouse tail tip (0.5cm long) or ear punches and processed using Qiagen DNeasy kit (Qiagen, UK), according to the manufacturer's instructions. Tissues were lysed overnight at 55^{o}C in a proteinase K lysis buffer (40mAU/mg protein). This enzyme is a serine protease which facilitates protein degradation to reveal nucleic acids. Samples were then incubated in an ethanol-lysis buffer and added to individual spin columns, which allowed the DNA to bind the silica gel membrane as a consequence of the differences in electron charges. The membranes were then washed twice by centrifugation with optimized buffer, which prepares the column for removal of the DNA. The elution buffer/DNA absorbance ratio at A_{260}/A_{280} (1.8-2.0) is an indicator of good DNA purity.

2.4.2.2 DNA amplification and visualisation

Polymerase chain reaction (PCR) was used to amplify the DNA. This technique facilitates the exponential amplification of DNA and enables further analysis of the DNA extract. The PCR protocol was originally provided by Gail Fraser from the University of Dundee and the settings were adapted to the Hatter Laboratory. The primer sequences were as follows. PTEN Wild type - 5' GTC TCT GGT CCT TAC TTC C 3', PTEN common - 5'TTG CAC AGT ATC CTT TTG AAG 3', PTEN neo/NEW - 5'ACG AGA CTA GTG AGA CGT GC 3'. 0.5μM primers (MWG, Germany), 2.5mM MgCl, 0.2mM dNTPs mix and 1unit Taq Polymerase (all from Promega, UK) were mixed with approx 10ng DNA, and run on a thermocycler under the conditions shown in Table 2.2. The amplified DNA was analysed on a 2% agarose gel with

ethidium bromide, which intercalates between nucleic acid bases and fluoresces orange when exposed to UV light. The PCR amplification products reveals either a wild type phenotype (from littermate control $PTEN^{+/+}$) or a haploinsufficient phenotype (from $PTEN^{+/-}$); consisting of one band running to 240bp or two bands running to 240bp and 320bp, respectively.

Table 2.2: PTEN PCR conditions.

Step	Temp (^{o}C)	Time (min)
1	94	5
2	94	0.5 (Separates dsDNA)
3	55	0.5 (Annealing of primers)
4	72	2 (DNA synthesis)
5	Cycle steps 2-4	34 cycles (Amplification)
6	72	7
7	4	Finish

2.5 PTEN ELISA (activity assay)

2.5.1 The concept of the ELISA assay

The PTEN activity assay was purchased from Echelon Biosciences Incorporated, USA and has been successfully used to detect PTEN phosphatase activity (Eickholt et al., 2007; Papakonstanti et al., 2007). The assay used was based on an Enzyme-Link ImmunoSorbant Assay (ELISA), which utilizes several antigen antibody binding reactions to quantify a protein of interest. Antibodies that are enzyme tagged can be used to assess the amount of target protein present in a sample. These enzymes are used to produce a detectable signal, which

can be measured either using a substrate that will emit a colour or fluorescence. A description of the assay used to detect PTEN phosphatase activity is outlined in Figure 2.8.

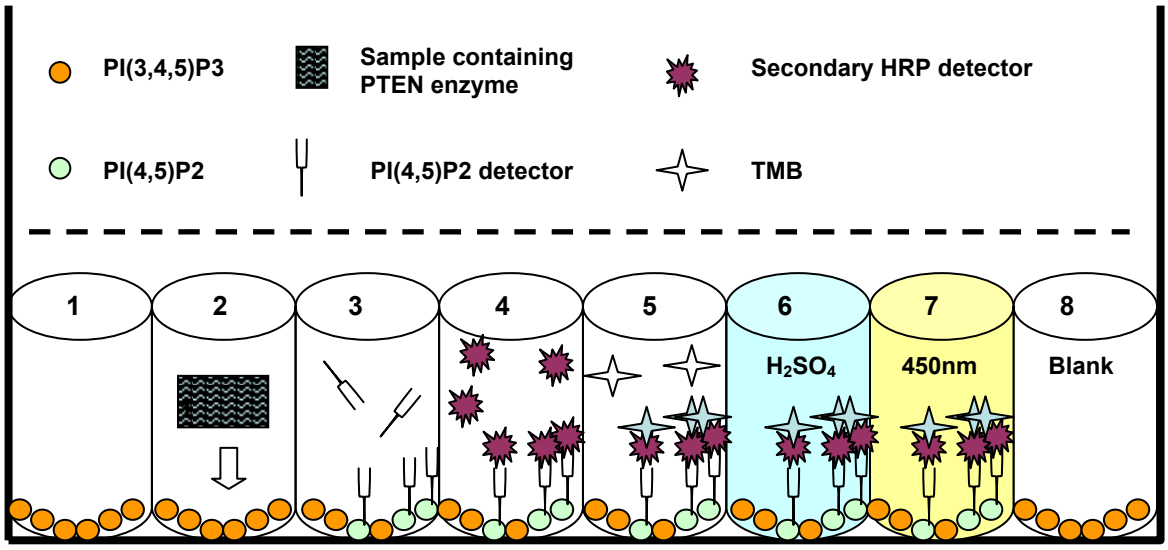

Figure 2.8: Steps involved in the PTEN ELISA assay, used for detecting PTEN phosphatase activity. 1) phosphatidylinositol 3 phosphate (PI(3,4,5)P3) was pre coated on the ELISA substrate plate. (Echelon, USA) 2) Myocardial tissue homogenates were incubated on the substrate plate. 3) Antibodies that recognised phosphatidylinositol 2 phosphate (PIP(4,5)P2) were then added. 4) A secondary antibody, which reacts with the PIP(4,5)P2 detection antibody, tagged with horseradish peroxidase (HRP) was added. 5) A tetra methyl benzidine (TMB) chromogenic reagent was then added. 6) The TMB reagent reacts with HRP to create a blue colour, which is proportional to the amount of PIP(4,5)P2. 7) sulfuric acid (H_2SO_4 was added to each well to stabilise and stop the reaction. The intensity of the blue colour could be measured at 450nm on an absorbance spectrophotometer.

2.5.2 Enzyme preparation

Myocardium samples were collected and homogenised as described in the Western blot protocol, below. According to the manufacturer's instructions, PTEN samples were diluted in PTEN enzyme reaction buffer (10mM HEPES, 150mM NaCl including 10mM dithiothreitol (DTT) added just prior to use). Samples were incubated on a substrate plate (pre-coated with PI(3,4,5)P3), in replicates of 3. Wells pre-coated in various concentrations of PI(4,5)P2 were provided with the assay and used as the standard curve. 10nM of the PTEN Enzyme (Echelon,USA) was purchased as a positive control. The sample wells were then incubated at 37^{o}C for 1hr. Sample wells were then washed 3x with 300ul TBS-Tween 20 ((Tris buffered saline (TBS)10mM Tris, 150mM NaCl, pH7.4) + 0.05% Tween 20).

2.5.3 Detection of PTEN activity by measuring conversion of PI(3,4,5)P3 into PI(4,5)P2

Detection of converted PI(4,5)P2 was initiated by the addition of the PI(4,5)P2 detector, provided with the assay. The PI(4,5)P2 detector was prepared in TBS-goat serum (TBS + 1% goat serum (Gibco/Invitrogen, UK). The reaction was incubated at RT for 1hr. Reaction wells were then washed 3x with 300ul TBS-Tween 20. The detector-PI(4,5)P2 reaction was then identified by the addition of a Horse Radish Peroxidase (HRP) conjugate solution, prepared in TBS-goat serum and incubated at RT for 1hr. Reaction wells were then washed 3x with 300ul TBS-Tween 20. Tetra methyl benzidine (TMB), a chromogenic substrate of HRP, was added to each well and incubated in the dark at RT for 15-30 min. In the presence of hydrogen peroxide, HRP oxidises TMB causing the emission of a blue colour. When sufficient colour was developed the assay reaction was terminated by adding a sulphuric stopping solution (0.5M sulphuric acid). This final oxidisation step of the TMB by the peroxide solution turns the reaction yellow. The absorbance of the samples were then measured, using a 96 well plate

absorbance reader (Dynex technologies, USA with a Revelation software platform) at 450nm wavelength. The average absorbance values were calculated and used as an indicator of PI(3,4,5)P3 conversion into PI(4,5)P2 which was therefore, indicative of PTEN phosphatase activity. An example of the expected standard curve was supplied with the assay protocol and is shown below in Figure 2.9.

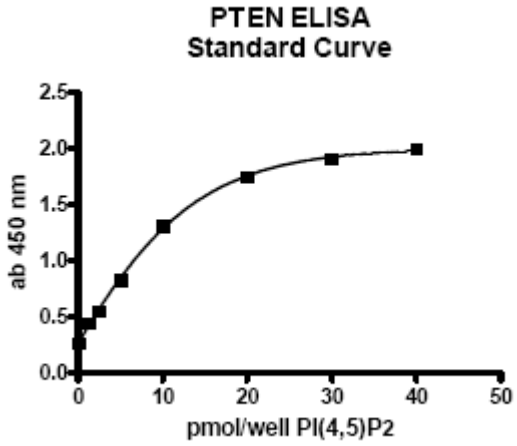

Figure 2.9: Expected phosphatidylinositol 2 phosphate (PI(4,5)P2) standard curve, provided in the Echelon PTEN ELISA assay kit.

2.6 Simulated ischaemia-reperfusion injury in an isolated cardiomyocyte cell model

We used a cellular model of ROS induced mitochondrial damage to determine the response of the mitochondria in isolated cardiomyocytes, to this aspect of simulated ischaemia-reperfusion injury. Ischaemia-reperfusion injury has been linked to the opening of the mPTP, therefore we use a cellular model to mimic this phenomenon (Halestrap et al., 2004). To investigate this primary adult cardiomyocytes were isolated from the myocardium of $PTEN^{+/-}$ mice and cells were loaded with the cationic dye, tetra methyl rhodamine methyl (TMRM) which is highly selective for normally functioning mitochondria due to its negative charge. A Confocal microscope was used to excite TMRM using a HeNe (Helium/Neon) 543nm laser.

When used at relatively high concentrations of 3μM, the fluorescence of the dye, highly concentrated within the mitochondria, is quenched. Upon mPTP opening the dye is released into the cytosol, the effective concentration in the larger volume is decreased, and detected as an increase in fluorescence. The excitation of the TMRM dye in the mitochondria generates ROS (predominantly superoxide, O_2^-) that induces mPTP opening and mitochondrial depolarisation (Zorov et al., 2000; Davidson et al., 2006). We measured the time to depolarisation as an indicator of ROS induced mitochondrial damage and cell death. This protocol is an established method that has been validated within the Hatter Cardiovascular Institute and is described in more detail below (Hausenloy et al., 2003; Davidson et al., 2006; Lim et al., 2008).

2.6.1 Isolation of ventricular cardiomyocytes

Mice were injected (i.p) with 500U of Heparin (CP Pharmacuticals,Wrexham, UK) 30 min prior to anaesthetic, which consisted of a 0.01ml/g i.p injection of a Ketamine (10mg/ml)/Xylazine (2mg/ml)/Atropine (0.06mg/ml) reagent. The heart was excised and immediately placed in ice cold calcium free perfusion buffer. The heart was trimmed and the aorta was rapidly cannulated with a 22 gauge murine cannula (ADinstruments, Oxford, UK) and secured with a 5/0 surgical silk tie. (Syneture Technologies,USA). The heart was attached to the Langendorff perfusion apparatus where it was perfused retrogradely at 3mls/min, with pre warmed (37^oC) oxygenated (95%O_2/5%CO_2) calcium free perfusion buffer for 4 min. Calcium free perfusion buffer consisted of 113mM NaCl, 4.7mM KCL, 0.6mM KH_2PO_4, 0.6mM Na_2HPO_4, 1.2mM $MgSO_4.7H_2O$, 12mM $NaHCO_3$, 10mM$KHCO_3$, 30mM Taurine, 10mM HEPES, 11mM Glucose and 10mM 2,3-Butanedione monoxime (BDM). The reagent, BDM, is used in the buffer to inhibit myocardial contraction during isolation. Time from heart excision to perfusion on the rig was within 3 min. The heart was then perfused with pre-warmed oxygenated digestion buffer for 10 min. Digestion buffer consisted of 220U/ml of type 2 Collagenase (Worthington,UK),

which breaks down the collagen connections in the heart and 55U/ml Hyaluronidase, which breaks down hyaluronic acid and is used to assist digestion by permeablising the cell membrane. These enzymes were dissolved in the calcium free perfusion buffer supplemented with 12.5μM $CaCl_2$.

Following the initial 10 min digestion step the ventricles were collected in 3-5mls of digestion buffer and torn apart for additional tissue disruption. The tissue was digested further by incubating the mixture with 95%O_2/5%CO_2 in a shaking incubator (170rev/min) at 37^oC for 5 min. A second and final digestion step was performed by adding 5mls fresh digestion buffer followed by 10 min incubation with 95%O_2/5%CO_2 in a shaking incubator at 37^oC. The following extraction steps were performed under sterile conditions. The ventricular cell suspension was transferred to a fresh tube and 5% foetal bovine serum (FBS) (Gibco/Invitrogen,UK) was added. The ventricular cells were centrifuged at a 600 relative centrifugal force (RCF) for 3 min to separate the larger, myocyte pellet. The smaller fibroblasts and remaining connective tissue in the supernatant were discarded. The myocyte cell pellet was re-suspended in a low calcium buffer, which consisted of the calcium free perfusion buffer supplemented with 12.5μM $CaCl_2$. Small volumes of calcium was re-introduced to the myocyte suspension every 4 min to gradually reach a final concentration of 1mM. The cells were then centrifuged at 600 relative centrifugal force (RCF) for 3 min and re-suspended in 1-2mls plating media which consisted of Medium-199 (Sigma,UK) supplemented with 2mg/ml Bovine Serum Albumin (BSA) (VWR, Lutterworth, UK) 0.66mg/ml Creatine, 0.662mg/ml Taurine, 0.322mg/ml Carnitine, 50U/ml Penicillin (Gibco/Invitrogen,UK) and 5μg/ml Streptomycin (Gibco/Invitrogen,UK) and 25μM blebbistatin a cell cycle and myosin II inhibitor. (Calbiochem, Nottingham,UK) The cell suspension was then added to a glass cover slip, 22mm diameter (VWR, Lutterworth, UK) pre-coated with laminin (1mg/ml) to aid cell adhesion. Cells were left to adhere for 1hr in the cell culture incubator (New Bruswick Scientific, Hertfordshire,UK) at 37^oC, 95%O_2/5%CO_2 and 90% humidity. Each cover slip was

washed with plating media and the adhered cardiomyocytes were supplemented with 1ml of fresh plating media. The morphology of a typical myocyte isolation preparation is shown below in Figure 2.10.

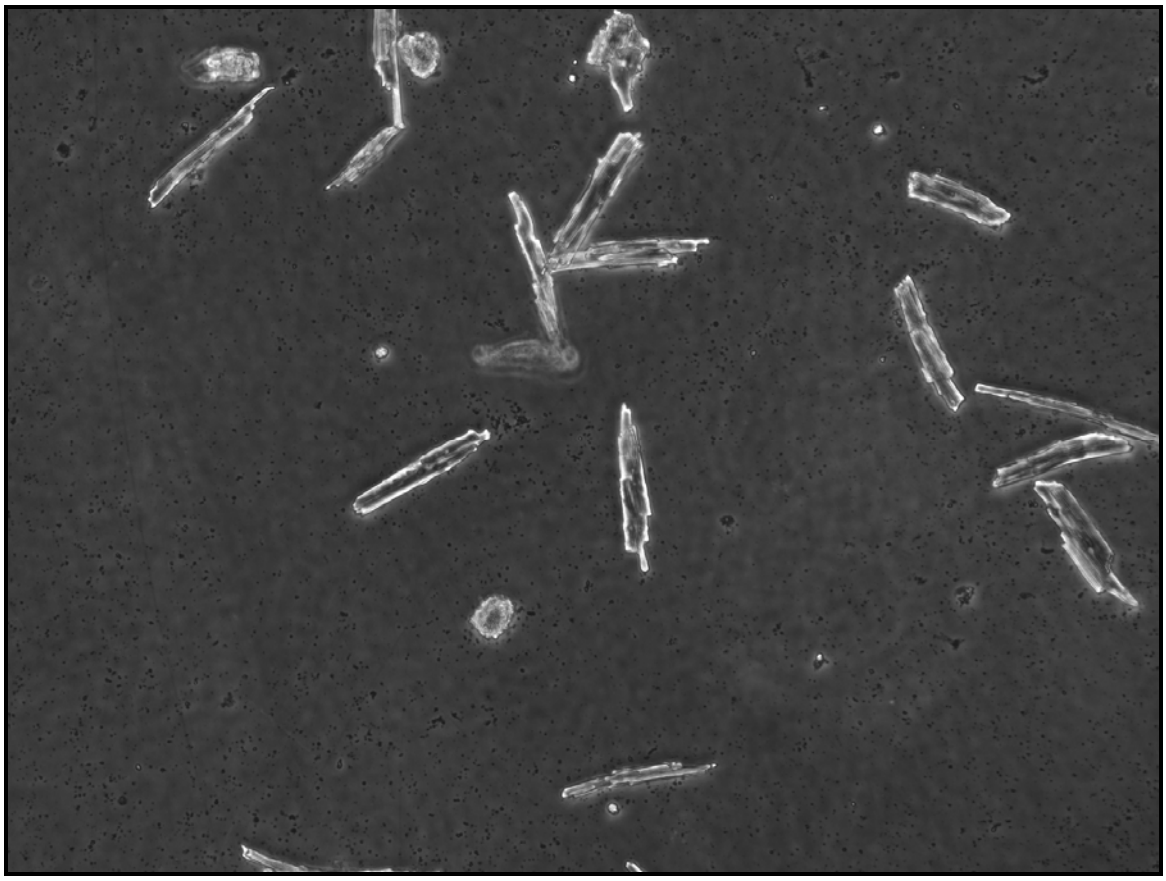

Figure 2.10: Typical morphology of isolated murine myocytes, viewed under light microscope.

2.6.2 Preparations of the cells for imaging mitochondria

The cover slip containing the isolated cardiomyocytes was removed from the plating media and gently blotted dry. The cover slip was then inserted into the confocal metal ring, as shown in Figure 2.11. Cells were covered with a 3μM solution of TMRM (Sigma,UK) diluted in imaging buffer (which consisted of low calcium perfusion buffer without BDM and supplemented with 10mM HEPES pH 7.4 to maintain pH and 1.2mM $CaCl_2$). The cells were

incubated with the dye for 15 min at room temperature. The TMRM containing media was removed and cells were incubated at RT for 5 min in either imaging buffer alone or CsA (0.4μM, diluted in imaging buffer) used as a positive control. Using microscope oil as an interface between the objective and cover slip the cells were mounted onto the confocal microscope ready for visualisation of the mitochondria.

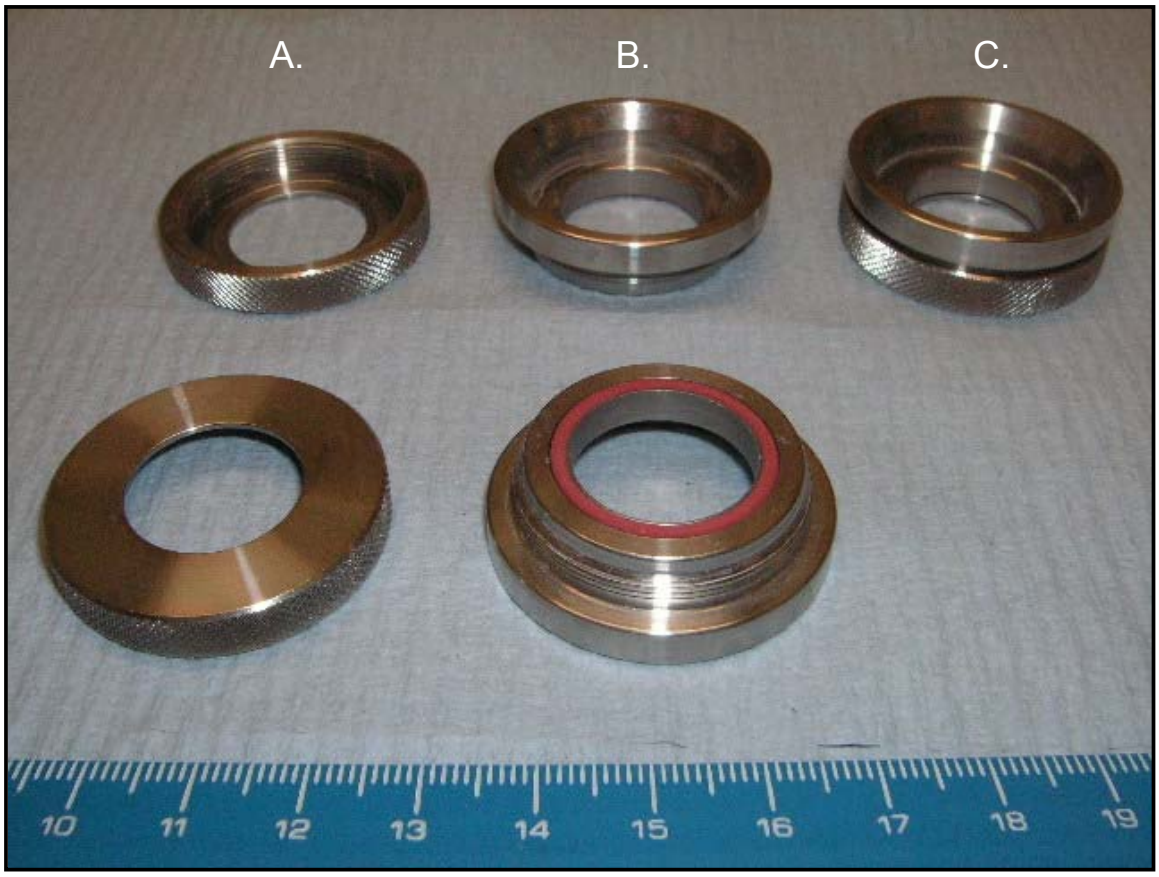

<u>Figure 2.11:</u> Metal rings (A,B) used to secure (C) cover slips, which are coated with myocytes, prior to viewing on the confocal microscope.

2.6.3 Visualising the mitochondria and measuring time to reactive oxygen species induced depolarisation.

Marvin Minsky was the founder of 3D microscopic imaging, using multiple fluorescent labelling, of living cells and tissues. The use of confocal microscopy has continued to expand (Paddock, 2000). We used pinhole confocal microscopy for fluorescent imaging of mitochondria. The cells on the cover slip were secured in the microscope chambers, as shown in Figure 2.11, and were mounted on the stage of a confocal microscope DMI3000B (Lecia Microsystems, Germany,) equipped with s 40x optical objective (numerical aperture was equal to 1.25) with immersion oil (Type F immersion oil, Leica, Germany). The Leica application suite for Advanced Fluorescence (LAS AF) was the software linking the confocal laser (Leica TCS SP5) to the microscope. The settings used to image the cells are described below and an example of the system set up is shown in Figures 2.12.

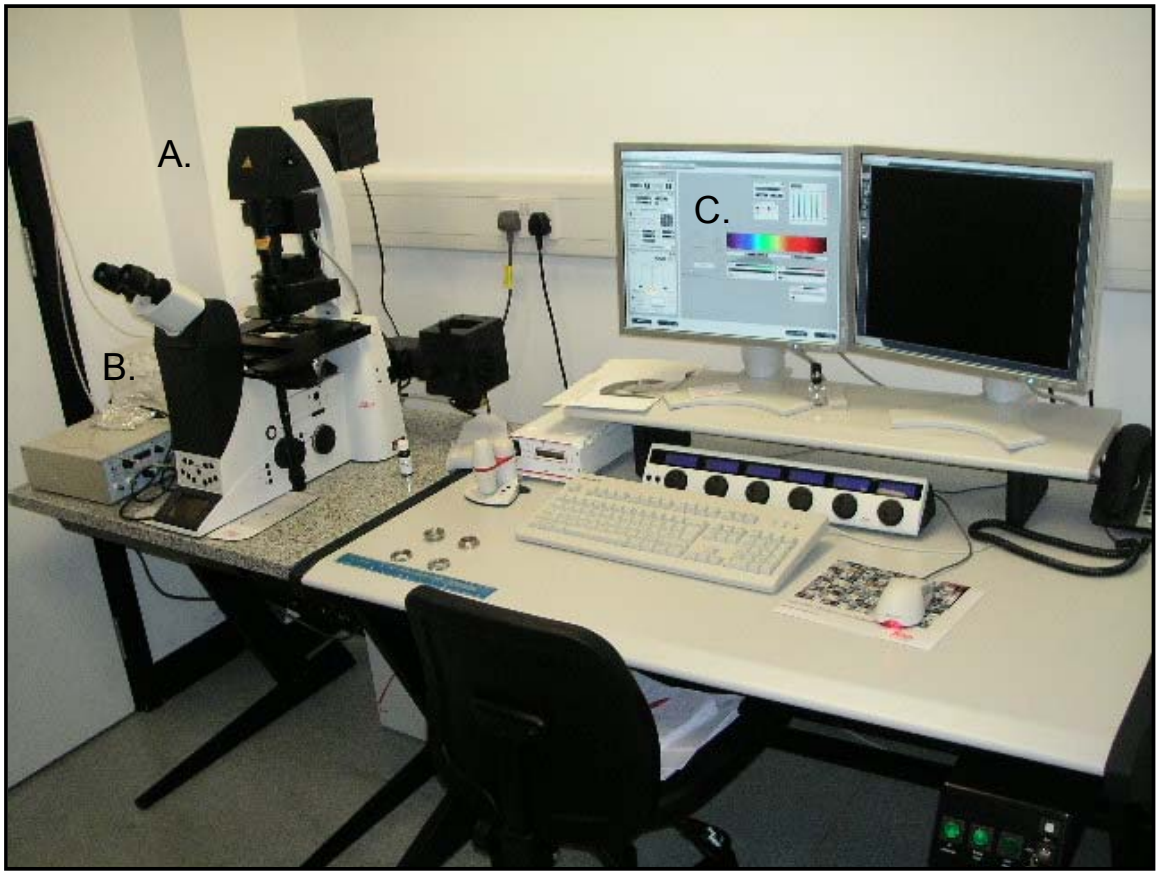

Figure 2.12: The equipment required for the Leica Application Suite, used for investigating time to cardiomyocyte depolarisation: A) confocal microscope, B) laser scan head and C) software and data acquisition point.

The TMRM dye is a positively charged lipophilic cation which will accumulate at high negative charge, as in the mitochondria. This fluorophore can be excited with a 543nm wavelength to emit a fluorescent signal which was collected using a long pass filter above 560nm. However, when used in a high concentration, the dye accumulates within the mitochondria and the fluorescence is quenched. When the dye is excited the contrast in fluorescence from quenched and non quenched TMRM provides an outline of the mitochondria in-situ. An example of the TMRM staining and imaging of the mitochondria is shown in Figure 2.13.

Following ischaemia-reperfusion the mPTP opens which can initiate signals for cell death (Crompton, 1999). Reoxygenation of an ischaemic area can signal the formation of the mPTP

to facilitate pore opening, rapid equilibration of ions across the membrane and a collapse of the mitochondrial membrane potential. This is an indicator of imminent cell death (Griffiths and Halestrap, 1995; Crompton, 1999). The excitation of the TMRM dye in the mitochondria can generate ROS (Zorov et al., 2000), which has been reported to induce the mPTP opening and mitochondrial depolarisation (Smith et al., 2006; Davidson et al., 2006). We used confocal microscopy and TMRM-generated ROS in isolated ventricular myocytes as a model of the injury that occurs at the mitochondria during reperfusion. The laser beam path settings on the Lecia Application Suite were as follows.

Confocal images were acquired using xyt (x, y, time) mode at a scan rate of 400Hz, with a pinhole size of 67.91μM and a zoom of 1 with a line average of 2 and a frame average of 1. This provided a 512x512 format image with an actual size of 387.50μM x 387.50μM (pixel size of 758.32nmx758.32nm). The HeNe laser used to excite the TMRM was set to 60% power, sufficient to generate ROS from the loaded TMRM. The image gain was set to 338V. Sequential images were acquired at 2.633s intervals until depolarisation occurred. An example of the images indicating mitochondrial depolarisation is shown in Figure 2.13. The TMRM dye showed individual mitochondria are located in a structured formation striated along the cell. Closer images were not collected at the time of this study and any attempts to zoom in on the original images collected during these experiments substituted resolution for magnification. Therefore, no further images are displayed in this thesis. Results are expressed as time to TMRM release and mitochondrial depolarisation.

The time from commencement of TMRM excitation until the time of depolarisation was recorded. Cyclosporine A (CsA), known to bind cyclophilin D, thus preventing the formation of the mPTP, and delaying pore formation, opening and mitochondrial depolarisation (Griffiths and Halestrap, 1995) and was used as a positive control. The time to depolarisation in isolated cardiomyocytes from $PTEN^{+/+}$ and $PTEN^{+/-}$ was compared with and without CsA.

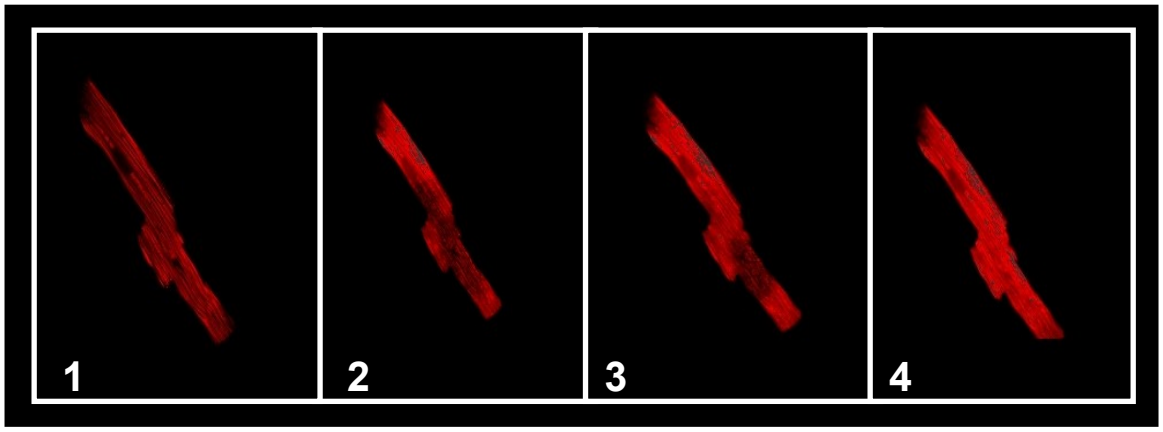

Figure 2.13: Fluorescent imagining of an isolated cardiomyocyte loaded with Tetra methyl rhodamine methyl dye. Frames 1-4 display the change in intensity as the dye is released from the mitochondria into the cytoplasm to indicate mitochondrial depolarisation.

2.7 Protein analysis using Western blot analysis

The protocol for Western blot analysis was originally described by W.N Burnette in 1981 and combines molecular and immunological technologies to analyse the expression of proteins (Burnette, 1981). Sodium dodecyl sulfate - polyacrylamide gel electrophoresis (SDS-PAGE) is used to separate proteins according to their molecular weight. Antibodies are used to visualise the levels of total protein expression or phosphorylation, specific to the protein of interest. The western blot protocols used in the Hatter Cardiovascular Institute have been validated and subsequently published (Mocanu et al., 2002; Bell and Yellon, 2003; Tsang et al., 2005), as described below. Western blot analysis enables a qualitative investigation of proteins separated by gel electrophoresis. Proteins are identified by their transfer to a membrane, which facilitates immuno-identification and analysis of specific proteins. An outline of the method used is shown in Figure 2.14.

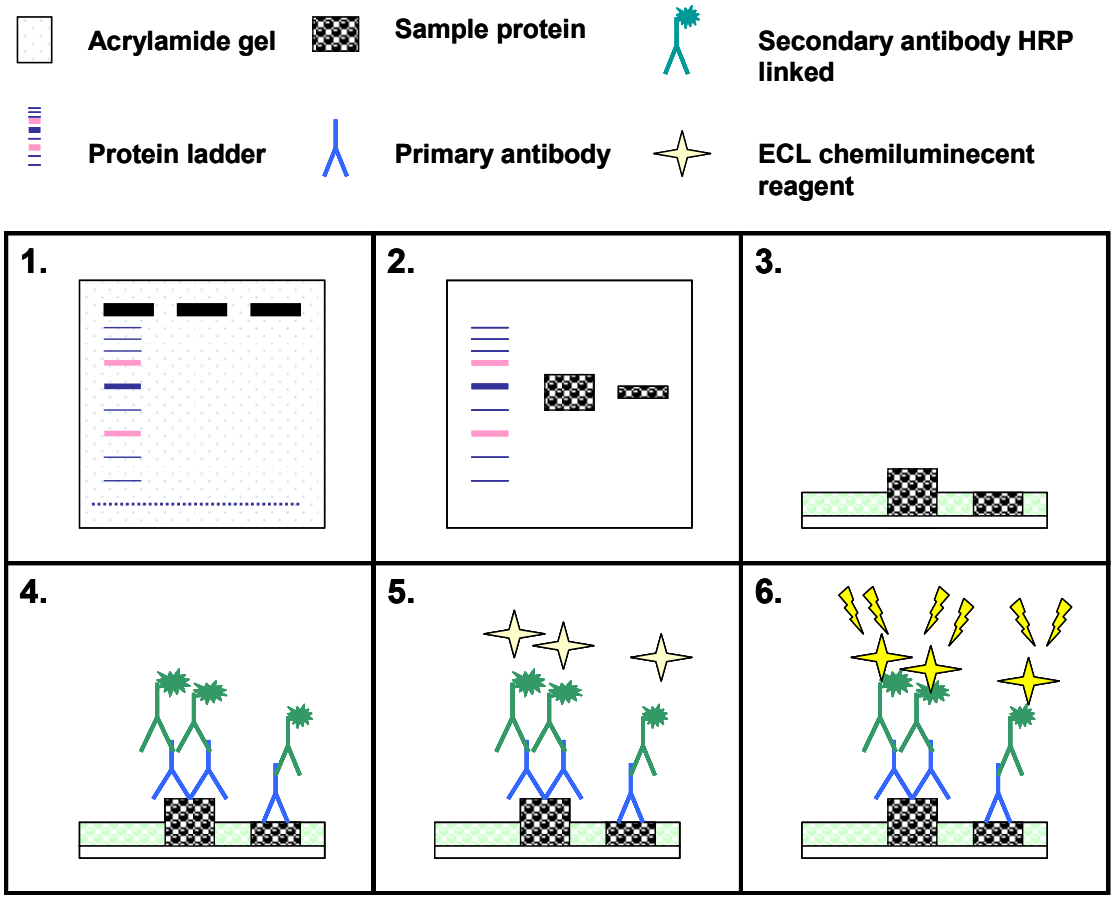

Figure 2.14: **A schematic presentation of the sodium disulphide poly acrylamide gel electrophoresis and Western blot techniques. 1) Sample proteins are loaded onto an acrylamide gel and separated by electrophoresis. 2) Proteins are transferred to a membrane. 3) The membrane is blocked with milk proteins. 4) Primary antibody to protein of interest binds the protein located on the membrane. 5) Secondary antibody conjugated to horse radish peroxidase (HRP), binds to primary antibody. 6) Electrochemiluminescence (ECL) reagent reacts with HRP and emits a light signal that is correlated to the amount of protein of interest.**

2.7.1 SDS-PAGE sample collection

2.7.1.1 Myocardial models

The protocols used to collect myocardial samples for Western blot analysis are described in more detail in the relevant experimental chapters. The ventricular tissue of all hearts was collected by rapidly trimming the aorta and atrial appendages. The remaining tissue was immediately snap frozen in liquid nitrogen and stored at -80^{o}C.

2.7.1.2 Cell models

Cell samples collected for Western blot analysis were prepared as follows. At the end of the experiment, cells were washed on ice with ice cold PBS. The washing buffer was removed and the cells were homogenised in whole cell lysis buffer (1 part suspension buffer (0.1M NaCl, 10mM Tris, 1mM (pH 8.0) EDTA, 2mM Sodium Pyrophosphate, 2mM NaF, 2mM B-glyerophosphate, protease cocktail and 0.5mM AEBSF) and 1 part sample buffer (l00mM Tris (pH 6.8), 200mM DTT, 2% SDS, 0.2% Bromophenol blue and 20% Glycerol). The cells were scraped from the surface of the cell culture plate with a pipette tip to ensure maximal whole cell lysis; samples were stored at -80^{o}C.

2.7.2 Protein extraction

2.7.2.1 Myocardial models

Cytoplasmic proteins were extracted from heart samples that were previously snap frozen in liquid nitrogen. Samples were homogenised in ice cold suspension buffer, on ice. Homogenates were centrifuged for 10 min at 12900 RCF at 4^{o}C. Small aliquots of extracted protein were quantified using a bicinchoninic acid assay (BCA) (Sigma, UK); This is a

colorimetric assay where peptide bonds in the protein samples reduce Cu^{2+}, present in the BCA reagent, to form Cu^{1+}. The bicinchoninic acid in the BCA reagent then chelates the $Cu1^{+}$, (a temperature sensitive reaction aided by cysteine, tyrosine and tryptophan amino acids in the protein samples producing a change in colour, from light green to purple. This change in optical density can be measured by an absorbance reader at a wavelength of 562nm, and is proportional to the level of protein in each sample. A BSA protein standard curve was created with each BCA assay. The extracted remaining protein, in suspension buffer, was then diluted at a 1:1 ratio in SDS sample buffer and heated to 95^{o}C for 10 min to ensure protein denaturation.

2.7.2.2 Cell models

Equal volumes of whole cell lysates (already collected in the cell lysis buffer) were heated at 95^{o}C for 10 min and were loaded directly to the acrylamide gel ready for protein separation by SDS-PAGE.

2.7.3 SDS-PAGE

2.7.3.1 Preparing and running PAGE

The SDS in the sample buffer is an anionic detergent which denatures proteins and provides a uniform charge across the samples. Therefore, when a current is applied the proteins loaded in the gel migrate according to their molecular weight and resistance in that matrix. A polyacrylamide gel is used to separate the proteins and is prepared by the polymerisation of acrylamide and bis-acrylamide. The polymerisation is initiated by the addition of ammonium persulfate (APS) and tetramethylethylenediamine (TEMED). This reaction releases free radicals causing the acrylamide to cross link and solidify which creates pores of equal size in

a 3D gel matrix. We used a 12.5% running gel (consisting of 12.5% acrylamide, 0.4M Tris, 0.1% SDS, 0.1% TEMED and 0.05% APS) and a 5% stacking gel (consisting of 5% acrylamide, 0.125M Tris, 0.1% SDS, 0.2% TEMED, 0.1% APS and 0.02% bromophenol blue) 30µg protein was loaded per lane with one lane per gel assigned for a standard precision plus protein marker (BioRad, UK). This protein marker is used for quality control when running and transferring the gel. In addition, the protein weight marker (containing bands of known molecular weight) can be used as a reference point for the identification of proteins of interest, based on molecular weight. Gels were run in 1x running buffer (10x = 144.2g glycine, 10g SDS, 30.3g Tris in a litre of dH_20) at 200V until the bromophenol reached the bottom and good separation of the protein marker occurred.

2.7.3.2 Protein transfer

To prepare the proteins for visualisation they were transferred from the acrylamide gel to Western blot transfer paper, Hybond electrochemiluminescence (ECL) (GE Health Care, UK). The nitrocellulose transfer paper and Whatman blotting paper were pre-soaked in 1x transfer buffer (10% 10x transfer buffer (10x transfer buffer = Glycine 144.2g, Tris 30.3g, in 1litre distilled water) 20% MeOH and 70% water. The gel and the membrane were sandwiched together between the Whatman paper. Air bubbles were removed, the cassette closed, loaded into the tank according to the direction of the protein transfer and immersed in transfer buffer. The protein transfer was set to run at 140mA overnight. When an electric current is applied to this set up the negatively charged proteins in the gel move towards the positive electrode and are caught on the nitrocelluose membrane. As a consequence, at the end of the protein transfer period a mirror image of the gel is formed.

2.7.4 Protein detection

Detection of the proteins on the Western blot membrane is based on immunological reactions, as shown in Figure 2.14, and requires antibody-antigen binding to localise proteins of interest (similar to an ELISA reaction). To visualise the proteins, membranes were probed with the antibody of interest which were identified using a chemiluminescence reaction. The membrane was incubated in 5% blocking buffer (5% marvel milk in 1x Tris buffered saline (TBS) containing 0. 1%Tween20 (TBS-Tween20) (10x TBS = Tris base 24.2g, NaCl 80.0g pH7.6) at RT for 1hr. The role of the blocking buffer was to cover up the remaining areas of the membrane with protein and therefore, to reduce non specific binding of the antibody of interest to the membrane. Thereafter, the membrane was rinsed 3 times with 1xTBS-Tween20. A primary antibody with specificity to an epitope on the protein of interest was diluted according to the manufacturer's instructions. Primary antibodies were diluted in 5% BSA made up in TBS-Tween20 and incubated with the membrane for a minimum of 2h at RT. The primary antibodies used were as follows: total AKT, phosphorylated AKT (for Ser473 and Thr308 phosphorylation sites), total PTEN, phosphorylated PTEN (for Ser/Thr 380/382&383 phosphorylation sites), total p53 and caspase 3 were all from Cell Signalling technologies, UK. SHIP2 and PHLPP were from Bethyl laboratories,USA and PINK1 was obtained from Abcam, UK. Additionally, antibodies used for analysis of equal protein loading, such as Beta Actin, alpha Tubulin and glyceraldehyde 3-phosphate dehydrogenase (GAPDH), were all from AbCam, UK and were used to normalise for any loading discrepancies. The primary antibodies were then washed off 3 times in 1xTBS-Tween20 and the secondary antibody (HRP linked) was prepared in 5% blocking buffer and incubated with the membrane for 1hr at RT according to the manufacturer's recommendations. After the final wash an ECL reagent (GE Healthcare,UK) was used to start the chemiluminescences reaction. The membranes were incubated in ECL reagent for 5 min before exposure to ECL Hyperfilm (GE Health care, UK). The ECL is a chemiluminescent reagent which contains peroxide acid, luminal and phenol. When this reagent is added to the membrane HRP, bound to the secondary antibody

which is attached to the protein of interest on the membrane, induces an oxidative reaction in the ECL reagent. Therefore, the emission of light correlates to the amount of HRP-primary/secondary antibody conjugate and this is indicative of the expression of the protein of interest bound to the membrane.

The Hyperfilm-autoradiography paper, which is sensitive to blue light (emission of light at 428nm wavelength), was exposed to the luminescence reaction. The paper was then incubated in developer (which catalysed the area of light sensitivity) followed by fixer solution (which stopped the reaction and dissolves the light sensitive coating). This reaction exposes a black band on the autoradiography paper and is an indicator of location and quantity of the protein of interest. These bands were scanned into the computer for densitometry analysis using NIH Image.3.63. The relative density of the scanned bands were compared and expressed in arbitrary units (A.U) or as percentage change from control.

Membranes requiring re-probing were washed and striped of antigen antibody reactions by submersing the membrane in Restore Plus Western blot stripping buffer (Thermo Scientific, USA). Membranes were stripped for 10 min at RT with gentle agitation. Membranes were washed 3 times before re-blocking and probing for additional proteins or house keeping proteins to normalise for lane loading.

2.8 Studies using H9c2 cells silenced for PTEN protein expression with small interfering RNA technology

2.8.1 Cell culture of H9C2 cells

H9c2 cells are an adherent rat cardiac cell line with myoblast morphology. These cells were originally sourced from the European Collection of Cell Cultures (ECACC) ECACC number

88092904 (Kimes and Brandt, 1976) and were obtained within UCL. An example of the cell morphology is shown in Figure 2.15. Cells were cultured in sterile conditions and were grown in culture media and maintained in a New Bruswick Scientific incubator at 37^{o}C in 95%O_2/5%CO_2 with 90% humidity. H9c2 cell culture media was MEM (minimum essential media with Earles salts and 2mM glutamine) (Invitrogen-Gibco,UK) culture media supplemented with 10% FBS (Invitrogen, Gibco), 50U/ml Penicillin (Gibco/Invitrogen,UK) and 5µg/ml Streptomycin (Gibco/Invitrogen,UK). Cells were sub-cultured when they grew to a confluence of 70-80%. This was achieved by covering cells in 0.25 % Trypsin/EDTA (Invitrogen/Gibco, UK) for 2 min at 37^{o}C, to detach the cells from the surface of the culture plate. Cells were then seeded at a 1 in 10 dilution, in a fresh 75 cm^2 growth culture flask (Orange Scientific, Belgium), this was performed twice a week. Growth of cells in clusters, groups or to confluence was avoided, as under these circumstances, H9c2 cells can differentiate into myotubules.

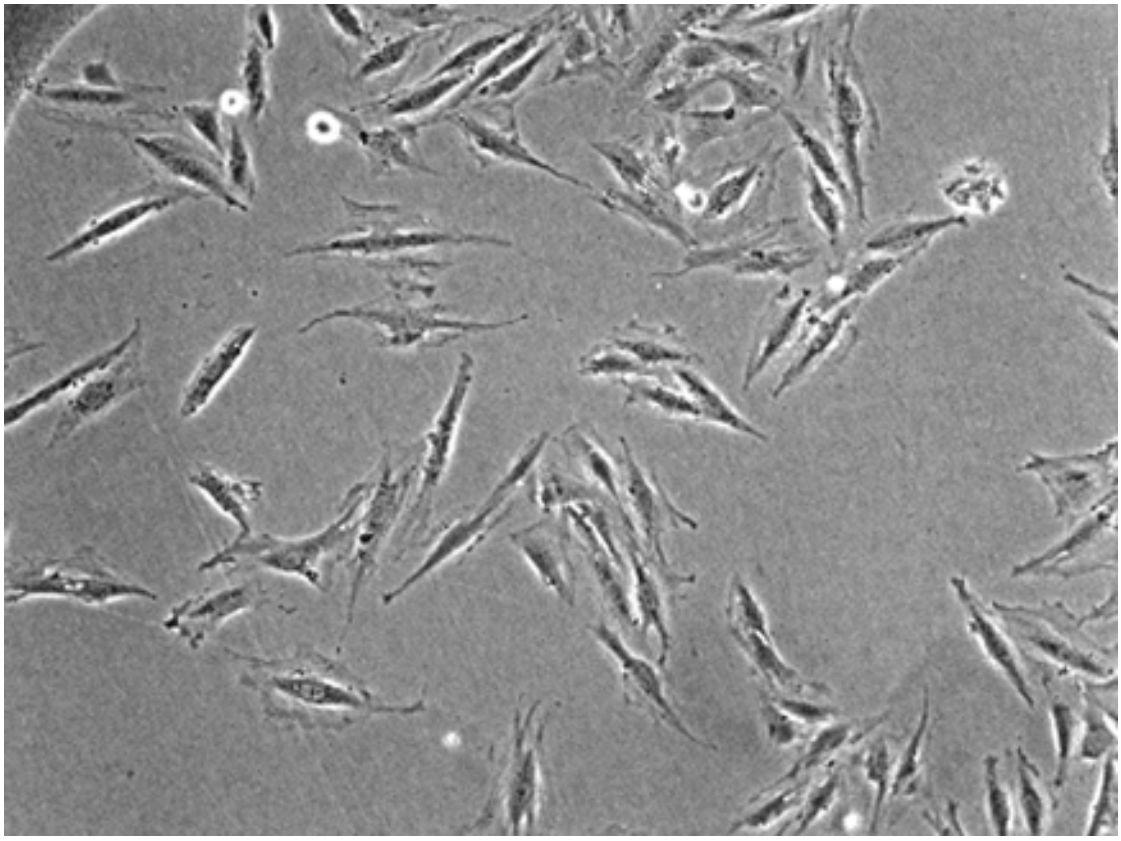

Figure 2.15: Typical morphology of the myoblast H9c2 cell line.

2.8.2 SiRNA knockdown of PTEN protein

In 2006 Fire and Mello won the Nobel Prize in Physiology and Medicine for their contributions to the discovery of RNA interference (Couzin, 2006). The discovery that double stranded RNA can suppress gene activity has led to much excitement and as a consequence the technology is evolving. An overview of the method is illustrated in Figure 2.16. The technique facilitates the manipulation of the cells' natural transcriptional and translational mechanisms to silence the expression of the specific protein of interest. The addition of double stranded RNA with specificity to a target transcript prevents the translation of that protein whilst the genome itself remains unaltered (Caplen et al., 2001).

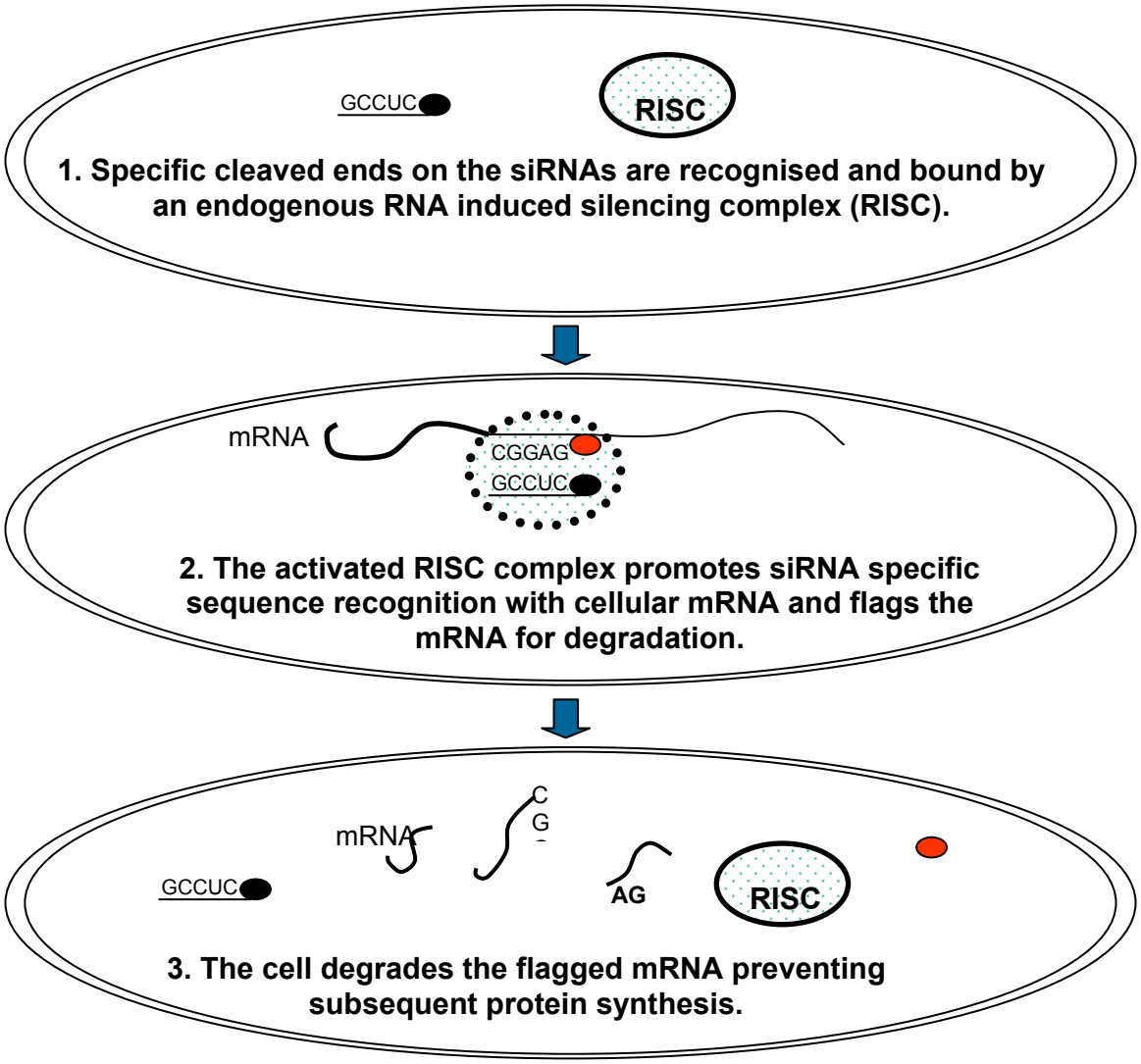

Figure 2.16: Principle of small interfering RNA (siRNA) induced silencing of target proteins. The siRNA complexes that are specific for the target protein, are recognised within the cell by a RNA-induced silencing complex (RISC). The cell attaches a degradation flag on anything that is bound to the siRNA, such as the protein transcripts for the target protein. This destroys the mRNA for the target and prevents protein synthesis. (RNA = ribonucleic acid, mRNA = messenger RNA)

The process of siRNA protein silencing was not previously established within the Hatter Institute. Therefore, we had to perform a number of optimisation studies to verify that it was

possible to knock down the expression of specific proteins in H9c2 cells. These experiments are described in more detail in chapter 7. An overview of the methods used in to study PTEN silencing with siRNA is described below.

Cells were sub-cultured; counted using a haemocytometer and seeded at 4,000cells/3.8cm^2 (in 12 well plates) (Sigma, UK). Immediately after seeding, cells were gently placed in the incubator (avoiding vortexing and pooling of cells) and left to adhere for 6-8h. Once they were adherent and their usual morphology had returned, cells were transfected with either reagent control or reagent-siRNA primers complex. The reagent-siRNA complex targeted either non coding scrambled primers (control), GAPDH or PTEN protein. All siRNA primers were purchased from Ambion. The sequences are shown in Table 2.3. GAPDH siRNA was used in the initial optimisation experiments and every experiment included a scrambled siRNA control. The Silencer® pre-designed PTEN primers were purchased from Ambion with a guarantee 1 out of 3 purchased siRNA primers would knockdown PTEN protein with 80% efficiency. The extent of the protein knock down was verified before routine use, by Western blot technique.

To transfect cells, the growth media was replaced with fresh culture media and transfection reagent was added to each well. The X-tremeGene siRNA transfection reagent, a multi lipid component, was used. A reagent-siRNA complex was generated at a 3:1 ratio of reagent (ul) to siRNA (ng), in 1/10th of the final well volume in serum and antibiotic free culture medium. This reagent-siRNA complex is required for membrane penetration and transfer of siRNA across cell membranes. Cells were transfected overnight for approximately 12h, after which the medium containing the transfection complex was replaced with fresh growth medium. We observed that the time for PTEN protein turnover (time for remaining PTEN to be degraded) within these transfection conditions was 60-72h, following which the medium was removed

and the cells were prepared for protein analysis (as described in the Western blot protocol) or induction of hypoxia-reoxygenation.

Table 2.3: The sequence of oligonucleotides for the siRNA primers used in this study. GAPDH = Glyceraldehyde 3-phosphate dehydrogenase, PTEN Phosphatase and tensin homolog deleted on chromosome 10 and siRNA = small interfering ribonucleic acid.

siRNA target	Anti-sense (5'-3')
• Scrambled Silencer® control siRNA	CCGUAUCGUAAGCAGUACUTT
• GAPDH Silencer® control siRNA	AAAGUUGUCAUGGAUGACCTT
• PTEN primer 1, Silencer® pre-designed to exon 2	ACAUCAUCAAUAUUGUUCCTG
• PTEN primer 2, Silencer® pre-designed to exon 5	UGAUAAGUUCUAGCUGUGGTG
• PTEN primer 3, Silencer® pre-designed to exon 5.	CAAGAUCUUCACAAAAGGGTT

2.8.3 Hypoxia-reoxygenation

An appropriate protocol for the induction of cell death using hypoxia-reoxygenation (duration of hypoxic buffer) in H9c2 cells was established, based upon past protocols and published techniques used at the Hatter Institute. We reinstated the methods for hypoxia and reoxygenation (duration and hypoxic buffer) (Smith et al., 2007; Lim et al., 2008). The hypoxia-reoxygenation protocol used in this thesis is described below.

Two culture plates were prepared in parallel (normoxia and hypoxia plates) and for each treatment and cells were seeded in replicates of 2 or more wells. After the 60 h transfection protocol, described above, cells were serum starved overnight: by replacing growth media

with serum free media. 12 h later media was removed and cells were either maintained in normoxia or incubated in hypoxic conditions, as described below.

2.8.3.1 Maintaining normoxia

Cell medium, was replaced with normoxic buffer (Table 2.4) and cells were placed in the standard cell culture incubator, as previously described, for 24h.

2.8.3.2 Induction of hypoxia

Cell media was replaced with hypoxic buffer (Table 2.4), which was designed to mimic ischaemic conditions. It contains no glucose, elevated potassium levels, lactate and is pH 6.7, reflecting the acidic conditions caused by the accumulation of lactate from increased glycolytic metabolism. The cells were placed in the hypoxic chamber (as shown in Figure 2.17) and maintained at 37^{o}C for 24h. The hypoxic chamber was designed and made in house. It is temperature protected and contains two one-way gas valves which enable the entry of nitrogen into the chamber and facilitates the displacement of oxygen. Thus re-entry of gases into the chamber is prevented providing a low oxygen environment.

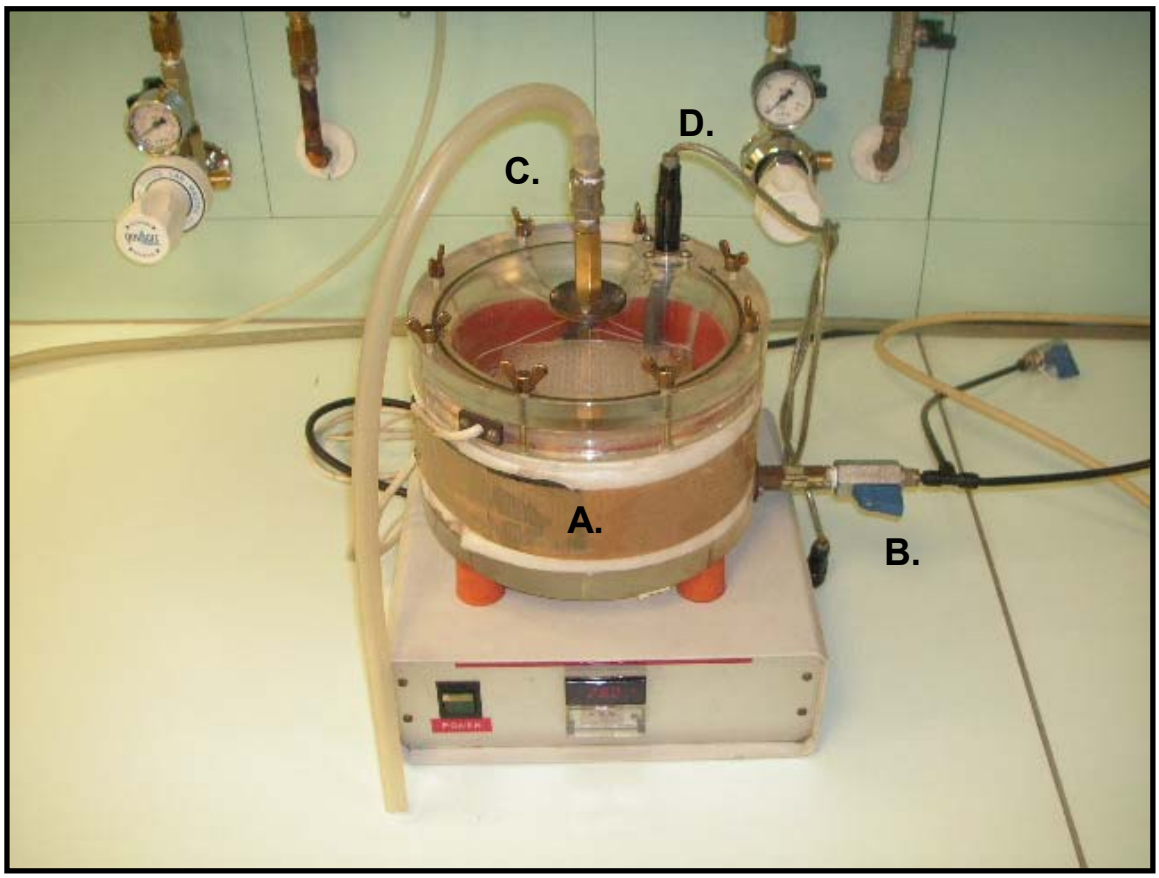

<u>Figure 2.17:</u> The hypoxic chamber used in the hypoxia-reoxygenation experiments: A) heating chamber, B) one way, gas inlet valve, C) one way, gas outlet valve and D) temperature sensor.

Table 2.4: The components of the normoxic and hypoxic buffer. These buffers are abased on a modified KREBS-Ringer N-2-hydroxyethylpiperazine N-2ethanesulfonic acid (HEPES) buffer (Rakhit et al., 2001).

Normoxic Buffer		Hypoxic Buffer	
Compound	**[Final] (mM)**	**Compound**	**[Final] (mM)**
• KH2PO4	1mM	• KH2PO4	1mM
• NaHCO3	10mM	• NaHCO3	10mM
• MgCl2.6H20	1.2mM	• MgCl2.6H20	1.2mM
• NaHEPES	25mM	• NaHEPES	25mM
• NaCl	98mM	• NaCl	74mM
• KCl	3mM	• KCl	16mM
• D-glucose	10mM		
• Na-Pyruvate	2mM	• NaLactate	20mM
• Bubble 95%O2/5%CO2		• Bubble Nitrogen	
• pH 7.4		• pH 7.4	
• $CaCl_2$	1.2mM	• $CaCl_2$	1.2mM
		• De-oxy glucose	5mM

2.8.3.3 Reoxygenation

Following 24hr incubation the cells were reoxygenated for 4hr. Normoxic or hypoxic buffer was removed and gently replaced with MEM growth media lacking FBS and containing propidium iodide (PI) at 10µg/ml (Molecular Probes, UK). Insulin (10µg/ml), known to prevent the injury induced by hypoxia-reoxygenation (Davidson et al., 2006) was used as a positive control. Reoxygenation buffer was used as a control for insulin. At the end of reoxygenation the medium was removed and cells were collected for Western blot analysis.

2.8.3.4 Analysis of cell viability

We performed experiments to determine the best method to asses H9c2 cell viability following hypoxia-reoxygenation. Firstly we investigated the detection of PI, which is a membrane impermeable dye however, when the cell membrane is permeable, as in necrosis or late stage apoptosis, the dye can enter the cell and bind to DNA (Jonassen et al., 2004). Fluorescence from the dye can be excited using a mercury lamp which causes the emission of a red fluorescence which can be recorded as an indicator of cell death.

Secondly, we investigated the changes in lactate dehydrogenase (LDH) release as an indictor of cell death. When the cell plasma membrane is permeabilised, enzymes such as lactate dehydrogenase (LDH) and creatine kinase are released and can be used as an indicator of cell damage (Jonassen et al., 2004). The CytoTox 96 Non-radioactive cytotoxicity assay (Promega, UK), was used in an attempt to measure cell viability in a secondary cell viability model. After reoxygenation, cell medium was collected and assayed following the manufacturer's instructions. Following a number of enzymatic reaction steps this assay measures the activity of LDH in samples. Firstly, lactate and NAD(+) in samples are converted by LDH into NADPH and pyruvate. Next, tetrazolium salts ((2-p(iodophynyl)-3-(p-nitrophynyl)-5-phenyltetrazolium chloride, present in the assay substrate mix, react with NAD(+) to create a red formazan product. In doing so this creates a change in optical density that can be measured at 490nm, which is symptomatic of LDH activity. This is a marker of LDL release and therefore can be used as an indicator of cell and viability (WROBLEWSKI and LADUE, 1955).

The results are presented as a ratio of released LDH in comparison to the total LDH extracted from remaining viable and adherent cells. Further optimisation experiments to detect LDH were required and are described in more detail in chapter 7. Cell suspension and cell lysate

samples were incubated in the assay lysis buffer for 60 min followed by the addition of assay substrate mix. Isolated LDH (provided as a positive control in the assay) at 1.6units/ml, 3.2units/ml and 6.4units/ml was used as a positive control. Changes in the colour were measured by reading the absorbance at 490nm.

Finally, we investigated the detection and changes in expression of cleaved caspase 3. The cleavage of caspase 3 is a determining step of apoptosis and therefore can be used as an indicator of cell damage (Kothakota et al., 1997). This was performed by assessing the expression of caspase 3 in whole cell lysates, collected after reoxygenation; as described in the Western blot protocol above. Antibodies detecting total and cleaved caspase 3, from Cell Signalling Technologies, UK) were used and the ratio of cleaved caspase 3 compared to the total caspase 3, was used as an indicator of cell death.

2.9 Statistics

For comparisons between two groups an unpaired t-test was used. For comparison between more than two groups a One Way ANOVA, using GraphPad Prism4 (GraphPad software inc, California, USA), was used; to analyse between groups the Bonferroni's multiple comparison post hoc test was used. Results were considered significant when $p \leq 0.05$. All results were displayed as group means ± standard error (SE) and the test used was specified in the legend of the appropriate graph.

3 Chapter 3 - Characterisation of the isolated perfused mouse heart model of global ischaemia-reperfusion injury.

3.1 Background and aims

The Langendorff model can be used for studying ischaemia-reperfusion injury in isolated perfused hearts, as described in chapter 2, section 2, and has previously been used within the Hatter Institute (Sumeray et al., 2000; Simpkin et al., 2007). However, optimisation experiments were performed to validate and further characterise the model of ischaemia-reperfusion injury in isolated mouse hearts. It was predicted that future experiments may require varying degrees of ischaemia-reperfusion.

Additionally, in advance of investigating the effects of PTEN inhibition on cardioprotection in isolated perfused mouse hearts, a positive control was required. For this purpose ischaemic preconditioning (IPC), which is initiated by inducing sub-lethal ischaemia and reperfusion cycles prior to a lethal ischaemic event, was selected. IPC is considered the most powerful protective mechanism against infarction (Murry et al., 1986; Yellon and Downey, 2003).

3.2 Experimental protocols, methods and hypothesis

The Langendorff perfusion apparatus was used to study the effects of ischaemia-reperfusion on isolated perfused mouse hearts, as described in chapter 2, section 2. Infarct size was assessed as an end point. To validate this model the effects of submersion buffer, mouse strain, duration of ischaemia and reperfusion, and various IPC protocols on myocardial infarction was investigated.

3.2.1 Infarction and ischaemic buffer

NIH Swiss white mice were used for the initial Langendorff characterisation studies. The level of infarction induced by 30 min stabilisation followed by 35 min ischaemia and 30 min reperfusion, was compared in the presence of either oxygenated (n=22) or non oxygenated (n=6) submersion buffer, as shown in Figure 3.1. It was hypothesised that the myocardium incubated in non oxygenated submersion buffer would incur a greater level of infarction following ischaemia-reperfusion.

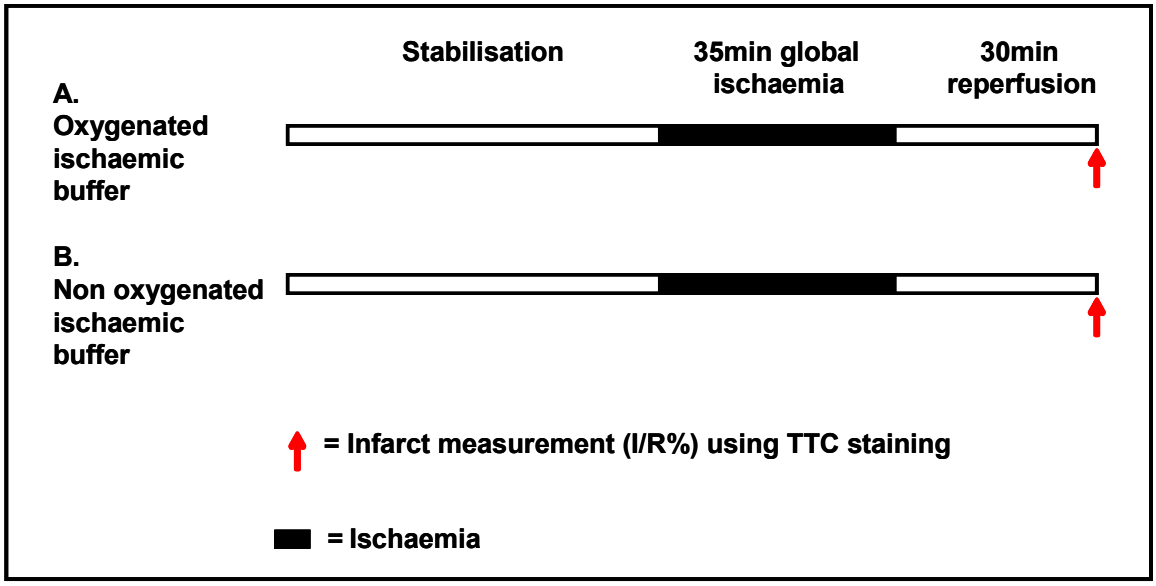

Figure 3.1: Langendorff perfusion protocols used to investigate ischaemia-reperfusion injury. In the presence of A) oxygenated submersion buffer or B) non oxygenated submersion buffer. I/R% = percentage of infarction to risk area TTC = triphenyltetrazolium chloride.

3.2.2 Infarction in different murine strains

The response to ischaemia-reperfusion injury in myocardium from the NIH Swiss White (n=28) and C57BL/J6 mice (n=17) was compared. The standard protocol of 30 min

stabilisation followed by 35 min ischaemia and 30min reperfusion, as shown in Figure 3.1 was used.

3.2.3 Infarction and duration of ischaemia and reperfusion

The infarction developed in C57BL/J6 myocardium, as a consequence of increasing durations of ischaemia (25, 35, 45, 55 min n=5, 17, 5 and 6, respectively) and reperfusion (30 and 120 min, n = 17 and 6, respectively) was investigated.

Sham hearts perfused without ischaemia, time matched to the control protocol, were also collected to establish any basal damage caused by the balloon and/or by the manoeuvres required by the hanging of the heart on the perfusion apparatus. (sham control for 30 and 120 min reperfusion, n = 4 and 4, respectively).

A) Increasing ischaemia time

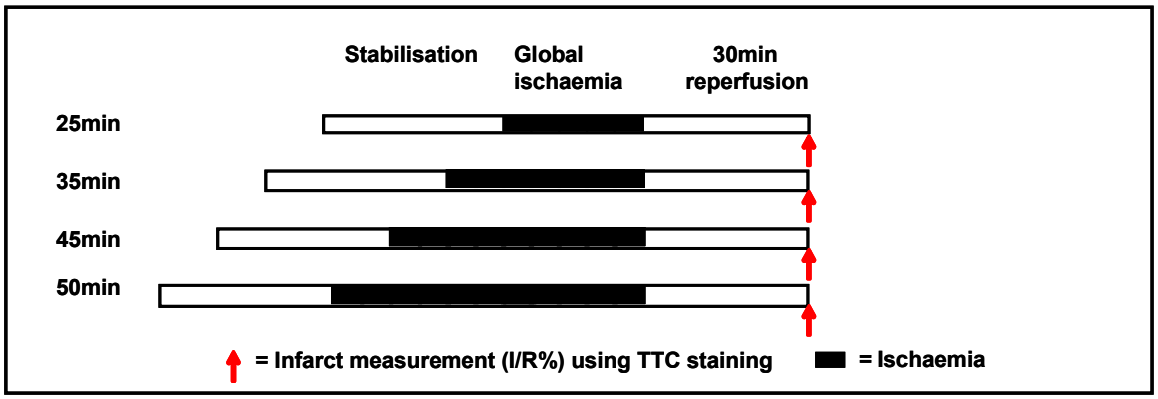

B) Increasing reperfusion time

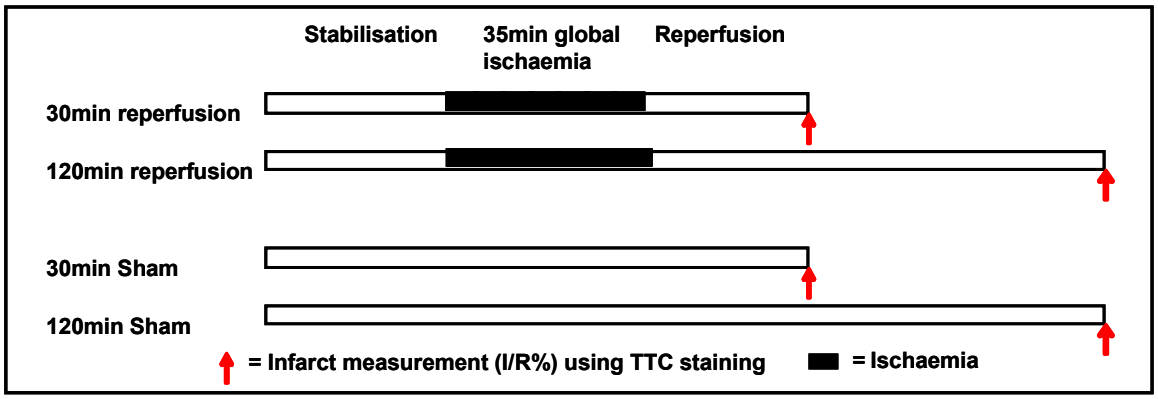

<u>Figure 3.2:</u> Langendorff perfusion protocols used to ischaemia-reperfusion injury: following different durations of A) ischaemia and B) reperfusion periods. I/R% = percentage of infarction to risk area TTC = triphenyltetrazolium chloride.

Various IPC protocols (listed below and shown in Figure 3.3) applied prior to the lethal ischaemia-reperfusion protocol, of 35 min ischaemia and 30 min reperfusion, were investigated in isolated perfused C57BL/J6 mouse hearts.

1) 1 cycle of 5 min ischaemia followed by 15min reperfusion (n=3).
2) 2 cycles of 10 min ischaemia followed by 10min reperfusion (n=3).
3) 1, 2, or 4 cycles of 5 min ischaemia followed by 5 min reperfusion (n=2,2 and 3, respectively).

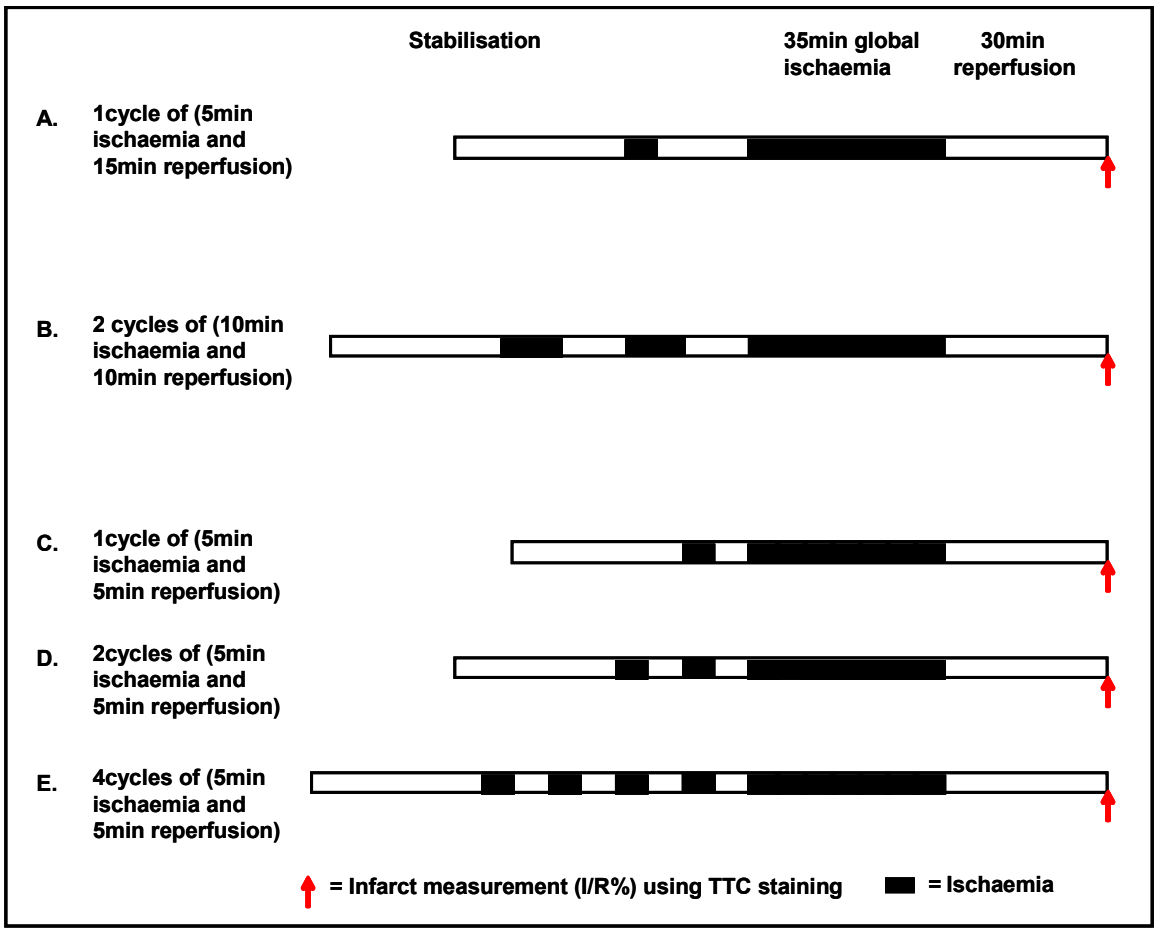

Figure 3.3: Different IPC protocols tested to investigate cardioprotection in isolated C57BL/J6 mouse hearts. I/R% = percentage of infarction to risk area TTC = triphenyltetrazolium chloride.

The best IPC protocol was selected based on results from these characterisation studies and previously established findings in the Hatter Cardiovascular Institute. In order to match the ischaemia-reperfused control hearts with the IPC hearts the stabilisation duration in control hearts was extended from 30 to 55 min, (n=5) as shown in Figure 3.4.

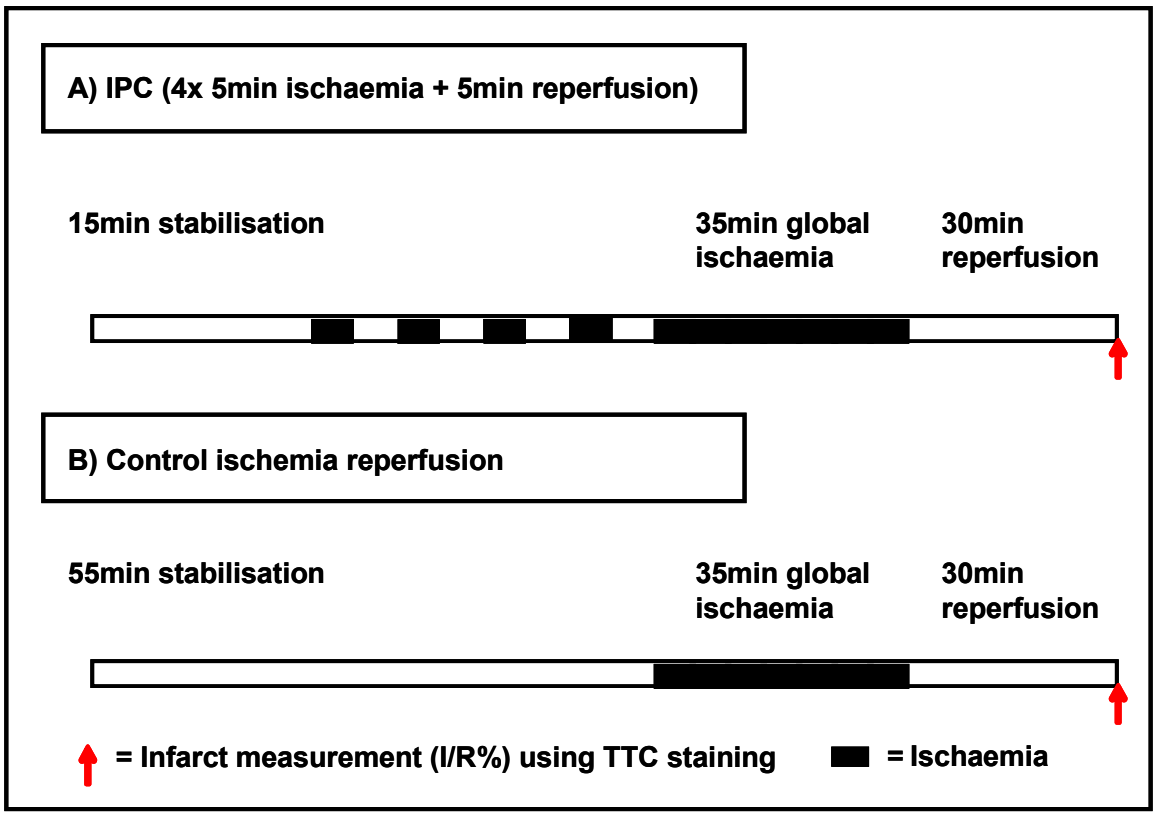

Figure 3.4: The selected IPC protocol used to investigate protection in isolated C57BL/J6 mouse hearts: A) IPC protocol and B) time matched control protocol. I/R% = percentage of infarction to risk area TTC = triphenyltetrazolium chloride.

3.3 Results

3.3.1 Infarction and the submersion buffer

Myocardium from NIH Swiss white mice were subjected to ischaemia-reperfusion, which consisted of 30 min stabilisation followed by 35 min global ischaemia and 30 min reperfusion, (30/35/30). Unexpectedly, the level of infarction incurred was small, 19.03 ± 1.83%. It was hypothesised that the presence of oxygenated submersion buffer surrounding the heart during ischaemia may provide protection due to the passive diffusion of the oxygen into the tissue. As shown in Figure 3.5 this hypothesis was not confirmed because no significant differences were observed when ischaemia-reperfusion injury was investigated in hearts

submerged in oxygenated (19.03 ± 1.83%) compared to non oxygenated submersion buffer (16.82 ± 1.07%).

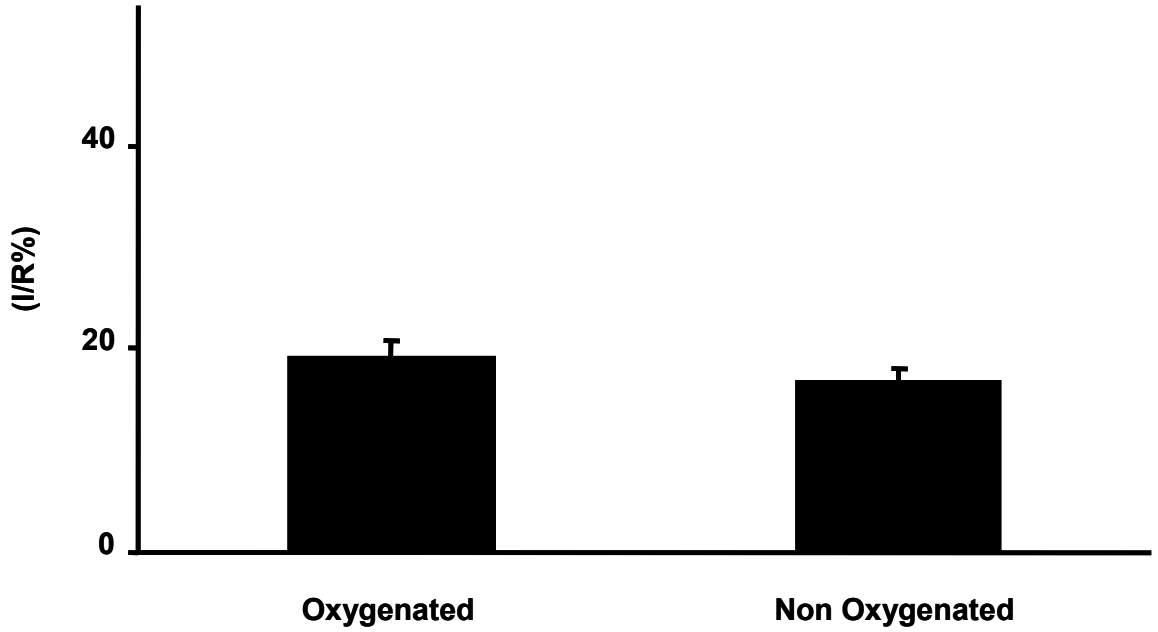

Figure 3.5: Percentage of infarction developed in the risk area (I/R%) in the NIH Swiss White mouse myocardium submersed in normothermic oxygenated (n=22) and non oxygenated (n=6) buffer during ischaemia. There was no statistical differences between groups, assessed using the Student's paired t-test.

3.3.2 Infarction in different murine species

In an attempt to explain the small infarct size in Swiss White mice, it was hypothesised that there may be different susceptibilities to myocardial ischaemia-reperfusion injury in different strains of mice. To investigate this, the level of infarction was compared using the control ischaemia-reperfusion protocol (30 min / 35 min / 30 min) in the myocardium from Swiss White and C57BL/J6 mice. As shown in Figure 3.6 the mean infarct size observed in C57BL/J6 myocardium was significantly higher than in NIH Swiss White myocardium (39.33 ± 3.47%, vs. 18.55 ± 1.43%,$p<0.005$).

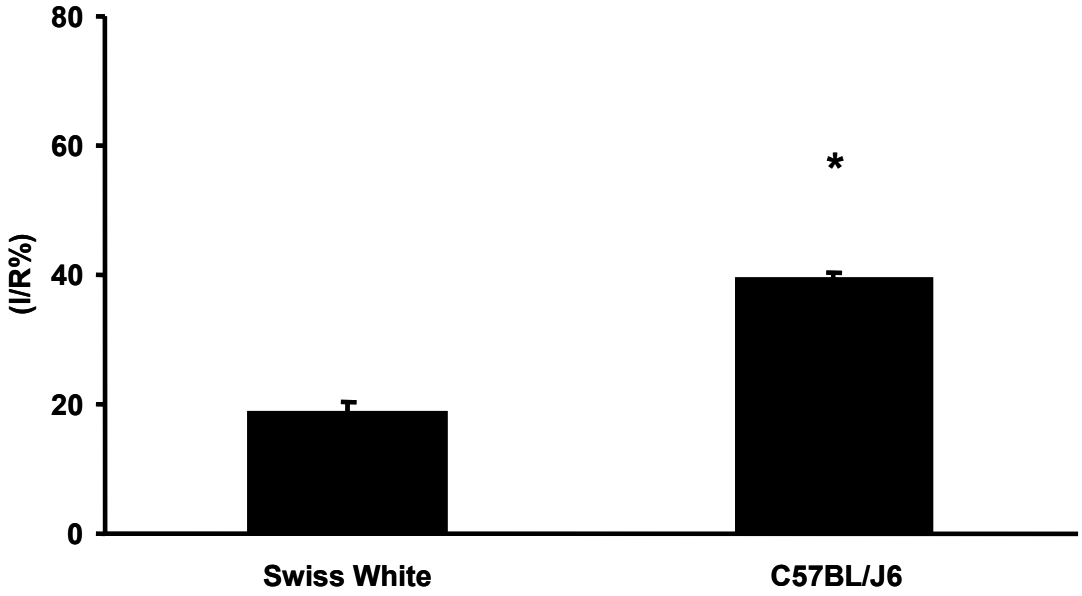

Figure 3.6: Percentage of infarction developed in the risk area (I/R%) in Swiss White mouse myocardium (n=28) and C57BL/J6 mouse myocardium n= 17. Statistical differences were assessed using the Student's paired t-test, (*=p<0.005).

3.3.3 Infarction and the duration of ischaemia and reperfusion

Further optimisation experiments were performed using the C57BL/J6 mouse model in which the hearts were subjected to various durations of ischaemia and reperfusion. The results, shown in Figure 3.7 indicate that, as the ischaemic time increases, infarct size is amplified. For example 25 min of ischaemia induced 28.29 ± 8.2% infarction. Increasing the ischaemic time, from 25min to 35 or 45 min was associated with an augmented infarct size to 39.33 ± 3.47% and 50.28 ± 2.71%, respectively. Furhter on when the ischaemic time was increased to 55 min an even greater infarct size was recorded; 54.92 ± 3.85%, $p<0.05$. The greatest injury occurred at 55 min ischaemia, alternatively the effect of 35 min ischaemia (39.33 ± 3.47%) appeared to be positioned in the linear part of the ischaemic effect response. Therefore, 30 min stabilisation and 35 min, ischaemia followed by 30 min reperfusion may

offer the most manipulative protocol for studying infarct size, whereby detection of changes in ischaemia-reperfusion injury may be more evident.

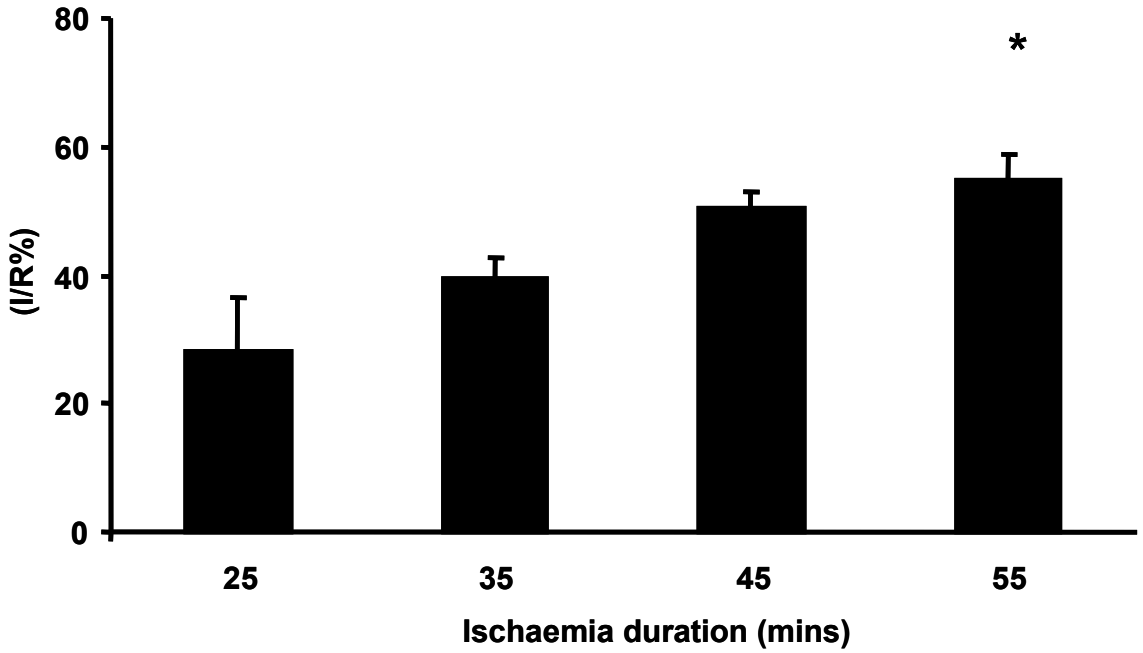

Figure 3.7: Percentage of infarction developed in the risk area (I/R%) in C57BL/J6 myocardium, stabilised for 30 min and subjected to varying durations of global ischaemia, (25min (n=5), 35min (n=17), 45min (n=5) and 55 min (n=6)) followed by 30 min reperfusion. Statistical differences were assessed using One Way ANOVA, (*=p<0.05, 25min to 55mins ischaemia).

In addition to investigating a range of ischaemic durations the effects of various periods of reperfusion on ischaemia-reperfusion injury were also explored. Figure 3.8 demonstrates the level of infarction following increasing durations of reperfusion, while stabilisation and ischaemia time remained fixed at 30 and 35 min respectively. The results indicate there is a significant increase in infarct size (61.72±3.26%, $p<0.001$) at 120 min reperfusion. Interestingly, in the sham (perfusion without ischaemia-reperfusion) hearts developed 6.4±1.56% infarction after 95min perfusion. This duration is equal with an experimental protocol of 30 min stabilisation, 35 min ischaemia and 30 min reperfusion. In comparison,

when the length of time on the perfusion apparatus was extended to 185 min (equating with 30 min stabilisation, 35 min ischaemia and 120 min reperfusion).

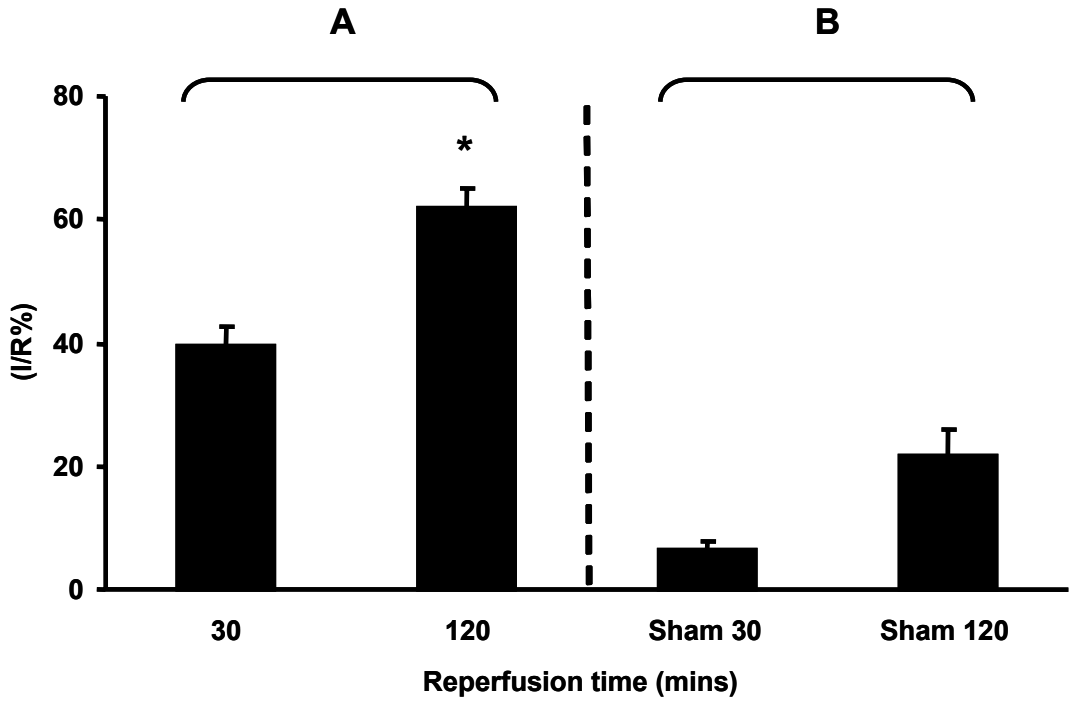

Figure 3.8: (A) Percentage of infarction developed in the risk area (I/R%) subsequent to 30 min stabilisation and 35 min ischaemia followed by either 30 min (n=17) or 120 min (n=6) reperfusion and (B) percentage of infarction developed in the risk area (I/R%) in sham (perfusion without ischaemia-reperfusion) hearts perfused for either 95 min (n=4) or 185 min perfusion (n=4). Statistical differences between 30min and 120min in group A and B were assessed using One Way ANOVA, *=p<0.001.

Heart rate, developed pressure, coronary flow rate and temperature were permenatly recorded throughout experimental protocols. Figure 3.9 represents an example of the haemodynamic recordings, collected during every experiment. Collected data was used to ensure that the hearts were functioning and that the recordings were within the inclusion/exclusion criteria throughout the experiments. However, our aim was not to investigate changes in heart function, we measured infarct size as an end point of the

experiments. Therefore, the haemodynamic recordings will not be presented further in this thesis. For investigating function as an end point there is a more reliable and consistant model of isolated perfused hearts, namely the “working heart model” which was not used in this study.

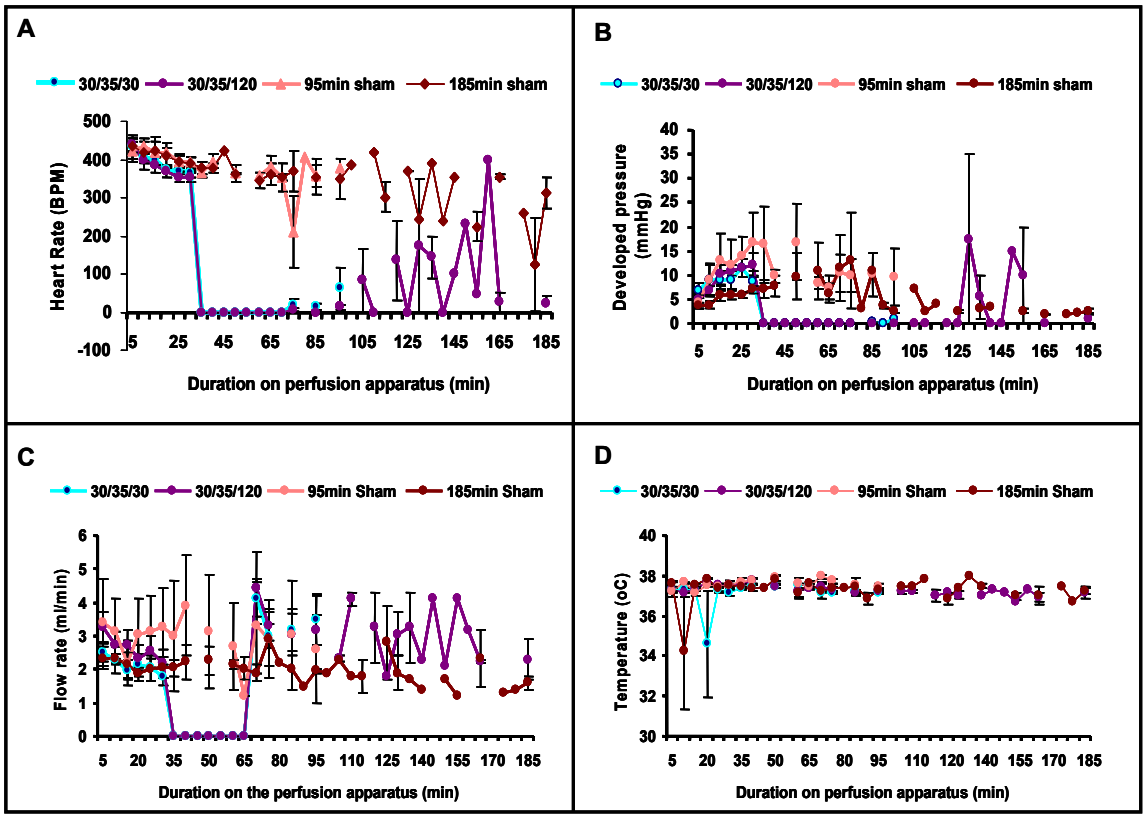

<u>Figure 3.9:</u> Example of haemodynamic measurements during experiments protocols of 30 min stabilisation and 35 min ischaemia followed by either 30 min (30/35/30, n=17) or 120 min (30/35/120, n=6) reperfusion. Data from sham (perfusion without ischaemia-reperfusion) hearts perfused for either 95 min (95min Sham, n=4) or 185 min perfusion (185min Sham, n=4) are also included. A) heart rate in beats per minute (BPM), B) developed pressure in mmHg, C) flow rate in ml/min and D) temperature in degrees celsius (°C).

3.3.4 Infarction and the ischaemic preconditioning protocol

The optimum number of preconditioning cycles required to protect the C57BL/J6 mouse myocardium, subjected to our protocol of 30 min ischaemia and 35 min reperfusion was investigated. Figure 3.10 and Figure 3.11 show the results of the IPC optimisation experiments. Historically, in the Hatter Institute, IPC in the mouse myocardium was induced using 4 cycles of 5 min ischaemia followed by 5 min reperfusion (Bell and Yellon, 2001). Other laboratories have induced protection with alternative protocols, for example 3 cycles of 5 min ischaemia (Lange et al., 2007). Conversely, 1 cycle of 5 min ischaemia and 15 min reperfusion has been used to initiate cardioprotection (Turcato et al., 2006). However, as shown in Figure 3.10 the alternative protocols investigated did not facilitate protection in our C57BL/J6 mouse model. In our hands, as presented in Figure 3.9, 4 cycles of 5 min ischaemia followed by 5 min reperfusion were required to confer protection in the C57BL/J6 myocardium. Infarction was reduced from 50.4± 4.6% in control to 38.2 ± 3.3% in the presence of 4 cycles of IPC stimulus (consisting of 5 min ischaemia and 5 min reperfusion) prior to lethal ischaemia.

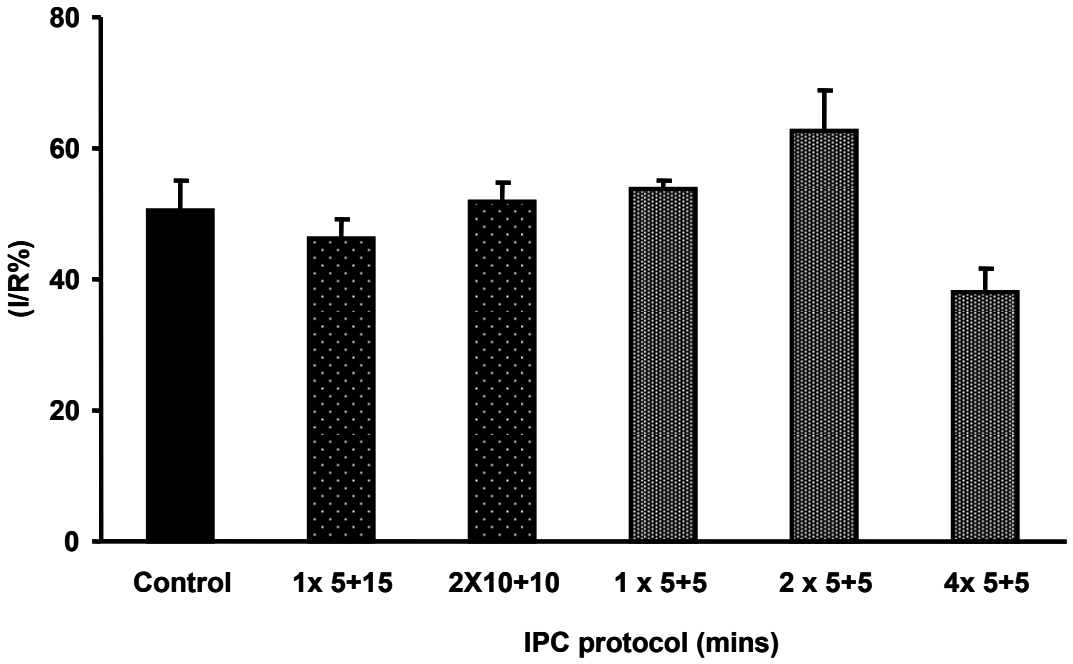

Figure 3.10: Percentage of infarction developed in the risk area (I/R%) in C57BL/J6 myocardium in control and following different ischaemic preconditioning (IPC) protocols, (1x 5+15 min ischaemia-reperfusion (n=3), 2x 10+10 min ischaemia-reperfusion (n=3), 1x5+5 min ischaemia-reperfusion (n=2), 2x5+5 min ischaemia-reperfusion (n=2) or 4x5+5 min ischaemia-reperfusion n=3)) prior to 35 min ischaemia followed by 30 min reperfusion. Statistical differences were assessed using One Way ANOVA. Details of the IPC protocols are shown in Figure 3.3.

The chosen IPC protocol of 4 cycles 5 min ischaemia and 5 min reperfusion lengthened the total myocardial perfusion time. Consequentially, in control hearts the stabilisation duration had to be extended to time match the IPC protocol prior to ischaemia. For more details on this protocol see Figure 3.4. The results are shown in Figure 3.11 and demonstrates a significant reduction in infarction ($35.4 \pm 4.09\%$, $p<0.05$).

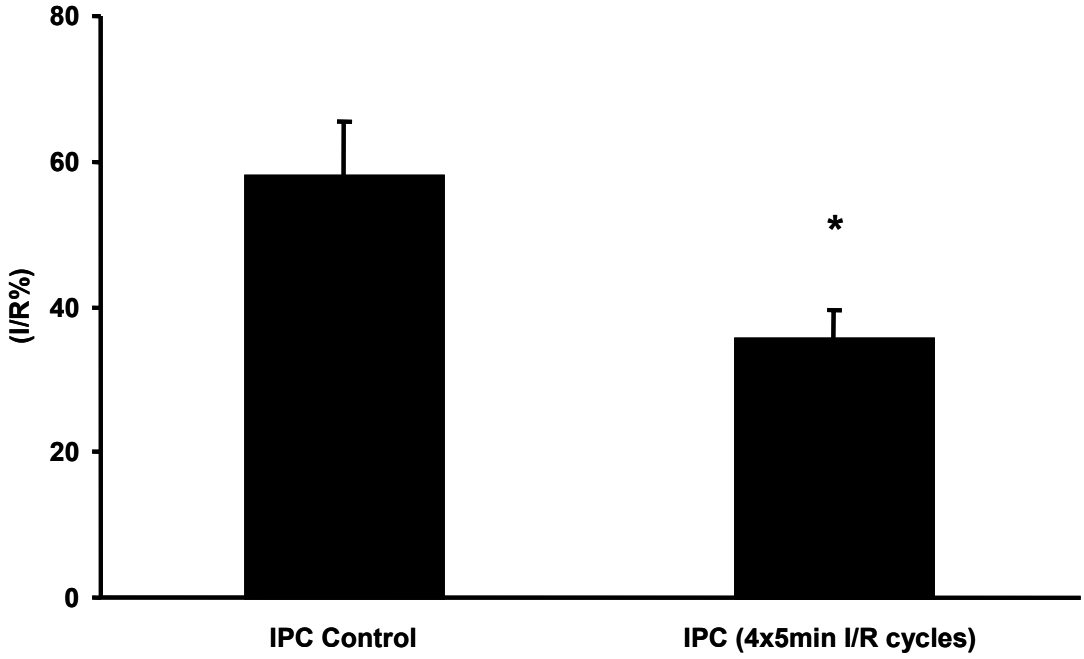

Figure 3.11: Percentage of infarction in the risk area (I/R%) in C57BL/J6 myocardium with extended 55 min stabilisation (to mirror the duration of the ischaemic preconditioning (IPC) stabilisation period) or IPC consisting of 4x5+5 min ischaemia-reperfusion: prior to 35 min ischaemia followed by 30 min reperfusion (n=5). Statistical differences were assessed using the students paired t-test, (*=p<0.05).

In summary, we aimed to characterise the Langendorff model investigating the effects of different durations of ischaemia and reperfusion and different IPC protocols on myocardial ischaemia-reperfusion injury. Our results show significantly larger levels of infarction in myocardium from C57BL/J6 mice compared to NIH Swiss White mice. Furthermore, using C57BL/J6 we demonstrate that as the ischaemia time is extended, the level of infarction is also increased. We concluded that 30 min stabilisation and 35 min ischaemia followed by 30 min reperfusion appears to provide a compliant platform to study ischaemia-reperfusion injury. As a positive control, protection using IPC in C57BL/J6 mouse myocardium was induced using 4 cycles 5 min ischaemia and 5 min reperfusion prior to the lethal ischaemia-

reperfusion protocol. Therefore, these ischaemia-reperfusion protocols were used as a starting point for subsequent studies in which we aim to examine the effects of PTEN inhibition on ischaemia-reperfusion injury in whole hearts.

3.4 Discussion

3.4.1 Infarction and strain variance

Initially, NIH Swiss white mice were used to validate the Langendorff technique, ensuring that reproducible infarct sizes were produced. However, it was found that myocardium from these mice develop very small levels of infarction. We thought the submersion buffer, used to keep the hearts at a constant temperature during ischaemia, may have provided some protection through capillary action and passive diffusion of oxygen into the myocardium. However, no significant differences in infarct size were observed from the use of oxygenated and non oxygenated submersion buffer.

Subsequently, to try and understand this, the level of myocardial infarction between different strains of mice was investigated. Myocardial ischaemia-reperfusion injury in the NIH Swiss white mice was compared to that of the C57BL/J6 strain. The C57BL/J6 myocardium developed significantly larger ($p<0.005$) levels of infarction, comparable to infarct data previously published in this strain (Eckle et al., 2006). Surprisingly, the infarct size in the NIH Swiss mice were significantly smaller. This demonstrates the importance of choosing an appropriate mouse strain to study myocardial protection. Not all strains have similar thresholds to ischaemia-reperfusion, posing the question as to why these differences are observed. To answer this, further investigations are required and may implicate new cellular pathways involved in resistance to ischaemia-reperfusion injury. To summarise, the oxygenation status of the submersion buffer does not affect infarct size. Furthermore, the C57BL/J6 mouse model gives the largest window of potential protection against ischaemia-reperfusion injury.

3.4.2 Infarction: duration of ischaemia and reperfusion

Previous studies have shown a direct relation between the length of ischaemia and myocardial infarct size (Eckle et al., 2006). The best and most practical duration of reperfusion is often debated. To ensure that the optimum ischaemia-reperfusion protocol, providing the biggest window of potential protection and reproducible data was used, the effect of different ischaemia and reperfusion durations on infarct size was investigated. It was observed that extended ischaemia durations corresponded with an increase in infarct size. Moreover increases in reperfusion time from 30 min to 120 min appeared to increase the infarct size; albeit to a limited extent. Similarly, it should be noted that this observation was also seen in sham hearts, which were time matched control hearts perfused without ischaemia. This may be due to the crystalloid perfusion buffer and/or the presence of the balloon in the left ventricle. This suggests that in our hands, as the time on the perfusion apparatus increases, the basal damage to the heart can further increase.

Throughout reperfusion it was observed that hearts show little or no visible ventricular activity. Some laboratories report functional recovery following global ischaemia in mice myocardium (Headrick et al., 2001). However this was not observed in our model of ischaemia-reperfusion injury and has not been recorded in the Hatter Institute previously (Simpkin et al., 2007; Smith et al., 2006; Bell and Yellon, 2003). To investigate any cardiac reserves following ischaemia in these hearts may involve infusing an ionotropic activator, such as adrenaline at reperfusion. As one would expect the act of perfusion using a Langendorff perfusion apparatus creates a basal level of injury. Additional studies may help understand this observation. Such investigations may include recording the effects on infarct size and cardiac reserves with and without the presence of the balloon. Furthermore, studies using a force transducer rather than a pressure transducer as used in other laboratories (Xi et al., 1998; Sumeray et al., 2000) may eliminate the need to use a balloon. The reduced recovery of function at the end of reperfusion in our C57BL/J6 model may be explained on the basis of

using a global versus a regional model of ischaemia. Rat hearts, undergoing global ischaemia released troponin at reperfusion however, this was not observed in rat hearts undergoing regional ischaemia (Feng et al., 2001). As troponin release is a measure of tissue damage, it is probable that complete functional recovery may never be obtained in models of global ischaemia (Jenkins et al., 1997). It also highlights the importance of comparing results between laboratories and awareness of the precise methods used in each group. Results from these studies suggest that the most reproducible and robust protocol of ischaemia-reperfusion injury, is with 35 min ischaemia and 30 min reperfusion.

3.4.3 Infarction and ischaemic preconditioning protocols.

Optimisation experiments for the IPC protocols were carried out in C57BL/J6 mice. Four cycles of 5 min ischaemia and 5 min reperfusion, prior to a lethal period of ischaemia gave significant ($p<0.05$) protection. Published models of ischaemia-reperfusion injury and IPC can be very different, especially in the mouse model. Other groups have shown protection in C57BL/J6 mice using 3 cycles of 5 min ischaemia and 5 min reperfusion (Lange et al., 2007), even 5 min ischaemia and 15 min reperfusion (Turcato et al., 2006). Eckle *et al.,* 2006 has undertaken similar IPC optimisation studies to our own and indicate there is a pattern for protection at 3 cycles but a significant protection only using 4 cycles IPC (Eckle et al., 2006). In our hands this model was used as a positive control. The optimisation experiments were completed and confirmed, by extending the stabilisation period of the IPC control protocol, to account for the increased time on the perfusion apparatus.

In summary, the data obtained in these preliminary experiments were used to choose the best protocol of ischaemia-reperfusion injury. It was decided that in myocardium from C57BL/J6 mice the protocol of 35 min ischaemia and 30 min reperfusion was the best to study ischaemia-reperfusion injury. Furthermore, using IPC as a positive control, it was

shown that 4 cycles of 5 min ischaemia and 5 min reperfusion was the best protocol to study IPC induced cardioprotection against ischaemia-reperfusion injury.

4 Chapter 4 – Chemical inhibition of PTEN using bpV(HOpic) and SF1773; investigating the response to ischaemia-reperfusion

4.1 Background, aims and hypothesis

4.1.1 bpV(HOpic)

The chemical bisperoxo (5-hyroxypyridine-2carboxy) oxovanadate (bpV(HOpic) (Figure 2.7) contains a vanadium ion. Vanadium compounds can mimic the effects of insulin and have anti diabetic effects (Posner et al., 1994; Huisamen, 2003). Others have shown that orthovanadate can increase AKT activity and decrease PTEN activity, which can protect against neuronal ischaemia-reperfusion injury. However, orthovanadate is a non specific general protein tyrosine inhibitor, which can confer protection by a number of mechanisms (Posner et al., 1994; Liem et al., 2004; Wu et al., 2006). The chemical bpV(HOpic) is a protein tyrosine phosphatase inhibitor, with 100 fold specificity for inhibiting PTEN over other tyrosine phosphatases and it can induce an increase in AKT activity (Schmid et al., 2004).

The effects of the PTEN inhibitor, bpV(HOpic) on ischaemia-reperfusion injury, in isolated perfused mouse hearts were investigated. It was hypothesised that the administration of the PTEN inhibitor bpV(HOpic) would activate the prosurvival PI3K/AKT pathway and confer cardioprotection against ischaemia-reperfusion injury.

4.1.2 SF1773 (Semafore)

The PTEN inhibitor, SF1773 (1-Anthraquinonesulfonanilide / 9,10-Dioxo-9,10-dihydro-anthracene-1-sulfonic acid phenylamide), was a kind gift from Semafore

Pharmaceuticals,USA. The specificity to inhibit other enzymes as well as its mechanisms of action are unknown. Observations of the chemical structure, shown in Figure 2.7 reveal that the compound lacks vanadium ions (as well as other ions known to inhibit PTEN, for example Zinc). This may indicate that SF1773 has an alternative mechanism of action for PTEN inhibition. For instance, a naturally occurring naphthoquinone derivative, shikonin has been reported to poses insulin like actions, inhibiting PTEN and tyrosine phosphatases (Nigorikawa et al., 2006). The authors of this work propose that shikonin binds to a shared motif in the PTEN's active site preventing substrate binding.

The chemical SF1773 is currently being developed as a specific PTEN inhibitor to target the side effects of chemotherapy. It is expected that this compound will temporarily minimise cell death in healthy cells and improve survival following chemotherapy. The effects of this drug on ischaemia-reperfusion injury, in isolated perfused mouse hearts were investigated. It was hypothesised that the administration of the PTEN inhibitor, SF1773, would confer cardioprotection against ischaemia-reperfusion injury.

4.2 Experimental protocols and methods

4.2.1 bpV(HOpic)

4.2.1.1 Ischaemia-reperfusion injury in the presence of bisperoxo (5-hyroxypyridine-2carboxy) oxovanadate (bpV(HOpic) in isolated perfused C57BL/J6 mouse hearts

The Langendorff perfusion apparatus was used to study the effects of ischaemia-reperfusion injury in isolated perfused C57BL/J6 mouse hearts, as described in chapter 2, section 2 and infarct size was assessed as an end point. The effect of bpV(HOpic) on ischaemia-

reperfusion injury was investigated. Isolated C57BL/J6 hearts were perfused with bpV(HOpic) (Calbiochem,UK) throughout reperfusion (at 0.02μM, 0.05μM, 0.1μM and 0.5μM, n=5, 5, 4 & 2, respectively) or throughout stabilisation and reperfusion (at 0.02μM,1μM and 10μM, n=3,7 & 5, respectively). Additionally, as a positive control, isolated C57BL/J6 hearts were perfused with sodium orthovanadate (Na_3VO_4 or orthovanadate) (Sigma, UK) at 5.4mM during stabilisation and reperfusion, n=6. The vehicle control for these drugs was water. These hearts were subjected to our standard ischaemia-reperfusion protocol, as shown in Figure 4.1 and the level of infarction was compared to that detected in C57BL/J6 myocardium perfused with control buffer (n=18). These initial drug concentrations were extrapolated from published data using an isolated PTEN enzyme, PIP3/PIP2, conversion assay. The authors of this study demonstrated an IC_{50} of 14nM. They also investigated the phosphorylation of AKT with bpV(HOpic) for which they obtained an EC_{50} of 20nM (Schmid et al., 2004). Using this study as a starting point the initial doses used in the study was 20nM. The effects of a range of concentrations, the maximum being 10μM were investigated.

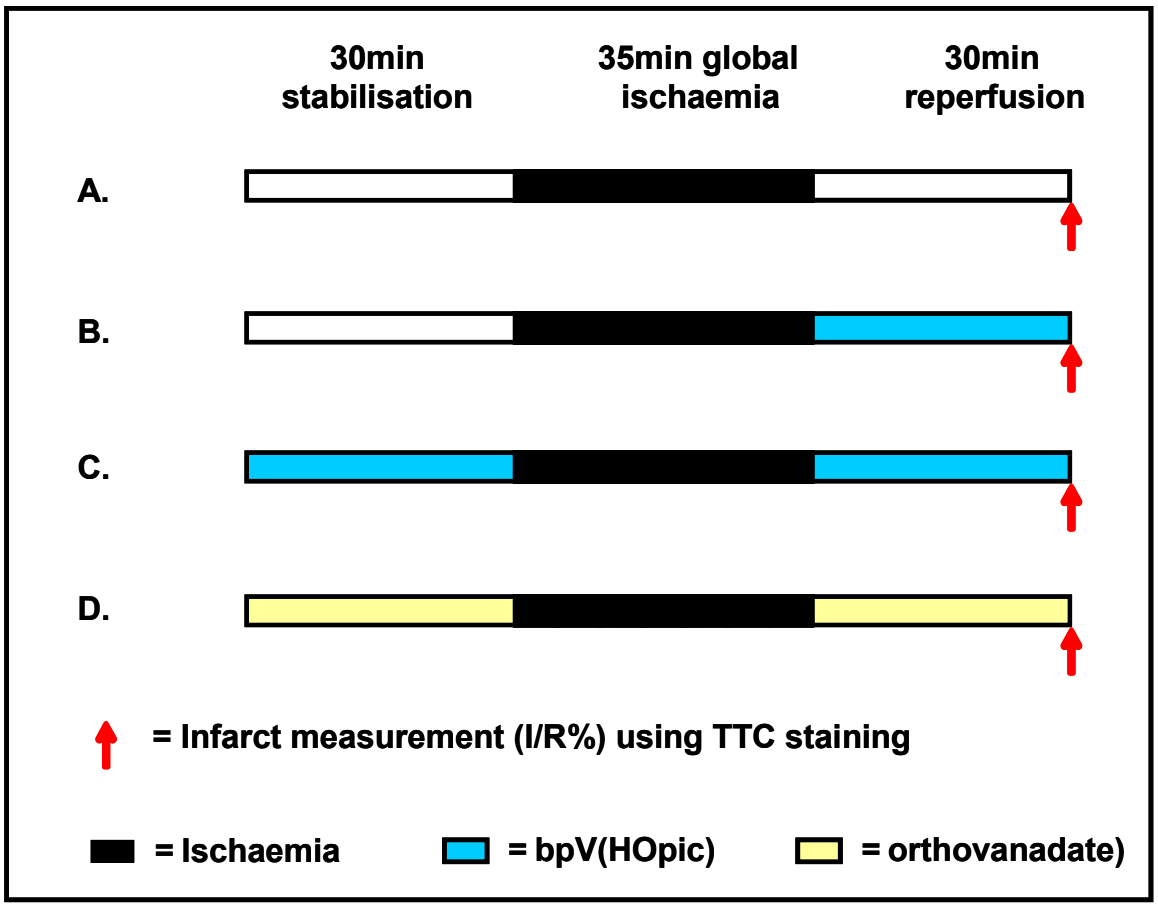

Figure 4.1: **The experimental protocols for investigating infarction in isolated C57BL/J6 mouse hearts perfused with: A) control buffer; B) bpV(HOpic) administered at and throughout reperfusion; C) bpV(HOpic) administered at and throughout stabilisation and reperfusion and D) orthovanadate administered as a positive control at and throughout stabilisation and reperfusion. The stock concentrations of these drugs were made up in water and subsequently diluted in Krebs buffer to the appropriate concentrations. I/R% = percentage of infarction to risk area TTC = triphenyltetrazolium chloride.**

4.2.1.2 Ischaemic preconditioning and bpV(HOpic) in isolated perfused C57BL/J6 mouse hearts

Infarction

The Langendorff perfusion apparatus was used to study the effects of IPC on ischaemia-reperfusion injury, in the presence or absence of 1μM bpV(HOpic). As described in chapter 2, infarct size was assessed as an end point. As an additional positive control the number of IPC cycles required to confer cardioprotection in isolated perfused C57BL/J6 mouse hearts in the presence or absence of bpV(HOpic) administered throughout stabilisation and reperfusion was investigated. We explored the effects of control, 2 and 4 cycles IPC (5 min ischaemia followed by reperfusion) in the presence (n= 4,4 and 3, respectively) and absence (n= 6,4 and 6, respectively) of bpV(HOpic) as shown in Figure 4.2.

Signalling

As shown in Figure 4.2 the protein expression of phosphorylated AKT (Ser473 and Thr308 phosphorylation sites), total AKT, phosphorylated PTEN (Ser380Thr382/383) and total PTEN was investigated, as a consequence of bpV(HOpic). We used Western blot techniques to investigate changes in protein expression and assessed the results using densitometry. Samples were collected immediately prior to the lethal ischaemic event (n=3). It has been shown that changes in AKT activity, which occur in response to IPC, can be detected subsequent to the IPC stimulus (Tsang et al., 2005). All samples were snap frozen in liquid nitrogen immediately after removal from the Langendorff rig and stored in -80^{o}C.

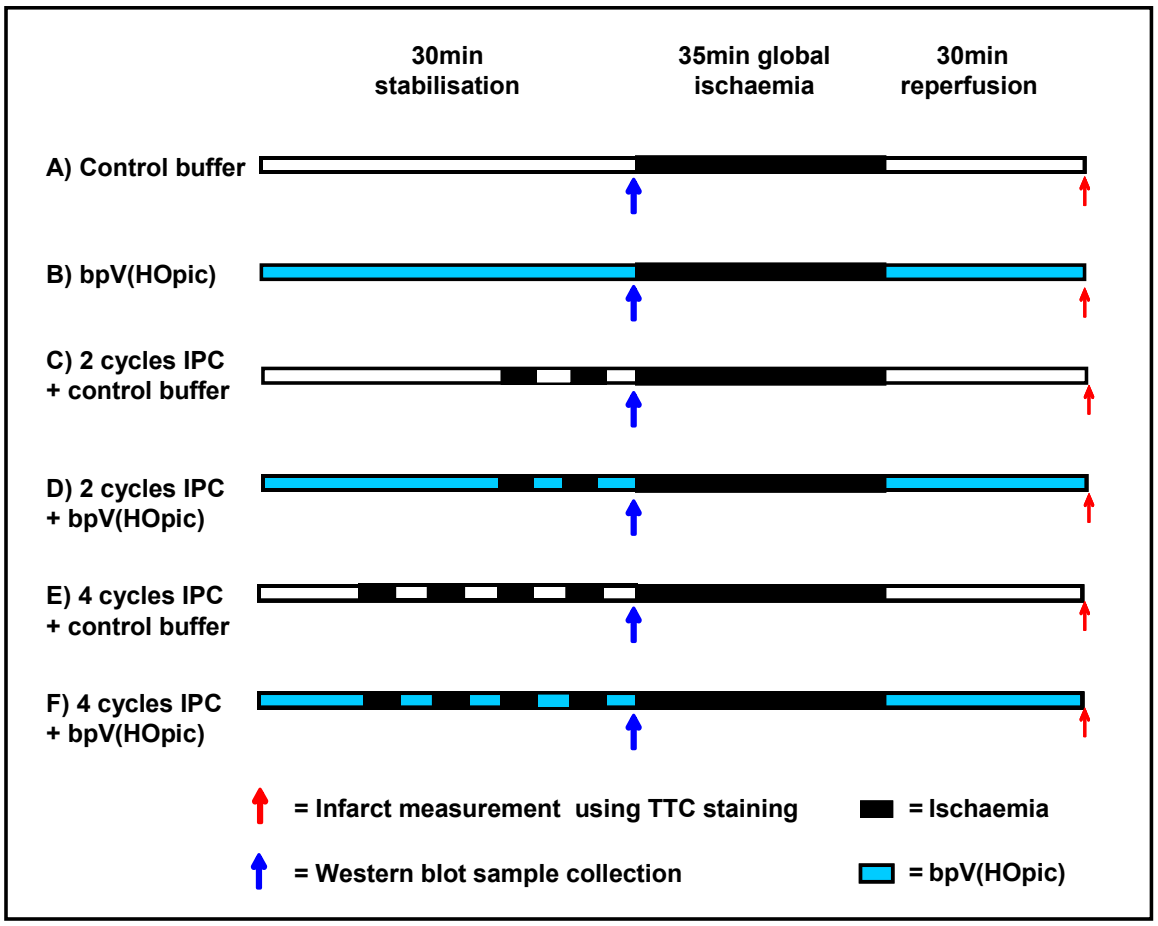

Figure 4.2: **The experimental protocols used to investigate ischaemia-reperfusion injury and cardioprotection with bpV(HOpic), administered throughout stabilisation and reperfusion in control and ischaemic preconditioned (IPC) isolated C57BL/J6 hearts. A) control buffer; B) bpV(HOpic); C) control buffer with 2 cycle IPC; D) bpV(HOpic) with 2 cycle IPC; E) control buffer and 4 cycles IPC and F) bpV(HOpic) with 4 cycles IPC. The stock concentration of bpV(HOpic) were made up in water and subsequently diluted in Krebs buffer to the appropriate concentrations. I/R% = percentage of infarction to risk area TTC = triphenyltetrazolium chloride.**

4.2.2 SF1773 compound

4.2.2.1 Ischaemia-reperfusion injury in the presence of SF1773 in isolated perfused C57BL/J6 mouse hearts

The Langendorff perfusion apparatus was used to study the effects of ischaemia-reperfusion injury in isolated perfused C57BL/J6 mouse hearts, as described in chapter 2, section 2; infarct size was assessed as an end point. The mechanisms of actions for SF1773 are unknown however, Semafore Pharmaceuticals,USA, report an IC_{50} of 221nM, for PTEN inhibition. A range of doses (0.06μM, 0.12μM, 0.24μM, 0.48μM and 0.96μM, n = 7,5,8,3 and 5, respectively) were perfused throughout stabilisation and reperfusion of isolated C57BL/J6 myocardium subjected to the standard ischaemia-reperfusion protocol, as shown in Figure 4.3.

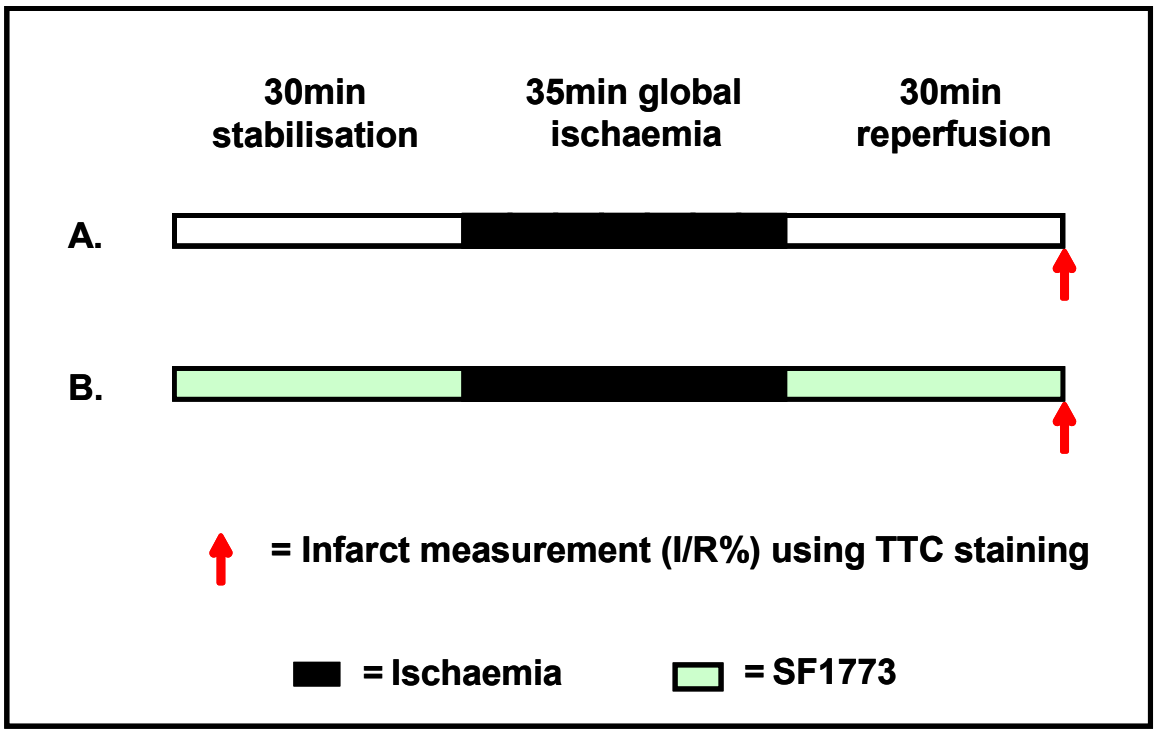

Figure 4.3: **Experimental protocols used to investigate the infarction in isolated C57BL/J6 mouse hearts perfused with: A) control buffer or B) SF1773 administered at and throughout stabilisation and reperfusion. The stock concentration of SF1773 was made up in dimethyl sulfoxide (DMSO) and subsequently diluted in Krebs buffer to the appropriate concentrations, the total amount of perfused DMSO was <0.01%). I/R% = percentage of infarction to risk area TTC = triphenyltetrazolium chloride.**

4.3 Results

4.3.1 bpV(HOpic)

4.3.1.1 Ischaemia-reperfusion injury in the presence of bisperoxo (5-hyroxypyridine-2carboxy) oxovanadate (bpV(HOpic) in isolated perfused C57BL/J6 mouse hearts.

The vanadium compound, bpV(HOpic), is a protein tyrosine phosphatase inhibitor with 100 fold specificity for inhibiting PTEN over other tyrosine phosphatases (Schmid et al., 2004). It was hypothesised that myocardial perfusion with bpV(HOpic) would pharmacologically inhibit PTEN and confer cardioprotection in our model of ischaemia-reperfusion injury. Initially, the effects of different concentrations of the inhibitor administered at reperfusion only were investigated. Figure 4.4 shows that there was no change in infarction in the presence of the varying concentrations of bpV(HOpic) when given at reperfusion only. The level of infarction in control myocardium was 48.95±3.4% compared to 48.08±7.02%, 51.24±6.96%, 60.55±2.93%, 59.05±4.45% infarction in myocardium perfused with 0.02μM, 0.05μM, 0.1μM and 0.5μM bpV(HOpic), respectively. It is important to note that the precise mechanism of action of this drug is not fully understood. However it seems to be effective for PTEN inhibition in the NIH3T3 cell line (Schmid et al., 2004). Subsequently, the inhibitor was administered throughout stabilisation and reperfusion, to ensure sufficient time was provided for the drug to enter the cells and take effect. Orthovanadate, a general protein tyrosine phosphatase inhibitor, was used as a positive control to demonstrate protection in our model. This inhibitor was administered at 5.4mM into the buffer throughout stabilisation and reperfusion. As shown in Figure 4.4 a significant reduction in infarction from 48.95±3.4% to 26.5±4.1%, $p<0.01$ was observed using orthovanadate, when administered throughout

stabilisation and reperfusion. However, no changes were observed using bpV(HOpic) at a range of concentrations under similar conditions.

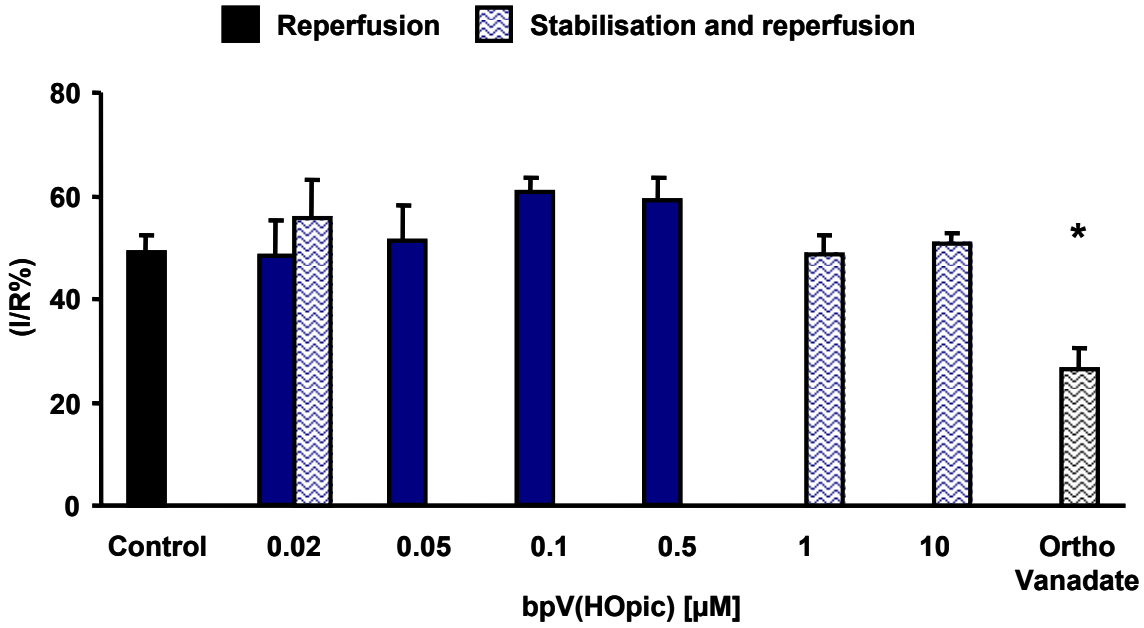

Figure 4.4: Percentage of infarction developed in the risk area (I/R%) in C57BL/J6 myocardium treated with the PTEN inhibitor, bpV(HOpic). Control in solid black bar (n=18); bp(HOpic) at reperfusion, (0.02µM, 0.05µM, 0.1µM & 0.5µM, n= 5, 5, 4 & 2, respectively) in solid blue bars; bpV(HOpic) throughout stabilization and reperfusion (0.02µM, 1µM, and 10µM, n= 3, 7, and 5, respectively) in hatched blue bars and orthovanadate throughout stabilization and reperfusion (n=6) in hatched black bars. One Way ANOVA, (*=p<0.01).

Unexpectedly, in the presence of orthovanadate, lower flow rates were observed at the beginning of stabilisation, for approximately 5 min. To eliminate the possibility of an IPC-like protection due to low flow ischaemia an additional group, in which 5 min of low flow (1.0ml/min) and reduced perfusion pressure (PP<50mmHg) was applied, to account for this observation. Figure 4.5 shows that there was no change in infarct size versus control (48.9±3.4%) to the 5 min low flow, low perfusion pressure group (47.6±4.2%).

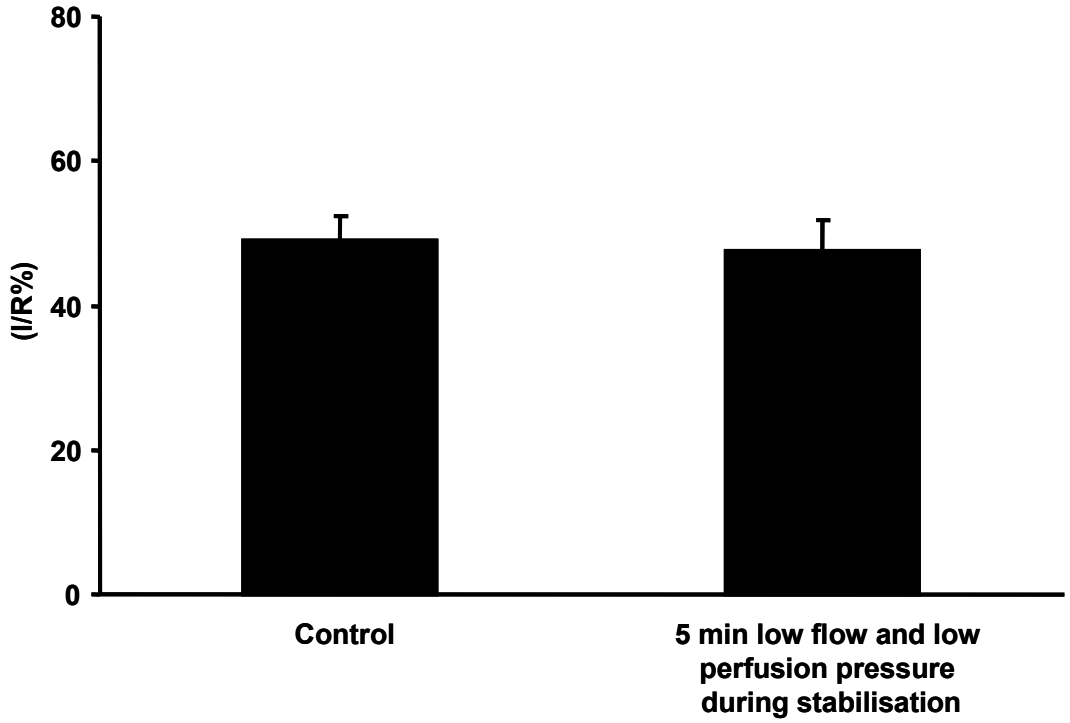

<u>Figure 4.5:</u> Percentage of infarction developed in the risk area (I/R %) in C57BL/J6 myocardium in controls (n=18) and in hearts subjected to a low flow stabilisation period, (n=5). There was no statistical differences between groups, assessed using the Student's paired t-test.

In summary, orthovanadate, a protein tyrosine phosphatase inhibitor, confers protection to ischaemia-reperfusion. However, perfusion with a specific PTEN inhibitor, bpV(HOpic) was not sufficient to induce cardioprotection in our model of isolated myocardial ischaemia-reperfusion injury. This unexpected result occurred regardless of using increasing concentrations and duration of perfusion with the PTEN inhibitor, bpV(HOpic).

4.3.1.2 Ischaemic preconditioning and bpV(HOpic) in isolated perfused C57BL/J6 mouse hearts

Infarction

It was hypothesised that, despite lack of protection against ischaemia-reperfusion injury in the presence of bpV(HOpic), perfusion with this PTEN inhibitor may decrease the level of infarction when other cardioprotective mechanisms are applied. To verify this hypothesis, the IPC stimulus required to confer protection was explored in a C57BL/J6 mouse model of ischaemia-reperfusion, in the presence of 1μM bpV(HOpic). The results presented in Figure 4.6 show the infarct size incurred subsequent to 35 min global ischaemia and 30 min reperfusion, preceded by 2 or 4 cycles IPC (5 min ischaemia and 5 min reperfusion). In hearts perfused with control buffer, protection was achieved with 4 cycles IPC and the level of infarction was significantly reduced from 49.0± 3.1% to 36.7± 3.1%, $p<0.05$. In the presence of 1μM bpV(HOpic), protection was observed with 4 cycles IPC and the level of infarction was reduced from 53.10± 3.4% to 25.6± 4.5%, $p<0.001$. In the presence of bpV(HOpic) protection was also observed even with 2 cycles IPC, where infarction was significantly reduced to 23.9 ± 3.89%, $p<0.001$).

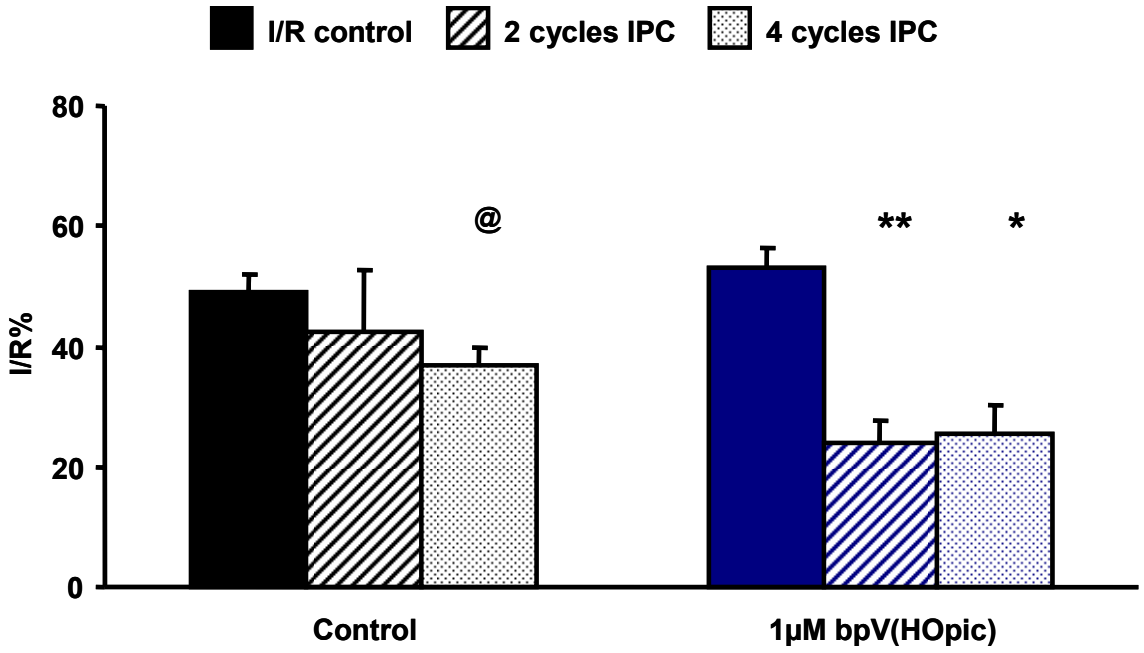

Figure 4.6: Percentage of infarction developed in the risk area (I/R%) in C57BL/J6 myocardium subjected to ischaemic preconditioning (IPC) in the presence of 1µM bpV(HOpic) administered in the buffer throughout stabilisation and reperfusion. Solid bars = ischaemia-reperfusion (I/R) control (no IPC); striped bars = 2 cycles IPC and dotted bars = 4 cycles IPC (n=4 or more). The statistical differences were assessed from bpV(Hopic) control using One Way ANOVA (*=p<0.01, **=p<0.01). In the buffer control group a significant reduction in infarction at 4cycles IPC compared to I/R control was recorded only using Student's t test (@=p<0.05).

Signalling Pathways

We have shown that the cumulative IPC stimulus, required to reduce infarct size, is lower in the presence of bpV(HOpic). Therefore, the potential cell signalling that may be involved was investigated. It was hypothesised that the phosphorylation (hence activation) of the pro survival protein AKT would be increased as a consequence of perfusion with the PTEN inhibitor, bpV(HOpic). In the isolated hearts perfused with bpV(HOpic) (no ischaemic injury) a significant increase in the ratio of phosphorylated AKT was observed. Levels of phosphorylated AKT (at Ser473 phosphorylation site) was increased from 0.139 $\pm$ 0.02 A.U in

buffer control to 0.401 ± 0.045 A.U, $p<0.0024$ following perfusion of bpV(HOpic), as shown in Figure 4.7. Furthermore, phosphorylated AKT (Thr308) was increased from 0.174 ± 0.05 A.U in buffer control to 0.443 ± 0.028 A.U, $p<0.01$ subsequent to perfusion of bpV(HOpic), as shown in Figure 4.8.

Additionally, the expression of phosphorylated AKT in conjunction with the IPC stimuli was further investigated. The results investigating phosphorylated AKT (at Ser473 phosphorylation site) are shown in Figure 4.7. Perfusion with control buffer in the presence of 4 cycles IPC induced a significant increase in expression of phosphorylated AKT (Ser473 site) (from 0.139 ± 0.02 A.U in the control to 0.245 ± 0.026 A.U, $p<0.05$ in the presence of 4 cycles IPC). No changes were observed following 2 cycles IPC. Perfusion of bpV(HOpic) did not induce any further increases following 2 and 4 cycles IPC. However the level of phosphorylated AKT(Ser473) was significantly higher than the untreated hearts even without IPC.

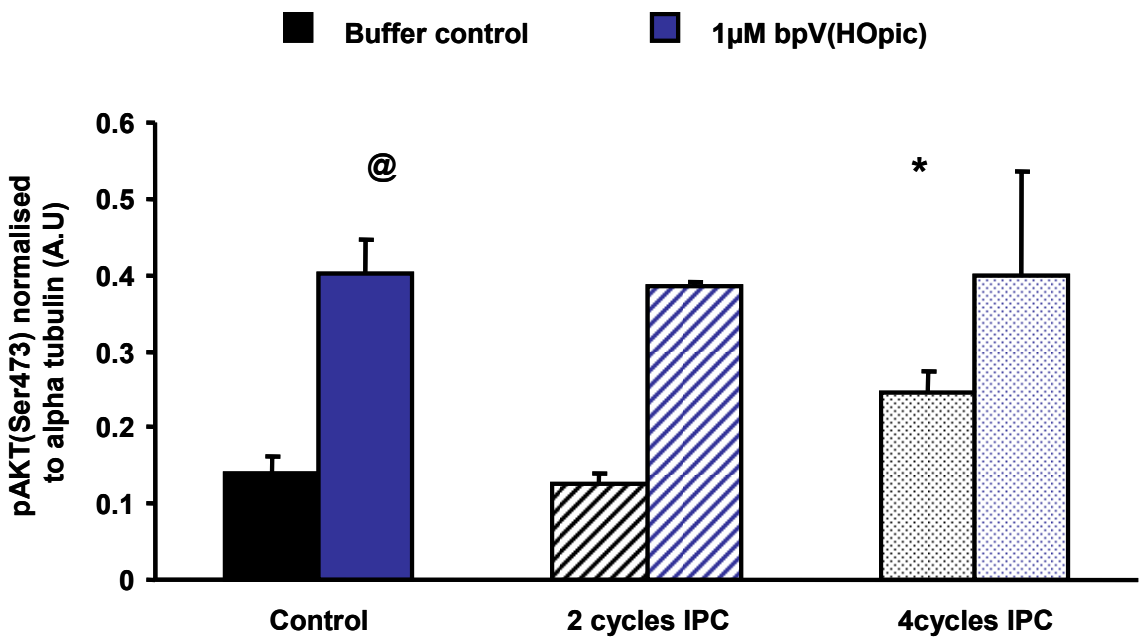

Figure 4.7: Phosphorylated (p) AKT (Ser473 site) protein expression in C57BL/J6 myocardium subjected to ischaemia-reperfusion control (solid), with 2 (stripes) or 4 (dots) cycles of ischaemic preconditioning (IPC); perfused with buffer control (black bars) or 1μM bpV(HOpic) (blue bars) (n=3). Statistical differences were assessed from control and from bpV(HOpic) groups, using One Way ANOVA (*=p<0.05 in control group only). A Student's t test was used to investigate the significant difference between buffer control and bpV(HOpic) subjected to the control protocol, (@=p<0.05).

The results from our studies investigating phosphorylated AKT (at the Thr308 site) are shown in Figure 4.8. Examples of the Western blots used to investigate the phosphorylation of AKT at 473 and 308 sites are displayed in Figure 4.10. Interestingly, following 2cycles of IPC the expression of AKT(308) was reduced when control buffer and significantly, $p<0.05$, when bpV(HOpic) was perfused throughout the heart. Perfusion with control buffer or bpV(HOpic) during 2 and 4 cycles IPC caused no further significant differences in expression. Perfusion with bpV(HOpic) during 2 cycles of IPC increased the expression profile of phosphorylated AKT (at the Thr308 site), when compared to the same IPC stimulus in the presence of control buffer. Additionally, in hearts perfused with bpV(HOpic) there was an increase in

phosphorylated AKT (at Thr308 site) during 4 cycles IPC (0.306± 0.053 A.U) compared to 2 cycles IPC (0.171 ± 0.04 A.U), however, these changes were not significant.

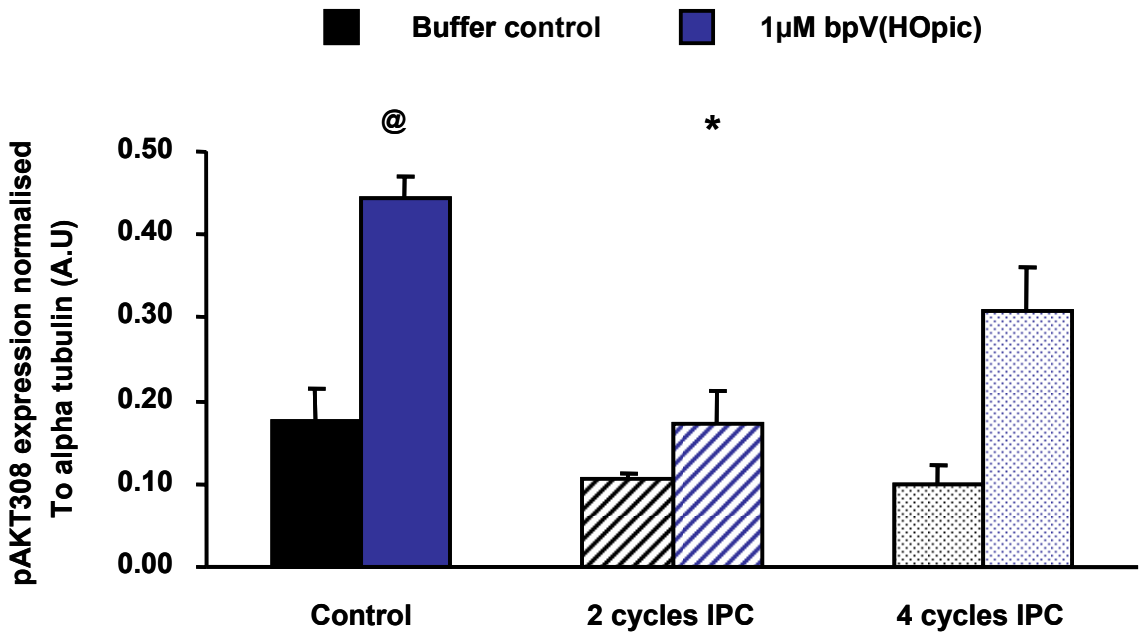

Figure 4.8: Phosphorylated (p) AKT (at Thr308 site) protein expression in C57BL/J6 myocardium subjected to ischaemia-reperfusion control (solid), 2 (stripes) or 4 (dots) cycles of ischaemic preconditioning (IPC); perfused with buffer control (black bars) or 1µM bpV(HOpic) (blue bars) (n=3). Statistical differences were assessed in control and bpV(HOpic) groups, using One Way ANOVA (*=p<0.05 in bpV(HOpic) group only). A Student's t test was used to investigate the significant difference between buffer control and bpV(HOpic) subjected to the control protocol, (@=p<0.01). The vehicle control used was water.

PTEN

The PTEN inhibitor was perfused throughout the myocardium over a period of 95 min. Figure 4.9 represents the expression values of phosphorylated PTEN (at Ser380, Thr382/383 sites), which can be indicative of PTEN activity (Cai and Semenza, 2005; Al Khouri et al., 2005; Wu et al., 2006). Examples of the Western blots are displayed in Figure 4.10. No significant

changes in phosphorylated PTEN levels were observed. However, perfusion with bpV(HOpic) during 4 cycles of IPC provided a small, but not significant, reduction in the level of phosphorylated PTEN, from 0.665 ± 0.01 A.U to 0.469 ± 0.07 A.U. It appears that in our samples, perfusion with the bpV(HOpic) may not modify the phosphorylated PTEN expression profile, during this time frame.

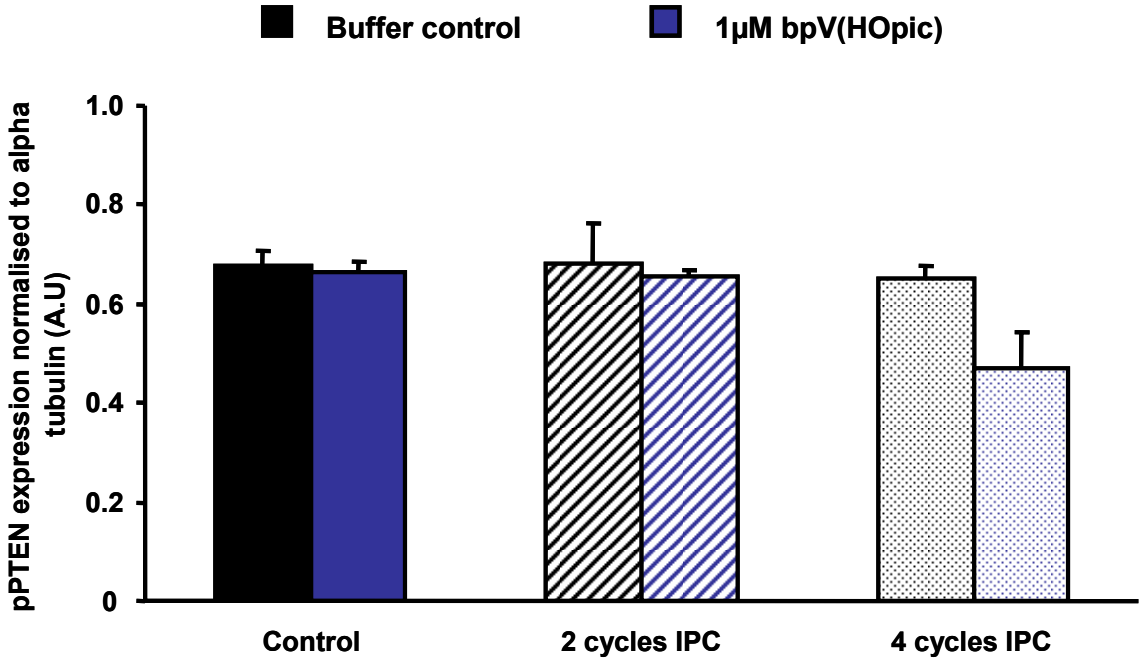

Figure 4.9: Phosphorylated (p) PTEN (Ser380, Thr382/383 sites) protein expression in C57BL/J6 myocardium subjected to ischaemia-reperfusion: control (solid bars), 2 cycles of ischaemic preconditioning (IPC) (stripes) or 4 cycles of IPC (dots) prior to ischaemia; perfused with either buffer control (black bars) or bpV(HOpic) (blue bars) (n=3), Statistical differences were assessed using One Way ANOVA.

Perfusion with bpV(HOpic) increased the activation of the PI3K/AKT pathway, however this increase was not sufficient to confer cardioprotection against myocardial ischaemia-reperfusion injury. Nevertheless, when combined with IPC, the threshold of protection was decreased and the infarct size was reduced with less IPC stimuli.

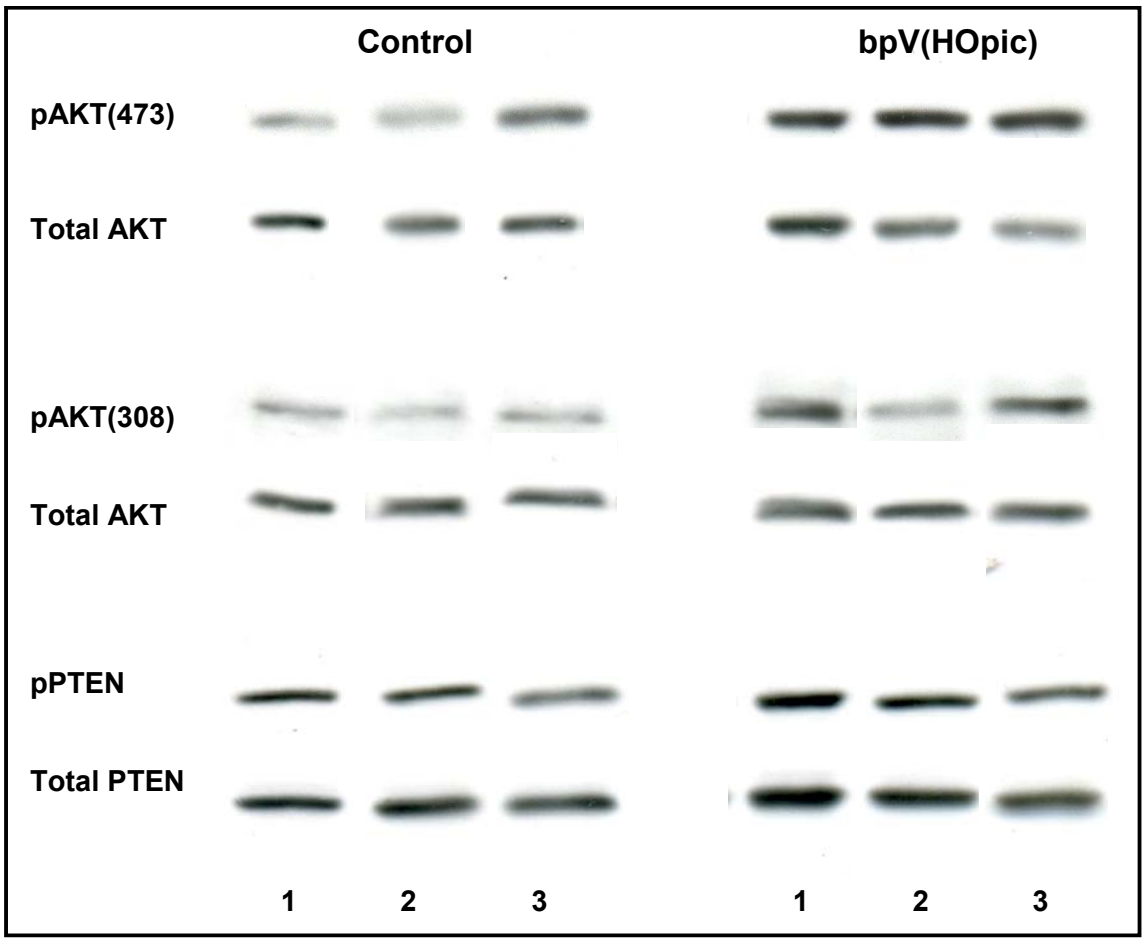

Figure 4.10: **Examples of Western blots obtained when investigating total and phosphorylated (p) AKT (473 and 308 sites) and PTEN (Ser380, Thr382/383 sites) protein expression in C57BL/J6 myocardium subjected to (1) ischaemia-reperfusion control, (2) 2 cycles ischaemic preconditioning (IPC) or (3) or 4 cycles IPC; perfused with either buffer control or bpV(HOpic).**

4.3.2 SF1773 (Semafore)

4.3.2.1 Ischaemia-reperfusion injury in the presence of SF1773 (Semaphore) in isolated perfused C57BL/J6 mouse hearts

It was hypothesised that the perfusion with SF1773, an alternative PTEN inhibitor, in C57BL/J6 myocardium would induce cardioprotection against ischaemia-reperfusion injury. Based on our investigations using bpV(HOpic) and orthovanadate, the drug was perfused throughout stabilisation and reperfusion periods, using different concentrations (from 60 to 960nM). The results are displayed in Figure 4.11. Perfusion of SF1773 does appear to reduce cell death induced by our model of ischaemia-reperfusion however, no dose response effect was observed. Infarction following perfusion with vehicle control was 46.2 $\pm$ 1.7%. An infarct size of 36.96 $\pm$ 3.9%, 36.28 $\pm$ 2.5%, 40.6 $\pm$ 5.7% and 36.5 $\pm$ 2.5% was observed using 0.12 0.24, 0.48 and 0.96μM of SF1773, respectively. Only a significant reduction in infarction was observed at 0.24μM SF1773, ($p<0.05$) which may be due to the degree of variability in the infarct sizes, within these other groups.

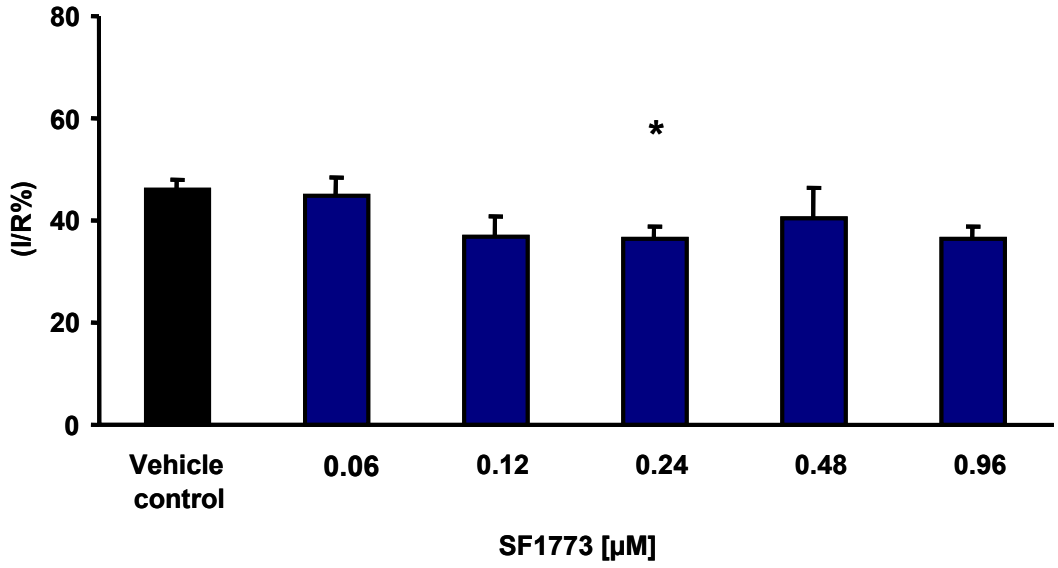

Figure 4.11: Percentage of infarction developed in the risk area (I/R%) in vehicle control (solid black bar, n= 11) and in myocardium perfusion with SF1733 (0.06µM, 0.12µM, 0.24µM, 0.48µM and 0.96µM, (blue bars, n= 7, 5, 8, 3 and 5, respectively). Statistical differences were assessed using One Way ANOVA, (*=p<0.05).

4.4 Discussion

4.4.1 bpV(HOpic)

4.4.1.1 Ischaemia-reperfusion injury in the presence of bisperoxo (5-hyroxypyridine-2carboxy) oxovanadate (bpV(HOpic) in isolated perfused C57BL/J6 mouse hearts.

Historically, vanadium compounds are reported to have effects on the cardiovascular system, increasing blood pressure and decreasing force of myocardial contraction (Borchard et al., 1981). They are also reported to have effects on PTEN, blocking its function (Schmid et al., 2004). According to the literature bpV(HOpic) is a specific pharmacological inhibitor of PTEN

(Schmid et al., 2004). This drug was used in our model of ischaemia-reperfusion injury to investigate this potential cardioprotective agent. It was hypothesised that the administration of bpV(HOpic) would induce cardioprotection against ischaemia-reperfusion injury by decreasing the level of PTEN. This drug is a protein tyrosine phosphatase inhibitor with specificity for PTEN due to a 100 fold greater inhibitory activity over other tyrosine phosphatases (Schmid et al., 2004). The results from these studies showed that the administration of the drug, given in increasing concentrations at reperfusion alone, did not confer protection in our model of ischaemia-reperfusion injury. Other groups have shown that administration of drugs, such as leptin in pancreatic and hypothalamic cells, can modulate PTEN stability within 30 min (Ning et al., 2006). Therefore administration of bpV(HOpic) at reperfusion may not be sufficient to effect PTEN/PI3K/AKT pathway before the irreversible damage caused by ischaemia-reperfusion injury transpires. Hence, it was predicted that perfusion of bpV(HOpic) given prior to ischaemia may provide protection against infarction. However, when bpV(HOpic) was perfused throughout stabilisation and reperfusion, no reductions in infarction were observed.

In our experiments orthovanadate was administered as a positive control. A significant ($p<0.01$) level of protection against ischaemia-reperfusion injury was recorded. This observation is in agreement with work by Liem et al., 2004 who perfused orthovanadate in a model of myocardial ischaemia-reperfusion and demonstrated cardioprotection. Monitoring for any non specific drug effects during perfusion of the isolated mouse hearts was performed. It was observed that a brief and temporary reduction in flow upon the administration of orthovanadate (at stabilisation), typical of a vasoconstrictor-like function, occurred. Further studies to investigate the effects of 5 min low flow and low perfusion pressure in control hearts were applied in order to mimic this functional effect and showed no protection. This suggests that the reduction in infarction using orthovanadate was not due to

the reduction of flow and perfusion pressure (i.e IPC like effect), and that alternative mechanisms are responsible.

Similar to our findings, others have shown that orthovanadate can reduce infarction following ischaemia-reperfusion (Liem et al., 2004). The authors of this study attributed the protection to the opening of K_{ATP} channels (Liem et al., 2004). In addition orthovanadate has been shown to inhibit the NaK-ATPase (Svoboda et al., 1984). Orthovanadate is a general protein tyrosine phosphatase inhibitor (Schmid et al., 2004). Huisamen *et al*, 2003 showed that orthovanadate can increase phosphorylated AKT levels and induce glucose uptake in isolated rat cardiomyocyte. As yet the direct effects on PTEN have not been investigated, this may be important for future studies, as orthovanadate can protect against brain ischaemia-reperfusion injury and has been shown to phosphorylate and inhibit PTEN (Wu et al., 2006).

The lack of protection against ischaemia-reperfusion, with bpV(HOpic) was unexpected. In contrast, other groups have shown protection in other tissues using similar inhibitors of PTEN. In a study investigating axon cell growth by Arevalo et al 2006 the PTEN inhibitor bpV(pic) (dipotassium bisperoxo(picolinato) oxovanadate) was used to facilitate cell growth. In lung epithelial cells PTEN inhibitors bpV(phen) and bpV(pic) increased the levels of phosphorylated AKT (at the Ser473 site) and decreased the time to wound healing in a scratch model of injury (Lai et al., 2007). In this monolayer assay of wound healing, 2μM of the inhibitors was used (Lai et al., 2007). This protective concentration is similar to the highest dose used in our isolated whole heart model of ischaemia-reperfusion injury. It is possible that, a higher dose of bpV(HOpic) may be required to induce cardioprotection, since it is difficult to extrapolate results obtained using cell models for application in a whole organ model. It may also be argued that at higher concentrations the specific effects could be lost and other phosphatases might also be affected. Further difference can be highlighted in the lung injury model, described above, as epithelial cells are proliferative cells unlike

cardiomyocytes. By 48h the scratch wound was fully healed regardless of any pro survival intervention. In contrast, within our experiments cardiomyocytes, which are differentiated cells, were investigated and as an end point cell death was measured. Ischaemia-reperfusion is a severe stress and potentially, the amount of PTEN inhibition may not be sufficient to protect the myocardium subjected to our ischaemia-reperfusion protocol.

Schmid et al., 2004 have investigated the effects of many bisperoxovanadium compounds on specific PTEN inhibition and provided a short list of their most potent inhibitors. To achieve this, the group stimulated NIH3T3 cells with insulin and monitored the phosphorylation of AKT in the presence of the PTEN inhibitors. Furthermore they investigated the lipid phosphatase activity of recombinant PTEN in the presence of the PTEN inhibitors and PI(3,4,5) used a malachite green reagent to detect the changes in phosphate release (Schmid et al., 2004). In this study their most potent PTEN inhibitor, published at the time was bpV(HOPic). Subsequently, this group have communicated data which show better vanadium based PTEN inhibitors, which was not known or available at the time of our studies (Rosivatz et al., 2006). There may be functional differences between these vanadium compounds in situ. For example Lai et al.,2007 investigated 2 of these inhibitors in their lung cell wound healing model and observed that bpV(phen) caused LDH release, whereas bpV(pic) did not effect cytotoxicity (Lai et al., 2007).

An additional explanation for the lack of cardioprotection in the presence of bpV(HOpic) may be due to the pharmacokinetics and pharmacodynamics of the drug. Initially, we perfused the PTEN inhibitor at reperfusion only, and saw no reduction in infarction. Subsequently the drug was perfused throughout stabilisation to afford sufficient time for PTEN inhibition. The half life and the duration of action of this inhibitor are unknown. Therefore it may be possible that during ischaemia (35min) the effects on PTEN are lost enabling full activation of residual

PTEN at reperfusion. Future work to address this issue could include administered the drug at stabilisation and measuring AKT activity at reperfusion.

In summary, we observed no reductions in infarction using 0.02-10μM bpV(HOpic) and were able to demonstrate cardioprotection only by using the positive control orthovanadate. However, due to the non-specific actions of this general tyrosine phosphatase inhibitor further investigations using orthovanadate as an inhibitor of PTEN were not pursued.

4.4.1.2 Ischaemic preconditioning and bpV(HOpic) in isolated perfused C57BL/J6 mouse hearts

Infarction studies

The cardioprotection obtained by IPC in isolated C57BL/J6 mouse hearts perfused with or without bpV(HOpic) was investigated. Myocardial infarction was compared following ischaemia-reperfusion alone or ischaemia-reperfusion preceded by 2 or 4 cycles of IPC (5 min ischaemia and 5 min reperfusion). IPC stimulates the activity of the PI3K/AKT pathway (Yellon and Hausenloy, 2005). As shown in Figure 4.6, a reduced threshold for IPC induced protection in the presence of bpV(HOpic) was observed. Hearts perfused with control buffer were significantly ($p<0.05$) protected with 4 cycles IPC whereas myocardium perfused with bpV(HOpic) was significantly ($p<0.01$) protected with both 2 and 4 cycles IPC, respectively. This finding positively supports our hypothesis that the presence of a PTEN inhibitor can facilitate cardioprotection.

Schmid et al., 2004 were the first to identify bpV(HOpic) as an inhibitor of PTEN (Schmid et al., 2004). Interestingly, the in vitro assay they use to demonstrate PTEN inhibition required the addition of insulin. This indicates that the effect of PTEN inhibition is detected or amplified once the PI3K/AKT pathway has been stimulated, with insulin. Inhibitors of PTEN can

manipulate the PI3K/AKT pathway, causing significant biological changes (Cai et al., 2008b; Lai et al., 2007; Zhang et al., 2007). The results obtained in this study indicate that in order to demonstrate the cardioprotective effects of this drug, a stimulus of the PI3K/AKT pathway seems to be required.

Further evidence supporting our results is offered by studies investigating the effects of increased PTEN level in the myocardium. Goto Kakazaki rats are a well known model of diabetes and their isolated hearts express higher PTEN levels than wild type animals (Mocanu et al., 2006). These rats have a de-sensitised PI3K/AKT pathway in conjunction with an increased PTEN level (Tsang et al., 2005). This may be why Tsang *et al.,* 2005 demonstrated the myocardium from these rats exhibit a higher threshold to IPC, where 3 cycles of IPC were required to induced protection in these rats compared to the usual 1 cycle in their WT controls. Therefore the threshold of IPC appears higher in the Goto Kakazaki rat myocardium (Tsang et al., 2005). In addition, studies by Cai and Semenza in 2005, showed that changes occur to PTEN activity during IPC stimuli. This work provides supporting evidence that PTEN can be manipulated in the heart and that its down regulation may be involved in survival following ischaemia-reperfusion injury (Cai and Semenza, 2005). Moreover, work by Huisaman in 2003 demonstrates that vanadate can lower the signalling sensitivity in the heart, The combination of sub-maximal concentrations of 1mM vanadate with 10mM insulin induced an additive response similar to that seen with 100nM insulin alone (Huisamen, 2003). Not only does this implicate vanadate as a modulator of the PI3K/AKT pathway it may also indicate that there are mechanisms which can increase the sensitivity of stimulated PI3K/AKT signalling.

In summary, perfusion of isolated C57BL/J6 mouse hearts with bpV(HOpic) is not able to reduce infarction from ischaemia-reperfusion alone, in our model. However, when associated

with IPC, which is known to activate the PI3K/AKT, the threshold to cardioprotection is reduced.

Signalling studies

AKT

Cardiomyocytes incubated with vanadate, a general tyrosine phosphatase inhibitor, express a higher level of phosphorylated AKT(Huisamen, 2003). General tyrosine phosphates inhibitors such as vanadate can inhibit PTEN and have also been shown to induce increases in the level of AKT phosphorylation (Posner et al., 1994; Schmid et al., 2004; Lai et al., 2007). However, such compounds are not specific for PTEN inhibition and alternative compounds such as bpV(HOpic) have been shown to have more specificity (100fold) for PTEN inhibition over general tyrosine phosphatase inhibition (Schmid et al., 2004). We hypothesised that myocardial perfusion with the PTEN inhibitor bpV(HOpic) would increase the phosphorylation of the pro survival protein AKT, uniquely in cardiac tissue. Indeed we observed a significant increase in phosphorylation of AKT at both Thr308 and Ser473 phosphorylation sites, $p<0.01$. Increases in the phosphorylation of AKT have been associated with cardioprotection (Bell and Yellon, 2003; Hausenloy and Yellon, 2004a; Baines et al., 1999). However, in our study the increase in AKT phosphorylation due to bpV(HOpic) was not sufficient to protect against infarction in our model of ischaemia-reperfusion injury.

Nevertheless, we confirmed that IPC (4 cycles IPC in our mouse model of ischaemia-reperfusion injury) significantly ($p<0.05$) increased phosphorylation of AKT at Ser473 site (Hausenloy et al., 2005; Cai et al., 2008a). Furthermore, no significant changes in AKT phosphorylation were observed at 2 cycles IPC. It was shown that bpV(HOpic) reduced the threshold for protection, where 2 cycles IPC conferred protection, compared to 4 cycles in control. However, no additional significant changes in AKT phosphorylation were observed between control, 2 and 4 cycles of IPC. The reason for this is not clear, future work to

address this issue may include assessing the activity of alternative prosurvival signalling pathways, in the presence of bpV(HOpic) and IPC, such as JAK/STAT or p42/p44 pathway.

Conversely, the level of AKT phosphorylation in the presence of bpV(HOpic) is higher than that observed in the control IPC. This finding is discussed below. Further experiments addressing this issue may provide additional information, such as investigating the level of phosphorylated AKT following ischaemia and reperfusion.

PTEN

In the presence of bpV(HOpic) no significant changes in PTEN phosphorylation, which can be an indicator of PTEN inactivity and instability were observed (Wu et al., 2006; Ning et al., 2006). It is unknown if this drug activates enzymes that can phosphorylate (Ser380,Thr382/383 sites) and inactivate PTEN, such as CK2 (Ning et al., 2006). However, in the brain, the inhibition of PTEN using bpV(pic) and PTEN antisense technology has been associated with further increases in PTEN tyrosine phosphorylation and degradation, AKT(Ser473) phosphorylation and a reduction in JNK1 phosphorylation. These changes have been associated with neuroprotection against brain ischaemia (Zhang et al., 2007). Such phosphorylation events were not recorded and cardioprotection against ischaemia-reperfusion in our myocardial model of ischaemia-reperfusion injury was not observed. The mechanisms of PTEN inhibition by bpV(HOpic) are unknown, however past papers showed that vanadium has properties similar to phosphate ions (Lindquist et al., 1973). These compounds can inhibit enzymes involved in phosphoryl transfer reactions, such as phosphoglycerate mutase which is involved in glucose metabolism (Climent et al., 1981). It is suggested that vanadium mimics the structure of phosphate transition states causing associative displacement and potentially, protein instability (Climent et al., 1981). Therefore, it could be considered that changes in the phosphorylation of PTEN may not accurately reflect

the state of PTEN activity. Further experiments may include investigating the level of PTEN ubiquitination in the presence of bpV(HOpic).

bpV(HOpic) and IPC

IPC activates many other signalling pathways in addition to PI3K/AKT. In the presence of bpV(HOpic) the effects on the PTEN/PI3K/AKT pathway may not be sufficient to reduce infarction following ischaemia-reperfusion alone. However the combination of sub maximal IPC stimulus and the PTEN inhibitor seems to promote the signals for protection, possibly due to further PTEN modulation. For example, IPC can generate ROS which is known to inhibit PTEN (Kwon et al., 2004; Cai and Semenza, 2005). As discussed in Chapter 6, additional PTEN inhibition, possibly due to the generation of ROS during IPC may explain the reduction in the threshold to IPC; in the presence of bpV(HOpic). A proposed hypothesis for how PTEN may be further inhibited in the presence of either a PTEN inhibitor or genetic deletions is shown in Figure 6.24.

To conclude, in the presence of the PTEN inhibitor bpV(HOpic) the changes detected in the PI3K/AKT signalling were not sufficient to confer cardioprotection in our mouse model of ischaemia-reperfusion. However, once the PI3K/AKT pathway had been stimulated by IPC, the presence of the PTEN inhibitor reduced the threshold for protection induced by IPC.

4.4.2 SF1773 (Semafore)

4.4.2.1 Ischaemia-reperfusion injury in the presence of SF1773 (Semafore) in isolated perfused C57BL/J6 mouse hearts

The use of SF1773, a specific PTEN inhibitor, donated by Semafore Pharmacuticals was investigated, in our model of myocardial ischaemia-reperfusion injury. The initial dose used

was recommended by Semafore Pharmaceuticals, which tested the IC_{50} value for the drug by measuring the ability of isolated PTEN to convert PIP3 into PIP2. Using this drug in a range of concentrations, from 0.06 to 0.96μM, a small but significant ($p<0.05$) reduction in infarction against ischaemia-reperfusion injury was observed. However, a dose response effect with this compound was not detected. Only at 0.24μM was significance recorded, at the additional doses of 0.12, 0.48 and 0.96μM a small but insignificant reduction in infarct size was found. This may be because the standard error at these doses was to large. Other cardioprotective agents demonstrate dose response effects against ischaemia-reperfusion injury, such as adenosine or bradykinin (Maddock et al., 2002; Bell and Yellon, 2003). Therefore, if this reduction in infarction is a real effect the physiological relevance of this finding in terms of cardioprotection may be debated. It is possible that the bioavailability of the drug in a whole organ model is reduced and therefore provides limited biological effects, and increasing the concentrations further may address this issue. However, little is known about its mechanisms of action in PTEN inhibition. Therefore, we did not pursue the use of SF1773 as a PTEN inhibitor in our models of ischaemia-reperfusion injury.

In conclusion, the effects of chemical inhibitors of PTEN on myocardial ischaemia-reperfusion injury were investigated. No protection was observed in the presence of bpV(HOpic) alone. However, when the PI3K pathway was stimulated by IPC, the threshold of protection was reduced in the presence of this drug. Using SF1773 (semaphore) a small reduction in infarction was recorded, however; no dose response effect was detected.

5 Chapter 5 – Biochemical modulation of PTEN using the p53 inhibitor pifithrin alpha

5.1 Background, aims and hypothesis

It has been demonstrated that p53, a transcription factor implicated in cell survival and death, can up regulate PTEN (Stambolic et al., 2001). Down regulation of the tumour suppressor p53 has been associated with a decrease in PTEN (Wang et al., 2005; Tang and Eng, 2006). Pifithrin alpha (PFTα) is a p53 inhibitor; however, its exact mechanism of action is not clear. The chemical structure of this compound is shown in Figure 2.7. Intra peritoneal injections of PFTα in rats can reversibly inhibit p53 dependent apoptosis caused by myocardial and renal ischaemia-reperfusion injury (Kelly et al., 2003; Liu et al., 2006). Furthermore, in mice, the deleterious effects of chemotherapy have been reduced using PFTα (Komarov et al., 1999).

We aimed to establish whether it is possible to manipulate PTEN activity by modulating the levels of p53. If successful, this could provide a tool for investigating the effects of PTEN reduction on ischaemia-reperfusion injury. It was hypothesised that reducing the level of p53 (using the known inhibitor PFTα) would down regulate PTEN expression and that these hearts would be protected against ischaemia-reperfusion injury.

5.2 Experimental protocol and methods

NIH Swiss White mice (20-30g) were subjected to one of the following conditions every 24h for 3days, via i.p injection (n=5 in each group). These experiments were performed at the very start of this body of research and at that time we were using NIH Swiss White mice in our studies, see Chapter 3.

1) Sham (0.9% saline)
2) Vehicle (0.1% DMSO/0.9%saline)
3) PFTα (2.2mg/kg PFTα in 0.1% DMSO/0.9% saline)

Four hours following the final injection cervical dislocation was performed and hearts were rapidly excised into ice cold Krebs-Henseleit buffer containing approx 500U heparin. Hearts were rapidly trimmed and the atrium and any blood clots were removed.

Samples were then immediately snap frozen in liquid nitrogen and processed for Western blot analysis, as described in Chapter 2, section 6. Thereafter, the expression of total p53, phosphorylated and total PTEN (Ser380,Thr382/383 phosphorylation sites) and phosphorylated and total AKT (Ser473 phosphorylation site) was investigated.

5.3 Results –Reducing PTEN levels using the p53 inhibitor pifithrin

The results are shown in Figures 5.1, 5.2, 5.3 and 5.4 respectively. No significant differences were observed between sham, vehicle and PFTα groups. A small, but non significant, decrease in total p53, between the vehicle control group and the PFTα treated group was detected. However, under these experimental conditions this decrease was not sufficient to elicit changes in PTEN and, ultimately, in AKT expression.

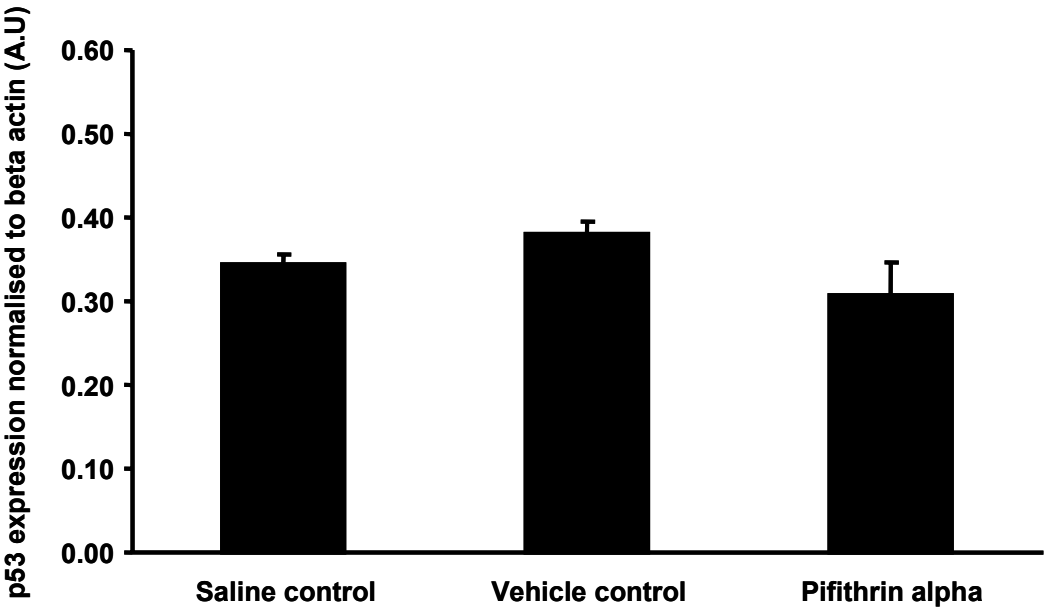

Figure 5.1: **Total p53 protein expression in the myocardium from Swiss White mice exposed to saline control (0.9% saline), vehicle control (0.1%DMSO/0.9% saline) or 2.2mg/kg PFTα (0.1%DMSO/0.9% saline) every 24h for 3 days, (n=5). There was no statistical differences between groups, assessed using the Student's paired t-test.**

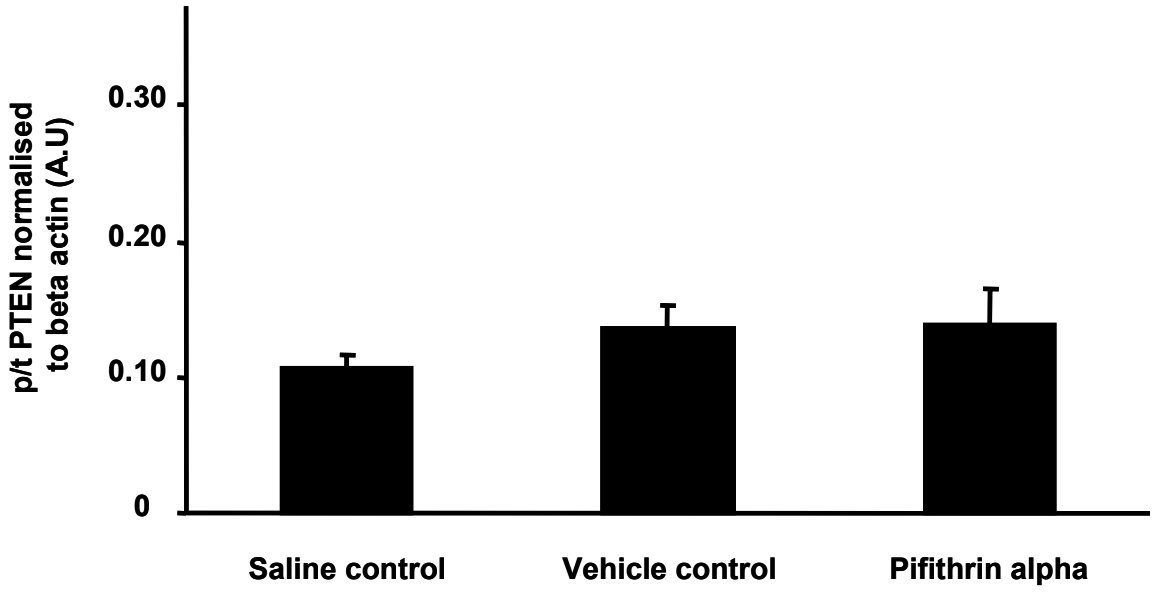

Figure 5.2: **Phosphorylated versus to total PTEN (p/t) protein expression in myocardium from Swiss White mice exposed to saline control(0.9% saline), vehicle control (0.1%DMSO/0.9% saline)or 2.2mg/kg PFTα (0.1%DMSO/0.9% saline) every 24h for 3 days, (n=5). There was no statistical differences between groups, assessed using the Student's paired t-test.**

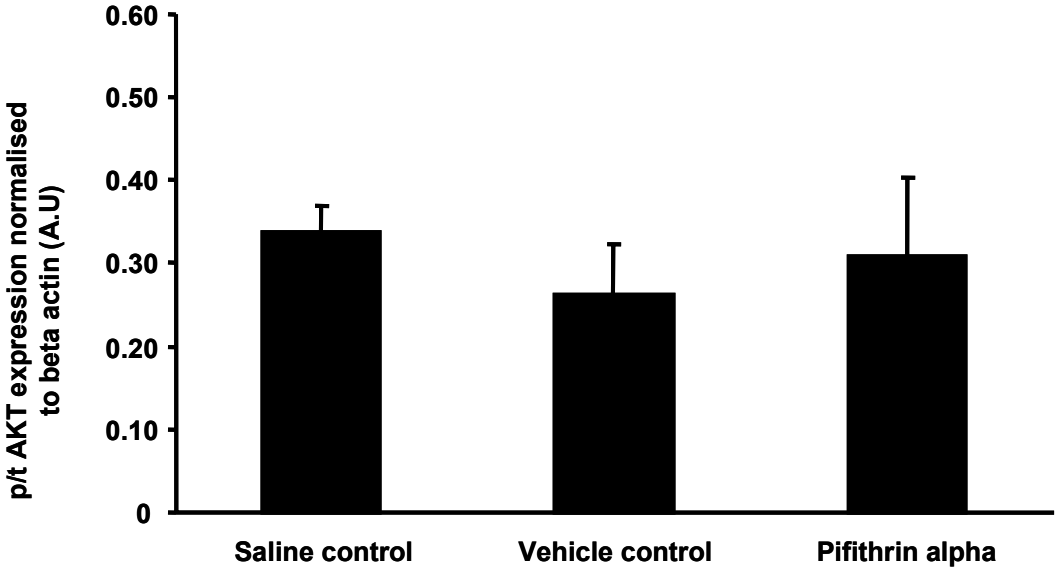

Figure 5.3: **Phosphorylated versus to total (p/t) AKT (at Ser473 phosphorylation site) protein expression in myocardium from Swiss White mice exposed to saline control(0.9% saline), vehicle control (0.1%DMSO/0.9% saline) or 2.2mg/kg PFTα (0.1%DMSO/0.9% saline) every 24h for 3 days, (n=5). There was no statistical differences between groups, assessed using the Student's paired t-test.**

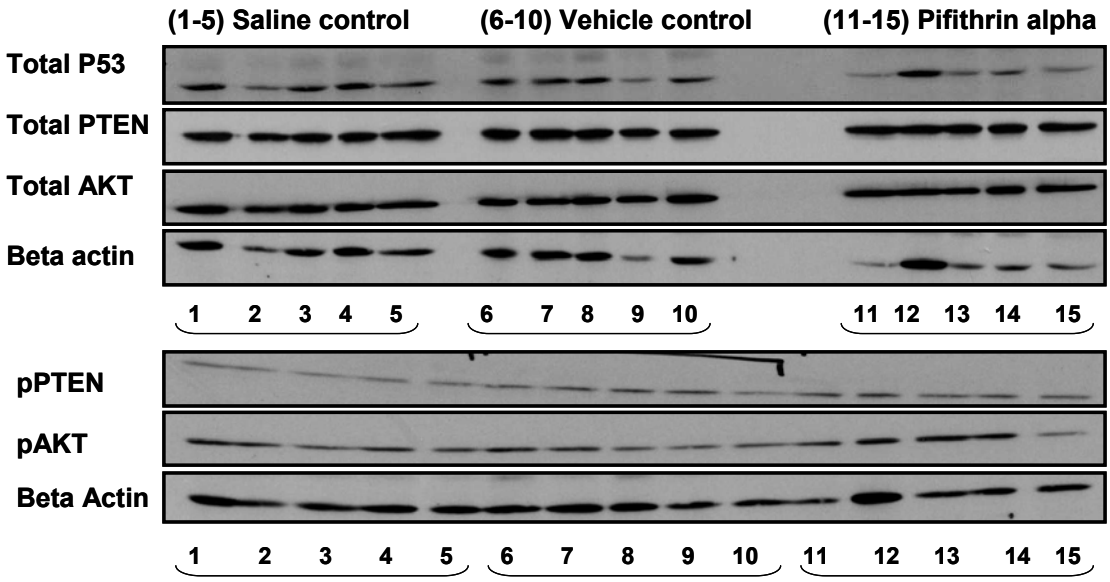

Figure 5.4: **Representative Western blots of the results shown in Figure 5.1-5.3.**

5.4 Discussion

5.4.1 Reducing PTEN levels using the p53 inhibitor pifithrin alpha

The tumour suppressor, p53 can up regulate the transcription of PTEN (Stambolic et al., 2001). Therefore, it was predicted that the inhibition of p53 using PFTα, (a p53 inhibitor), would decrease the level of PTEN and maybe up regulate the PI3K/AKT survival pathway. We aimed to investigate if PFTα can be used as a tool for studying PTEN inhibition on ischaemia-reperfusion injury.

Our results do not show any significant differences in the expression of p53, PTEN and AKT following the administration of PFTα. A possible explanation may be the absence of p53 activation. Apoptotic stimuli such as UV light or doxorubicin are commonly used to up regulate p53 (Komarov et al., 1999; Wang et al., 2005). In MEF cells UV light up regulated p53 and induced cell death which was attributed to an increase in BAX induced membrane permeability. This effect was independent of its promoter activity (Chipuk et al., 2004). The authors of this work observed that, in the absence of UV light, this effect was abolished (Chipuk et al., 2004), indicating that part of p53 apoptotic effects are dependent on a stress stimulus such as UV light.

In addition, a longer duration of PFTα administration may also be required. Eipel *et al,* have used this compound for up to 7 days in a hepatic model of tissue regeneration (Eipel et al., 2005). Moreover, p53 knock out mice are available and may provide a more direct model to investigate the link of p53 to PTEN in the myocardium. These mice manifest cardioprotection against ischaemia-reperfusion injury (Matsusaka et al., 2006) and we predict down regulation of PTEN may contribute to this protection.

The mechanism by which PFTα induces p53 inhibition is unknown. It was identified that PFTα may not alter the expression of p53, however, it can affect p53 function, as assessed by p21 and BAX expression. This implies that the total protein expression does not effect the protein function. Localisation of p53 can be important to cell signalling. In the presence of PFTα a reduction in p53 localisation at the nucleus and mitochondria can be observed following ischaemia-reperfusion (Kelly et al., 2003). Others have shown that PFTα is cardioprotective in a rat model of ischaemia-reperfusion injury (Mocanu and Yellon, 2003; Liu et al., 2006). Collectively this indicates that PFTα is cardioprotective by means of a number of different mechanism; from protein transcription to direct effects on mitochondrial survival (Stambolic et al., 2001; Kelly et al., 2003; Chipuk et al., 2004). PTEN reduction is included in this list; however, we were unable to demonstrate this.

In summary, administration of PFTα did not reduce protein expression of p53 or PTEN and no changes were observed in AKT. Hence, we decided that our treatment with PFTα does not offer a reliable tool for reducing myocardial PTEN; therefore we aimed to investigate alternative methods for inhibiting PTEN.

6 Chapter 6 –The effect of ischaemia-reperfusion injury in myocardium from PTEN haploinsufficient mice

6.1 Aims, hypothesis and experimental protocols

Mice with PTEN deletions (PTEN haploinsufficient mice heterozygous for $PTEN^{+/-}$) exhibit multiple organ neoplasms, enhanced cell proliferation and defective apoptotic abilities. Their homozygous littermates ($PTEN^{-/-}$) do not survive gestation further than embryonic day E6.5 (Podsypanina et al., 1999). In response to insulin, myocytes from these $PTEN^{+/-}$ mice have enhanced glucose uptake and increased levels of AKT activity (Wong et al., 2007). The main hypothesis of this study was that the myocardium from these mice would be protected against cell death, induced by ischaemia-reperfusion. On commencement of this investigation the PTEN haploinsufficient ($PTEN^{+/-}$) mouse model was not available commercially. As a kind gift, 2 breeding pairs were donated from Dundee University. Therefore, it was necessary to establish a breeding programme and characterise the strain within our colony prior to studying the response to ischaemia-reperfusion injury. The steps taken to investigate the hypothesis are listed below in brief and are described in more detail further in this chapter. The methods, results and discussion for each section are as follows.

1) Characterising the PTEN$^{+/-}$ mouse
    - Monitoring breeding
    - Measuring body weight and blood glucose
    - Measuring myocardial PI3K/AKT/PTEN signalling

2) Investigating the response of the PTEN$^{+/-}$ myocardium to ischaemia-reperfusion injury
    - Measuring the response of isolated hearts to ischaemia-reperfusion injury
    - Measuring the response of isolated cardiomyocytes to ROS induced mitochondrial damage

3) Investigating the response of the PTEN$^{+/-}$ myocardium to ischaemic preconditioning
    - Measuring the ischaemic preconditioning protocol required to induce protection in isolated hearts
    - Measuring myocardial PI3K/AKT/PTEN signalling

4) Investigating reasons for the lack of protection against ischaemia-reperfusion injury in the PTEN$^{+/-}$ mouse
    - Measuring alternative regulators of the PI3K/AKT/PTEN pathway
    - Measuring alternative mechanisms that contribute to ischaemia-reperfusion injury

6.2 Characterising the PTEN$^{+/-}$ haploinsufficient mouse model

6.2.1 Experimental protocols

6.2.1.1 Monitoring Breeding

With the support of the Biological Service Unit within UCL, the breeding pattern of the PTEN haploinsufficient mice (PTEN$^{+/-}$) was monitored. All animals were genotyped prior to experimentation. Tail or ear DNA was extracted and analysed by PCR amplification, thereafter, the DNA was separated and visualised by agarose gel electrophoresis, as described in chapter 2 section 4.2.

6.2.1.2 Measuring body weight and blood glucose

Prior to experimentation the body weights of the haploinsufficient mice and their littermate controls were recorded. In addition to measuring body weight, non fasting blood glucose levels were measured from the tails, immediately following cervical dislocation, n=6. An Accu-Chek® compact plus glucose meter (Roche, UK) was used to monitor glucose levels. The results were expressed in mmol/L.

6.2.1.3 Monitoring myocardial PTEN/PI3K/AKT signalling

Possible changes in the activity and protein expression of the PTEN/PI3K/AKT pathway were investigated by measuring PTEN lipid phosphatase activity and the expression of phosphorylated PTEN and AKT.

6.2.1.3.1 Measuring PTEN lipid phosphatase activity

The PTEN lipid phosphatase activity was investigated in the $PTEN^{+/-}$ myocardium and it was hypothesised that there would be a reduced PTEN activity in these hearts compared to littermate controls. The lipid phosphatase activity was estimated using an Echelon ELISA assay, as described in chapter 2, section 4.3, Samples were collected from isolated hearts perfused on the Langendorff apparatus, without ischaemia-reperfusion, as shown in Figure 6.1 A and described in chapter 2, section 1, n=3 and each heart was examined in replicates of 3.

Optimisation experiments were performed to further validate this assay, for the detection of PTEN phosphatase activity, within the Hatter Institute. We investigated the most efficient dilution of myocardial homogenate to use in the assay. It was hypothesised that there would be a reduction in PTEN phosphatase activity in the $PTEN^{+/-}$ myocardium.

6.2.1.3.2 Measuring PTEN and AKT expression

The levels of PTEN and AKT were investigated in the $PTEN^{+/-}$ mouse hearts, using Western blot analysis, as described in chapter 2, section 6. Samples were collected from isolated hearts perfused on the Langendorff perfusion apparatus for 10 min, with no ischaemia, as shown in Figure 6.1, A, n=3. This perfusion was done in order to ensure that blood contaminants were removed from the tissue.

PTEN - Phosphorylated and total levels of PTEN. Phosphorylated PTEN expression is indicative of PTEN inactivity (Ning et al., 2006; Wu et al., 2006; Zhang et al., 2007). Therefore, it was hypothesised that in the $PTEN^{+/-}$ myocardium there would be an increase in phosphorylated PTEN and a decrease in total PTEN, compared to hearts from $PTEN^{+/+}$ mice.

AKT - Full activation of the pro survival kinase AKT requires phosphorylation of amino acids Ser473 and Thr308 (Alessi et al., 1996). The profile of these two phosphorylation sites were investigated. It was hypothesised that in the PTEN$^{+/-}$ myocardium there would be an increase in phosphorylated AKT.

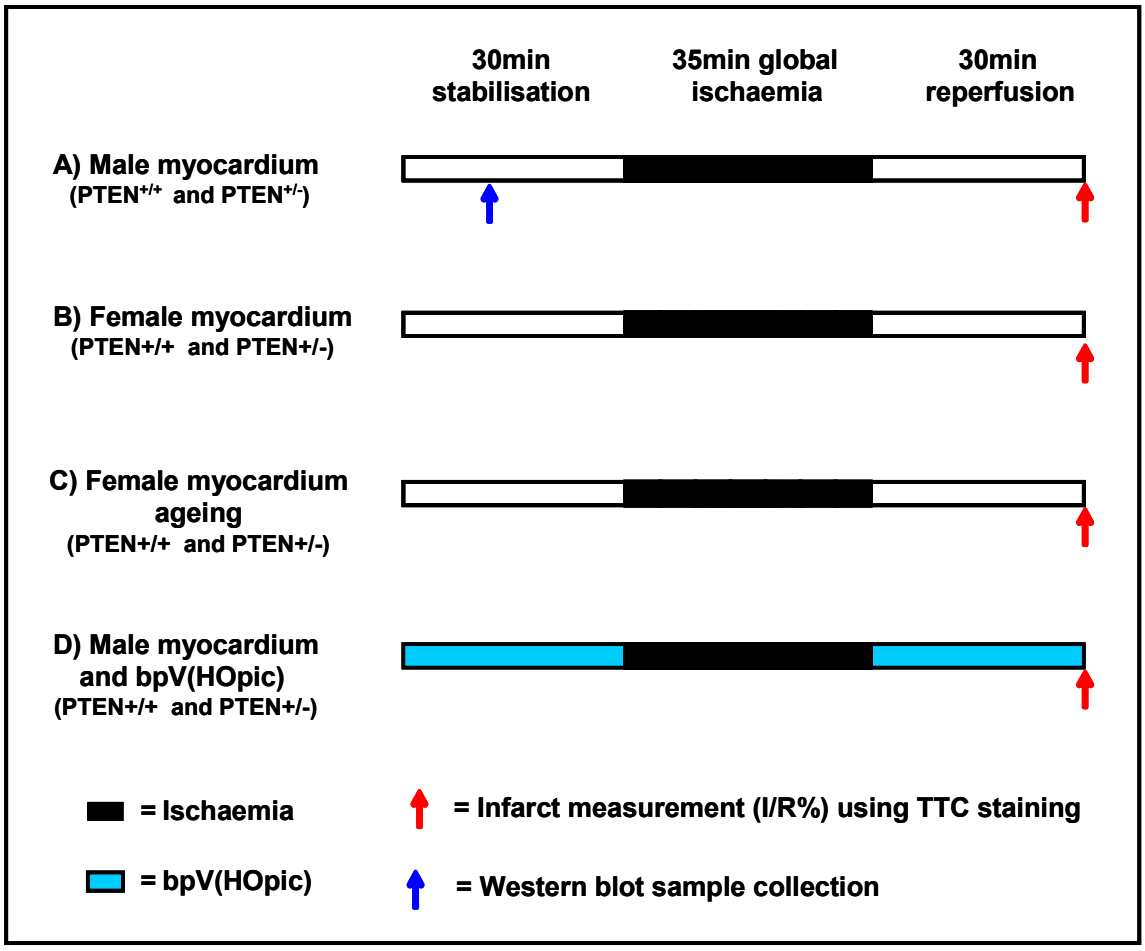

Figure 6.1: Experimental protocols used to investigate infarction in isolated hearts from PTEN$^{+/+}$ and PTEN$^{+/-}$ mice. A) male hearts; B) female hearts; C) Ageing (20wk vs 10wk) female hearts; D) male myocardium perfused with the PTEN inhibitor bpV(HOpic). I/R% = percentage of infarction to risk area TTC = triphenyltetrazolium chloride.

6.2.2 Results

6.2.2.1 Breeding

PTEN haploinsufficient mice were good breeders if pairs were establish at a young age (6-8 weeks). On average, a litter produced 6-8 pups. However, due to the onset of tumour development, breeding periods were short. $PTEN^{+/-}$ females were especially sensitive and only produced a total of 3-5 litters: in contrast $PTEN^{+/-}$ males bred 2-3 times longer. Therefore, preferentially we paired ($PTEN^{+/+}$ females) with ($PTEN^{+/-}$ males); producing litters containing 50:50% average $PTEN^{+/+}$ to $PTEN^{+/-}$ phenotypes. As previously mentioned, $PTEN^{-/-}$ animals are not viable and the embryos die in uterus (Podsypanina et al., 1999). The presence of $PTEN^{-/-}$ pups were therefore, not observed in our litters.

$PTEN^{+/+}$ samples amplified 2 PCR products: a non-specific band running as 100base pairs (bp) and a second band running as 240bp. $PTEN^{+/-}$ samples amplified a total of 3 PCR products, with a third additional band running as 320bp. A photographic representation of the PCR products from a typical litter is shown in Figure 6.2.

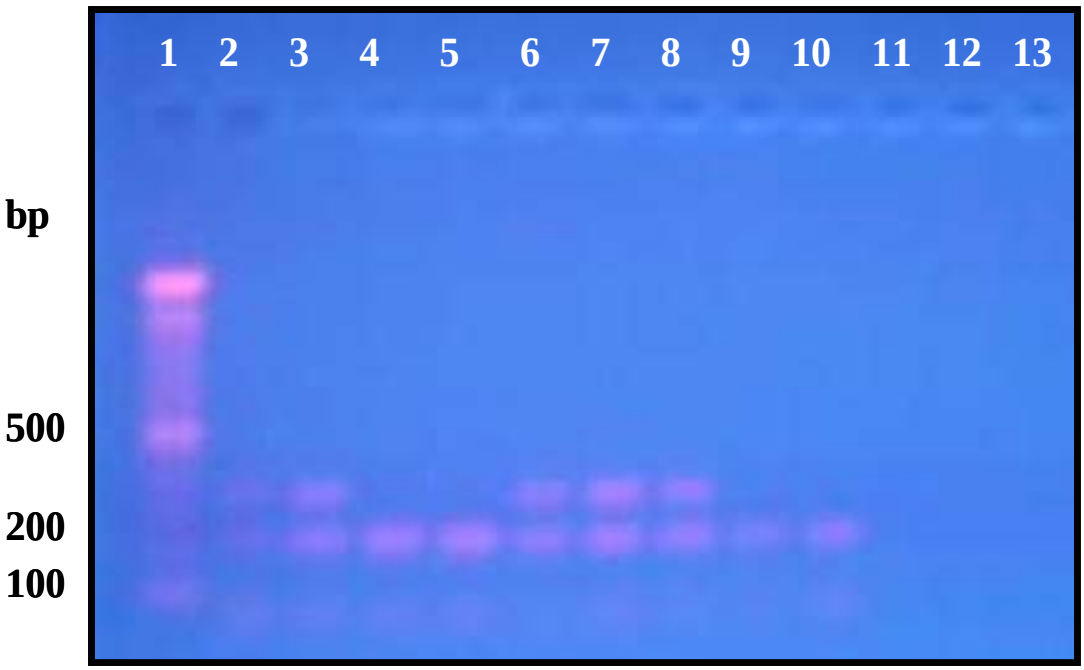

Figure 6.2: **Photographic example of genotyping a litter containing PTEN$^{+/+}$ and PTEN$^{+/-}$ mice. Lane 1 = 100 base pairs (bp) ladder. Lane 2 = positive control donated from Dundee University. Lanes 3,6,7 and 8 = PTEN$^{+/-}$ mice; lanes 4,5,9 and 10 = PTEN$^{+/+}$. Lanes 11-13 = negative controls containing no Taq Polymerase.**

6.2.2.2 Body weight and blood glucose

Body weight

Figure 6.3 displays the body weight of the mice. As expected males are heavier than females, for example PTEN$^{+/+}$ males weigh 29.17 ± 1.21g compared to PTEN$^{+/+}$ females weighing 22.33±0.619g. However, in PTEN$^{+/-}$ males and females only, a small insignificant increase in weight was observed. For example the female PTEN$^{+/+}$ mice weighed an average of 22.33±0.619g compared to the PTEN$^{+/-}$ mice which had an average weight of 23.816±0.97g.

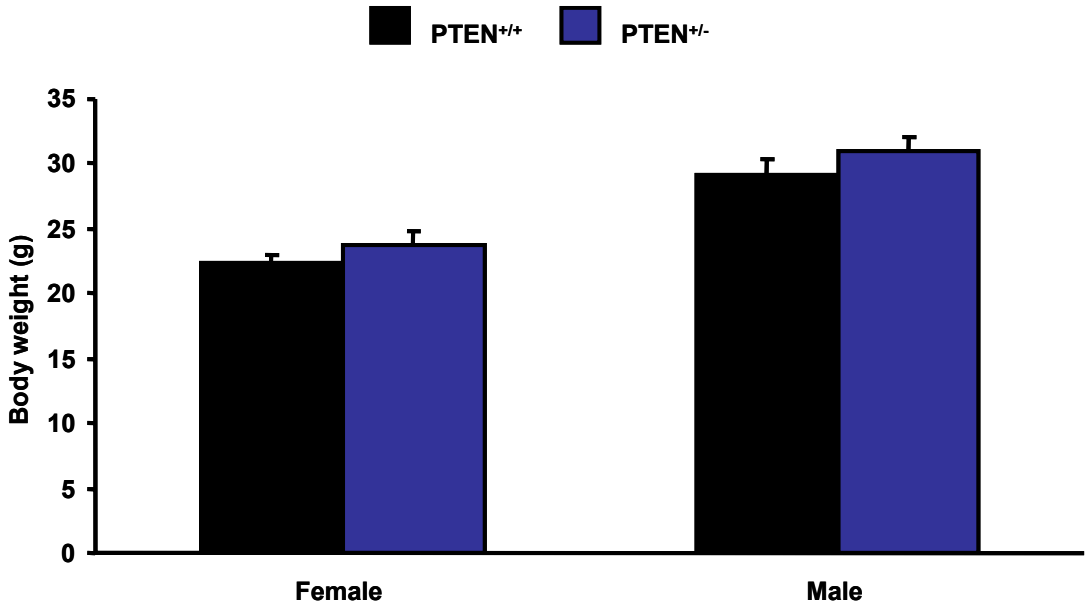

Figure 6.3: **Female and male body weight in grams (g) in PTEN$^{+/+}$ (black bars) compared to PTEN$^{+/-}$ (blue bars) mice (n=6). There was no statistical differences between groups, assessed using the Student's paired t-test.**

Blood glucose

Figure 6.4 displays the values of the blood glucose measured from tail samples (non-fasted). No differences in blood glucose were observed between PTEN$^{+/+}$ and PTEN$^{+/-}$mice. Male blood glucose was reduced from 11.06±0.29mmol/L in PTEN$^{+/+}$ mice to 10.34±0.33mmol/L in the PTEN$^{+/-}$mice, however, this change was not significant.

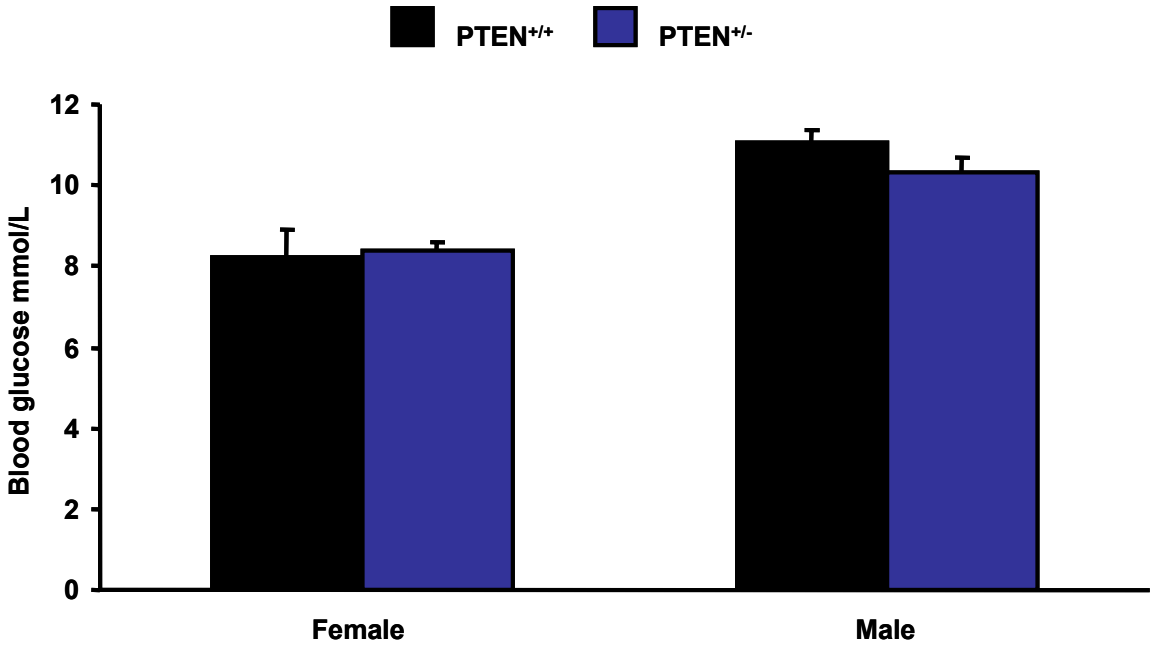

Figure 6.4: **Female and male blood glucose (mmol/L) from PTEN$^{+/+}$ (black bars) compared to PTEN$^{+/-}$ (blue bars) mice (n=6). There was no statistical differences were assessed using the Student's paired t-test.**

6.2.2.3 Myocardial PTEN/PI3K/AKT signalling

6.2.2.3.1 Myocardial PTEN lipid phosphatase activity

The lipid phosphatase activity was estimated using an ELISA assay which monitors the level of PI(3,4,5)P3 that is converted into PI(4,5)P2, and is recorded by changes in absorbance (O.D). The results are displayed in Figure 6.5 which represents the average OD values obtained from basal PTEN$^{+/-}$ hearts without any ischaemia-reperfusion. There were no significant differences in PI(3,4,5)P3 phosphatase activity between PTEN$^{+/-}$ and their PTEN$^{+/+}$ littermates.

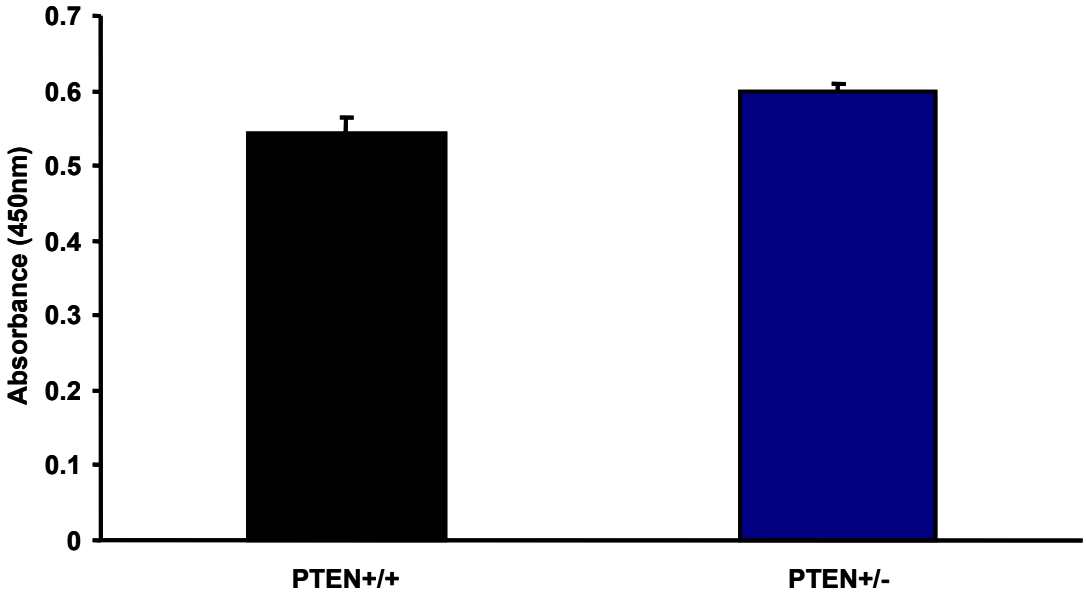

Figure 6.5: PTEN lipid phosphatase activity in the myocardium of the PTEN$^{+/+}$ (black bars) compared to PTEN$^{+/-}$ (blue bars) mice, samples were homogenised in suspension buffer and assayed using the Echelon PTEN ELISA kit, (n=3). There was no statistical differences between groups, assessed using the Student's paired t-test.

These results were surprising, as it was expected that the myocardium from PTEN$^{+/-}$ mice would have less phosphatase activity. The following results show what we did to investigate if this effect was real or if they reflected an operator error. Figure 6.6 and Figure 6.7 show the optimisation steps performed in our investigations. Figure 6.6 demonstrates the typical absorbance values obtained with the PI(4,5)P2 standard curve provided in the ELISA assay kit. As shown in Figure 6.6 a sample from PTEN$^{+/+}$ myocardium provided an OD values of 0.542±0.02 O.D. It was observed that although the samples were not at the lowest point of the standard curve neither were they in the most linear part of the scale, approx 0.75 O.D.

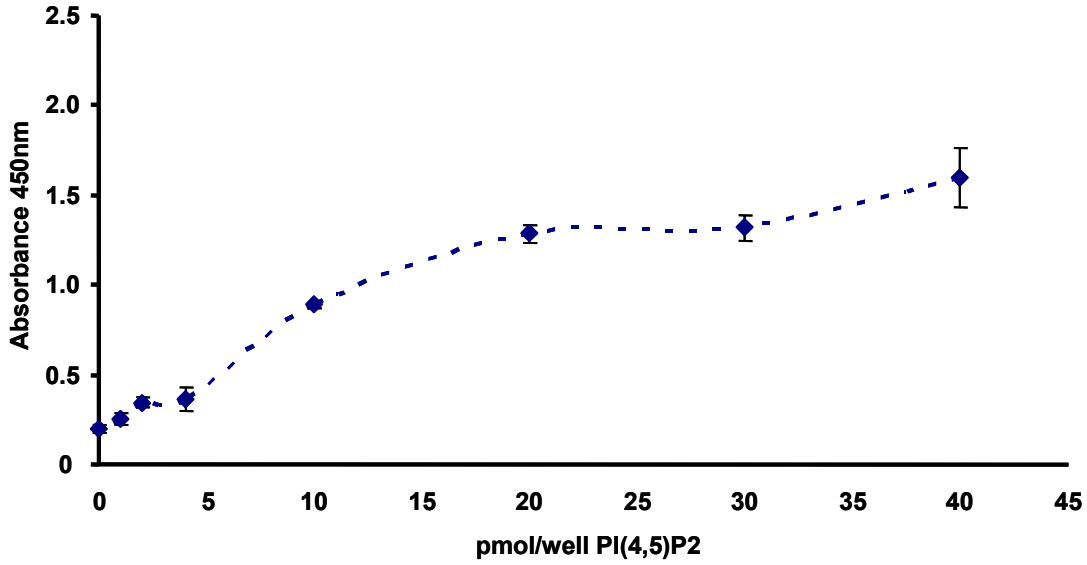

Figure 6.6: Illustration of the phosphatidylinositol 2 phosphate (PI(4,5)P2) standard curve required for the PTEN lipid phosphatase ELISA activity assay (n=3).

We have included the assay optimisation results with the aim to explain why no differences in PTEN lipid phosphatase activity were observed in the $PTEN^{+/-}$ myocardium. Figure 6.7 indicates that as you dilute the myocardial homogenate samples, the OD value increases. This indicates that, when our enzyme preparation was diluted, more PI(4,5)P2 was converted. These preliminary optimisation results suggested that a component in the myocardial homogenate buffer may be interfering with the activity of PTEN in our lysed samples. In summary, we could not confidently address the question regarding PTEN activity in the $PTEN^{+/-}$ hearts using this model.

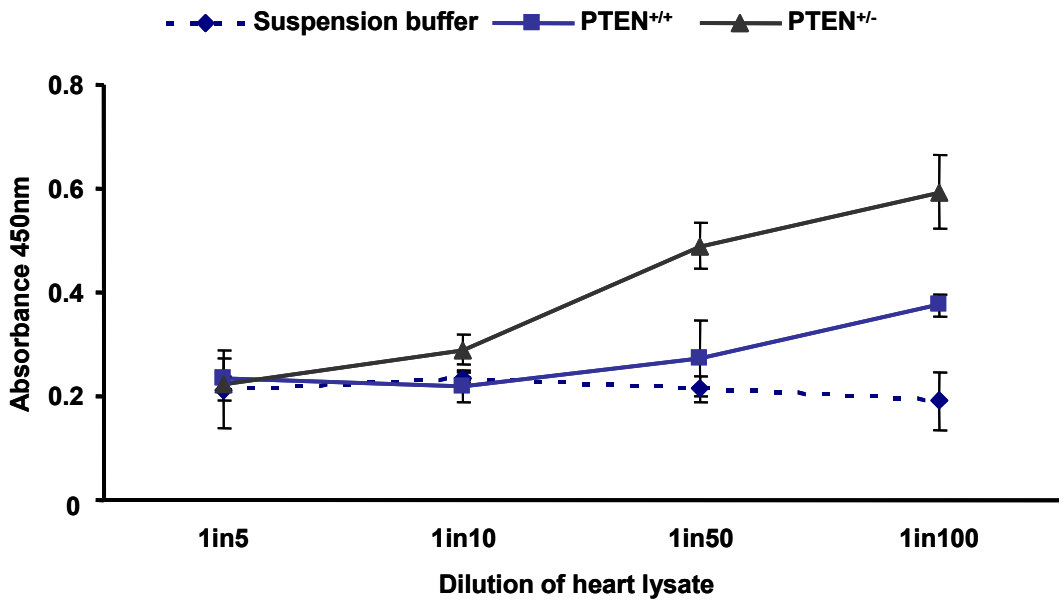

Figure 6.7: Optimisation data for the PTEN lipid phosphatase ELISA activity assay, investigating dilutions of myocardial sample homogenate (n=2).

6.2.2.3.2 The expression of myocardial PTEN and AKT in the PTEN$^{+/-}$ myocardium

PTEN

It was hypothesised that in the PTEN$^{+/-}$ myocardium there would be reduced level of total PTEN expression and/or increased levels of phosphorylated PTEN expression (indicative of PTEN inactivity). As predicted, the basal level of total PTEN was significantly ($p<0.05$) reduced from 0.84±0.1 arbitrary units (A.U) in PTEN$^{+/+}$ controls to 0.35±0.07 A.U in haploinsufficient PTEN$^{+/-}$ myocardium, shown in Figure 6.8. In addition, a small but significant ($p<0.05$) increase in phosphorylated PTEN in the PTEN$^{+/-}$ mice was also observed, being increased from 1.12 ± 0.07 A.U in PTEN controls$^{+/+}$ to 1.40 ± 0.09 A.U in the PTEN$^{+/-}$ myocardium, as shown in Figure 6.9. These results demonstrate a reduced PTEN expression and also indicate the remaining PTEN may be less active in the PTEN haploinsufficient myocardium.

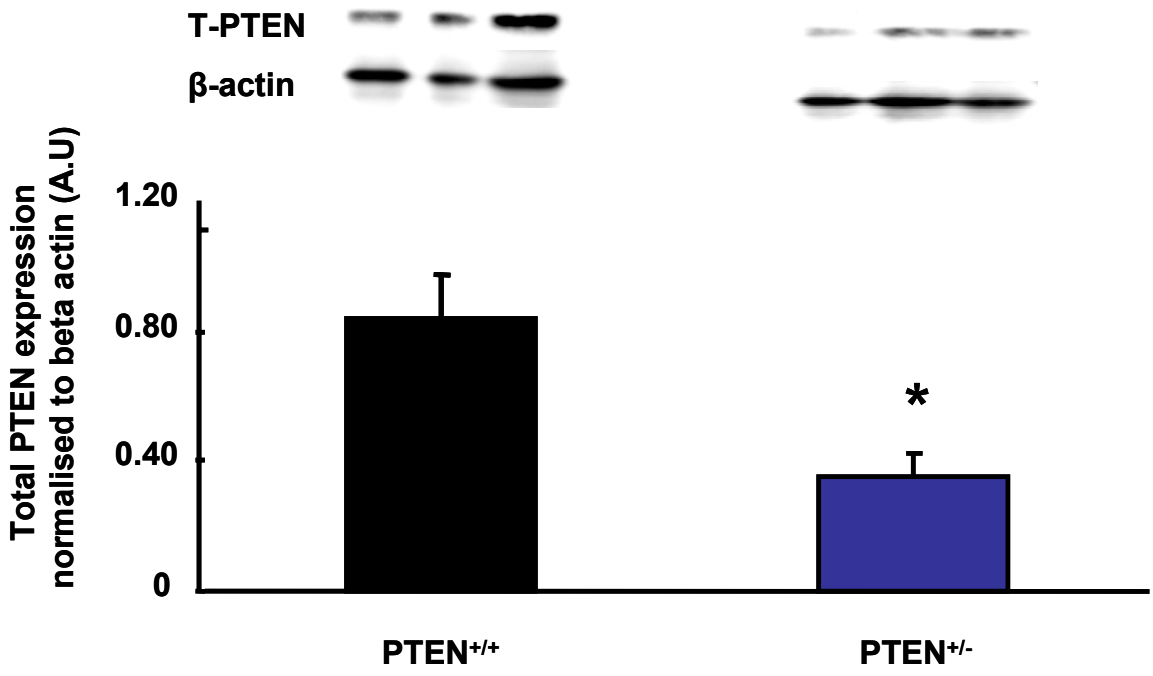

Figure 6.8: **Total PTEN protein expression in myocardium from PTEN$^{+/+}$ (black bars) compared to PTEN$^{+/-}$ (blue bars) mice (n=3). Statistical differences were assessed using the Student's paired t-test, (*p<0.05).**

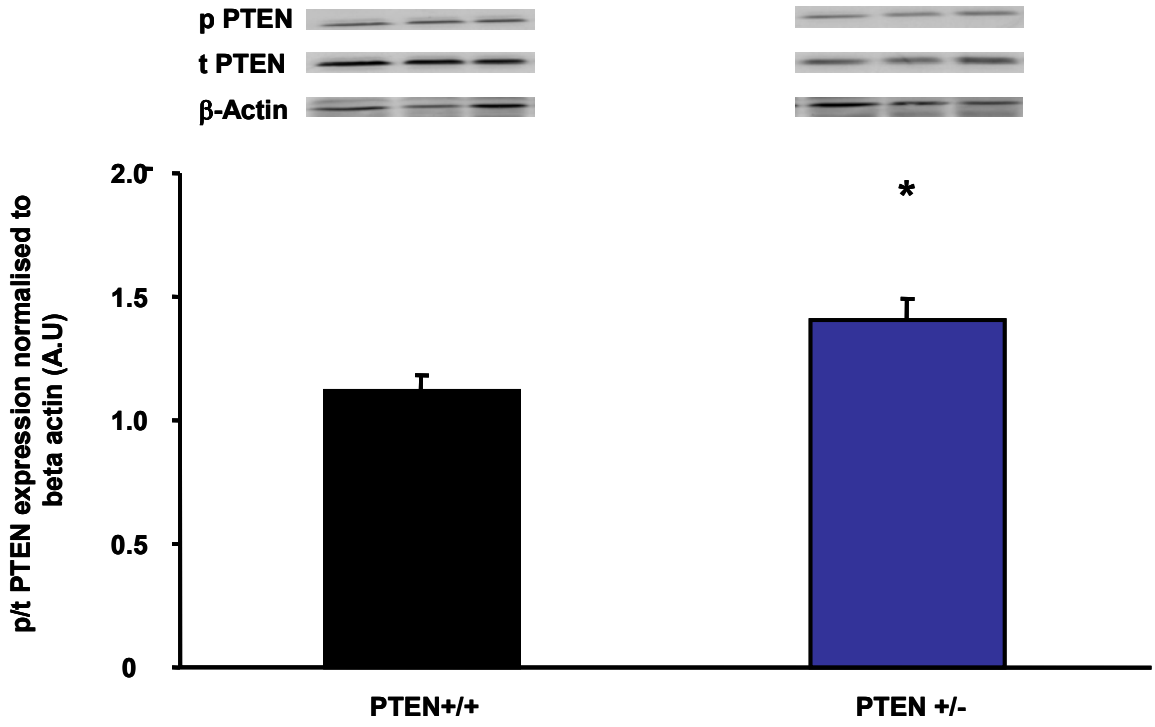

Figure 6.9: Phosphorylated PTEN (p/t PTEN) protein expression in myocardium from PTEN$^{+/+}$ (black bars) compared to PTEN$^{+/-}$ (blue bars) mice (n=3). Statistical differences were assessed using the Student's paired t-test, (*p<0.05).

AKT

It was hypothesised that in the PTEN$^{+/-}$ myocardium there would be an increased expression of phosphorylated AKT (indicative of AKT activity). As predicted, the basal level of phosphorylated AKT, at the Ser473 phosphorylation site, was significantly increased in PTEN$^{+/-}$ haploinsufficient myocardium. The levels were increased to 0.62±0.156 A.U from 0.20±0.088 A.U, $p<0.05$, in control myocardium, as shown in Figure 6.10. Furthermore, a significant ($p<0.05$) increase in phosphorylation of AKT at the Thr308 phosphorylation site was observed in the PTEN$^{+/-}$ myocardium. The levels were increased to 0.27±0.037 A.U from 0.10±0.035 A.U in the control myocardium, as shown in Figure 6.11.

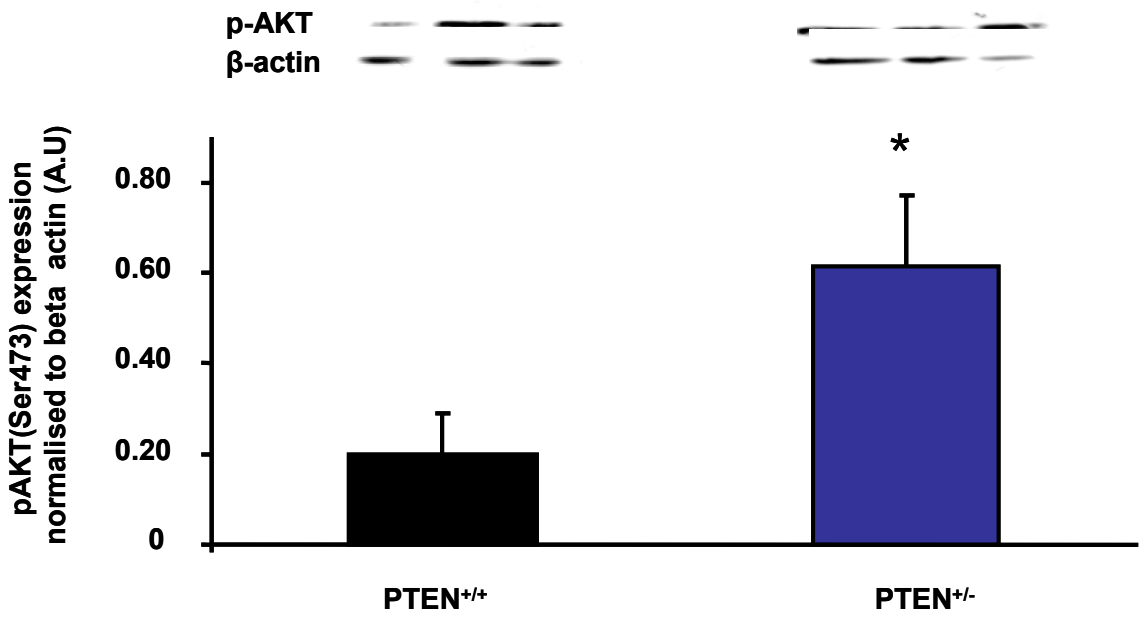

Figure 6.10: **Phosphorylated AKT at Ser473 site (pAKT(Ser473)) protein expression in myocardium from PTEN$^{+/+}$ (black bars) compared to PTEN$^{+/-}$ (blue bars) mice (n=3). Statistical differences were assessed using the Student's paired t-test, (*p<0.05).**

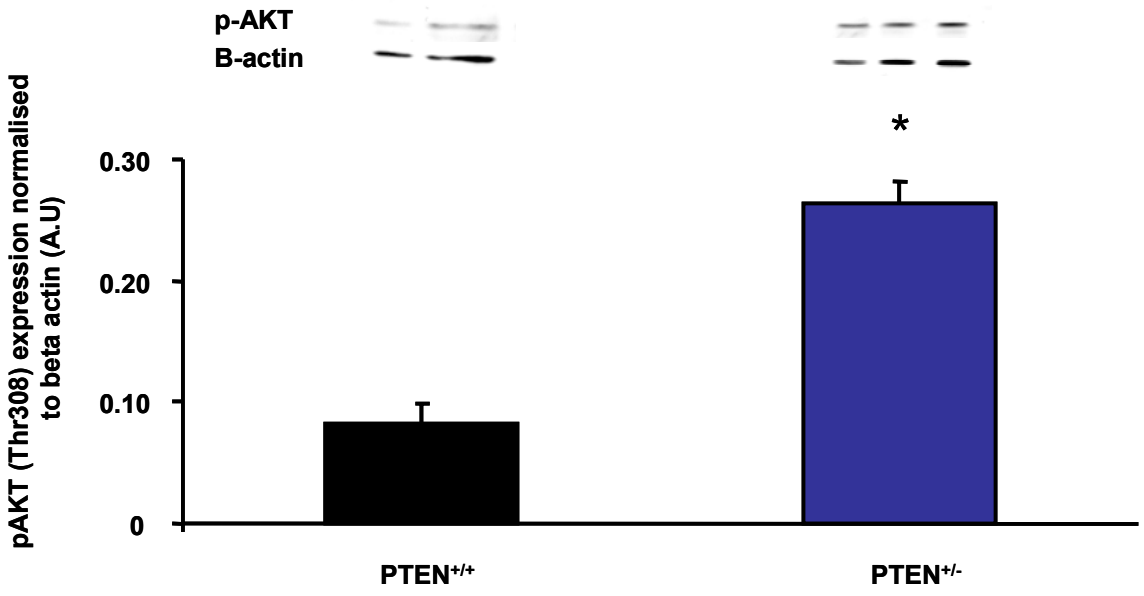

Figure 6.11: **Phosphorylated AKT at Thr308 site (pAKT(Thr308)) protein expression in myocardium from PTEN$^{+/+}$ (black bars) compared to PTEN$^{+/-}$ (blue bars) mice (n=3). Statistical differences were assessed using the Student's paired t-test, (*p<0.05).**

Taken together this data indicate that the myocardium from the PTEN haploinsufficient mice have a significant reduction in PTEN expression and increased AKT phosphorylation in comparison to their $PTEN^{+/+}$ littermate controls. This may have consequences for the survival of the ischaemic-reperfused myocardium.

6.2.3 Discussion

6.2.3.1 Characterising the $PTEN^{+/-}$ haploinsufficient mouse model

As shown by Podsypanina et al., 1999 and Wong et al., 2007, and in this study, we demonstrated that the $PTEN^{+/-}$ mice were heterozygous for PTEN. No significant differences in body weight or blood glucose was observed between $PTEN^{+/-}$ and $PTEN^{+/+}$ mice, 10-15 weeks of age. In contrast Wong et al., found a small but significant reduction in tail vein blood glucose in the $PTEN^{+/-}$ mice, undergoing ad libitum feeding. They recorded blood glucose levels directly from the tail vein, as 7.1±0.4 mmol/L from the $PTEN^{+/+}$ mice compared to 6.3±0.2 mmol/L from the $PTEN^{+/-}$ mice. We recorded higher levels of blood glucose from our mouse colony, 11.06±0.29 mmol/L in the $PTEN^{+/+}$ controls and 10.34±0.33 mmol/L in the $PTEN^{+/-}$ mice.

6.2.3.2 PTEN haploinsufficiency and myocardial PTEN/PI3K/AKT signalling

The aim of this section was to investigate the functional consequences of the PTEN mutation in the myocardium from our PTEN haploinsufficient mouse colony. Myocardial PTEN phosphatase activity was investigated, using an Echelon PTEN ELISA kit, which detects the level of PI(3,4,5)P3 that is converted into PI(4,5)P2. In addition the level of phosphorylated

and total PTEN and AKT expression in the myocardium from these mice was investigated, using Western blot analysis.

6.2.3.2.1 Myocardial PTEN lipid phosphatase activity

It was expected that in the in $PTEN^{+/-}$ myocardium there would be a reduction in PTEN lipid phosphatase activity. However, no changes in the PI(3,4,5)P3 phosphatase activity between $PTEN^{+/-}$ and $PTEN^{+/+}$ hearts were detected. These results were surprising however, the data from the assay optimisation studies indicate that the signals obtained in these samples were not large enough to detect potential differences between $PTEN^{+/+}$ and $PTEN^{+/-}$ myocardium. Furthermore, the manufacturer of this kit only provided a protocol for detecting activity in cell lysates, not whole organ lysates. Western blot suspension homogenate buffer (described in chapter 2.7) was used to assay myocardial samples. Consequentially, when this buffer was diluted, we observed that the assay signal was amplified. It is not clear to us what the reasons for this are. A possible explanation could be that the ingredients on the cell lysis buffer, such as sodium pyrophosphate, may be inhibiting PTEN and or the ELISA assay. This may explain the observation that as the buffer was diluted the activity of PTEN appeared to increase. However, these observations may be due to changes on the ELISA assay itself, such as the substrate (PIP3). Regardless of the mechanisms of this interference, future work would require the investigation and application of an alternative homogenisation buffer, as discussed in section 6.4.3. Our results indicated that the suspension buffer may have interfered with the assay.

Even though the standard curve worked well our results indicated that calculating the level of PI(4,5)P2 conversion in whole hearts, using our ELISA technique may not be reliable. In summary, we could not confidently address the question regarding PTEN activity in the $PTEN^{+/-}$ hearts using this model.

6.2.3.2.2 The expression of myocardial PTEN and AKT

PTEN

It was hypothesised that in the $PTEN^{+/-}$ myocardium there would be a reduction in total PTEN protein expression and/or an increase in phosphorylated PTEN expression, indicative of PTEN inactivity (Ning et al., 2006; Wu et al., 2006). As predicted, in the $PTEN^{+/-}$ myocardium the basal level of total PTEN was reduced, by 58% and the phosphorylated compared to total PTEN was significantly increased ($p<0.05$). This indicates that in the PTEN haploinsufficient myocardium there is a decreased level of PTEN expression and that the remaining PTEN may be less active. The individual blots used to assess these differences, shown in Figure 6.9, are not the best quality however; these findings were consistant when repeated.

The PTEN mouse model used contained a heterozygous mutation, meaning that there was a remaining allele with normal PTEN function. This may explain the reason why no further reductions in total PTEN protein were observed. The level of PTEN reduction, recorded in these mice can vary between groups. Bayascas et al., 2005 have shown a reduction in the expression of PTEN in the liver. These changes were not significant, however a significant increase in the phosphorylation of AKT was observed in the $PTEN^{+/-}$ mice (Bayascas et al., 2005). In contrast, Huang et al., 2005 recorded a 50% reduction in the levels of liver and myocardial PTEN expression (Huang et al., 2008). In these knockout mice the effected region is within Exon 5 of the PTEN gene, which has been linked to activity (Podsypanina et al., 1999). Our $PTEN^{+/-}$ mouse colony tests positive for this deletion. As described by Podsypanina et al., 1999, these mice are predisposed to the development of tumours in proliferative tissue such as prostate and endometrial tissue, supporting the fact that an allele for PTEN has been deleted (Podsypanina et al., 1999). Our data coincides with work published by others indicating the total protein reduction in these mice can be minimal yet still have physiological consequences (Podsypanina et al., 1999). For example these mice exhibit

insulin hypersensitivity (Wong et al., 2007) and we have observed an increased incident of tumours. This suggests that there is insufficient PTEN function and up regulation of growth and survival pathways. Others groups have shown that the remaining PTEN appears to have reduced PTEN activity (Bayascas et al., 2005; Wong et al., 2007). Post translational modifications can also affect PTEN, for example phosphorylated PTEN is associated with reduced activity. Furthermore, PTEN phosphorylation by CK2 can inhibit activity and additionally make the phosphatase more susceptible to further phosphorylation and inactivation (Al Khouri et al., 2005; Ning et al., 2006).

AKT

It was hypothesised that the myocardium from $PTEN^{+/-}$ mice would have an increased expression of phosphorylated AKT (indicative of AKT activity). As predicted, the basal level of phosphorylated AKT (at Ser473 and Thr308 phosphorylation sites) was significantly increased in PTEN haploinsufficient myocardium ($p<0.05$). The individual blots used to assess this are shown in Figure 6.10 and are not the best quality, nevertheless the findings were consistent when repeated. Other laboratories have also successfully measured increases in AKT phosphorylation as an indicator of PTEN inactivity, in cells (Schmid et al., 2004; Lai et al., 2007) and in the brain (Wu et al., 2006). The data shown in this section indicates that the PI3K/AKT signalling pathway is up regulated in the $PTEN^{+/-}$ myocardium.

6.3 Investigating the response of the PTEN$^{+/-}$ myocardium to ischaemia-reperfusion injury

6.3.1 Experimental protocols

The response of PTEN haploinsufficiency to simulated ischaemia-reperfusion injury was investigated. An isolated heart model of ischaemia-reperfusion injury and an isolated cardiomyocyte model of ROS induced mitochondrial damage was used. As described in chapter 2, section 2 and 5, respectively. It was hypothesised that the PTEN$^{+/-}$ myocardium would be more resistant to ischaemia-reperfusion induced cell death due to up regulation of the PI3K/AKT prosurvival pathway.

6.3.1.1 Ischaemia-reperfusion injury in isolated perfused mouse hearts

As a standard, male mice are the preferred choice for use in experiments that investigate myocardial infarction, in order to avoid the possibility of cardioprotective effects from estrogens. Therefore, the following experiments, primarily used male mice. However, we aimed to maximise the use of each litter and additional validation studies entailed the use of female mice.

1) Isolated perfused male PTEN$^{+/-}$ and PTEN$^{+/+}$ myocardium (n=6) were subjected to the standard protocol of ischaemia-reperfusion, as shown in Figure 6.1 and the level of infarction was measured as an endpoint. It was hypothesised that the PTEN$^{+/-}$ myocardium will bestow protection against ischaemia-reperfusion injury.

2) Female, PTEN haploinsufficient mice develop tumours more readily than males; which reflects a higher activation of the PI3K/AKT pathway (Podsypanina et al., 1999).

Therefore it was additionally hypothesised that the female PTEN$^{+/-}$ myocardium may be better protected against ischaemia-reperfusion injury. We subjected isolated perfused female PTEN$^{+/-}$ and PTEN$^{+/+}$ myocardium (n=6) to our standard protocol of ischaemia-reperfusion, as shown in Figure 6.1,B and measured infarction as an endpoint.

3) Tumour progression in these mice is positively correlated with age. (Podsypanina et al., 1999). Therefore, it was additionally hypothesised that a better protection may be achieved with age and that the older PTEN$^{+/-}$ myocardium would develop smaller infarcts than the littermate controls. The effect of PTEN haploinsufficiency in the aging myocardium was investigated and the infarct size in mice at 10wks to mice at 20wks of age was compared. Female mice were used in this investigation and subjected to our standard protocol of ischaemia-reperfusion, as shown in Figure 6.1,C, n= 5.

4) The PTEN haploinsufficient mouse is a congenital model of PTEN down regulation in which the PTEN/AKT pathway is expected to be affected (Wong et al., 2007). However, an allele remains native for PTEN. We aimed to maximise PTEN inhibition in these mice using the PTEN inhibitor bpV(HOpic). Consequently, it was hypothesised that perfusion of the PTEN$^{+/-}$ myocardium with the PTEN inhibitor bpV(HOpic) would bestow an even bigger reduction in infarction following ischaemia-reperfusion injury. Isolated PTEN$^{+/-}$ and PTEN$^{+/+}$ myocardium (male, 10-15wks) were perfused with either control buffer or with buffer containing 1μM of bpV(HOpic) (n=5) throughout stabilisation and reperfusion, as shown in Figure 6.1,D. The vehicle control for this drug was water. Infarction was measured as an endpoint.

6.3.1.2 Response of isolated cardiomyocytes to ROS induced mitochondrial damage

Opening of the mitochondrial permeability transition pore has been associated with the final stages of cell death and plays an important role in ischaemia-reperfusion injury (Halestrap et al., 2004). Primary cardiomyocytes were isolated from PTEN haploinsufficient mouse hearts and subjected to ROS induced mitochondrial damage, as described in Chapter 2, section 5. ROS was generated in the mitochondria to mimic reperfusion injury (Hausenloy et al., 2003). The time to mitochondrial depolarisation was measured and compared to that recorded from $PTEN^{+/+}$ littermate control cells. As a positive control, CsA (0.4μM) was administered as an inhibitor of mPTP opening, 15 min prior to ROS stimulation. Cells were isolated from 3 hearts in separate experiments (n=3), which provided 37±2 cells for each condition tested. It was hypothesised that cardiomyocytes from the $PTEN^{+/-}$ myocardium would exhibit a delay in the time to mPTP opening, compared to myocytes from littermate control myocardium.

6.3.2 Results

6.3.2.1 Ischaemia-reperfusion injury in isolated perfused $PTEN^{+/-}$ myocardium

Isolated perfused male $PTEN^{+/-}$ myocardium were subjected to the standard protocol of ischaemia-reperfusion injury. Unexpectedly, no protection in response to ischaemia-reperfusion was detected in the haploinsufficient myocardium as shown in Figure 6.13. Isolated hearts from male $PTEN^{+/-}$ mice developed an infarct size of (42.1± 5.0%) which was similar to the infarction developed in male $PTEN^{+/+}$ hearts 45.6±3.3%. Furthermore, no difference in the heart function prior to ischaemia or at reperfusion was observed.

As mentioned above, it was hypothesised that the female PTEN$^{+/-}$ myocardium may be more resistant to ischaemia-reperfusion. These mice develop tumours more readily than males and therefore appear to be more effected by the mutation (Podsypanina et al., 1999). However, as shown in Figure 6.12, again no protection was observed in the female PTEN$^{+/-}$ myocardium. These female PTEN$^{+/-}$ hearts developed a similar infarct size (52.2± 6.2%) compared to male PTEN$^{+/-}$ and PTEN$^{+/+}$ myocardium.

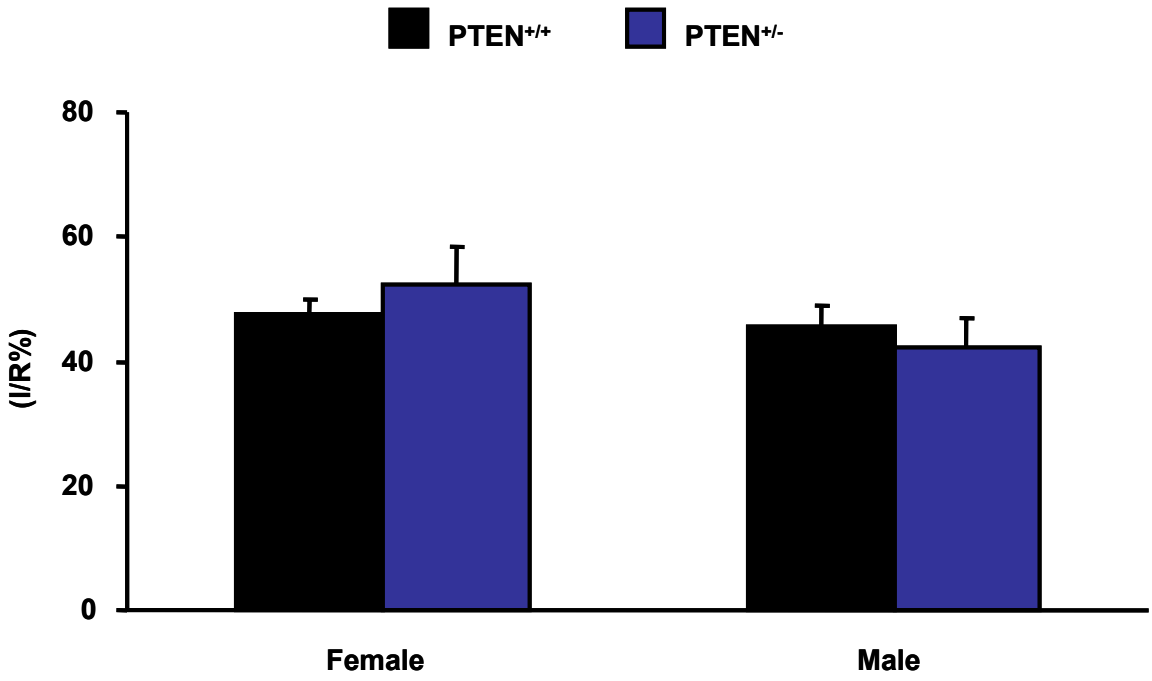

Figure 6.12: Percentage infarction developed in the risk area (I/R%) in male and female PTEN$^{+/+}$ and PTEN$^{+/-}$ myocardium subjected to ischaemia-reperfusion injury (n=6). There was no statistical differences between groups, assessed using the Student's paired t-test.

As described on page 210, tumour progression in these mice is positively correlated with age (Podsypanina et al., 1999). Therefore, it was hypothesised that the protection may be increased in older PTEN$^{+/-}$ myocardium. However, no significant differences were recorded between myocardium from mice 10 weeks of age compared to those at 20 weeks of age, as

shown in Figure 6.13. The isolated hearts from PTEN$^{+/+}$ mice at 20 weeks of age developed an infarct size of 51.9±5.98% which was similar to hearts from PTEN$^{+/-}$ mice of the same age (42.88± 5.17%).

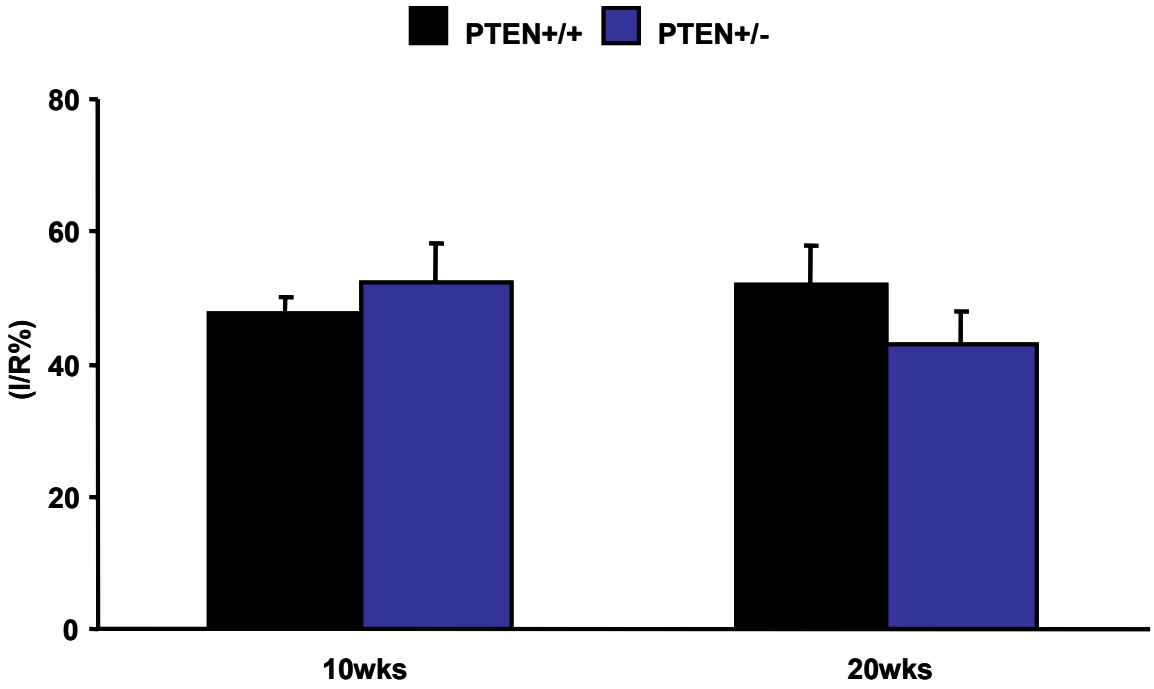

Figure 6.13: Percentage infarction developed in the risk area (I/R%) in female PTEN$^{+/+}$ and PTEN$^{+/-}$ myocardium subjected to ischaemia-reperfusion: at 10wks and 20wks of age (n=5). No significant differences were identified, assessed using a One way ANOVA test.

The PTEN haploinsufficient mouse is a congenital model containing a PTEN mutation and as previously shown, the PTEN/AKT pathway is affected in these mice. However, an allele remains native for PTEN. Consequently, it was hypothesised that perfusion of the PTEN inhibitor bpV(HOpic) in the PTEN$^{+/-}$ myocardium would bestow protection against ischaemia-reperfusion injury. Surprisingly, again no significant differences in the level of infarction were recorded, as shown in Figure 6.14. For example isolated hearts perfused with 1μM

bpV(HOpic) from PTEN$^{+/+}$ developed an infarct size of 39.16±6.5% which was similar to the PTEN$^{+/-}$ hearts which developed an infarct size of 37.14± 3.15%.

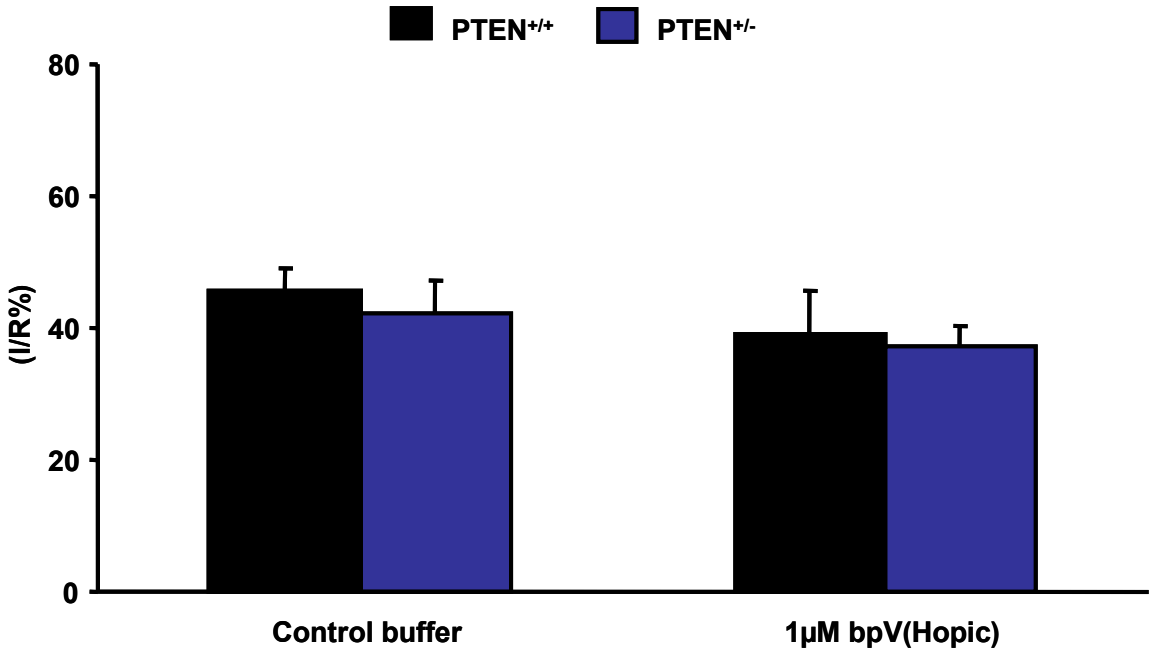

Figure 6.14: Percentage infarction developed in the risk area (I/R%) in male PTEN$^{+/+}$ and PTEN$^{+/-}$ myocardium (10-15wks) subjected to ischaemia-reperfusion in the presence and absence of bpV(HOpic) (n=6). No statistical differences observed using a One way ANOVA test.

In summary, the PTEN haploinsufficient myocardium appears to have enhanced activity of the PI3K/AKT pro survival pathway. However, this level of activation is not sufficient to induce protection against our models of myocardial ischaemia-reperfusion injury.

6.3.2.2 Isolated PTEN$^{+/-}$ cardiomyocytes and ROS induced mitochondrial damage

We investigated whether cardiomyocytes isolated from the PTEN$^{+/-}$ myocardium were protected against ROS induced mPTP opening. It was hypothesised that there would be a delay in the time to mPTP opening. The results are shown in Figure 6.15 and indicate there is no significant difference in time to mPTP opening in myocytes isolated from PTEN$^{+/-}$ (195 $\pm$ 2 sec) myocardium compared to the PTEN$^{+/+}$ (224 $\pm$ 4 sec) cardiomyocytes. As expected, incubation of isolated cardiomyocytes with CsA delayed the time to mPTP opening. CsA reduced time to mPTP opening to 366 $\pm$ 64 sec in PTEN$^{+/-}$ myocytes and 351 $\pm$ 74 sec in PTEN$^{+/+}$ myocytes. No differences in the time to mPTP opening were detected between PTEN$^{+/-}$ and PTEN$^{+/+}$ myocytes incubated with CsA.

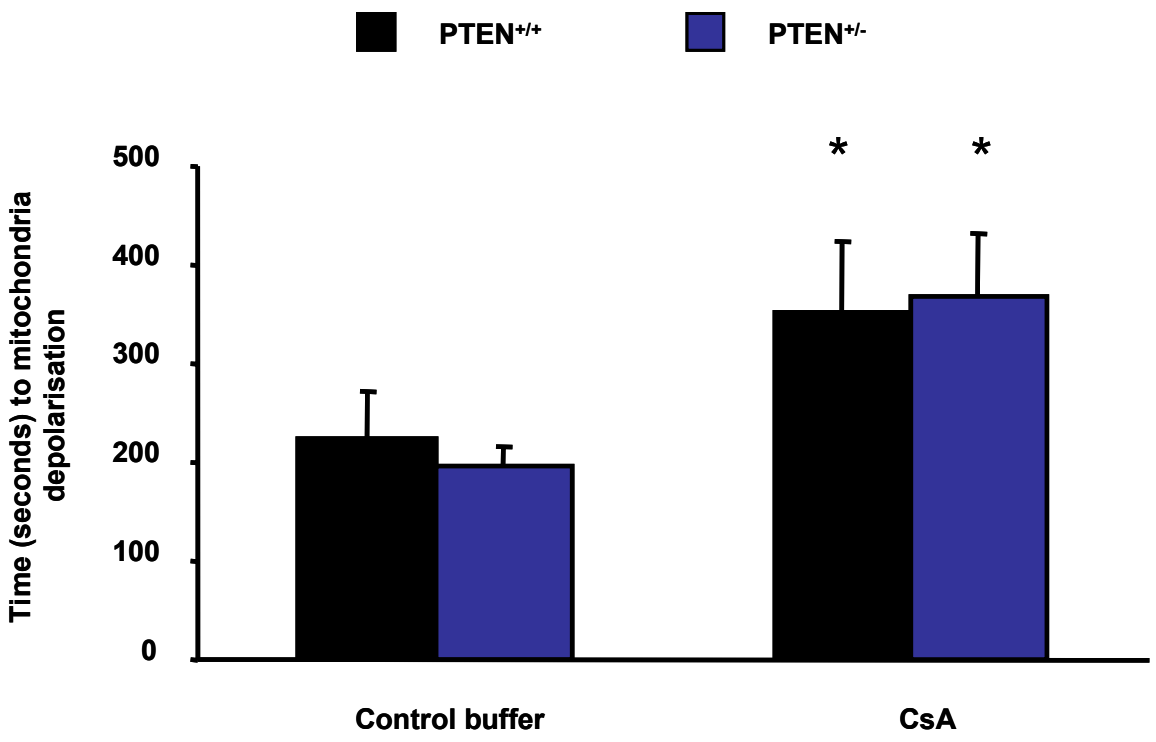

Figure 6.15: Time to ROS induced mitochondrial depolarisation, time to mitochondrial permeability transition pore (mPTP) opening in PTEN$^{+/+}$ and PTEN$^{+/-}$ mouse cardiomyocytes with or without cyclosporine A (CsA), an inhibitor of mPTP (cells isolated from 3 hearts, providing 37±2 cells for each condition). Statistical differences were assessed using the students paired t-test, compared to each control (*= p<0.05).

In summary, reducing PTEN (either using a chemical inhibitor or a genetically manipulated mouse strain) does not confer protection against myocardial infarction; despite AKT activation. However, because AKT activation is increased, it was hypothesised that the threshold for cardioprotection is lowered in the PTEN$^{+/-}$ hearts. IPC was selected as the model to verify this hypothesis.

6.3.3 Discussion

6.3.3.1 The response of isolated hearts to ischaemia-reperfusion injury

It was hypothesised that the genetic disruption of PTEN would facilitate a decrease in myocardial ischaemia-reperfusion injury. However, PTEN haploinsufficient mice did not present with any further protection against ischaemia-reperfusion in comparison to their littermate controls. Firstly, isolated perfused myocardium from male $PTEN^{+/-}$ mice were subjected to our standard protocol of ischaemia-reperfusion, and unexpectedly no protection was detected, as the infarct size was similar to the level from their $PTEN^{+/+}$ littermates. Additionally, it was hypothesised that the female $PTEN^{+/-}$ myocardium may be more resistant to ischaemia-reperfusion, however, no protection was observed relative to littermate controls. In light of these observations, it was hypothesised that protection may be achieved in the older $PTEN^{+/-}$ myocardium, however, no significant differences were recorded between myocardium from mice 10 weeks of age compared to those at 20 weeks of age. Cai et al., 2008 have studied ischaemia-reperfusion injury in HIF1α heterozygous knockout mouse, in their experiments they used mice that were 24 weeks old (Cai et al., 2008a). Unfortunately, we could not investigate $PTEN^{+/-}$ mice older than 20 weeks, as they exhibited the onset of tumours and needed to be euthanased. The PTEN haploinsufficient mouse is a congenital model of PTEN down regulation and, as we have shown, the PTEN/PI3K/AKT pathway is affected in these mice. However, as discussed previously, one allele remains wild type for PTEN. Consequently, it was hypothesised that perfusing the PTEN inhibitor bpV(HOpic) through the $PTEN^{+/-}$ myocardium would bestow protection against ischaemia-reperfusion injury. Surprisingly, even under these conditions, no significant differences in infarct size were recorded.

Interestingly, Crackower *et al*., 2002 have produced a homozygous knock out (-/-) of PTEN, organ targeted for mouse hearts and skeletal muscle only. Consequently, the hearts become hypertrophic and had impaired contractility (Crackower et al., 2002). This is a different knock out model to the one used in this study, however the finding by Crackower *et al.,* 2002 highlighted that the complete ablation of PTEN can have major physiological implications, such as cardiac hypertrophy and reduced myocardial contractility.

6.3.3.2 The response of isolated cardiomyocytes to ROS induced mitochondrial damage

The opening of the mPTP in relation to apoptosis and myocardial ischaemia-reperfusion injury has been studied (Griffiths and Halestrap, 1995; Halestrap et al., 2004; Argaud et al., 2005a). Interestingly, isolated rabbit hearts were perfused with CsA or the non immunosuppressive derivative NIM811 are protected against ischaemia-reperfusion injury. Mitochondria isolated from these hearts required a higher concentration of Ca^{2+} overload in order to open the mPTP and induce cell death (Argaud et al., 2005a). The authors of this work attributed cardioprotection in the myocardium to this delay in mPTP opening.

In order to investigate weather $PTEN^{+/-}$ cardiomyocytes are protected against mPTP opening; an isolated cardiomyocyte model of mPTP opening was used. This assay was a secondary model of simulated ischaemia-reperfusion injury, which mimics the accumulation of mitochondrial ROS that occurs during reperfusion. It was hypothesised that there would be a delay in the time to mPTP opening in isolated $PTEN^{+/-}$ cardiomyocytes compared to myocytes from $PTEN^{+/+}$mice. As a positive control cardiomyocytes from littermate controls were incubated with CsA. In agreement with work published by others (Lim et al., 2008; Halestrap et al., 1997; Argaud et al., 2005a) it was demonstrated that CsA provided a delay in mPTP opening in the myocardium from $PTEN^{+/+}$ and $PTEN^{+/-}$ mice. Conversely, no significant

differences in time to mPTP opening was observed in isolated myocytes from $PTEN^{+/-}$ compared to $PTEN^{+/+}$ mice. No differences in the time to mPTP opening were detected between $PTEN^{+/-}$ and $PTEN^{+/+}$ myocytes in the presence of CsA, verifying that down regulation of PTEN does not confer protection against ROS induced mitochondrial damage.

In this study, the TMRM dye was used as an indicator of mPTP opening, which is a widely used method (Lawrence et al., 2004; Davidson et al., 2007). Additionally, it is also possible to detect mPTP opening by using the green fluorescent dye, calcein-AM, which accumulates throughout the cell but can be visualised in the mitochondria by quenching cytosolic fluorescence using colbolt chloride. When the mPTP opens calcein moves out and the fluorescence is quenched (Hausenloy et al., 2004a; Saotome et al., 2009). It would be interesting to use this dye to confirm our results; however, because the positive control (CsA) worked in our model, we can assume that the results will be the same. However, incubation of cardiomyocytes from $PTEN^{+/-}$ mice with a subprotective dose of a PI3K/AKT activator, such as insulin, in may cause a delay in the time to mPTP opening when compared to a similar treatment in myocytes from $PTEN^{+/+}$ hearts.

Results with all knock out models should be interpreted with care as there may be adaptation or compensation to the lack of the target that is knocked out. The absence of cardioprotection against ischaemia-reperfusion injury in the $PTEN^{+/-}$ mice could be explained by compensatory mechanisms, such as up regulation of alternative lipid phosphatases. The PI3K/AKT pathway is also negatively regulated by the lipid phosphatase SHIP2 (Chi et al., 2004), which has specificity for the 5' phosphate of PI(3,4.5)P3 to produce PI(3,4)P2 whereas PTEN has specificity for the 3' phosphate creating PI(4,5)P2 (Chi et al., 2004), as shown in Figure 1.6. Surprisingly, the inhibition of SHIP2 was not associated with formation of cancers. Unlike PTEN, which acts on basal AKT activity, SHIP2 acts on stimulated levels of AKT (Lazar and

Saltiel, 2006). Therefore, this makes it a potentially attractive target for cardiovascular research and, possibly, an alternative target to PTEN (Pesesse et al., 1997).

In addition to SHIP2, other phosphatases such as PHLPP and PP2A can negatively regulate the PI3K pathway, directly inactivating AKT (Sugano et al., 2005; Gao et al., 2005a; Zuluaga et al., 2007). These phosphatases could be up-regulated in the PTEN haploinsufficient mice and could be classed as targets of cardioprotection in their own right. It is important to investigate these alternative negative regulators of the PI3K/AKT pathway in the myocardium of our PTEN haploinsufficient mice.

6.4 Investigating the response of the PTEN$^{+/-}$ myocardium to ischaemic preconditioning

6.4.1 Experimental protocols

IPC is regarded as the most powerful mechanism for cardioprotection and is often used as a positive control in myocardial survival studies (Yellon and Downey, 2003). Cardioprotection was investigated in the PTEN haploinsufficient myocardium, the aim was to determine the IPC protocol required to confer protection in these mice. The Langendorff model of isolated perfused myocardium was used to study the effects of IPC on ischaemia-reperfusion injury, as described in chapter 2, section 2. We investigated the effects of the perfusion protocols listed below on 1) infarction and 2) cell signalling.

1) The response to IPC in the PTEN$^{+/-}$ and PTEN$^{+/+}$ myocardium was investigated. The level of infarction developed in response to ischaemia-reperfusion alone or preceded by 2,4,or 6 cycles of IPC, n= 5, was recorded. Each IPC cycle consisted of 5 min ischaemia followed by 5 min reperfusion, as shown in Figure 6.16.

2) The cell signalling that occurred in the myocardium subjected to IPC was investigated by exploring the response to ischaemia-reperfusion alone or preceded by 4 or 6 cycles of IPC, n= 3. Western blot analysis, as described in chapter 2, section 2 was used to investigate the level of PTEN and AKT as a consequence of IPC in the PTEN haploinsufficient myocardium. Phosphorylated and total levels of PTEN (Ser380,Thr382/383 sites) and AKT(Thr308 and Ser473 sites) were measured. Previously, it was shown that changes in AKT activity during IPC can be detected following the IPC stimulus (Tsang et al., 2005). Therefore, samples were collected immediately prior to the lethal ischaemic event, as shown in Figure 6.16. These samples were used to investigate the PTEN lipid phosphatase activity during IPC, using the Echelon PTEN ELISA assay, as described in chapter 2, section 4. It was hypothesised, that in the $PTEN^{+/-}$ hearts, as a consequence of IPC there would be further increases in the PI3K/AKT signalling.

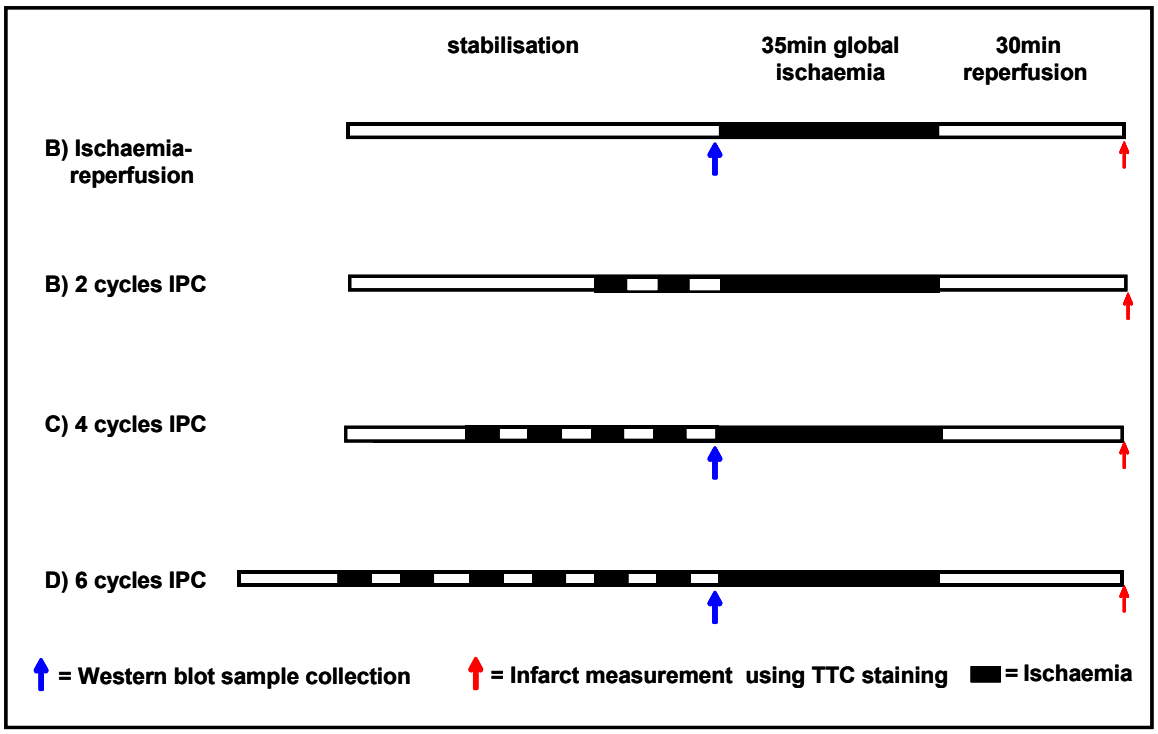

Figure 6.16: Experimental protocols used to study ischaemia-reperfusion injury and cardioprotection in isolated PTEN$^{+/+}$ and PTEN$^{+/-}$ myocardium. Investigating the number of ischaemic preconditioning (IPC) cycles required to confer protection, where 1 cycle consists of 5 min ischaemia followed by 5 min reperfusion. Comparing: A) ischaemia-reperfusion alone; B) 2 cycles IPC; C) 4 cycles IPC and D) 6 cycles IPC. I/R% = percentage of infarction to risk area TTC = triphenyltetrazolium chloride.

6.4.2 Results

6.4.2.1 IPC in the isolated perfused PTEN$^{+/-}$ myocardium

Cardioprotection in the PTEN haploinsufficient myocardium was investigated, the aim was to explore the minimal IPC stimulus protocol required to confer protection in these mice. Myocardial infarction following ischaemia-reperfusion alone or ischaemia-reperfusion preceded by 2,4,or 6 cycles of IPC (5 min ischaemia and 5 min reperfusion) was investigated.

The results are shown in Figure 6.17 and indicate that fewer cycles of IPC are needed in the PTEN$^{+/-}$ haploinsufficient mouse heart to confer tissue salvage. Protection was induced as a consequence of 6 cycles IPC in the PTEN$^{+/+}$ and PTEN$^{+/-}$ myocardium. In these groups, infarction was significantly reduced from 44.71 ± 1.97% in ischaemia-reperfusion control to 30.87 ± 5.06% ($p<0.05$) in the PTEN$^{+/+}$ myocardium and similarly was reduced from 44.28 ± 4.36% to 28.33 ± 2.66% ($p<0.05$) in the PTEN$^{+/-}$ myocardium. Interestingly, only in the PTEN$^{+/-}$ myocardium, 4 cycles of IPC stimulus also significantly reduced infarction to 29.07.± 3.05% $p<0.05$, an effect not observed in the PTEN$^{+/+}$ myocardium. These results indicate the myocardium from PTEN haploinsufficient animals have a reduced threshold for IPC induced cardioprotection.

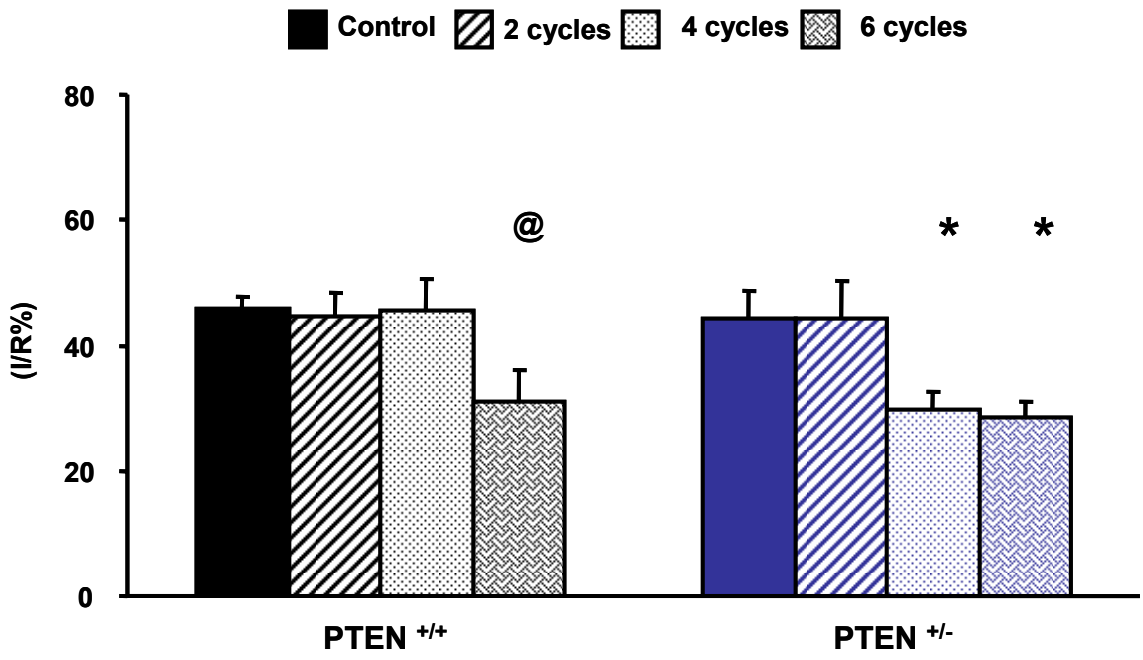

Figure 6.17: Percentage infarction developed in the risk area (I/R%) in male PTEN$^{+/+}$ and PTEN$^{+/-}$ hearts subjected to ischaemia-reperfusion (solid bars); with 2 (stripes); 4 (dots) or 6 (bricked) cycles of ischaemic preconditioning (IPC) (n=5). Statistical differences were assessed using One Way ANOVA, @=$p<0.05$ in PTEN$^{+/+}$ and *=$p<0.05$ in PTEN$^{+/-}$).

6.4.2.2 Expression of PTEN/PI3K/AKT pathway in IPC induced cardioprotection

It was hypothesised that the PI3K/AKT pathway in the $PTEN^{+/-}$ mouse myocardium would be increased by our IPC protocol. Tissue collected following the IPC protocol was measured for PTEN lipid phosphatase activity using the PTEN ELISA kit and the expression of phosphorylated and total PTEN and AKT using Western blot analysis. The results are described below.

PTEN lipid phosphatase activity in IPC

No significant differences in the absorbance values were observed in samples obtained from $PTEN^{+/-}$ or $PTEN^{+/+}$ myocardium subjected to either perfusion control, 4 or 6 cycles of IPC; as shown in Figure 6.18. As previously stated (in chapter 6, section 2) we are not confident that the ELISA kit is sensitive enough for measuring PTEN activity in homogenised tissues.

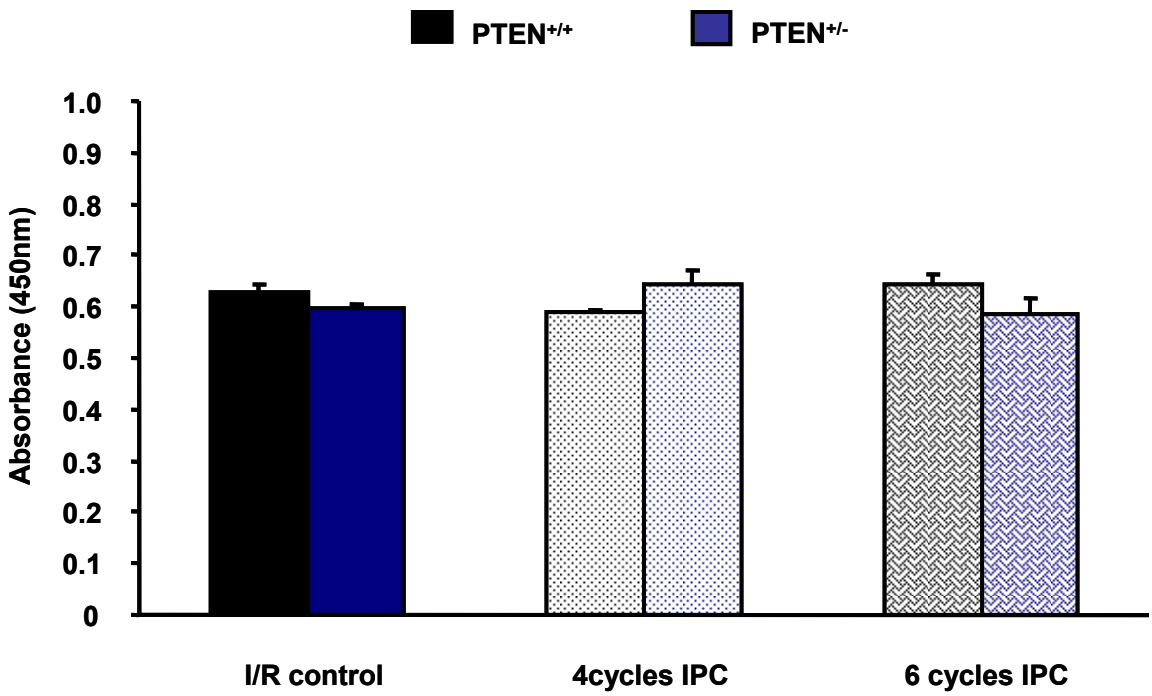

Figure 6.18: PTEN lipid phosphatase activity in the PTEN$^{+/+}$ and PTEN$^{+/-}$ myocardium subjected to ischaemia-reperfusion (solid bars); with 4 (dots) or 6 (bricked) cycles of ischaemic preconditioning (IPC) (n=3). Statistical differences were assessed using One Way ANOVA.

PTEN protein expression

Figure 6.19 presents the data obtained following investigations into phosphorylation of PTEN (Ser380,Thr382/383) during preconditioning of the PTEN$^{+/-}$ myocardium. It shows that basal, non preconditioned, non ischaemic PTEN$^{+/-}$ hearts expressed a significantly ($p<0.01$) higher level of PTEN phosphorylation, (1.26 ± 0.0126, A.U) compared to PTEN$^{+/+}$ (0.67 ± 0.03, A.U) hearts, indicative of PTEN inactivity. Following 4 cycles of IPC a significant ($p<0.01$) increase in phosphorylation of PTEN (Ser380,Thr382/383) is observed in the PTEN$^{+/-}$ myocardium, compared to PTEN$^{+/+}$ hearts subjected to ischaemia reperfusion control. The phosphorylation of PTEN (Ser380,Thr382/383) in PTEN$^{+/-}$ myocardium was higher than PTEN$^{+/+}$ myocardium at 4 (0.99 ± 0.20) and 6 cycles (0.73 ± 0.05) of IPC, however this differences was not

significant. Examples of the Western blot scans showing PTEN$^{+/-}$ myocardium with and without IPC are displayed in Figure 6.20.

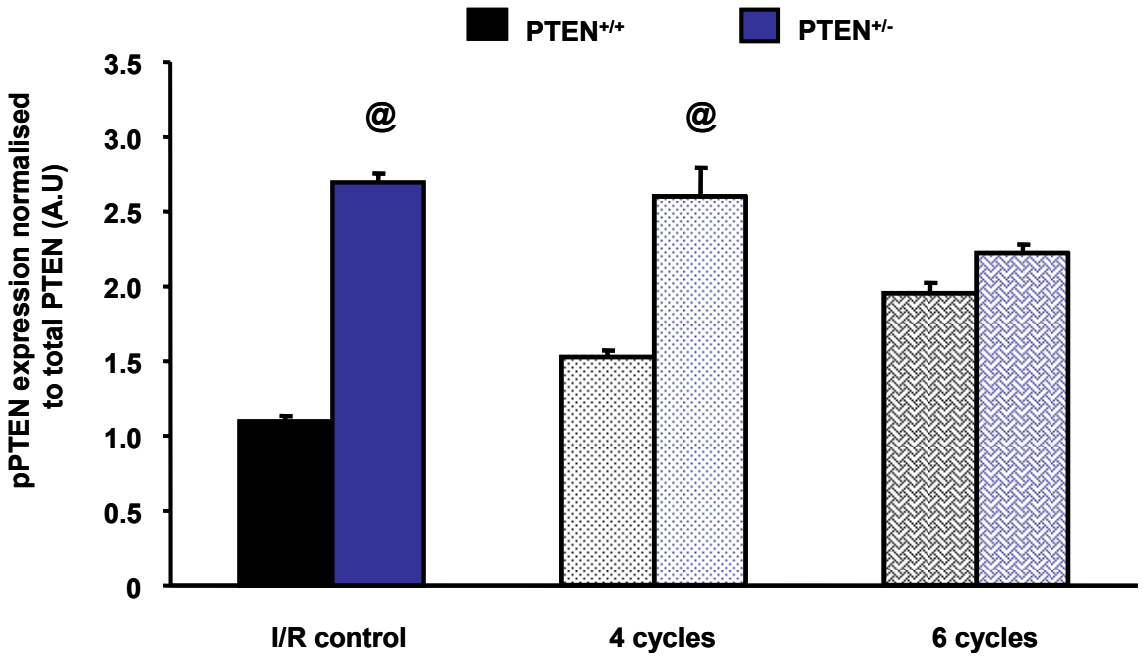

Figure 6.19: Phosphorylated (p) PTEN (at Thr380/Ser382/383 sites) protein expression in PTEN$^{+/+}$ and PTEN$^{+/-}$ myocardium subjected to ischaemia-reperfusion control (solid bars); and 4 (dots) or 6 (bricked) cycles of ischaemic preconditioning (IPC) (n=3). Statistical differences were assessed using One Way ANOVA, @=p<0.01 compared to PTEN$^{+/+}$ I/R control.

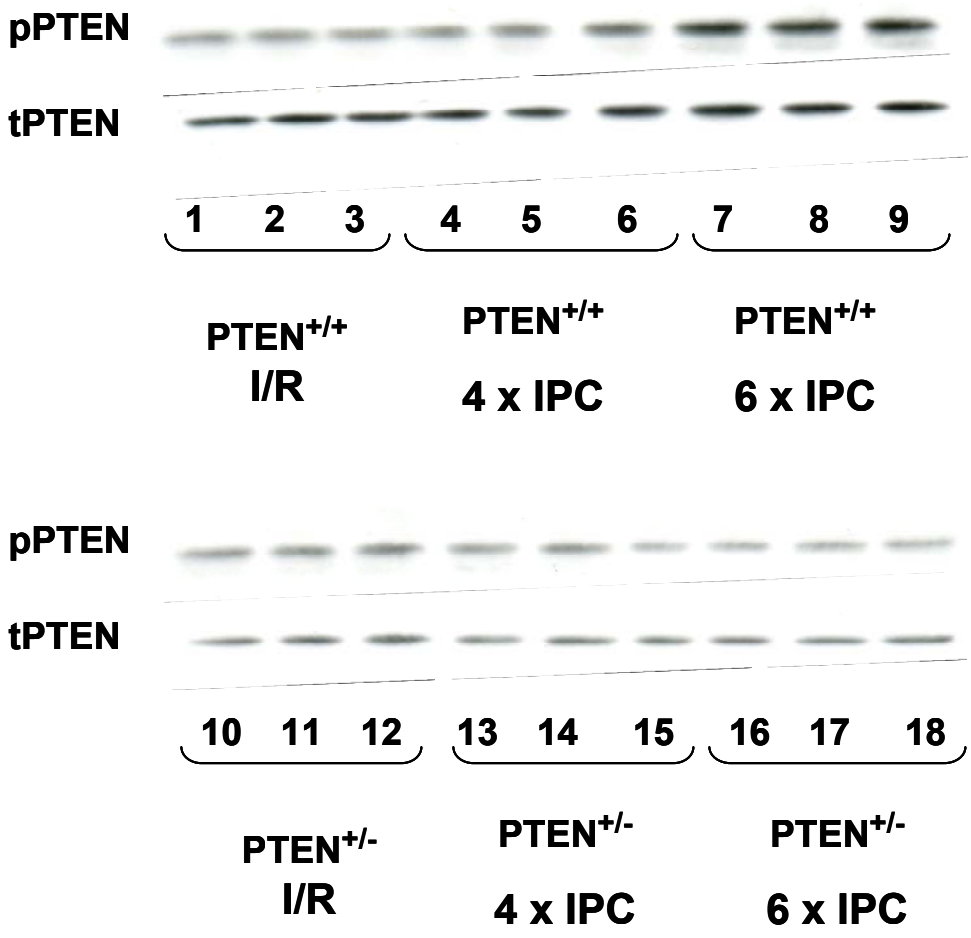

Figure 6.20: Example of Western blots illustrating total and phosphorylated (p) PTEN (at Thr380/Ser382/383 sites) in $PTEN^{+/+}$ and $PTEN^{+/-}$ myocardium subjected to ischaemia-reperfusion control, 4 or 6 cycles of ischaemic preconditioning (IPC).

AKT protein expression

Figure 6.21 and Figure 6.22 illustrate the phosphorylation of AKT at Ser473 and Thr308 phosphorylation sites (respectively) in the preconditioned $PTEN^{+/-}$ myocardium. Figure 6.23 represents the Western blot scans. As previously shown, phosphoryation of AKT at Ser473 and Thr308 phosphorylation sites is significantly increased in $PTEN^{+/-}$ compared to $PTEN^{+/+}$ hearts that were subjected to perfusion control, (no preconditioning). The phosphorylation of AKT at Ser473 phosphorylation site is significantly increased during 4 as well as 6 cycles of ischaemic preconditioning, in both $PTEN^{+/+}$ and $PTEN^{+/-}$ hearts. However, the infarct data

shows that PTEN$^{+/+}$ hearts are not protected with 4 cycles IPC. This may highlight the importance of the phosphorylation of AKT at Thr308 in cardioprotection. Figure 6.22 shows that, while the haploinsufficient hearts have already high levels of phosphorylated Thr308 and are protected by IPC, PTEN$^{+/+}$ hearts are protected at only at 6 cycles when the level of Thr308 phosphorylation in higher to that at 4 cycles.

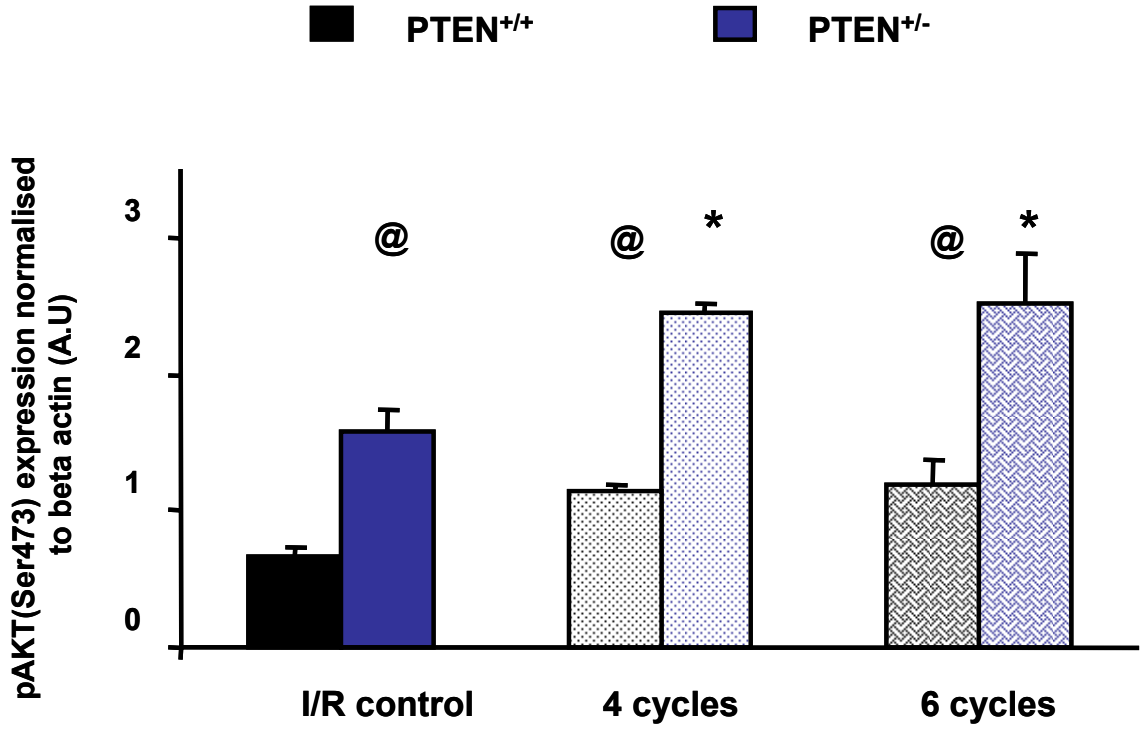

Figure 6.21: Phosphorylated (p) AKT (at Ser473 site) in PTEN$^{+/+}$ and PTEN$^{+/-}$ myocardium subjected to ischaemia-reperfusion control (solid bars); or 4 (dots) or 6 (bricked) cycles of ischaemic preconditioning (IPC). Statistical differences were assessed using one way ANOVA, @=p<0.05 compared to PTEN$^{+/+}$ baseline (non preconditioned) and *=p<0.05 compared to PTEN$^{+/-}$ baseline (non preconditioned) (n=3).

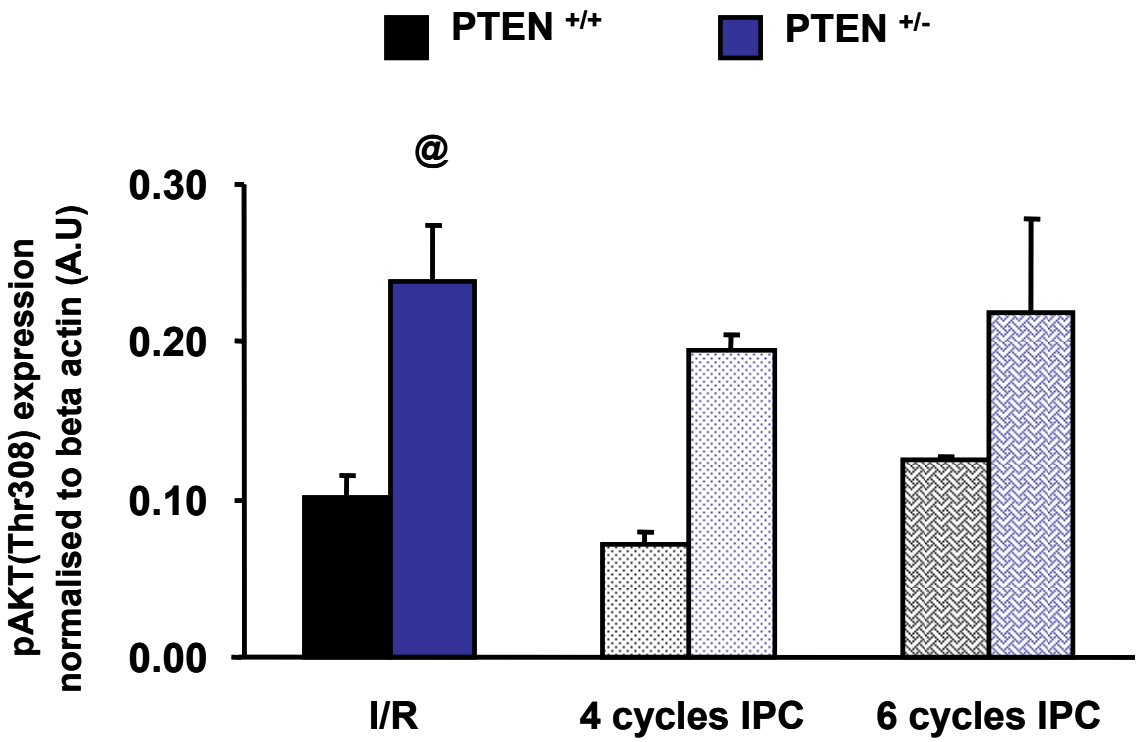

Figure 6.22: **Phosphorylated (p) AKT (at Thr308 sites) expression in PTEN$^{+/+}$ and PTEN$^{+/-}$ myocardium subjected to 4 (dots) or 6 (bricked) cycles of ischaemic preconditioning (IPC). Statistical differences were assessed using One Way ANOVA, @=p<0.05 compared to PTEN$^{+/+}$ baseline (non preconditioned), (n=3).**

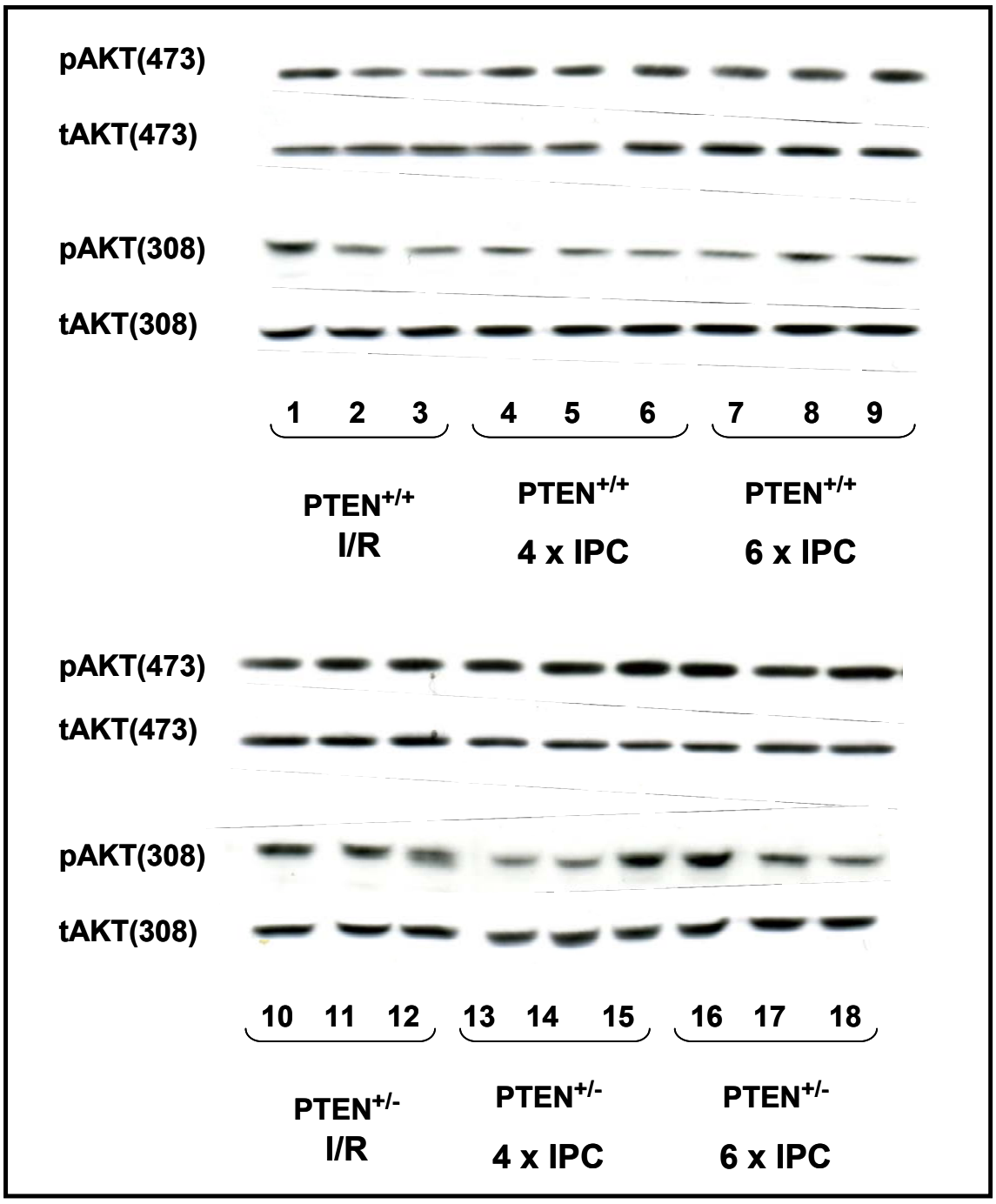

Figure 6.23: **Examples of Western blots illustrating total and phosphorylated (p) AKT (Ser473 and Thr308 sites) protein expression in $PTEN^{+/+}$ and $PTEN^{+/-}$ myocardium subjected to (1) ischaemia-reperfusion control, (2) 2 cycles of ischaemic preconditioning (IPC) or (3) 4 cycles IPC.**

In summary, in the isolated PTEN haploinsufficient myocardium, which already has a higher basal level of phosphorylated AKT compared to littermate controls, IPC increases the phosphorylation of AKT at Ser473 phosphorylation sites above the basal levels. In the $PTEN^{+/-}$ myocardium cardioprotection induced by IPC was achieved with less IPC stimuli: in which 4 and 6 cycles conferred protection. In contrast the littermate controls were protected with only 6 cycles of IPC. Thus it appears that the $PTEN^{+/-}$ myocardium may have an increased sensitivity towards cardioprotection.

6.4.3 Discussion

IPC in isolated perfused myocardium

Reducing PTEN (either using a chemical inhibitor or by using a genetically manipulated mouse strain) does not confer myocardial protection against ischaemia-reperfusion injury; despite AKT activation. Nevertheless, as described in chapter 4, section 3.1.2 perfusion of bpV(HOpic) in an isolated heart model of ischaemia-reperfusion injury reduces the threshold for IPC; it was predicted that the $PTEN^{+/-}$ myocardium may follow similar patterns for protection. Therefore the threshold for tissue salvage in the $PTEN^{+/-}$ myocardium was investigated and it was predicted that the threshold may be lowered in these hearts.

As predicted, there was a reduced threshold to cardioprotection in the myocardium from $PTEN^{+/-}$ mice. $PTEN^{+/+}$ controls were significantly protected ($p<0.05$) with 6 cycles whereas, $PTEN^{+/-}$ hearts were significantly ($p<0.05$) protected with 6 and 4 cycles of IPC stimuli, an effect not observed in the $PTEN^{+/+}$ myocardium. These results indicated that the myocardium from $PTEN^{+/-}$ mice had a reduced threshold for IPC induced cardioprotection. This finding positively supports our hypothesis that PTEN inhibition can be cardioprotective by contributing to the reduction of infarct size following ischaemia-reperfusion injury.

Similarly, Wong *et al,* have used these PTEN haploinsufficient mice to investigate insulin sensitivity. This group showed that in these mice, injections of insulin cause enhanced glucose uptake, increased insulin receptor substrate signalling activity and increased phosphorylation of AKT compared to littermate controls (Wong et al., 2007). Additionally, as described in Chapter 1, PTEN and the PI3K/AKT signalling pathway has a role in the development of diabetes. Mice lacking the insulin receptor substrate develop a diabetic phenotype and have disruption of pancreatic cells and loss of insulin (Kushner et al., 2005). When these mice are crossed with the PTEN haploinsufficient mice (developed by Podsypanina *et al.,* 1999) the sensitivity to insulin is restored, glucose injections can be tolerated, phosphorylated AKT is increased and the diabetic phenotype is abolished (Kushner et al., 2005). This indicated that, PI3K/AKT signalling can be further enhanced with insulin or glucose in the presence of reduced PTEN. This also highlights the very interesting possibility, that the capability to induce IPC (which is diminished in diabetic animals (Tsang et al., 2005; Mocanu et al., 2006)) might be restored in mice that are engineered to contain the $PTEN^{+/-}$ allele, or those that are treated with the PTEN inhibitor bpV(HOpic).

The data presented in this thesis indicates that, to demonstrate the functional effects of PTEN mutation in the PTEN haploinsufficient myocardium, a stimulus of PI3K/AKT pathway, above basal level, is required. Studies performed by Cai and Semenza in 2005 demonstrated changes which occur in PTEN during IPC stimuli. As discussed in chapter 4 and in more detail below, Their work provides supporting evidence that PTEN can be manipulated and reduced in the heart by IPC which is implicated to be involved in survival after ischaemia-reperfusion injury (Cai and Semenza, 2005). In the PTEN haploinsufficient mouse heart, which have a native allele for functional PTEN, IPC may contribute to the protection by reducing PTEN activity further; this idea is discussed in greater detail below.

To conclude, PTEN haploinsufficiency alone is not able to reduce infarction from ischaemia-reperfusion injury. However, when associated with an increase in PI3K/AKT activity, PTEN haploinsufficiency can induce cardioprotection by reducing the threshold to protection obtained with IPC.

Expression of PI3K/AKT/PTEN pathway in IPC induced cardioprotection

Tissue collected subsequent to the IPC protocol was measured for PTEN lipid phosphatase activity using the PTEN ELISA kit and expression of phosphorylated and total PTEN and AKT, using Western blot analysis.

PTEN lipid phosphatase activity in IPC

No significant differences in lipid phosphatase activity were observed in samples obtained from myocardium that had been subjected to ischaemia-reperfusion control, 4 or 6 cycles of IPC, from either $PTEN^{+/-}$ or $PTEN^{+/+}$ mice. However, significant changes in the PTEN lipid phosphatase activity have been observed during IPC (Cai and Semenza, 2005). In this study the malachite green reagent, which detects free phosphates, was used as an indictor of lipid phosphatase activity (Schmid et al., 2004; Connor et al., 2005; Cai and Semenza, 2005). As previously described we are not confident that the ELISA kit we used is adequate for measuring PTEN activity in homogenised whole tissues. Other groups have used this PTEN ELISA to measure lipid phosphatase activity (Eickholt et al., 2007; Papakonstanti et al., 2007). Differences include, the sample type (whole heart compared to cancer cell lines) and the enzyme preparation (tissue homogenation compared to PTEN imunoprecipitation prior to assaying the phosphatase activity). Therefore, more time is needed in order to develop the use of this assay for assessing samples obtained from whole hearts.

PTEN protein expression

Previously, we showed that basal, non preconditioned, non ischaemic $PTEN^{+/-}$ hearts manifest an increase in the level of PTEN phosphorylation, which is indicative of PTEN inactivity. The data from these IPC studies showed a similar increase in PTEN phosphorylation in $PTEN^{+/-}$ compared to $PTEN^{+/+}$ hearts. In the IPC samples, an increase in phosphorylation of PTEN was observed in the $PTEN^{+/+}$ myocardium subjected to 6 cycles IPC. The level of PTEN phosphorylation in the $PTEN^{+/-}$ myocardium was significantly higher at 4 cycles of IPC ($p<0.05$) compared to $PTEN^{+/+}$ control hearts. The phosphorylation of PTEN is associated with enzyme inactivity and as described previously, CK2 phosphorylation of PTEN encodes protein instability, ubiquitination and proteasomal degradation (Torres and Pulido, 2001). This indicates that in the $PTEN^{+/-}$ myocardium, overall there may be more inactive PTEN. These results are in agreement with work by others, associating PTEN phosphorylation with PTEN inactivation (Torres and Pulido, 2001; Al Khouri et al., 2005; Ning et al., 2006).

AKT protein expression

Previously, we showed that basal, non preconditioned, non ischaemic $PTEN^{+/-}$ hearts contained increased levels of AKT phosphorylation. Following these IPC studies an additional increase in AKT phosphorylation was induced in the $PTEN^{+/-}$ myocardium. The phosphorylation of AKT at the Ser473 phosphorylation site was significantly increased with 4 as well as 6 cycles of IPC in both $PTEN^{+/+}$ and $PTEN^{+/-}$ hearts. However, the infarct data showed that $PTEN^{+/+}$ hearts are not protected with 4 cycles IPC. This may highlight the importance of phosphorylation of AKT at the Thr308 phosphorylation site in cardioprotection. The $PTEN^{+/+}$ hearts are protected only after 6 cycles, when the level of Thr308 phosphorylation is different to that at 4 cycles. Therefore, this amplified phosphorylation may be necessary for cardioprotection in the $PTEN^{+/+}$ hearts to counterbalance the effects of PTEN.

The $PTEN^{+/-}$ myocardium was not protected against ischaemia-reperfusion alone; however, a reduced threshold for IPC induced cardioprotection was recorded in these hearts. Furthermore, in addition to activation of the PI3K/AKT pathway, other signalling events occur in IPC that may account for these observations. The IPC protocol consists of cycles of sub lethal ischaemia-reperfusion. Paradoxically, this procedure generates 'beneficial' ROS (Baines et al., 1997). ROS can oxidise and reversible inhibit PTEN.(Connor et al., 2005; Kwon et al., 2004) It has been shown that IPC induced ROS production can inhibit PTEN. (Cai and Semenza, 2005). In addition, the sub lethal ischaemia generated in IPC is sufficient to up regulate hypoxia inducible factor 1 alpha (HIF1α), which is thought to regulate PTEN function during the IPC trigger which contributes to ROS signalling and consequentially activation of the PI3K/AKT pathway. (Cai et al., 2008a). The data in this thesis shows that in the PTEN haploinsufficient myocardium cardiprotection is induced, because a reduction in the threshold of IPC was observed. In an attempt to explain this observation it could be hypothesised that these results were caused by further inhibiting PTEN due to a form of positive feedback. Whereby IPC/ROS induced inhibition of PTEN may be amplified in the PTEN haploinsufficient myocardium. This idea is outlined in Figure 6.24. We hypothesise that during IPC the PTEN hapolinsufficient myocardium would contain a greater amount of oxidised PTEN compared to their littermate controls. Importantly, alternative pathways that are activated in IPC should be investigated in future studies, such as JAK/STAT and p42/p44 pathways, which have a protective role in IPC.

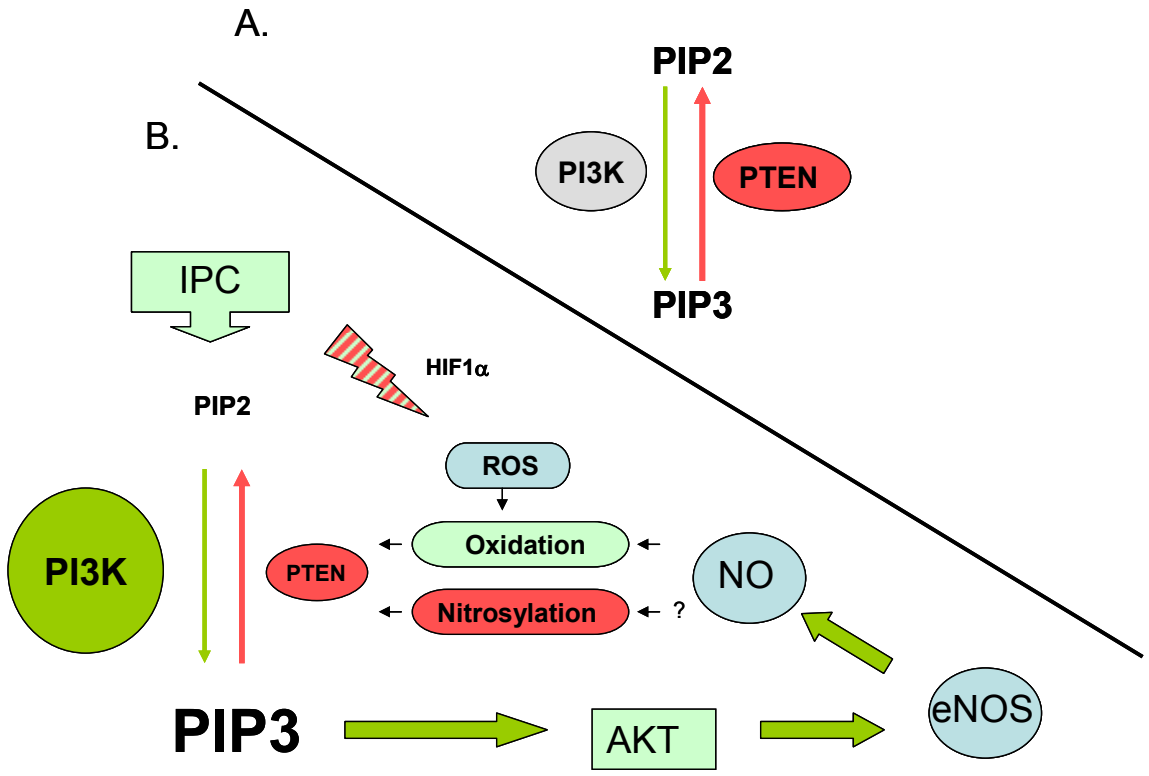

Figure 6.24: Proposed hypothesis for further reduction of PTEN activity during Ischaemic preconditioning (IPC) in the presence of either a PTEN inhibitor or genetic deletions of PTEN. A) Cellular PTEN activity under basal conditions. B) Cellular PTEN activity as a consequence of IPC. Inhibition of PTEN by oxidation and potential positive feedback causing further PTEN inhibition when PTEN is inhibited using a PTEN inhibitor such as bpV(HOpic) or in the presence of PTEN deletions. However nitrosylation has been shown to inhibit PTEN (Pei et al., 2009), which may act to control such situations chronically. HIF1α = hypoxia inducible factor 1 alpha, NOS = nitric oxide synthasse, NO = nitric oxide, PIP2 = phosphatidylinositol 2 phosphate, PIP3 = phosphatidylinositol 3 phosphate, PI3K = phosphatidylinositol 3 kinase and ROS = reactive oxygen species.

To summarise, in the isolated PTEN$^{+/-}$ myocardium, IPC increased the phosphorylation of AKT at Ser473 and Thr308 phosphorylation sites, above the baseline, which is already higher

than in the control littermates. However, no additional changes in phosphorylation of PTEN were observed. Nevertheless, IPC induced cardioprotection was achieved with less IPC stimuli. In the $PTEN^{+/-}$ myocardium 4 and 6 cycles induced protection, whereas only 6 cycles conferred protection in littermate controls. Thus it appears that the $PTEN^{+/-}$ myocardium may have an increased sensitivity towards cardioprotection.

6.5 Investigating reasons for the lack of protection against ischaemia-reperfusion injury

6.5.1 Experimental protocols

6.5.1.1 Investigating alternative regulators of the PI3K/AKT pathway

We aimed to investigate potential changes in the $PTEN^{+/-}$ myocardial cell signalling network, which may compensate for altered function of PTEN. The protein expression of other potential down regulators of the PI3K/AKT pathway was investigated, using Western blot analysis as described in chapter 2, section 6, samples were collected as shown in Figure 6.1, (n=3).

Firstly, the level of phosphatases known to reduce the PI3K/AKT pathway was measured, as described in chapter 1, section 4. The level of SHIP2, PHLPP, and PP2A was recorded. It was hypothesised that these phosphatases would be increased in the $PTEN^{+/-}$ myocardium to compensate for the partial loss of PTEN.

6.5.1.1.1 Investigating PINK1 expression

As described in chapter 1, section 5, the level of PTEN induced kinase 1 (PINK1), a mitochondrial pro survival kinase, can be increased by the re-expression of cellular PTEN

(Unoki and Nakamura, 2001). However, the association of PTEN and PINK1 in the myocardium is currently unknown. Therefore, the expression of PINK1 was investigated in the $PTEN^{+/-}$ and $PTEN^{+/+}$ myocardium, n=3, as shown in Figure 6.1,A, using Western blot analysis as described in chapter 2, section 6. It was hypothesised that there would be a reduced level of PINK1 in the $PTEN^{+/-}$ myocardium.

6.5.1.2 Investigating alternative contributors of ischaemia-reperfusion injury

Finally, alternative mechanisms that may explain the lack of protection against ischaemia-reperfusion injury were investigated in the $PTEN^{+/-}$ myocardium. In addition to its lipid phosphatase activity PTEN has a role in maintaining DNA stability and cell cycle (Shen et al., 2007). Cells in a pro apoptotic state have been associated with DNA fragmentation and can be visualised on an agarose gel, as an increase in DNA fragments, which can be observed as a laddering effect (Fliss and Gattinger, 1996). It was hypothesised that the $PTEN^{+/-}$ myocardium, which expresses a reduced level of PTEN protein, may be more susceptible to cell damage. To assess this DNA laddering and caspase 3 activation was investigated in the $PTEN^{+/-}$ hearts, as outlined below.

1) Myocardial tissue was collected at the end of the final IPC reperfusion cycle, as shown in Figure 6.16, and described in Chapter 2, section 6 (n=3-5). DNA was extracted from $PTEN^{+/+}$ and $PTEN^{+/-}$ myocardium and the level of DNA fragmentation was monitored subsequent to control, ischaemia-reperfusion, 4 and 6 cycles IPC, as described in chapter 2, section 2. Equal quantities of DNA were separated by agarose gel electrophoresis and visualised using ethidium bromide. It was hypothesised that the $PTEN^{+/-}$ myocardium may exhibit an increase in DNA laddering.

2) Caspase 3 activity in the PTEN$^{+/-}$ myocardium was investigated, as a marker of cell damage. Samples were collected without ischaemia-reperfusion, as shown in Figure 6.16, and was investigated using Western blot analysis, and described in chapter 2, section 6. Caspase 3, is activated when it is cleaved, producing a pro death fragment (Nicholson et al., 1995; Kothakota et al., 1997). The caspase 3 antibody used in this study detects cleaved and uncleaved caspase 3. Therefore, the total caspase 3 value was estimated by adding the A.U value obtained from the uncleaved caspase 3 band (running to 35kDa) with the A.U acquired from the cleaved caspase 3 fragment (running to 17kDa). The level of caspase activation was obtained by comparing the ratio of cleaved and uncleaved caspase 3. It was hypothesised that there may be an increase in the basal level of caspase 3 activation.

6.5.2 Results

6.5.2.1 Alternative regulators of the PI3K/AKT pathway

Originally, it was assumed that the PTEN$^{+/-}$ myocardium would manifest cardioprotection against ischaemia-reperfusion injury. However, thus far, a reduction in the level of infarction following 35 min ischaemia and 30 min reperfusion was not observed. In the following experiments we aimed to investigate potential explanations for this lack of protection observed in the PTEN haploinsufficient myocardium. It was hypothesised that changes may occur in the cell signalling network, which may compensate for altered expression of PTEN. Therefore, the expression of other potential down regulators of the PI3K/AKT pathway, such as the phosphatases SHIP2, PHLPP and PP2A (which are described in chapter 1, were investigated.

The data, presented in Figure 6.25, 6.26 & 6.27 shows that there were no significant changes in the expression of either SHIP2, PHLPP or PP2A, respectively, between $PTEN^{+/+}$ and $PTEN^{+/-}$ myocardium.

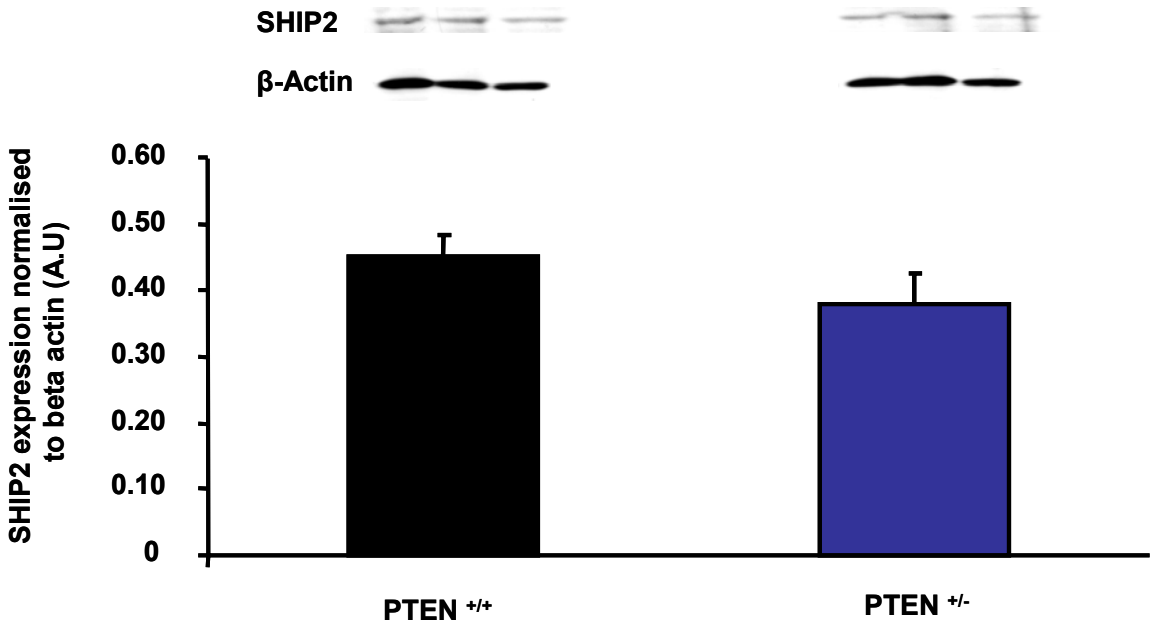

Figure 6.25: **SRC homology 2 containing inositol 5 phosphatase 2 (SHIP2) protein expression in $PTEN^{+/+}$ and $PTEN^{+/-}$ myocardium, normalised to beta actin. (Arbitrary Units = A.U.) No statistical differences were observed, assessed using the Student's paired t-test, (n=3).**

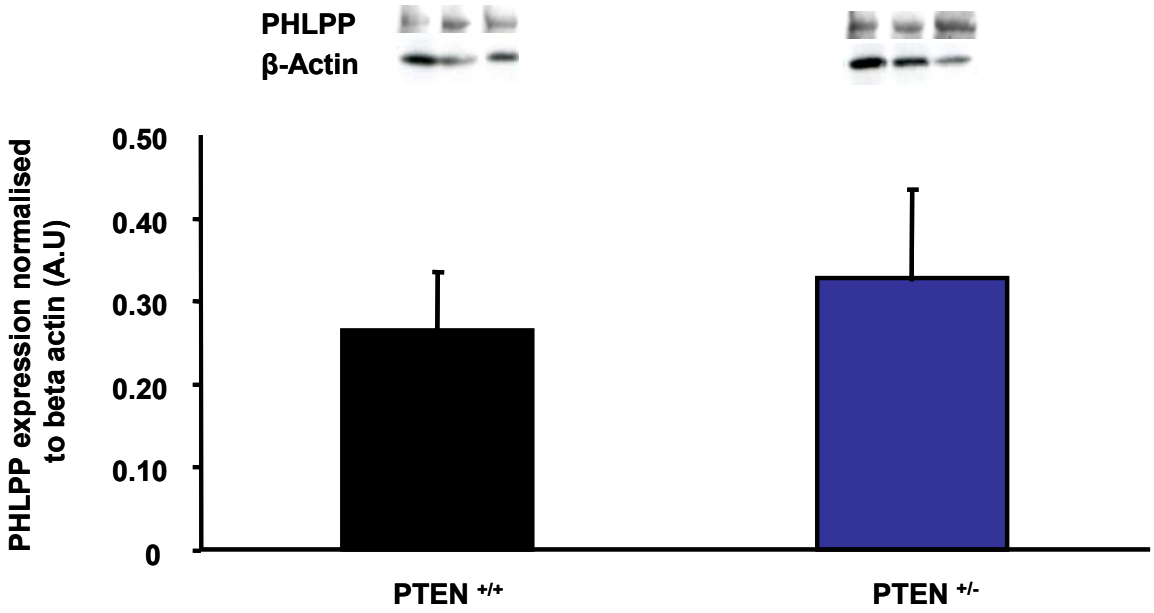

Figure 6.26: **PH domain leucine rich repeat protein phosphatase (PHLPP) protein expression in PTEN$^{+/+}$ and PTEN$^{+/-}$ myocardium, normalised to beta actin. (Arbitrary Units = A.U.) No statistical differences were observed, assessed using the Student's paired t-test, (n=3).**

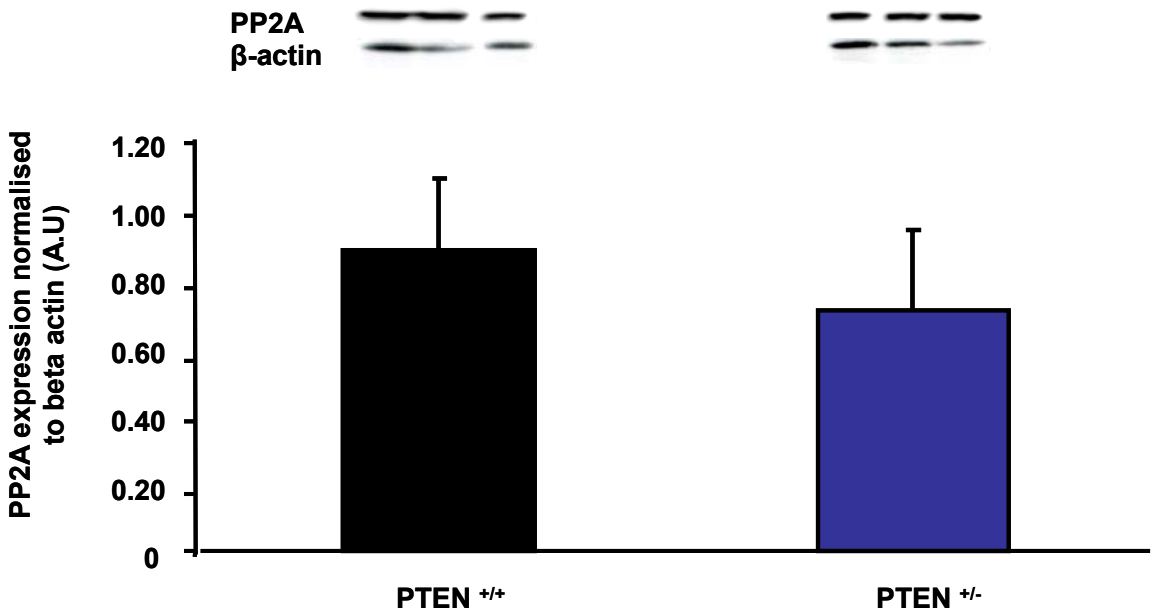

Figure 6.27: **Protein phosphatase 2A (PP2A) protein expression in PTEN$^{+/+}$ and PTEN$^{+/-}$ myocardium, normalised to beta actin. (Arbitrary Units = A.U.) No statistical differences were observed, assessed using the Student's paired t-test, (n=3).**

6.5.2.1.1 PTEN Induced Kinase 1 (PINK1) expression

As described in Chapter 1, PINK1 is a prosurvival mitochondrial kinase that is up regulated in cells by the expression of PTEN (Unoki and Nakamura, 2001; Petit et al., 2005). The association of PTEN and PINK1 in the myocardium is currently unknown. Interestingly, it was observed that PINK1 expression was reduced in the $PTEN^{+/-}$ myocardium. Figure 6.28 displays the PINK1 expression data and showing that $PTEN^{+/-}$ myocardium expressed significantly less PINK1 protein (25.6 ± 1.6 A.U, $p<0.05$) compared to their littermate controls (31.4 ± 1.4 A.U). The decrease in PINK1 may contribute to the lack of cardioprotection against ischaemia-reperfusion in the $PTEN^{+/-}$ myocardium; however, this hypothesis needs further investigation.

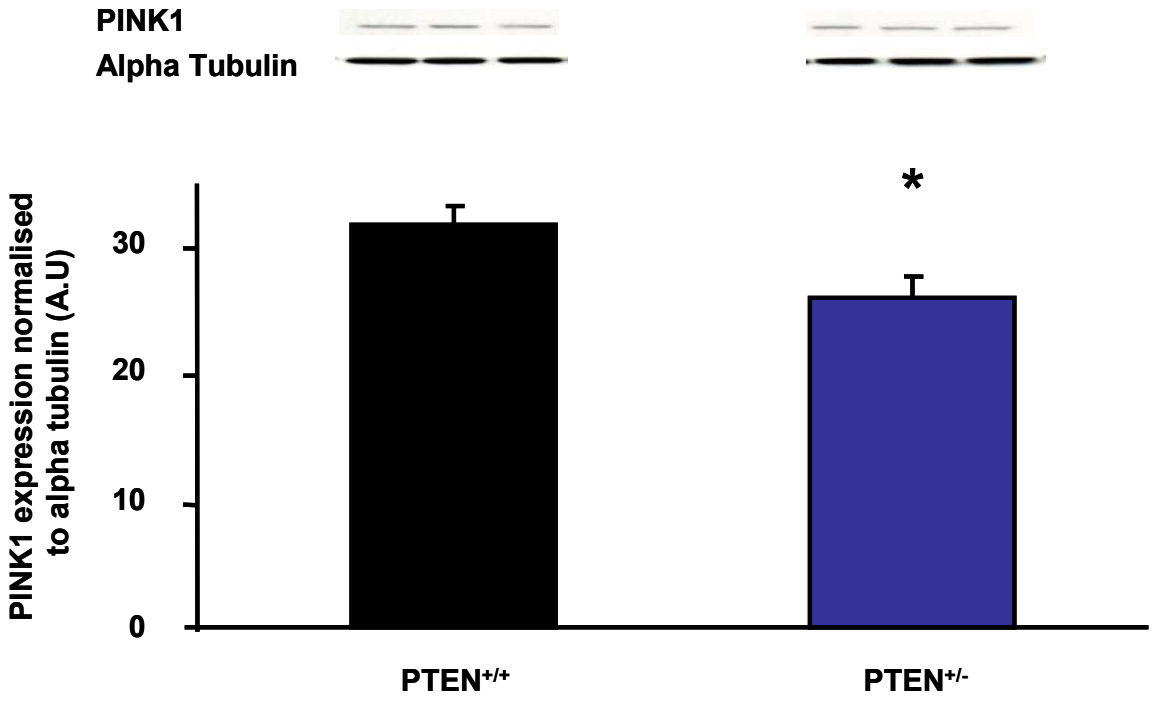

Figure 6.28: PTEN induced kinase 1 (PINK1) protein expression in $PTEN^{+/+}$ and $PTEN^{+/-}$ myocardium, normalised to beta actin. Expressed in Arbitrary Units (A.U), (n=3). Statistical differences were observed, assessed using the Student's paired t-test, (*$p<0.05$).

6.5.2.2 Alternative contributors of ischaemia-reperfusion injury

Alternative mechanisms for the lack of protection in the $PTEN^{+/-}$ myocardium were also investigated. In addition to its lipid phosphatase activity, it has been demonstrated that PTEN plays a role in maintaining DNA stability (Puc and Parsons, 2005; Shen et al., 2007). It was hypothesised that the $PTEN^{+/-}$ myocardium, which expresses reduced PTEN protein, may exhibit damaged DNA. The results are presented in Figure 6.29 however, they are difficult to compare and therefore inconclusive because clear DNA fragments are not identifiable. Nevertheless, a slightly greater degree of DNA smearing occurs in $PTEN^{+/-}$ myocardial extracts. In summary, the relation between the degree of DNA fragmentation and PTEN level in the myocardium does not seem to be proven by our data and more investigations are needed.

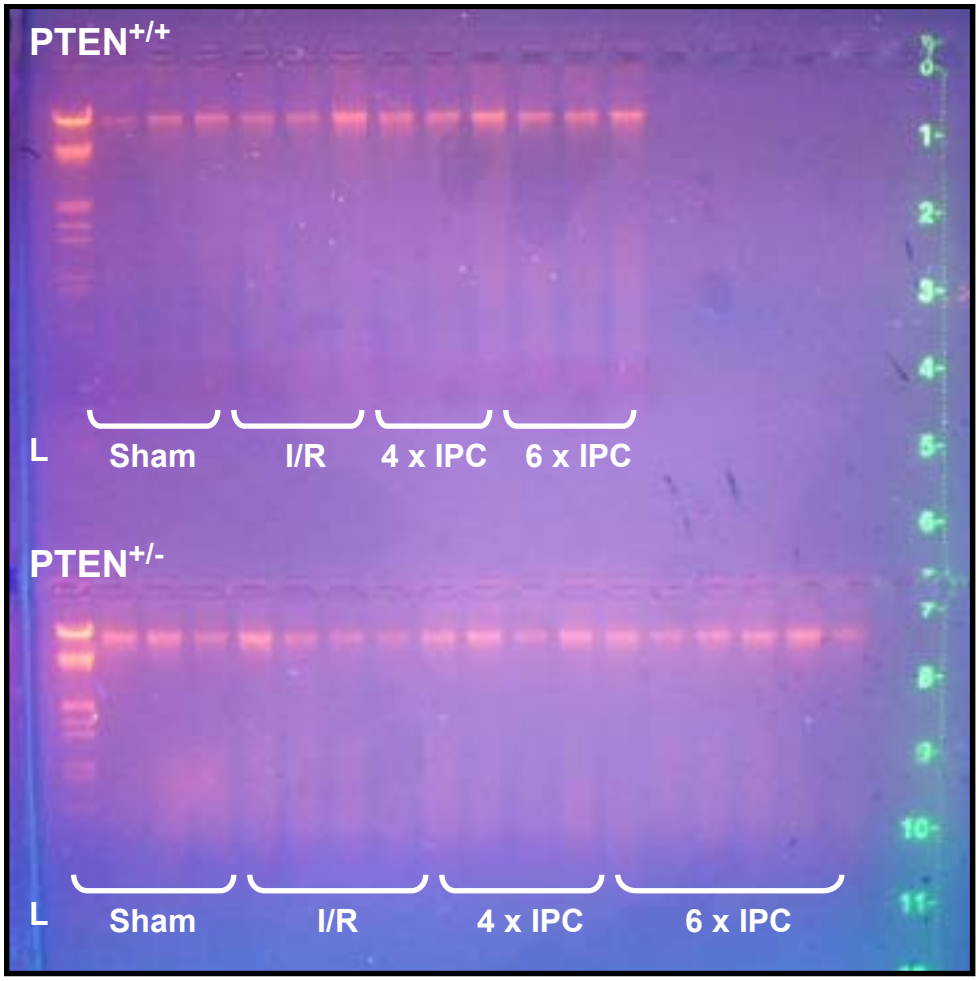

Figure 6.29: DNA separation in myocardium subjected to sham, ischaemia-reperfusion control (I/R), 4 and 6 cycles ischaemic preconditioning (IPC). DNA was extracted from whole hearts using the Qiagen DNA extraction kit and quantified using a spectrophotometer. A DNA ladder (L) and ethidium bromide (orange) was used to visualise the results.

Additionally, the expression of caspase 3 was investigated as a marker of cell damage. The results were investigated by Western blot techniques, analysed by densitometry and are displayed in Figure 6.30. No changes in the expression of caspase 3 cleavage in the $PTEN^{+/+}$ mycocardium (0.488 ± 0.158 A.U) compared to $PTEN^{+/-}$ hearts (0.502 ± 0.195 A.U) were observed. Representative blots are shown in Figure 6.31 , it should be noted that the quality

of the blots are not good and future work may include repeating these experiments to provide clearer data.

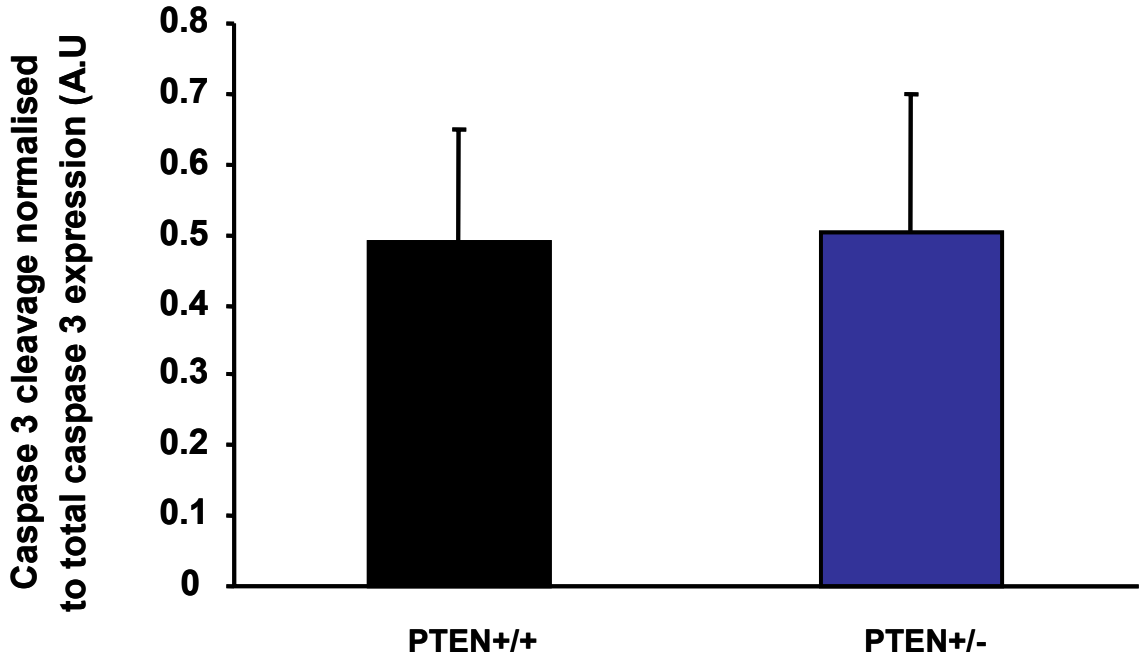

Figure 6.30: Cleavaed caspase 3 normalised to total caspase 3 expression in PTEN$^{+/+}$ and PTEN$^{+/-}$ myocardium. Expressed in Arbitrary Units (A.U). No statistical differences were assessed using the Student's paired t-test, (n=3).

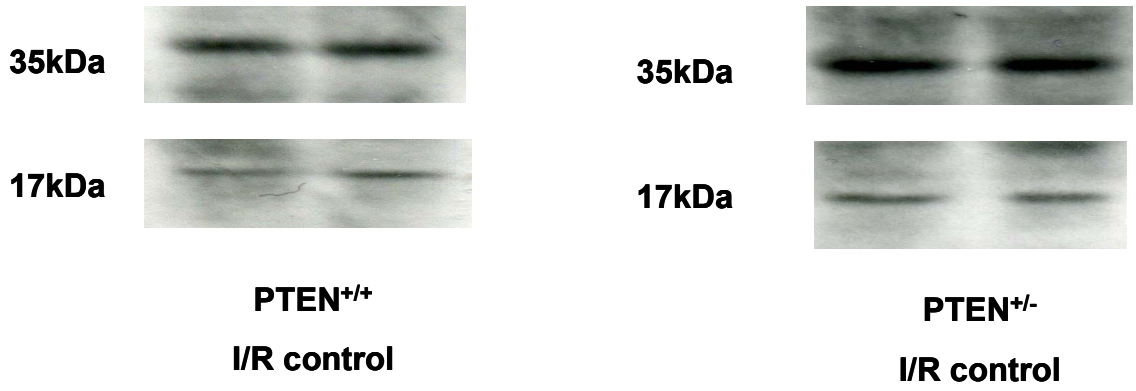

Figure 6.31: Example of western blots illustrating the cleaved (active 17kDa) and intact (inactive 25kDa) caspase 3 in PTEN$^{+/+}$ and PTEN$^{+/-}$ myocardium subjected to ischaemia reperfusion (I/R) control (perfused without ischaemia).

To summarise, no differences in the expression of other phosphatases known to negatively regulate PI3K/AKT activity, such as SHIP2, PHLPP and PP2A were observed in the PTEN$^{+/-}$ myocardium. Furthermore, no changes in cell stability, as measured by DNA fragmentation and caspase 3 cleavage were detected. Nonetheless, we discovered a reduction in the expression the pro survival mitochondrial kinase PINK1.

6.5.3 Discussion

6.5.3.1 Alternative regulators of the prosurival PI3K/AKT pathway

Originally, it was predicted that the PTEN$^{+/-}$ myocardium would manifest cardioprotection against ischaemia-reperfusion injury, however, this was not confirmed in our studies. Therefore, we aimed to investigate potential explanations for this lack of protection. It was hypothesised that there may be compensatory signalling mechanisms occurring in these hearts to counteract the altered expression of PTEN. Therefore, the expression of other potential down regulators of the PI3K/AKT pathway, such as SHIP2, PHLPP and PP2A were investigated in the PTEN$^{+/-}$ myocardium. The results showed that no differences in total protein levels were observed. However, we did not investigate the activities of these phosphatases.

Additionally, future work may include investigating the localisation and activity of these phosphatases. Interestingly, studies in cell lines showed that PTEN or SHIP2 reduction using siRNA can enhance the level of phosphorylation of AKT in the presence of LY294002, a PI3K inhibitor. Interestingly, following the incubation with LY294002 and the dual reduction of PTEN and SHIP2, AKT was eventually dephosphorylated (Sharrard and Maitland, 2006). This work indicates alternative phosphatase/s other than PTEN and SHIP2 can dephosphorylate

AKT, however, the authors of this work do not attempt to address the identity of these phosphatases.

Recently, a second isoform of PHLPP (PHLPP2) has been discovered, it contains 50% homology to PHLPP1 with a predicted molecular weight of 150kDa and similarly, dephosphorylates AKT at the Ser473 site (Brognard et al., 2007). Activation of the PI3K/AKT pathway using EGF increases the phosphorylation of AKT. The deletion of PHLPP1 and PHLPP2 stimulated a 30 fold increase in the EGF induced increase in phosphorylation of AKT (Brognard et al., 2007). Therefore, it would be interesting to investigate the levels of PHLPP2 in our $PTEN^{+/-}$ hearts.

Interestingly, PHLPP1 can bind and dephosphorylate AKT at the Ser473 of AKT isoforms 2 and 3. In contrast PHLPP2 binds to and dephosphorylates AKT at the Ser473 of AKT isoforms 1 and 3 (Brognard et al., 2007). AKT1 is involved in growth and proliferation and AKT2 is involved in glucose homeostasis (Brognard et al., 2007; Heron-Milhavet et al., 2006). We also investigated PP2A, and inhibition of this phosphatase in rat adipocytes, using okadaic acid, has been shown to cause an increase in phosphorylation of AKT1. In contrast, the authors of this work showed no changes in the phosphorylation of AKT2 (Resjo et al., 2002). The results from our study showed that no changes in PHLPP1 or PP2A were observed in the $PTEN^{+/-}$ myocardium. However, it would be interesting to establish which AKT isoforms are affected in the $PTEN^{+/-}$ myocardium.

Other regulators of the PI3K/AKT pathway

The results from this study indicate that the levels of, SHIP2, PHLPP and PP2A are not altered in the $PTEN^{+/-}$ myocardium. However, the list of negative regulators of the PI3K/AKT pathway is much larger than this, some of which are discussed below. The Src homology domain 2 (SH2) containing tyrosine phosphatase 1 (SHP1) is known to negatively regulate

Fas receptor signalling. SHP1 inhibition using siRNA confers cardioprotection against myocardial ischaemia-reperfusion (Sugano et al., 2005). Similarly, the Src homology domain 2 (SH2) containing tyrosine phosphatase 2 (SHP2) is a phosphatase that has been associated with regulating cell growth (Zito et al., 2007). In fibroblasts SHP2 appears to negatively regulate cell size, in periods of low ATP. The authors of this work conclude that SHP2 controls the cell growth by suppressing the mTOR/p70S6K pathway (Zito et al., 2007). The levels of SHP1 or SHP2 may be enhanced in the $PTEN^{+/-}$ myocardium.

In addition, skeletal muscle and kidney enriched inositol phosphatase (SKIP), a 50kDa lipid phosphatase that dephosphorylates PI(3,4,5)P3 to PI(4,5)P2, can negatively regulate the PI3K/AKT pathway (Ijuin and Takenawa, 2003). Over expression of SKIP in CHO cells can decrease insulin stimulated phosphorylation of AKT and inhibited insulin stimulated glucose uptake (Ijuin and Takenawa, 2003).

Finally, the potential impact of unknown or novel phosphatases yet to be discovered is discussed. Phosphatase activities are complex and can be tightly regulated. Already 2 splice variants of PHLPP have been discovered (Brognard et al., 2007). There is evidence that a novel phosphatases with homology to PTEN exists. These are known as 1) the Transmembrane Phosphatase with Tensin Homology (TPTE) and 2) the PTEN homolog inositol lipid phosphatase (TPIP). These are 2 splice variants which, to date, have been localised to the testis, stomach and brain. Nonetheless, these phosphatases may be regulated in other tissues (Walker et al., 2001).

It is important to note that in this section the quality of some of the western blots are not high, in some cases. For example the blots for SHIP2 and PHLPP appear dirty. In addition, some of the loading controls are not equal, as in the representative blots used for PHLPP and PP2A. Therefore, the results must be interpreted with caution. Future work would include

repeating for loading control and optimising the conditions required for probing larger proteins such as SHIP2 and PHLPP.

In summary, the expression of SHIP2, PHLPP and PP2A were investigated in the $PTEN^{+/-}$ myocardium. Dissimilar to the hypothesis, our results showed that the total protein expression of these phosphatases in our samples appeared unchanged in the $PTEN^{+/-}$ myocardium. This indicates that in our samples the total expression of these phosphatases did not change to compensate for the PTEN mutation.

PTEN Induced Kinase 1 (PINK1) expression

It has been shown that in endometrial cancer cells (HEC-151) the expression of PINK1 is dependent on the level of PTEN (Unoki and Nakamura, 2001), however, the association of PTEN and PINK1 in the myocardium is currently unknown. PINK1 is frequently researched in the brain and mutations have been associated with Parkinson's disease. In neuronal tissue, PINK1 deficiency results in changes in mitochondrial morphology and decreased mitochondrial membrane potential (Wood-Kaczmar et al., 2008). Over expression of PINK1 can protect against H_20_2 induced oxidative stress, by preventing cytochrome c release (Pridgeon et al., 2007). Mitochondrial PINK1 co-localises with and phosphorylates TNF receptor associated protein (TRAP1), also known as heat shock protein (HSP)75, and HSP90 where is thought to have a role in protein stability, cell viability and prevention of mPTP opening (Wang et al., 2007a; Lin and Kang, 2008b). Our data shows that in the $PTEN^{+/-}$ myocardium changes in PTEN level cause a small but significant ($p<0.05$) reduction in PINK1. Collectively, this and other published studies indicate that PINK1 is essential for mitochondrial integrity and function. It is most abundantly expressed in the heart (Mills et al., 2008), however, the precise mechanism involved in cell survival, has yet to be investigated.

In summary, it was hypothesised that the level of PINK1 would be reduced in the PTEN$^{+/-}$ myocardium, which may explain the lack of protection against ischaemia-reperfusion in these hearts. A small but significant ($p<0.05$) decrease in PINK1 expression was observed in these hearts. Our results suggest that in the PTEN$^{+/-}$ hearts any possible protection due to an increased activation of the PI3K/AKT pathway may be counterbalanced by the deficiency in mitochondrial PINK1. This may, in part, explain the lack of cardioprotection against ischaemia-reperfusion injury in the PTEN$^{+/-}$ myocardium; however, this hypothesis needs further investigation. Moreover, PINK1 may be a novel cardioprotective kinase in its own right.

6.5.3.2 Alternative contributors to ischaemia-reperfusion injury

In addition to negatively regulating the PI3K/AKT pathway, PTEN has a role in maintaining DNA stability (Puc and Parsons, 2005; Shen et al., 2007). However, our results were inconclusive and we were not able to investigate our hypothesis completely. Reasons for this may be due to experimental approach. The method we used to investigate DNA fragmentation did not seem to work and may have prevented the detection of DNA laddering in our samples. Fliss and Gattinger, 1996 showed that in rat hearts detection of DNA laddering, as an indicator of apoptosis, required the induction of ischaemia using permanent coronary occlusion. More importantly the myocardium had to be reperfused for 3-4 hours (Fliss and Gattinger, 1996). The authors of this work showed that 2 hours of reperfusion was not sufficient to detect a laddering effect and observed a similar DNA smearing pattern to that in our samples. This may indicate that sufficient time to observe any changes in DNA stability was not operational in our experiments. Collectively, these observations create an additional discussion point about the association and detection of necrosis and apoptosis in ischaemia reperfusion injury. Smearing of DNA can be interpretated as necrotic activity, whereas a laddering effect can be used to indicate apoptotic events within a sample (Kajstura et al.,

1996; Fliss and Gattinger, 1996; Taimor et al., 1999; Kim et al., 2003). Therefore, this may signal that there is more necrotic activity in our samples. However, this work may indicate that the methods we used to study DNA fragmentation may not be sensitive enough to detect the level of apoptosis and DNA fragmentation occurring in our samples.

Secondly, caspase 3 cleavage expression was investigated as a marker of cell damage. However, no significant differences between $PTEN^{+/+}$ and $PTEN^{+/-}$ myocardium could be detected. Similarly, this may be due to the experimentation design, as heart samples were not subjected to lethal ischaemia-reperfusion injury.

In summary, in the $PTEN^{+/-}$ myocardium no changes were observed in the expression of phosphatases that are involved in decreasing PI3K/AKT activity, such as SHIP2, PHLPP and PP2A. No significant decrease in cell stability, as measured by DNA fragmentation and caspase 3 cleavage was observed. However, a decrease in the expression of the pro survival mitochondrial kinase PINK1 was discovered, which may be a cardioprotective kinase its own right, and may in part explain the lack of protection against ischaemia-reperfusion in the $PTEN^{+/-}$ hearts.

6.5.4 Chapter summary

In conclusion, the PTEN haploinsufficient data indicates that there was reduced levels of total PTEN expression in $PTEN^{+/-}$ myocardium. Furthermore, PTEN activity may be decreased, as indicated by an increase in phosphorylated PTEN expression. Consequently, increases in AKT activity were observed. However, this increase in AKT activity was not sufficient to confer cardioprotection, either in isolated cardiomyocytes or in isolated perfused hearts, subjected to simulated ischaemia-reperfusion injury. Subsequent to investigating the role of possible compensatory signalling mechanisms in the $PTEN^{+/-}$ myocardium, we revealed that a reduction in PINK1 occurs. Nevertheless, IPC induced cardioprotection is achieved with less

stimuli, thus is appears that the $PTEN^{+/-}$ myocardium may have an decreased threshold for cardioprotection.

Obtaining a specific and reliable manipulation of PTEN levels and activity has been problematic. Inhibitors are limited and are not readily investigated, reliable or readily available. PTEN haploinsufficiency studies have proved useful to us and others (Wong et al., 2007; Bayascas et al., 2005; Podsypanina et al., 1999). However, we have to ask if it is the best tool for investigating the role of PTEN in cardioprotection?

The PTEN KO mice used in this study have a PTEN haploinsufficient phenotype ($PTEN^{+/-}$), their homozygous littermates with total knock down of PTEN ($PTEN^{-/-}$) do not survive gestation; and therefore were not valid for use in our studies (Podsypanina et al., 1999). In this PTEN haploinsufficient model all tissues are affected and there is a proportion of residual PTEN remaining that preserves function. Perhaps a model of cardiac tissue specific inhibition may prove a more powerful tool in understanding the biological importance and role of PTEN in ischaemia-reperfusion injury.

7 Chapter 7 – Reduction of PTEN using small interfering RNA

7.1 Background, aims and hypothesis

Within this thesis, the isolated perfused myocardial model of ischaemia-reperfusion injury was primarily used to study the effects of PTEN reduction on cell death. Additionally, we also used an isolated cardiomyocyte model of ROS induced mitochondrial damage. However, neither of these experimental models conferred significant protection against ischaemia-reperfusion injury, as shown in chapters 4 and 6. Therefore, we decided to go one step further and study the effects of PTEN silencing, using small interfering RNA, in a cellular model of hypoxia-reoxygenation.

As described in Chapter 2.8, siRNA silencing is a technique involving the manipulation of the cells' own transcription and translation mechanisms, to silence the expression of the protein of interest. The addition of double stranded RNA with specificity to a target protein prevents the synthesis of that protein (Caplen et al., 2001).

Initially, the method for knockdown of PTEN protein levels in H9c2 cells was optimised using various pre-designed siRNA constructs with specify to PTEN. It was hypothesised that PTEN protein knockdown in H9c2 cells, using siRNA with specificity to PTEN, would confer protection against hypoxia-reoxygenation injury.

7.2 Experimental protocols and methods

7.2.1 Optimising protein silencing using siRNA

Transfection of siRNA and protein knockdown are dependent on transfection efficiency and the rate of the target protein turnover in the cells used (H9c2 in this case). In our initial optimisation experiments we investigated the effect of:

1) Transfection reagent, comparing Fugene6, FugeneHD and X-tremeGENE (Roche,UK)
2) The ratio of transfection reagent (µl): siRNA(ng) (1:1-5-1),
3) Transfection time (24-72h),
4) Primer set (1-3),
5) siRNA concentration (100pmol/well-5pmol/well) and
6) Cell number on protein silencing.

These initial optimisation experiments were performed in 6 and 12 well culture plates. (Orange Scientific, Belgium) These experiments focused on identifying the most effective method for transfecting H9c2 cells. To explore the effects of these variables on transfection efficiency, we investigated the following:

1) The effect of different transfection reagents on transfection. Fluorescently tagged siRNA was not available for us to use at the time of this study. We compared the transfection reagents Fugene6 and the recently modified FugeneHD; at various reagent (l) to plasmid expressing green fluorescent protein (GFP) (ng) ratios (1:1-4:1).

   Transfection efficiencies were estimated by counting the percentage of total cells expressing and translating the GFP: a positive cell was counted as green, an example

of which is shown below in Figure 7.1. Average number of cells counted per condition was 114.5±8.7.

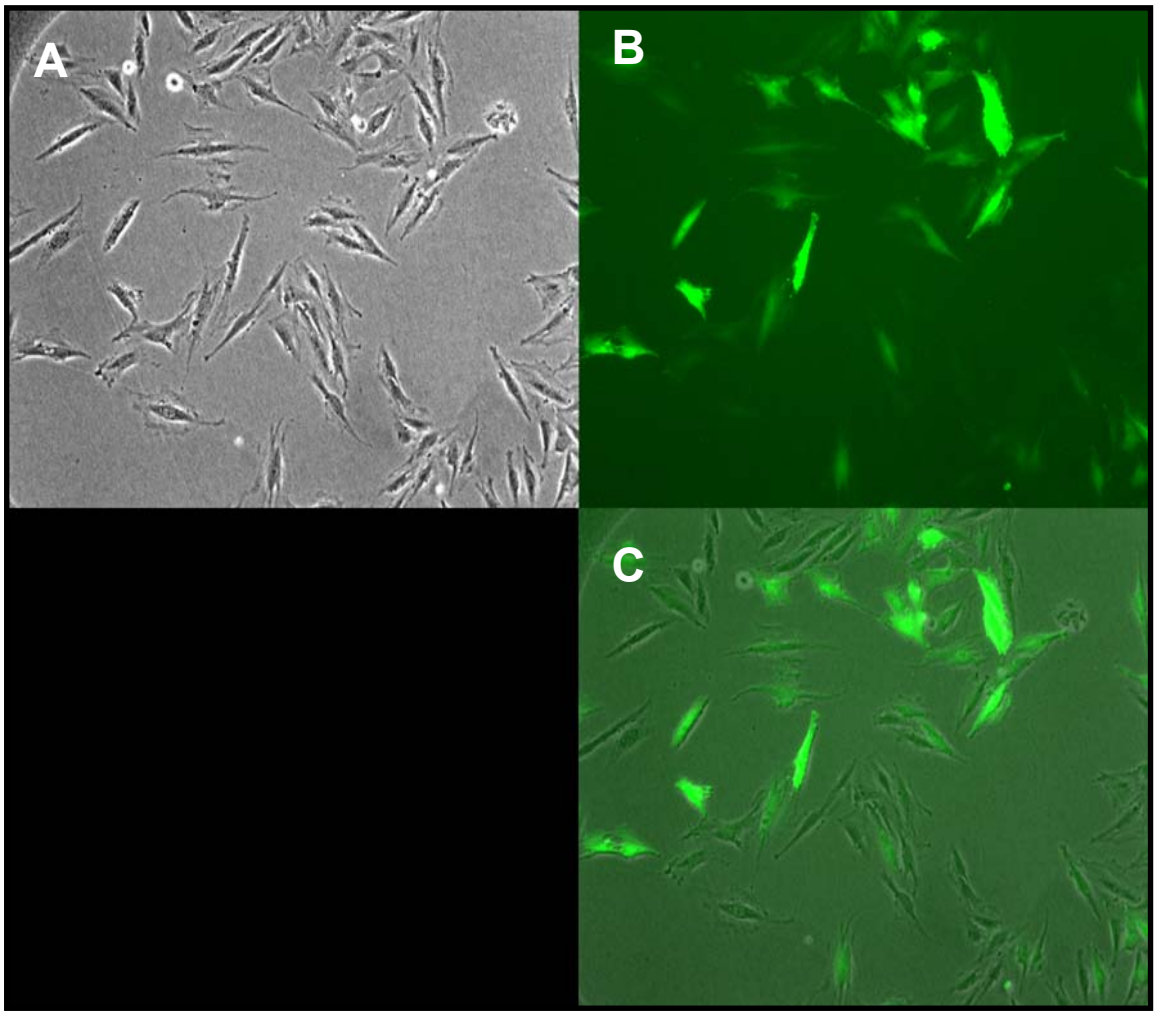

Figure 7.1: Example of the transfection efficiency using FugeneHD, in H9c2 cells (A, light image) identified by overlapping the green fluorescence (as a measure of green fluorescent protein (GFP) uptake) image (B) to identify the % of total cells transfected with the GFP that translate the green fluorescence (C).

2) The effects of different transfection reagents on protein expression; initially the certified GAPDH siRNA was used as a positive control.

Principally, we aimed to achieve a reduction in translational activity. Therefore, GAPDH protein expression was investigated in the presence of GAPDH siRNA, which was used as a positive control to confirm that the process of siRNA silencing works in our laboratory.

Transfection reagents FugeneHD or the siRNA specific transfection reagent, X-tremGENE were used to investigate GAPDH protein expression. Protein expression was compared, using either GAPDH specific siRNA (Ambion, UK) or scrambled siRNA (no transcript specificity) n=2 performed in 6 well plates. Protein expression was investigated using Western blot analysis and assessed changes by densitometry, described in more detail in chapter 2.6.

3) The effects of GAPDH siRNA concentration and transfection reagent to siRNA ratio, on GAPDH protein expression.

The effects of various concentrations (100,50 and 25pmol) and ratios of transfection reagent(ul) to GAPDH siRNA(ng) (2:1, 3:1 and 5:1) on GAPDH protein expression, n=2 were investigated. These experiments were carried out in 12 well plates, to assess the effects of reducing well size and therefore cell number on protein knockdown. This is because hypoxia-reoxygenation experiments are performed in 12 well plates.

4) The effects of PTEN siRNA primer sequence and concentration of siRNA on PTEN protein expression

The Silencer® pre-designed PTEN primers were purchased from Ambion with a guarantee that 1 out of 3 purchased siRNA primers would knockdown PTEN protein

with 80% efficiency. Therefore the changes in PTEN protein using 100pmol siRNA and X-tremGENE transfection reagent at 3 to 1 ratio in 6 well plates, n=2 were investigated.

5) The effects of PTEN siRNA concentration and duration of transfection using PTEN primers 1 and 3 on PTEN protein expression.

We strived to achieve maximal PTEN protein knockdown and therefore, optimisation studies focused on the PTEN primers 1 and 3. The PTEN protein knockdown after 48 and 72h, in the presence of 50 and 100pmol and X-tremGENE transfection reagent at 3 to 1 ratio in 12 well plates, n=2 was investigated.

6) The effects of PTEN siRNA concentration of using primer 3 per 4,000 cells

We aimed to attain the maximal PTEN protein knockdown possible in our hands. The PTEN siRNA primer 3 was investigated. Cells were incubated for 72h at a range of concentrations (30pmol/well-5pmol/well) with X-tremGENE transfection reagent at 3 to 1 ratio, in 12 well plates (in the presence of 4,000cells which was the number of cells/well of a 12 well plate required for subsequent hypoxia-reoxygenation experiments.), n=4.

7.2.2 Response to hypoxia-reoxygenation: optimising and inducing cell death

The level of cell death in H9c2 cells silenced for PTEN protein expression was investigated following our protocol of hypoxia-reoxygenation injury, as described in chapter 2.8 and outlined in Figure 7.2. Different methods were investigated to measure cell damage, such as percent of adherent cells positive for propidium iodide (PI), lactate dehydrogenase (LDH) release, and caspase 3 cleavage, which are described below. As a positive control cells were

incubated with insulin (10µg/ml) at the onset of reoxygenation. The vehicle control used for insulin was reoxygenation buffer.

1) Propidium iodide

Injured or damaged cells with permeabilised membranes permit the penetration of dyes such as propidium iodide (PI), the detection of which can be used to monitor cell death (Jonassen et al., 2004).

Injured cells were identified by counting the percentage of adherent H9c2 cells staining positive for PI (red), n=4. It was expected that, following hypoxia-reoxygenation the number of PI stained cells would increase in comparison to cells maintained in normoxia. It was hypothesised that fewer cells, silenced for PTEN protein expression, would stain positive for PI following hypoxia-reoxygenation. Insulin was used as a positive control, which was expected to reduce the number of cells staining positive for PI following hypoxia-reoxygenation.

2) LDH

Additionally, injured or damaged cells with perturbed membranes permit the release of cellular components such as LDH, usually located in the cytosol. The ratio of released LDH into the culture media compared to the remaining LDH levels can be used in order to estimate cell viability (Jonassen et al., 2004). LDH release following hypoxia-reoxygenation was measured using an LDH/cytotoxic assay kit from Promega, UK, as described in chapter 2.8. The absorbance of samples was measured and the results were expressed in A.U; relating to the total LDH present. Total LDH was the sum of LDH measured in cell supernatant and the LDH measured in the remaining whole cell population, n=4.

As a part of the assay optimisation experiments the effects of sample dilution on the sensitivity of the assay was investigated. The absorbance values obtained with various dilutions of neat LDH enzyme, supplied in the assay kit as a positive control were measured: 1.6units/ml, 3.2units/ml and 6.4units/ml were compared to the values obtained for buffer control (culture media only, no cell content).

It was expected that, following hypoxia-reoxygenation, LDH released would be increased compared to cells maintained in normoxia. Furthermore, it was hypothesised that following hypoxia-reoxygenation LDH release would be lower in cells silenced for PTEN protein expression and used insulin as a positive control.

3) Caspase 3 cleavage

Injured or damaged cells may undergo an increase in apoptosis, which can be reflected by an increase in the activation of caspases. The end effector caspase, caspase 3, is cleaved and therefore activated in apoptosis; producing a pro death fragment (Nicholson et al., 1995; Kothakota et al., 1997). The extent of caspase 3 cleavage was measured using Western blot analysis, as described in chapter 2.6. The results were normalised to the total caspase 3 levels and expressed as a percentage of control. The total caspase 3 value was estimated by combining the A.U value obtained from the uncleaved caspase 3 fragment (running to 35kDa) with the A.U acquired from the cleaved caspase 3 fragment (running to 17kDa), n=4.

It was expected that, following hypoxia-reoxygenation greater caspase 3 cleavage would occur compared to those cells maintained in normoxia. Furthermore, it was hypothesised that following hypoxia-reoxygenation caspase 3 cleavage would be less in cells silenced for PTEN protein expression and, insulin was used as a positive control.

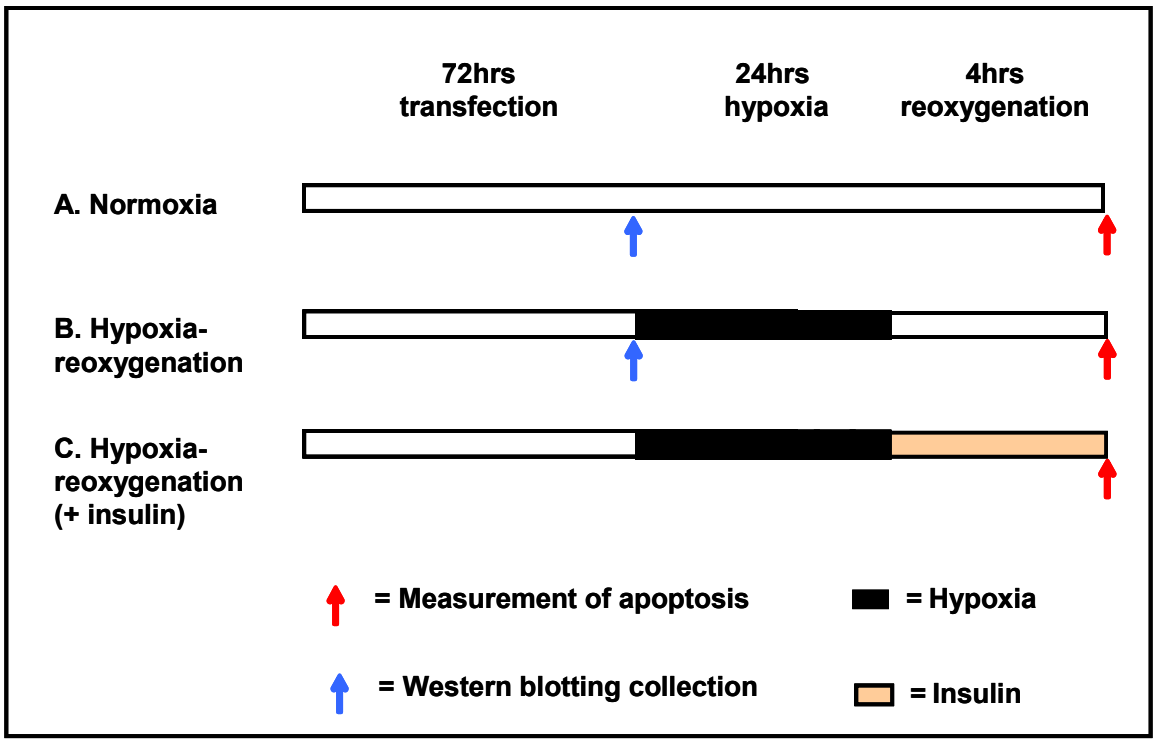

Figure 7.2: Hypoxia-reoxygenation protocol (24h hypoxia/4h reoxygenation) performed in H9c2 cells transfected with either scrambled (negative control) small interfering RNA (siRNA) or PTEN siRNA. Insulin at the onset of reoxygenation was used as a positive control, for which reoxygenation buffer was used as the vehicle control.

7.2.3 Possible compensatory signalling mechanisms in cells silenced for PTEN expression.

Previously, it was shown that the myocardium from PTEN$^{+/-}$ mice do not confer cardioprotection against our model of ischaemia-reperfusion injury. In these isolated hearts a reduced level of PINK1 expression was observed and it was proposed that this may be a possible explanation for the absence of protection in these hearts, as shown in chapter 6.

Similarly, in this chapter PINK1 protein expression was investigated in H9c2 cells silenced for PTEN protein expression. Western blot analysis was used, as described in chapter 2.6 to

measure this, n=3. It was hypothesised that cells silenced for PTEN would have lower levels of PINK1 protein expression.

7.3 Results

7.3.1 Optimising protein silencing using siRNA

1) Investigating the effect of different transfection reagents on transfection

Figure 7.3 represents the transfection efficiencies which were estimated by counting the percentage of total cells expressing and translating the GFP. The results indicate that there were no differences in the transfection ratios of reagent to DNA when comparing Fugene6 and FugeneHD transfection reagent. Nevertheless, the percentage of cells transfected efficiently was higher (59.4 ±5.1%) using Fugene HD compared to Fugene6 (24 ±2%)

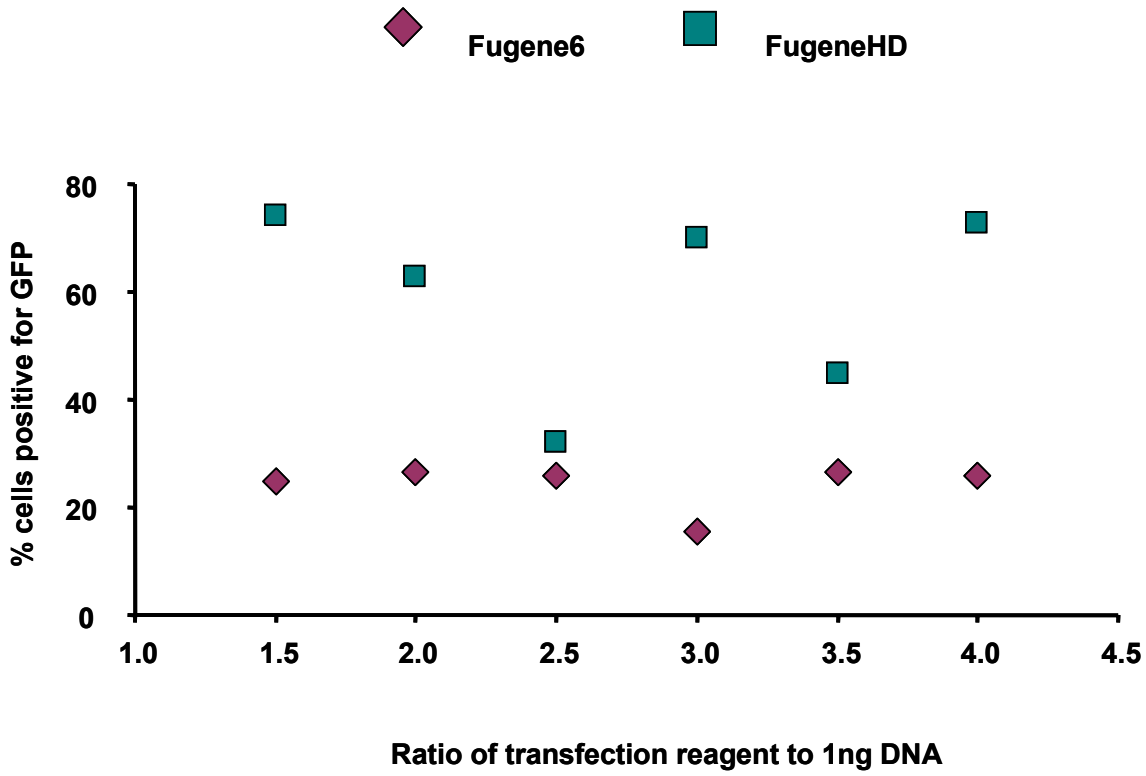

Figure 7.3: Transfection efficiency of Fugene6 (red diamonds) compared to FugeneHD (green squares) transfection reagent. Mimicking siRNA uptake in of H9c2 cells incubated with green fluorescent protein (GFP) measured by the % of cells fluorescing green.

2) Investigating the effects of different transfection reagents on protein expression; initially using the certified GAPDH siRNA as a positive control.

As shown in Figure 7.3 transfection of H9c2 cells with plasmid DNA expressing GFP was achieved using Fugene6. In contrast, as shown in Figure 7.4 GAPDH protein expression was not reduced in cells transfected using Fugene6. Nonetheless, GAPDH protein expression was reduced in cells transfected using X-tremGENE.

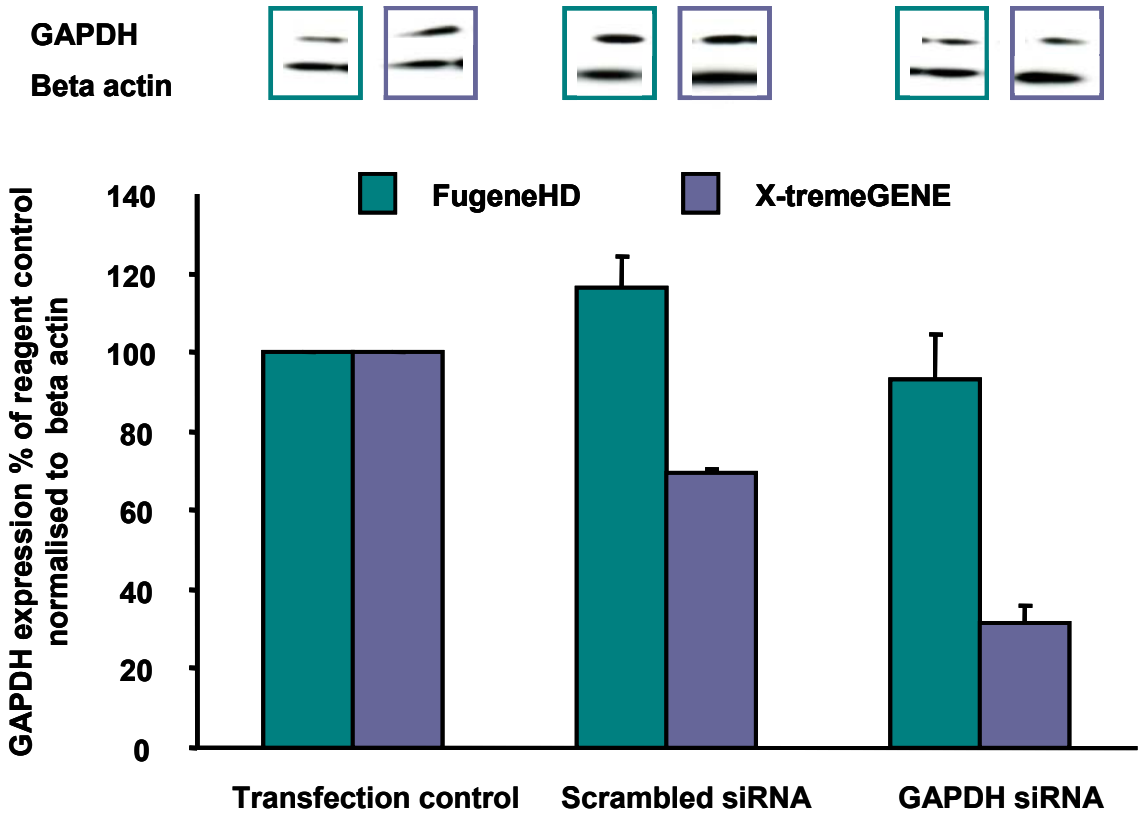

Figure 7.4: Transfection efficiency in H9c2 cells using FugeneHD (green bars) or X-tremeGENE (purple bars) transfection reagent, measured by assessing GAPDH protein expression normalised to transfection control using either scrambled siRNA or GAPDH siRNA (n=2).

3 The effects of GAPDH siRNA concentration and transfection reagent to siRNA ratio on GAPDH protein expression.

The results are shown in Figure 7.5 and highlight that 100 and 50pmol GAPDH siRNA provide maximal protein knockdown. The results also indicated that 3µls reagent to1ng of siRNA (3:1) provided the maximum and most specific GAPDH protein knockdown.

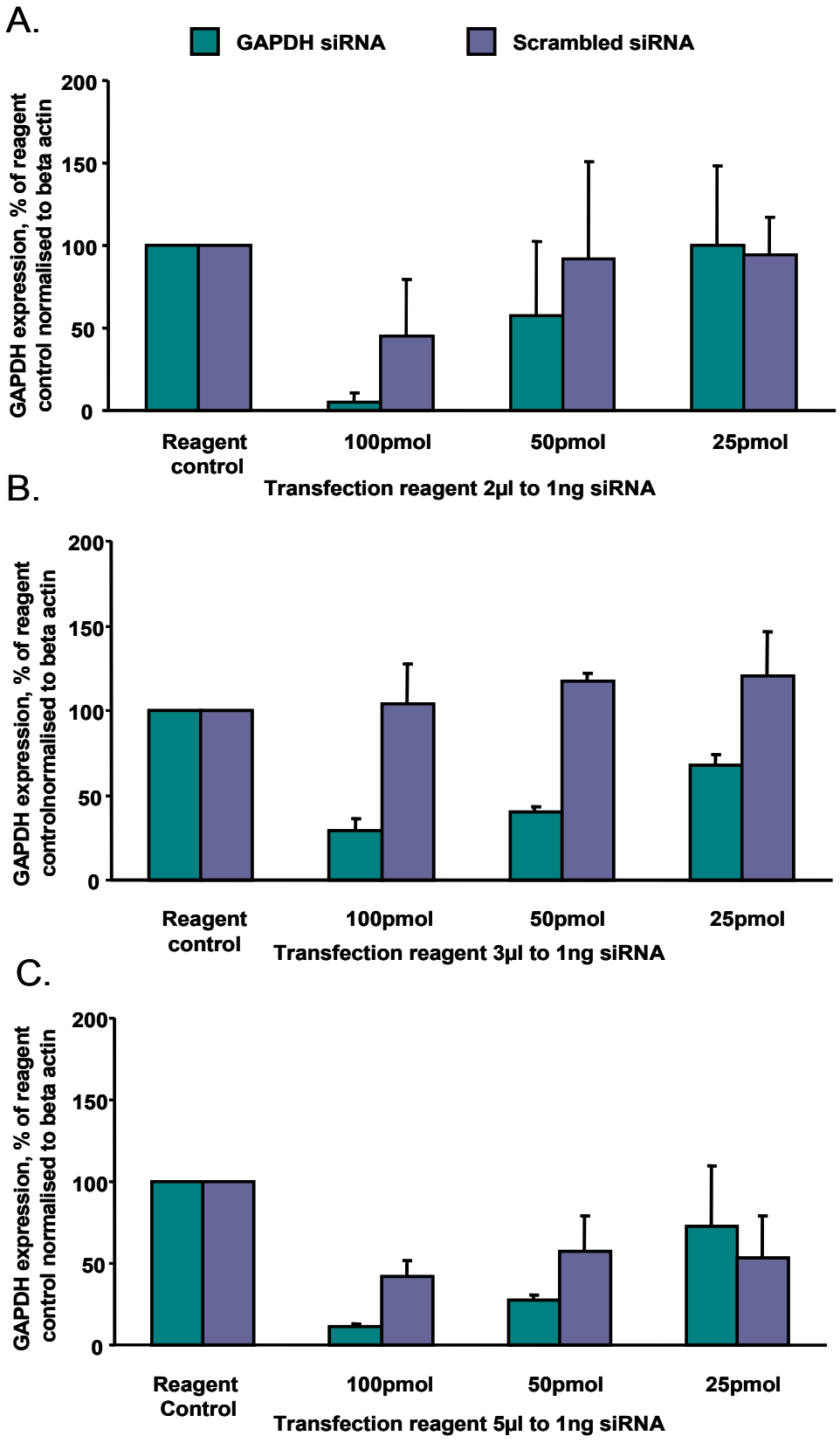

Figure 7.5: GAPDH protein knockdown with: A) 2:1, B) 3:1 or C) 5:1 ratios of transfection reagent (ul) to 1ng siRNA. 100pmol, 50 and 25pmol siRNA (n=2).

4) The effects of PTEN siRNA primer sequence and concentration of siRNA on PTEN protein expression

The initial studies investigating PTEN silencing were performed in 6 well plates. As shown in Figure 7.6, the preliminary studies indicated 2 out of the 3 primers successfully reduced the levels of PTEN (primer 1 and 3).

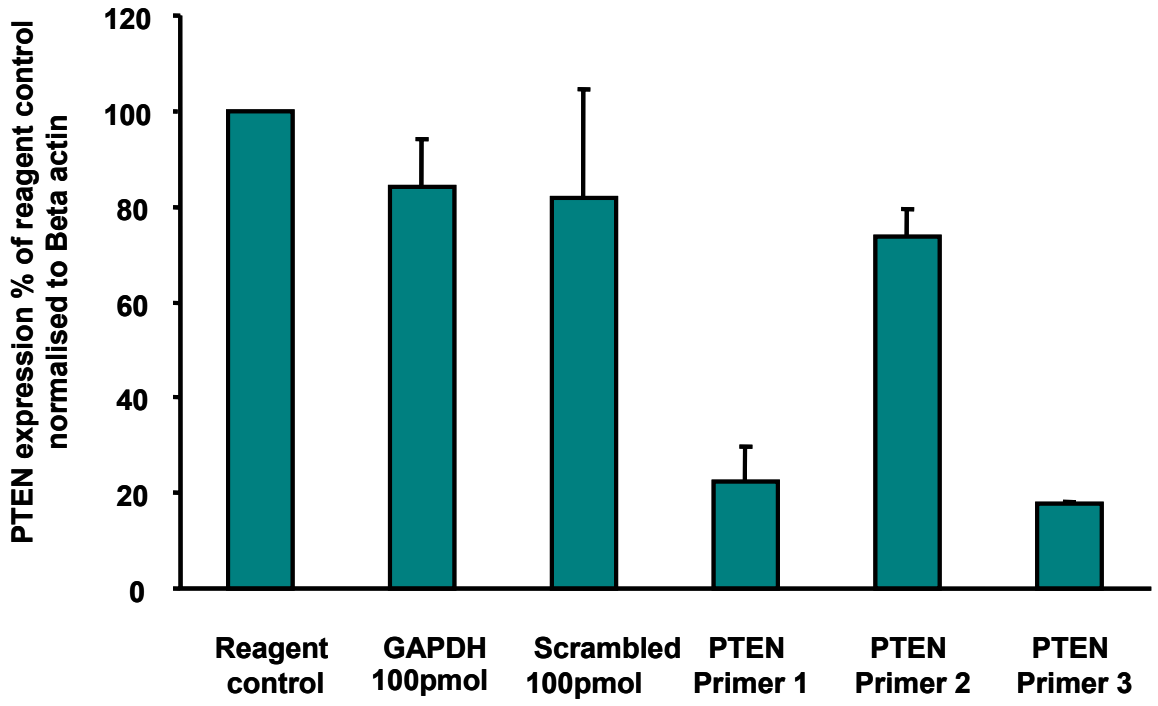

Figure 7.6: PTEN protein knockdown, investigating efficiency of 3 different PTEN siRNA primers at 100pmol, normalised to reagent control (n=2).

5) The effects of PTEN siRNA concentration and duration of transfection using PTEN primers 1and 3 on PTEN protein expression.

The results are shown in Figure 7.7 and indicate that the difference between PTEN protein expression at 48 and 72h is small. However, following 72h protein knockdown with primer 3 provided maximal silencing of PTEN protein.

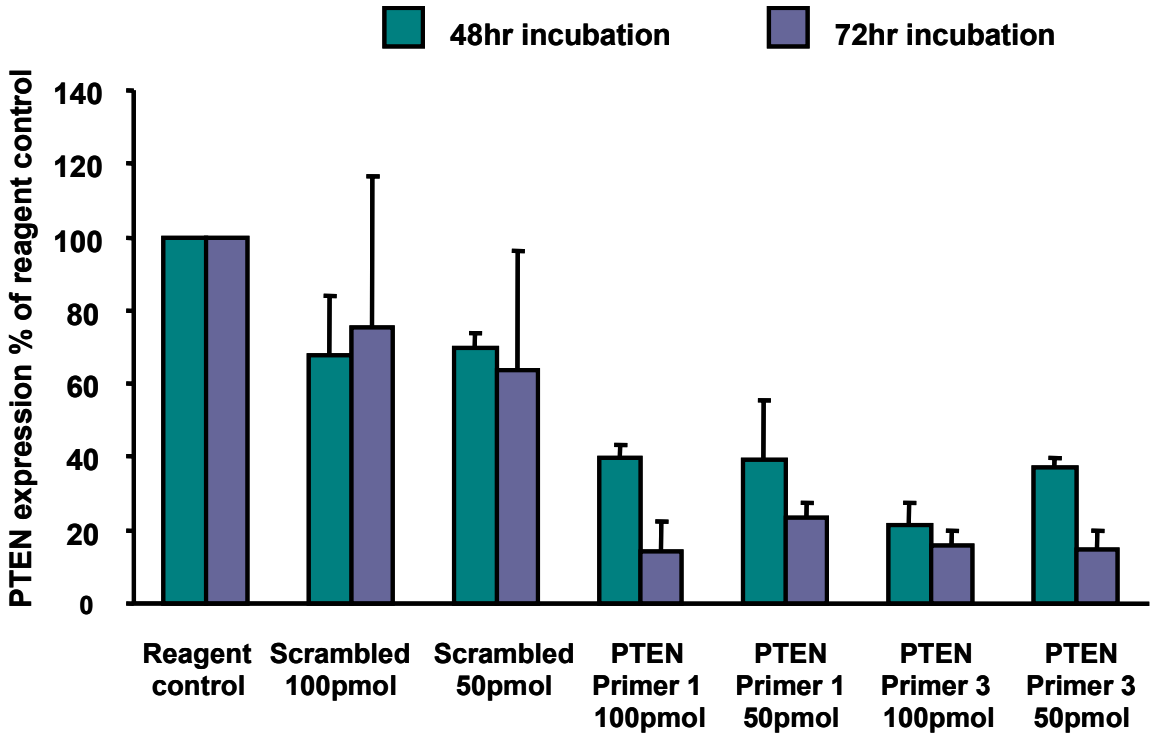

Figure 7.7: PTEN protein expression transfected with 100 and 50pmols PTEN siRNA primers 1 and 3 for either 48h (green bars) or 72h (purple bars), investigating maximal PTEN protein knockdown in 12 well plates (n=2).

6) The effects of PTEN siRNA concentration of using primer 3 per 4,000 cells

The results are shown in Figure 7.8 and shows that a dose response effect (of protein knockdown) occurs with varying concentrations of siRNA. The more siRNA present the more PTEN protein silencing was observed. Conversely, these results indicate that the scrambled siRNA had some off target effects, itself causing a reduction in PTEN protein expression at higher concentrations. This highlights the importance of including a scrambled siRNA control in all experiments with siRNA. The most efficient PTEN silencing occurred with 30pmol siRNA primer 3.

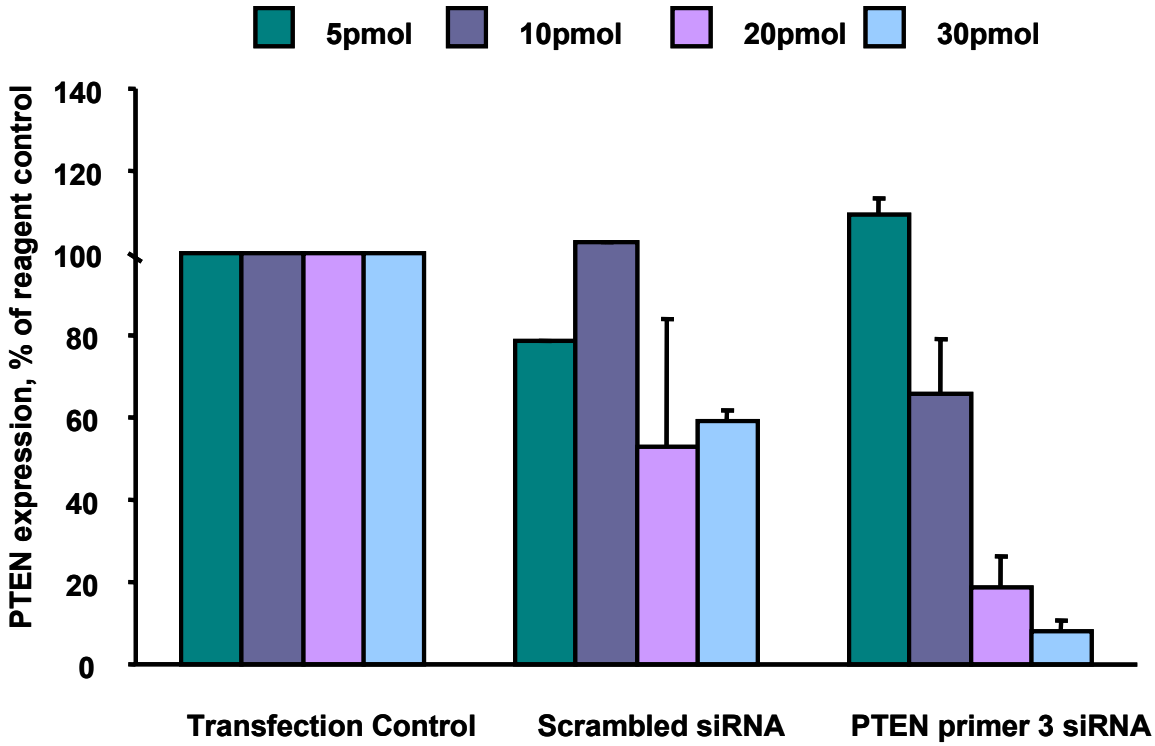

Figure 7.8: PTEN protein expression with 5 (green bars), 10 (purple bars), 20 (red bars) and 30 (light blue bars) pmol of PTEN siRNA primer 3 per 4,000 cells. Incubated for 72h (n=2).

In summary, the optimised method for siRNA induced PTEN silencing in H9c2 cells is described below. H9c2 cells were transfected with 30pmol/4,000cell/12 well plate using 3ul X-tremGene reagent to 1ng siRNA. Protein analysis was assessed 72h later conveying a significant ($p<0.001$) reduction in PTEN protein; PTEN expression was silenced to 17.6 ±4.0% of the scrambled siRNA control (100%), as shown in Figure 7.9.

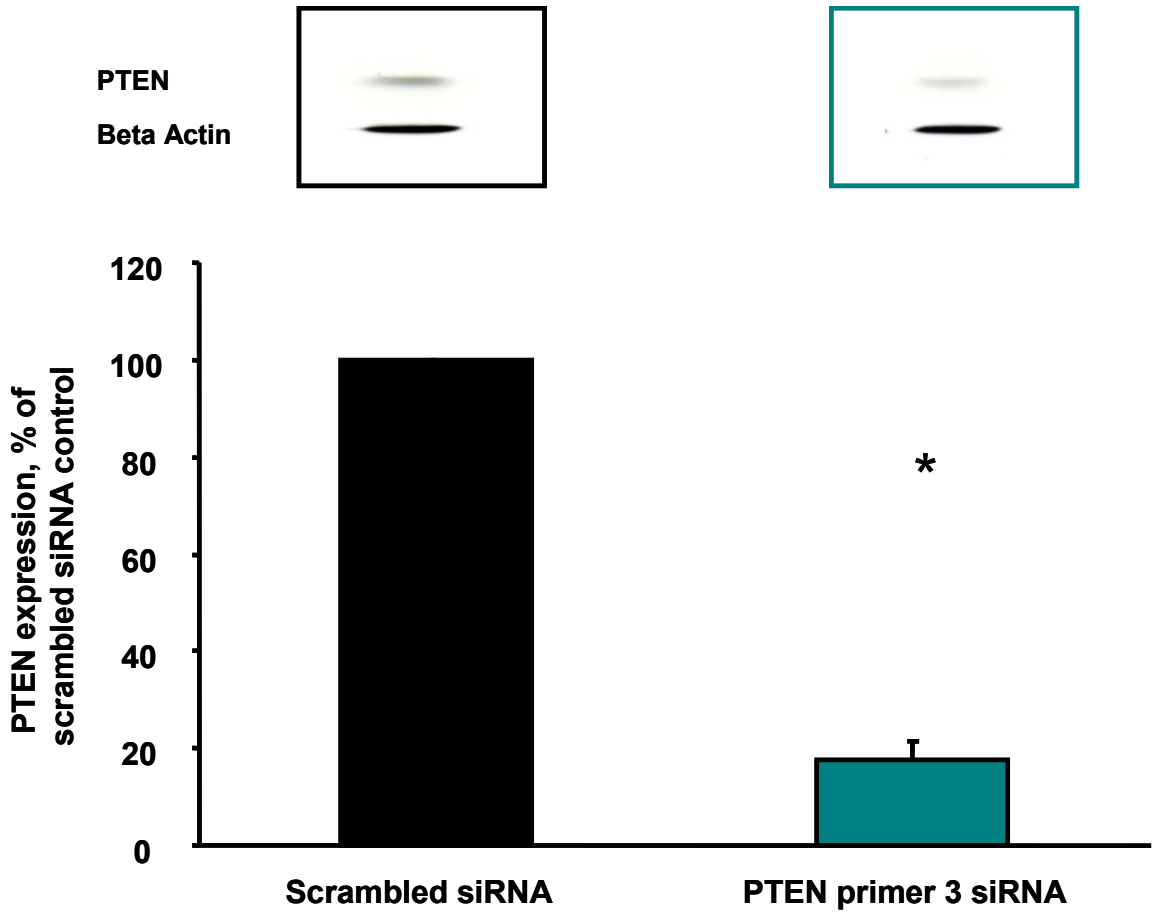

Figure 7.9: PTEN protein expression with 30pmol/4,000 cells of either scrambled siRNA (black bars) or PTEN primer 3 siRNA (green bars) transfected for 72h (n=4). Statistical differences were assessed using the Student's paired t-test, (*<0.001).

7.3.2 Response to hypoxia-reoxygenation injury: optimising and inducing cell death.

Measuring cell death following hypoxia-reoxygenation

Methods to measure cell death following hypoxia-reoxygenation were investigated, such as measuring the percent of adherent cells positive for propidium iodide (PI), lactate dehydrogenase (LDH) released, and caspase 3 cleavage: the results are described below.

1) Propidium iodide

To identify and assess injured cells the percentage of adherent H9c2 cells staining positive for PI (red) were counted. The results are shown in Figure 7.11. A significant increase in the number of cells staining positive for PI was observed in cells following hypoxia-reoxygenation (29.2 ± 3.8%) compared to cells maintained in normoxia (7.3 ± 1.3%, $p<0.005$). Figure 7.10 shows a representative example of the differences in PI staining in H9c2 cells subjected to hypoxia-reoxygenation compared to normoxia.

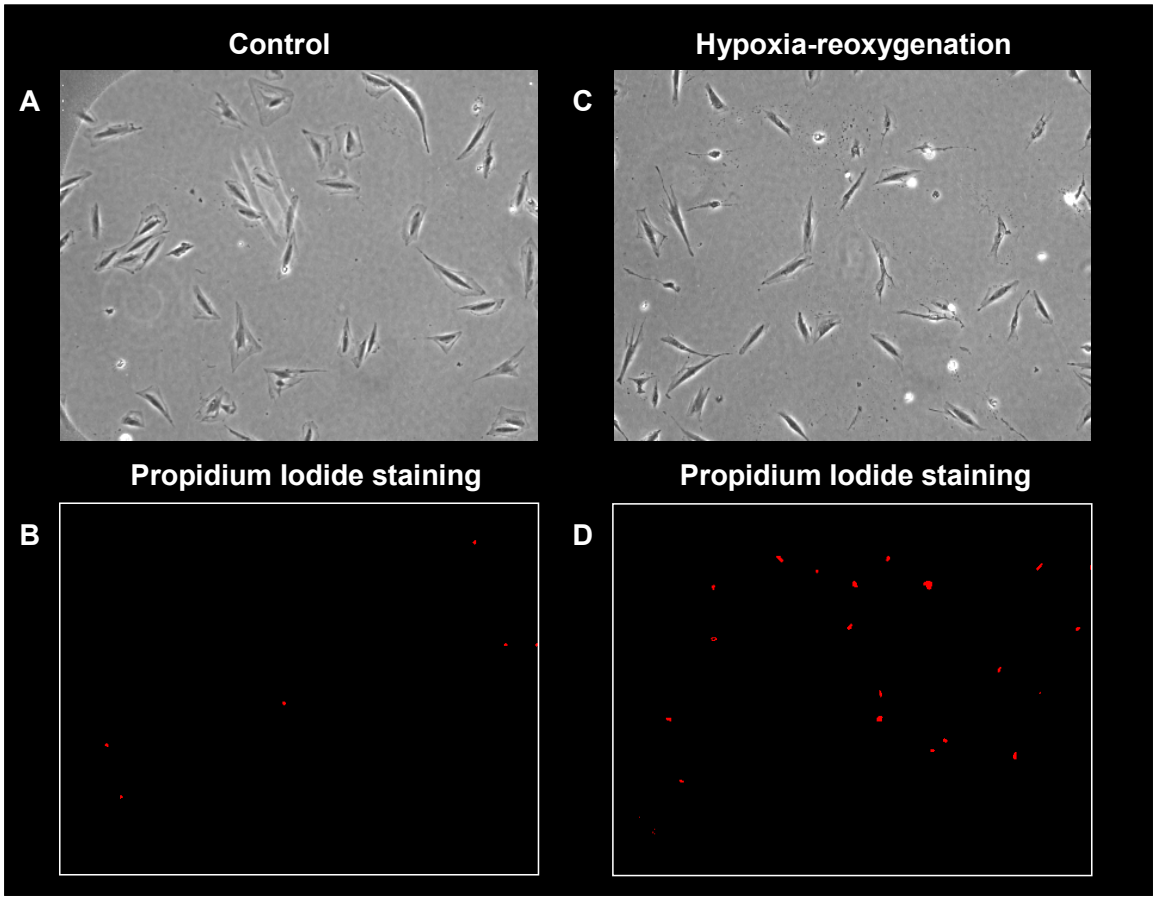

Figure 7.10: H9c2 cell viability: A) maintained in normoxic conditions or B) subjected to hypoxia-reoxygenation and C) the uptake of propidium iodide as indicated by red fluorescence in normoxia or D) following hypoxia-reoxygenation.

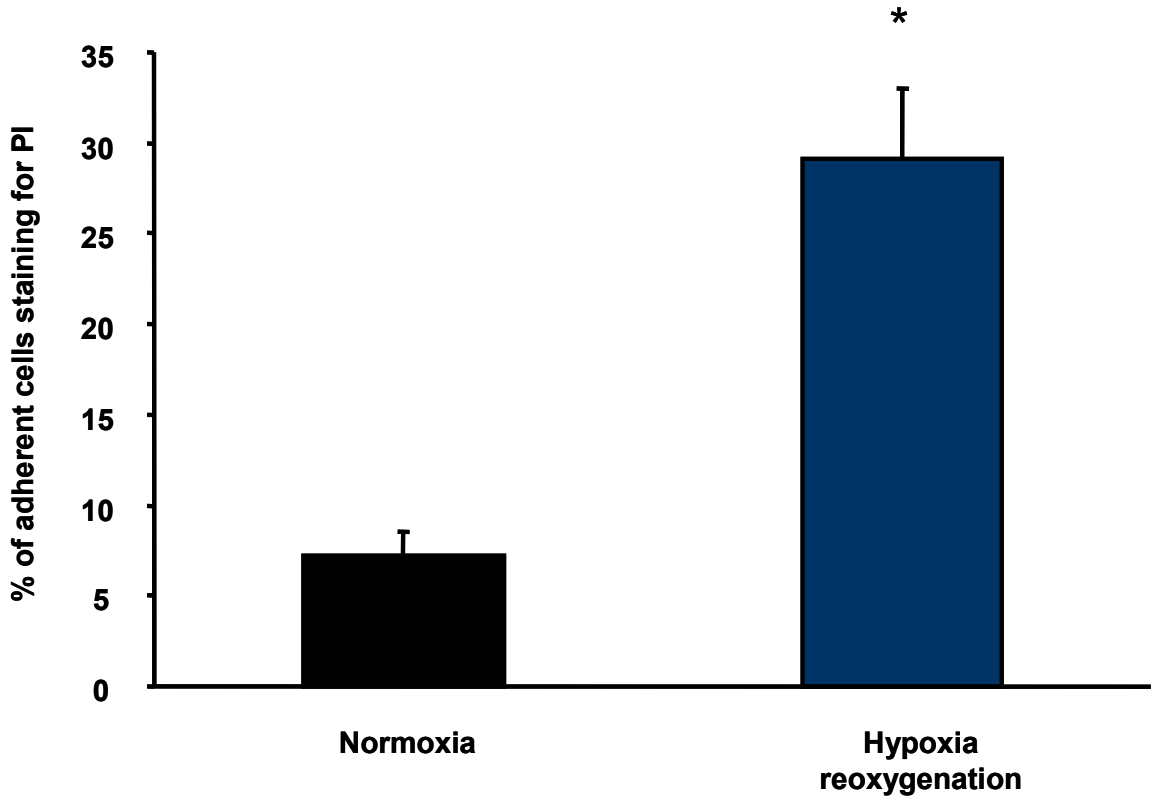

Figure 7.11: H9c2 cell viability monitored by visualising percentage of total cells positive for propidium iodide (PI) staining: normoxic conditions (black bars) or subjected to hypoxia-reoxygenation (blue bars) (n=4). Statistical differences were assessed using Student's paired t-test, (*<0.005).

It was hypothesised that fewer cells (silenced for PTEN expression) would stain positive for PI compared to cells transfected with control siRNA. However, we were not able to prove this, the results are shown in Figure 7.12 and indicate no significance differences in PI staining between cells transfected with PTEN specific siRNA and scrambled non specific siRNA. Unexpectedly, no reduction was observed in the presence of insulin. The variability in PI staining was large and the process of siRNA silencing in H9c2 cells appeared to cause some background staining. Therefore, alternative mechanisms to assess cell vulnerability subsequent to hypoxia-reoxygenation were explored.

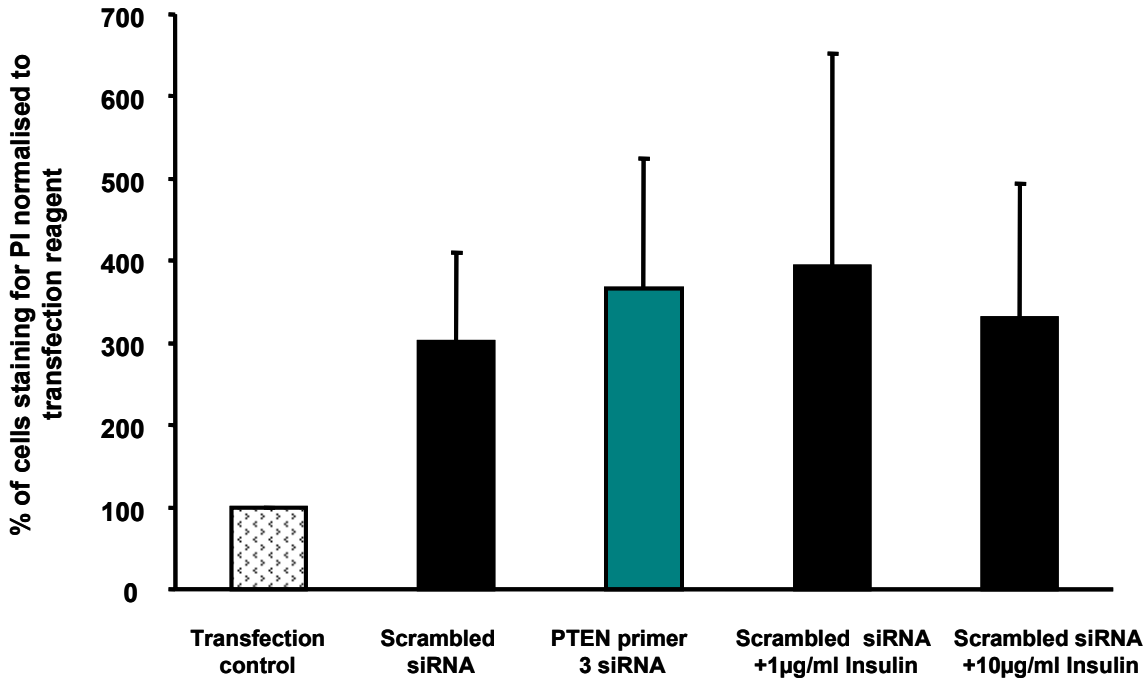

Figure 7.12: The effect of PTEN silencing on the number of cells staining positive for propidium iodide (PI) following hypoxia-reoxygenation (n=4). Reoxygenation buffer was used as a control for insulin. Statistical differences were assessed using One Way ANOVA.

LDH

LDH release was measured as an indicator of cell vulnerability following hypoxia-reoxygenation and was compared to that of the cells maintained in normoxia. It was hypothesised that there would be an increase in LDH release from cells subjected to hypoxia-reoxygenation injury. The results are shown in Figure 7.13, It was observed that an increase in LDH release occurred from cells subjected to hypoxia-reoxygenation (0.2590 ± 0.175 A.U) compared to cells maintained in normoxia (0.4119 ± 0.03 A.U). However, this increase was not significantly different.

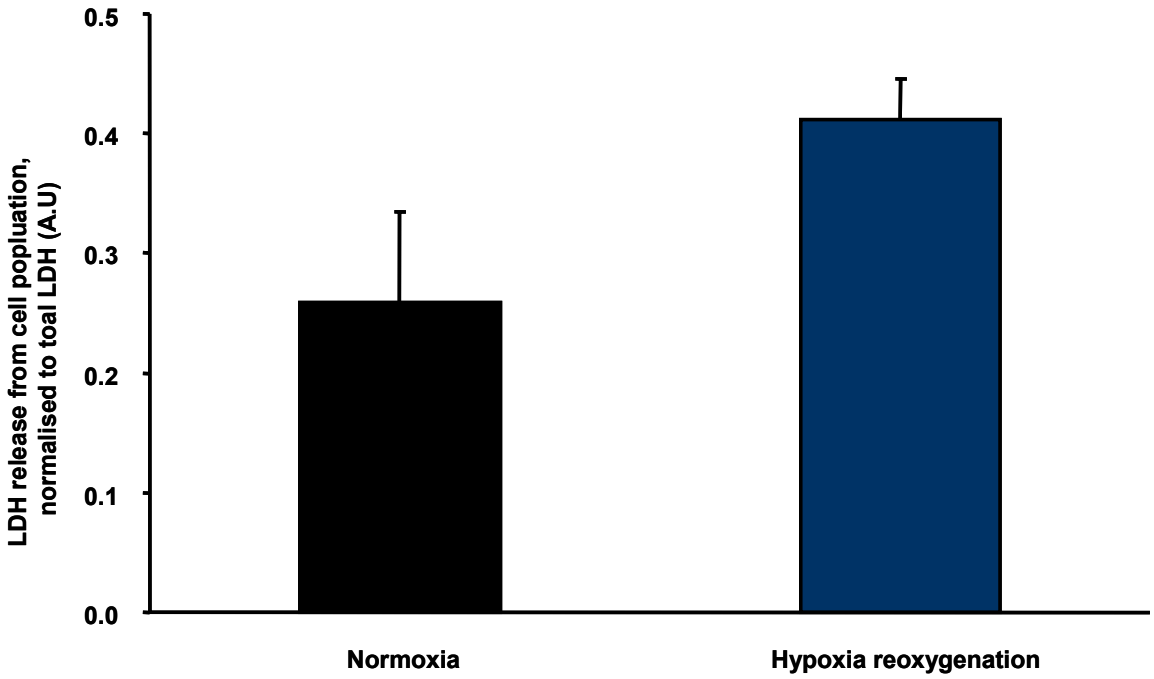

Figure 7.13: H9c2 cell viability following hypoxia-reoxygenation, monitored by detecting lactate dehydrogenase (LDH) release: LDH release from cells in normoxic conditions (black bars) compared to LDH release from cells subjected to hypoxia-reoxygenation (blue bars), expressed in arbitrary units (A.U). Statistical differences were assessed using the Student's paired t-test, (n=4).

As shown in Figure 7.14, following hypoxia-reoxygenation no significance differences in LDH release occurred between cells transfected with PTEN specific or scrambled siRNA. Furthermore, no reduction in LDH release was recorded in the presence of insulin at reoxygenation.

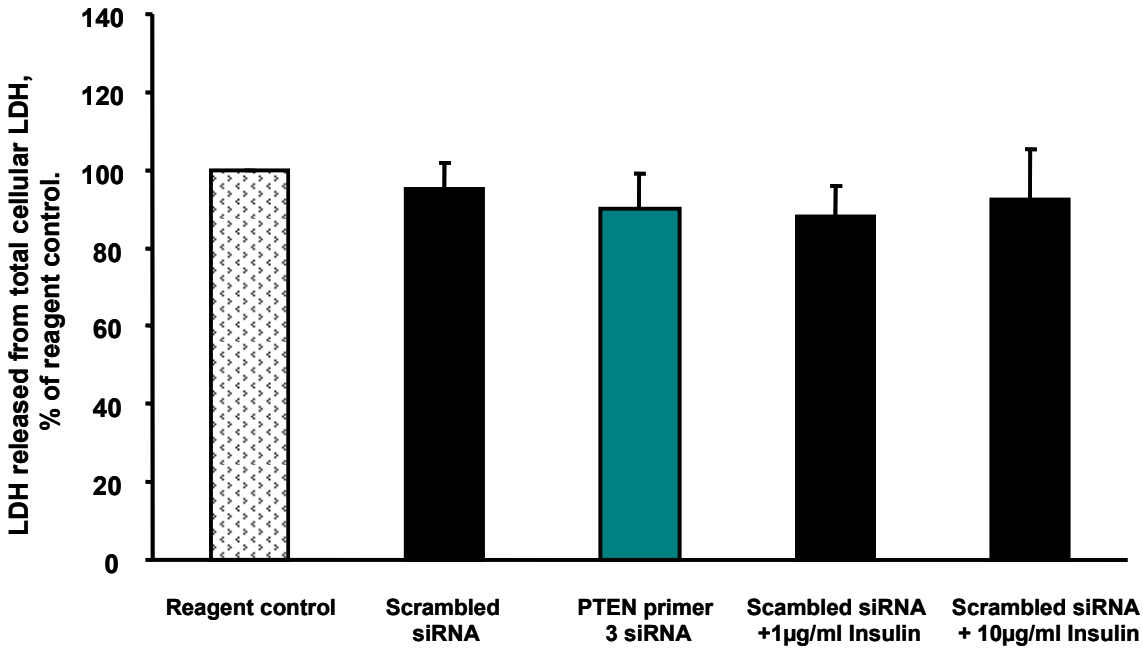

Figure 7.14: The effect of PTEN silencing on lactate dehydrogenase (LDH) release from cells maintained in normoxia (black bars) compared to cells subjected to hypoxia-reoxygenation (blue bars). Statistical differences were assessed using One Way ANOVA. (n=4).

To eliminate the possibility of any experimental set up errors, the effects of LDH sample dilution on the sensitivity of this assay were investigated. Figure 7.15 represents the typical absorbance values obtained with various dilutions of the neat LDH enzyme, supplied in the assay kit as a positive control. The absorbance values obtained in our samples were lower than the LDH positive control containing 1.6units/ml. Furthermore, the sample absorbance values were closer (but still higher) to the buffer control (culture media only, no cell contact). We investigated methods to increase the absorbance signal, however, these were unsuccessful. Therefore, alternative mechanisms to assess cell vulnerability subsequent to hypoxia-reoxygenation were explored.

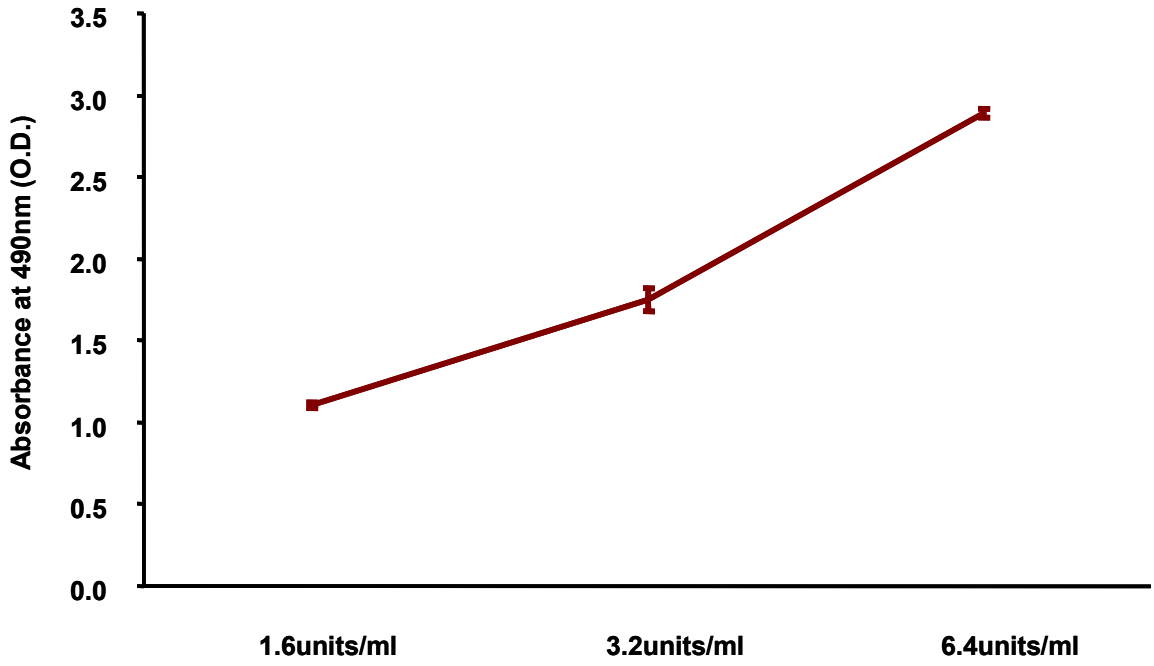

Figure 7.15: Absorbance (optical density (OD) values) obtained with various amounts of the lactate dehydrogenase (LDH) enzyme (used as a positive control) that was supplied with the LDH assay (replicates 2).

3) Caspase 3 cleavage

As shown in Figure 7.16, a significant increase in caspase 3 cleavage were observed in cells subjected to hypoxia-reoxygenation (231.9 ± 55.3%, $p<0.05$) compared to cells maintained in normoxia (100%).

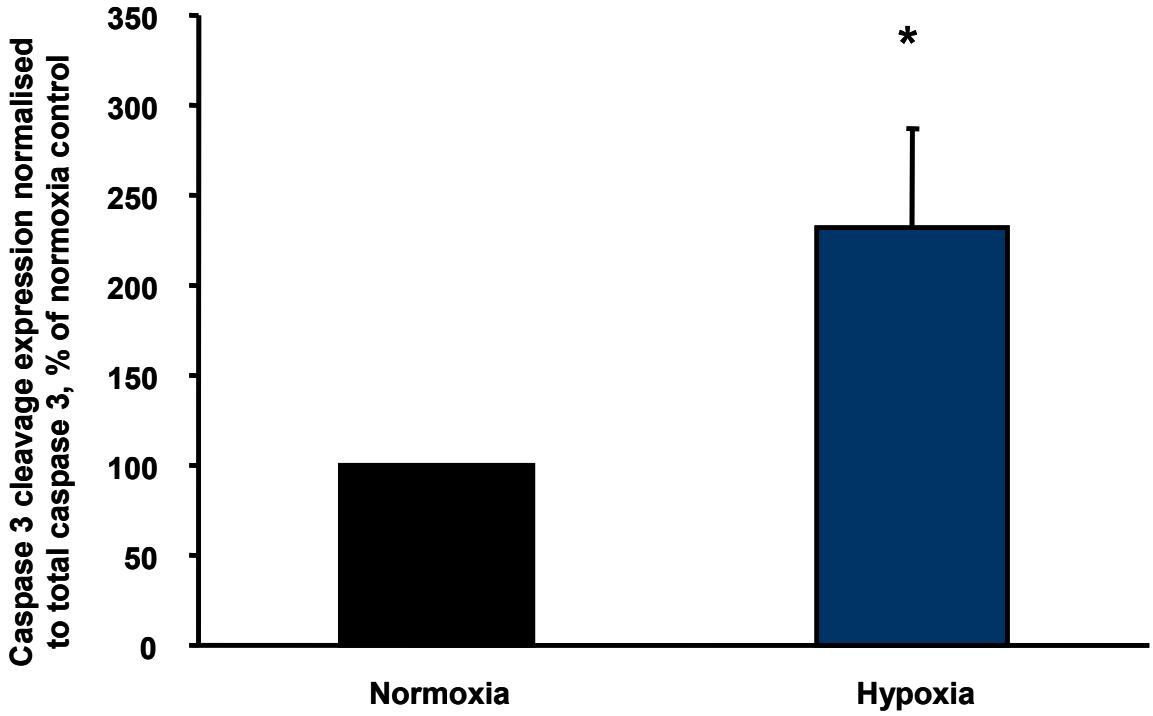

Figure 7.16: H9c2 cell viability monitored by detecting caspase 3 cleavage in cells maintained in normoxic conditions (black bars) compared to cells subjected to hypoxia-reoxygenation (blue bars). The caspase 3 cleavage is presented as a percent of the total caspase 3 expression (n=4). Statistical differences were assessed using Student's paired t-test, (*<0.05).

As shown in Figure 7.17 the addition of insulin at reoxygenation significantly reduced expression of caspase 3 cleavage fragment (38.83 $\pm$ 7.4%, $p<0.01$) compared to scrambled siRNA (100%). However, the expression of caspase 3 cleavage in cells silenced for PTEN was not reduced (120 $\pm$ 7.5%). Representative blots of caspase 3 in H9c2 cells are shown in Figure 7.18, it should be noted that the quality of the blots is not optimal due to changes in protein content in cell populations from normoxic and hypoxic populations and the presence and absence of siRNA. Future work may include repeating these experiments to provide clearer data.

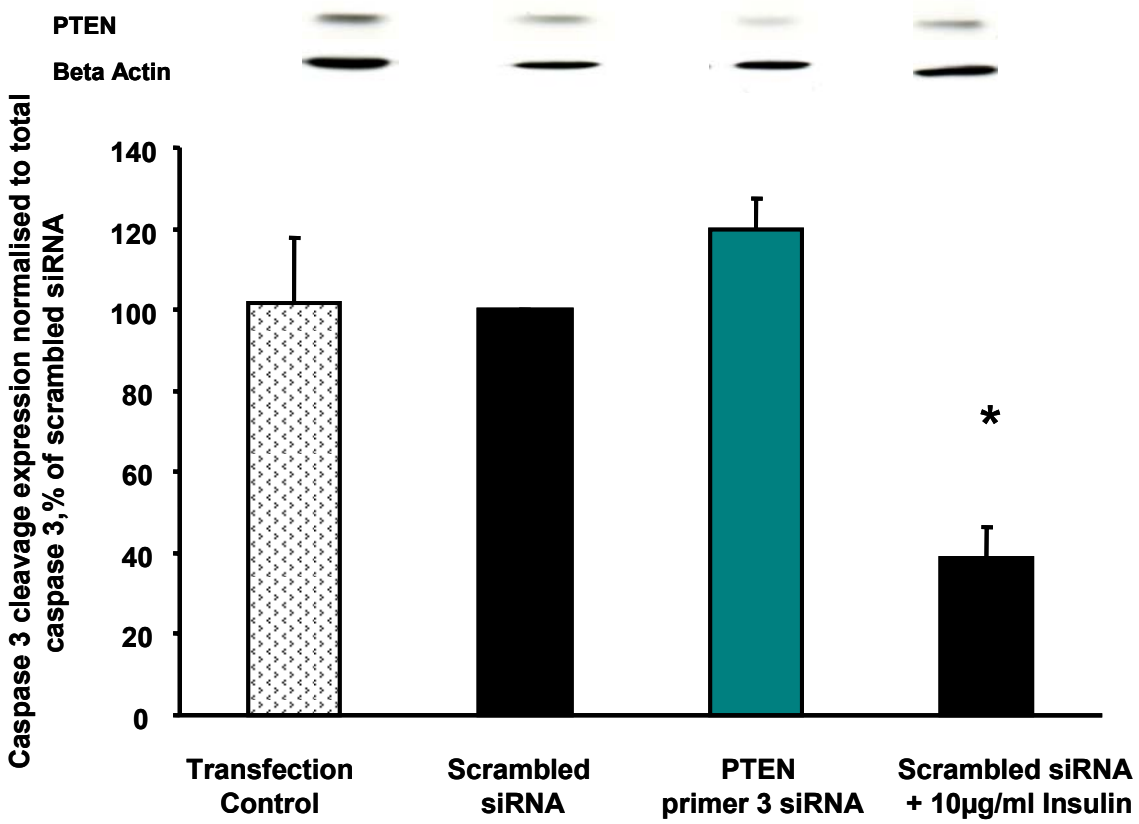

Figure 7.17: The effects of PTEN silencing following hypoxia-reoxygenation on the level of caspase 3 cleavage (n=4). Statistical differences were assessed using One Way ANOVA, (*<0.01).

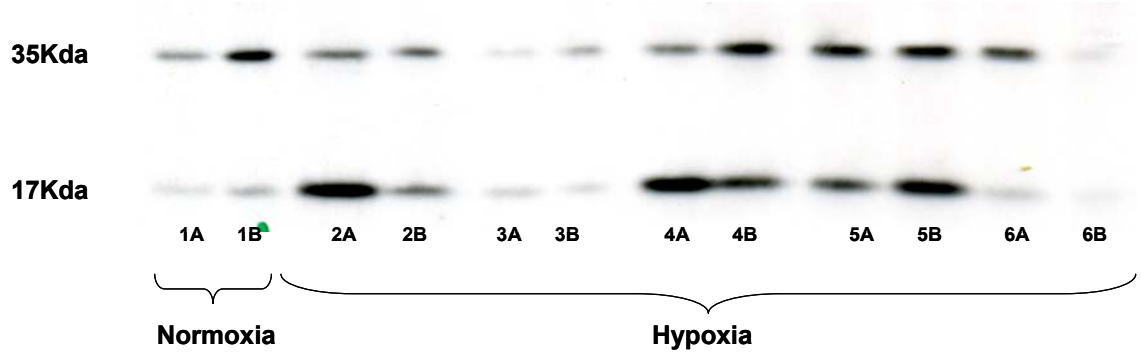

Figure 7.18: Example of Western blots illustrating cleaved (active 17kDa) and intact (inactive 35kDa) caspase 3 in H9c2 cells (samples in duplicate, A + B) subjected to normoxic conditions in the presence of 1 = transfection control and hypoxic conditions 2 = transfection control, 3 = scrambled siRNA, 4 = PTEN primer 3 siRNA, 5 = scrambled siRNA + 1µg/ml insulin and 6 = scrambled siRNA + 10µg/ml insulin.

7.3.3 Possible compensatory signalling mechanisms in cells silenced for PTEN protein expression

Possible compensatory signalling mechanisms that may explain the lack of protection in cells silenced for PTEN and subjected to hypoxia-reoxygenation injury were investigated. As shown in chapter 6 the myocardium from $PTEN^{+/-}$ mice was not protected against ischaemia-reperfusion injury. In the myocardium from these mice a reduction in PINK1 expression was detected. Therefore, PINK1 protein expression was investigated in H9c2 cells silenced for PTEN protein expression. As shown in Figure 7.19 the results demonstrates that cells silenced for PTEN express significantly less PINK1 (73.3 ± 15.3%, $p<0.05$) compared to cells incubated with scrambled siRNA (100.0%).

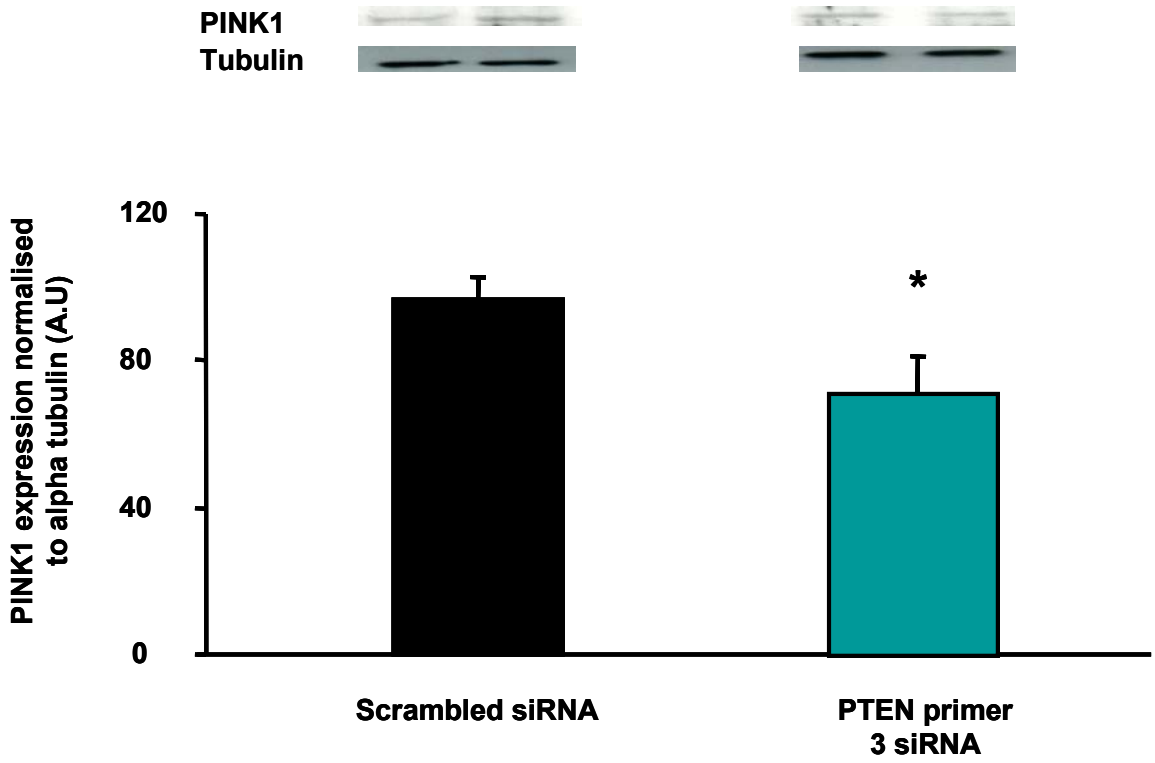

Figure 7.19: PTEN induced kinase 1 (PINK1) protein expression in H9c2 cells silenced for PTEN protein expression, expressed in arbitrary units (A.U). Statistical differences were assessed using Student's paired t-test, (*= <0.05), (n=3).

In summary, the PTEN protein expression was silenced by 82.4% in H9c2 cells, using siRNA specific for PTEN. Subsequent to hypoxia-reoxygenation the level of PI staining, LDH release and caspase 3 cleavage is increased. However, in cells treated with insulin (used as a positive control) measuring only the expression of caspase 3 cleavage was sufficient to detect a significant reduction in hypoxia-reoxygenation injury. Unexpectedly PTEN silencing in H9c2cells did not bestow protection against hypoxia-reoxygenation injury. In these cells a decrease in the expression of the mitochondrial pro survival kinase PINK1 was measured, which may in part explain the lack of protection against hypoxia-reoxygenation injury.

7.4 Discussion

As discussed in chapter 6, using KO models can be associated with a risk of adaptation or compensation to the knocked-out target. Small interfering RNA (siRNA) technology is widely employed as an alternative to KO models. SiRNA technology is based on a naturally occurring process and takes advantage of cellular transcription-translation mechanisms. Whereas, the DNA of the target remains unaltered, the mRNA levels are decreased, preventing the synthesis of the target protein. SiRNA can be effective within the timescale of several days, as opposed to genetic deletions which are typically present throughout the lifetime of the organism. Therefore, the application of siRNA technology may limit genetic adaptation and may provide a more beneficial tool for studying the role of PTEN inhibition on cardioprotection. Sugano *et al.,* 2005 have published positive studies using such techniques. For example, the administration of siRNA specific for the protein tyrosine phosphatase in vivo (to rats), can prevent SHP-1 activation and caused an increase in myocardial survival following ischaemia-reperfusion (Sugano et al., 2005). Owing to the limited number and specificity of tools to inhibit PTEN, it is common to observe the use of siRNA methods in published studies researching PTEN (Chang et al., 2006; Puri et al., 2007). For example PTEN was successfully silenced in mouse adipose tissue (Puri et al., 2007) and in HEK293 cells (Chang et al., 2006). The later study implicated apoptosis signalling with an increased activity of rho associated coiled coil protein kinase 1 (ROCK-1) and PTEN (Chang et al., 2006). In addition Butler *et al,* 2002 used antisense technology, which acts at the DNA level to prevent mRNA synthesis, to inhibit PTEN in a diabetic obese mouse (Butler et al., 2002). We planned to use siRNA as an alternative tool by which to reduce PTEN. Initially, this technology was optimised in H9c2 cells prior to studying the effects on hypoxia-reoxygenation injury. If these experiments had proved successful we could have potentially use this technique to asses the effects of PTEN reduction on whole hearts subjected to ischaemia-reperfusion injury.

7.4.1.1 Optimising protein silencing using siRNA

When trying to silence protein with siRNA the gene of interest, cell line and transfection technique must be considered. It was necessary to perform optimisation experiments with the aim of efficiently maximising protein knock down. Using scrambled (negative control), GAPDH (positive control) and PTEN siRNA, we aimed to obtain maximum protein knockdown. The effects of varying the transfection reagent type, concentration of transfection reagent and siRNA, cell number and duration of transfection. Three predesigned PTEN siRNA primers were purchased with a guarantee 1 out of these 3 primers would knockdown PTEN protein by 80%. Two out of the 3 primers were successful at silencing PTEN. We further optimised the use of one of the primers to maximise the level of protein knockdown.

It was shown that there was a dose response effect, associated with protein knockdown, whereby the more siRNA present the more protein silencing was observed. Conversely, these results indicate there were some off target effects of scrambled siRNA which affected PTEN protein expression. This is a common limitation of the approach, and we optimised protocols to keep this to a minimum. Furthermore, this work highlighted the importance of including a scrambled siRNA control in each experiment. Changes in protein expression were detected using Western blot techniques, which can be variable, as indicated by some large error bars in our results. This highlights another limitation of this assay and indicates the importance of including a number of replicates within each experiment.

The finalised method for siRNA-induced protein silencing in H9c2 cells is described below. H9c2 cells were transfected with GAPDH or PTEN siRNA at 50pmol and 30pmol (respectively) per well of a 12 well plate containing 4,000cells per well. siRNA was transfected using 3ul X-tremGene reagent to 1ng siRNA. Protein analysis was assessed 72h later conveying a significant ($p<0.001$) reduction in protein expression. The results were

compared to that of the scrambled siRNA control. PTEN expression was silenced by 82.4%, which conformed to the guaranteed knockdown of 80% or more when using siRNA primer constructs predesigned by Ambion, UK. Puri et al., 2007 knocked down PTEN by 70% in white adipose tissue incubated with 16nmol PTEN siRNA; which is comparable to our protocol and results (Puri et al., 2007). In addition, Chang et al., have used PTEN siRNA in HEK293 cells and successfully showed a reduction in the expression of PTEN. However, the authors of this work did not quantify the amount of protein reduction; instead they assessed this by measuring the level of phosphorylated AKT, which was increased by 56% (Chang et al., 2006).

7.4.1.2 Response to hypoxia-reoxygenation: optimising and measuring cell death.

The response of PTEN silencing in H9c2 cells subjected to hypoxia-reoxygenation injury was examined. It was hypothesised that reduced PTEN protein would protect against hypoxia-reoxygenation injury. To examine this we investigated ways of detecting cell death in our model of hypoxia-reoxygenation injury. Changes in propidium iodide staining, LDH release and caspase 3 cleavage were recorded.

Propidium iodide

Injured cells were assessed and localised following hypoxia-reoxygenation, by counting the percentage of adherent H9c2 cells staining positive for PI. It was observed that a significant ($p<0.005$) increase in PI staining occurred in cells subjected to hypoxia-reoxygenation. However, no differences were recorded between PTEN specific siRNA and scrambled siRNA. Similarly, the administration of insulin did not reduce the number of cells staining positive for PI. In these studies the variability of PI staining was large and the process of inducing siRNA into the H9c2 cells appears to increase PI staining. This variability may have been due to cell

type and or cell passage number. Each passage number correlates to the number of times the cell population has been sub cultured and is therefore an indicator of the total duration of cell culture and age. Older cells can be more susceptible to cell death (Hoffmann et al., 2001). It was noted that following reoxygenation a number of cells were dying and detaching from the well surface, and that this effect appeared random which may have been linked to uneven plating of the cells. Additionally, the hypoxia-reoxygenation protocol may have been too severe. These studies indicate that using PI as an indicator of cell death in H9c2 cells, following our hypoxia-reoxygenation protocol was not sufficient to detect changes in the level of cell death. Therefore, we aimed to find an alternative model for assessing cell vulnerability following hypoxia-reoxygenation in H9c2 cells.

LDH

LDH release was measured as an indicator of cell vulnerability following hypoxia-reoxygenation. It was observed that an increase in LDH release from cells subjected to hypoxia-reoxygenation occurred, however, this increase was not significantly different from cells maintained in normoxia. Additionally, H9c2 cells silenced for PTEN expression or cells stimulated with insulin showed no significance difference in LDH release. The absence of any differences in LDH release may have been due to an error in the experimental set up. The absorbance values obtained in our samples were lower than the 1.6units/ml LDH positive control supplied by the manufacturers of the LDH detection assay. Furthermore, the sample absorbance values were low, but still higher than the buffer control (culture media only, no cell contact). We have since found out that phenol red in cell culture media (like the media we used in reoxygenation) can interfere with this assay and should be avoided. Future work may include using a phenol free culture media to reoxygenate the cells in. Other groups have successfully used LDH release as an indicator of cell death however; it was not clear what media the samples were collected in (Potts et al., 2005; Taimor et al., 1999). However, to

save time we thought it was still necessary to explore an alternative mechanism for assessing cell death subsequent to hypoxia-reoxygenation.

Caspase 3 cleavage

Caspase 3 cleavage was measured using Western blot analysis, as an indicator of apoptosis and cell vulnerability following hypoxia-reoxygenation. A significant increase ($p<0.05$) in caspase 3 cleavage was observed, which was significantly reduced by the presence of insulin at reoxygenation ($p<0.01$). However, the expression of caspase 3 cleavage was not reduced in cells silenced for PTEN. Others have used caspase 3 cleavage as a method for detecting apoptosis (Stephanou et al., 2000; Hamacher-Brady et al., 2006b; Chang et al., 2006).

Cell death occurs after periods of hypoxia and reoxygenation, however, the importance of apoptosis and necrosis is still debated (Fliss and Gattinger, 1996; Ohno et al., 1998; Taimor et al., 1999; Lemasters et al., 2002; Potts et al., 2005). In this chapter, we did not address this issue, our aim was to measure cell death following hypoxia-reoxygenation. In the future it would be prudent to confirm the data obtained in a secondary model of cell vulnerability. We were not able to confirm our findings using either LDH or PI staining as these models had some practical limitations. Other groups have detected cell death using either Tunel staining for DNA fragmentation, Hoechst staining for chromatin condensation, Annexin V labelling of phosphatidylserine externalisation, immuno detection of cytochrome c and DNA laddering (Taimor et al., 1999; Hamacher-Brady et al., 2006a; Hamacher-Brady et al., 2006b). Alternatively, we could have used the trypan blue dye. Cellular exclusion of this dye can be used as an indicator of cell viability (Hansson and Schwartz, 1983). Future studies may entail using these methods to investigate the effects of PTEN silencing in H9c2 cells subjected to hypoxia-reoxygenation. Alternatively, we could try studying a different hypoxia-reoxygenation protocol, the method we used may be too severe, as a number of cells became rounded up and detached from the well surface following reoxygenation. Other groups studying hypoxia

reoxygenation in H9c2 cells have used quite different protocols. These ranging from 24hr hypoxia and 12hr reoxygenation, measuring Bax translocation as an end point (Hou and Hsu, 2005), to 6hr hypoxia and 12hr reoxygenation, measuring morphological changes and annexin V staining as an end point (Chen et al., 2002). Alternatively, a different myocardial cell line such as the HL1 cell line, which is an atrial myocyte cell line that maintains contractile properties (Claycomb et al., 1998), may respond differently to transfection of siRNA and hypoxia reoxygenation.

7.4.1.3 Investigating potential compensatory signalling effects in H9c2 cells silenced for PTEN expression.

By measuring caspase 3 cleavage we were not able to confirm our hypothesis, which predicted cells silenced for PTEN expression would have reduce cell death following hypoxia re-oxygenation. The reasons for this observation were explored. As shown in chapter 6, we showed that the myocardium from $PTEN^{+/-}$ mice was not protected against ischaemia-reperfusion injury. The myocardium from these mice express a reduced level of PINK1. This protein is a prosurvival kinase and drosophila with PINK1 mutations have muscle degeneration, altered mitochondrial morphology and reduced ATP levels. In the presence of paraquat, a complex I inhibitor, used to induce oxidative stress, these knockouts were less resistant to injury (Clark et al., 2006). The mechanisms for the protective effects of PINK1 is not fully understood, Clark et al., 2006 suggest this occurs by the phosphorylation and activation of Parkin. We investigated PINK1 protein expression in H9c2 cells silenced for PTEN protein expression. Our data indicates that cells silenced for PTEN have a small but significant ($p<0.05$) reduction in PINK1. This result is similar to the reduction in PINK1 expression in the $PTEN^{+/-}$ myocardium and may in part explain why we do not record protection when PTEN is reduced at the protein level. However, it should be noted that the individual blots used to assess this observation are illustrated in Figure 7.19 and are not the

best quality therefore; future work would include optimising the protocols according to the sample type and antibody used.

Previously, published studies have shown that in dopaminergic cells silenced for PINK1 expression using siRNA, PINK1 mRNA and protein levels were reduced by 87% and 80% respectively. And as a consequence, the authors of this work observed a 22% decrease in cell viability (Deng et al., 2005). Moreover, induction of oxidative stress using the pesticide and complex I inhibitor, rotenone, further reduced cell viability (Deng et al., 2005); indicating PINK1 reduction is associated with impaired response to oxidative damage and is required for survival. Inhibition of thioredoxin-interacting protein (Txnip) an endogenous inhibitor of thioredoxin, can decrease PTEN activity and increase, AKT activity and enhance insulin sensitivity in skeletal muscle. The authors of this work additionally observed impaired mitochondrial respiration in this tissue (Hui et al., 2008). In neuronal tissue, PINK1 deficiency results in changes in mitochondrial morphology and decreased mitochondrial membrane potential (Wood-Kaczmar et al., 2008). Collectively therefore, future work may include investigating the mitochondria morphology and function in our samples with reduced PTEN to confirm this idea. PINK1 was first identified in 2001 when PTEN was re-expressed in previously PTEN null cells. In this study PINK1 was one of the genes that was consequentially increased. Interestingly, an additional 72 genes were decreased as a result of PTEN re-expression (Unoki and Nakamura, 2001). These genes may provide novel targets for future survival studies.

In summary, PTEN expression was silenced in H9c2 cells by 82.4% using siRNA specific for PTEN. The cellular response of PTEN knockdown against hypoxia-reoxygenation injury was investigated. It was demonstrated that subsequent to hypoxia-reoxygenation, in cells transfected with scrambled siRNA, the level of PI staining, LDH release and caspase 3 cleavage was increased. However, only measuring the expression of caspase 3 cleavage

was sensitive enough to detect a significant reduction in injury when using insulin as a positive control. Unexpectedly, PTEN silencing in H9c2cells did not bestow protection against hypoxia-reoxygenation injury. A reduction in PINK1 expression in these hearts was observed, which may explain the lack of protection.

8 Chapter 8 –Future work and conclusions

8.1 Study limitations and future work

Measuring PTEN activity

Within this thesis we unsuccessfully attempted to optimise a PTEN ELISA assay for detecting PTEN lipid phosphatase activity in whole hearts. As discussed previously, in chapter 1, there are many ways in which PTEN activity can be reduced, for example changes to location, phosphorylation, oxidation, stability and degradation.(Connor et al., 2005; Trotman et al., 2007; Lai et al., 2007) Therefore, it is important to establish an additional reliable activity assay for use in tissue homogenates from whole hearts. Furthermore, we did not investigate the location of PTEN within the myocardial cell. Such investigation may lead to the identification of cytoplasmic versus membrane fractions of PTEN As described previously, in chapter 1, the location of PTEN has been linked to activity, for example cytoplasmic and nuclear PTEN has been associated with reduced PTEN lipid phosphatase activity (Wu et al., 2000a; Valiente et al., 2005; Lindsay et al., 2006).

Alternative PTEN inhibitors

Zinc and thioredoxin have been shown to reduce PTEN function in human airway epithelial cells (Wu et al., 2003; Meuillet et al., 2004). However, their specificity must be considered. In this study the effects of bpV(HOpic) on ischaemia-reperfusion injury were investigated. Additionally, other bisperoxvanadium compounds appear to have greater physiological effects with more specificity for PTEN, such as bpV(phen), bpV(pic) & VO-OHpic (Schmid et al., 2004; Rosivatz et al., 2006; Zhang et al., 2007).

The generation of tissue specific PTEN knockout mouse models may offer a greater degree of PTEN reduction sufficient to confer cardioprotection against ischaemia-reperfusion injury.

Such models are not commercially available and are difficult to obtain. Crackower *et al.,* in 2002 and 2008 have used cardiac specific PTEN mutant mice to show that inhibition of PTEN is associated with hypertrophy and reduced contractility. However, this group also showed that reduced PTEN confers protection against pressure overload, as shown by a reduction in the level of remodelling following permanent aortic banding (Crackower et al., 2002; Oudit et al., 2008). In 2009 Ruan *et al.,* published data showing that cardiac targeted PTEN inactivation protects against ischaemia-reperfusion injury (Ruan et al., 2009). In this study PTEN reduction was induced by daily injections of tamoxifan, which may be cardioprotective in its own right (Ek et al., 2008).

PTEN inhibition and the threshold for cardioprotection

We have shown that reducing PTEN function (by perfusing isolated C57BL/J6 mouse hearts with the PTEN inhibitor bpV(HOpic) and using the $PTEN^{+/-}$ myocardium) can reduce the threshold to IPC induced protection. Adenosine, bradykinin and insulin are pharmacological preconditioning mimetics that confer cardioprotection against ischaemia-reperfusion (Baines et al., 1999; Maddock et al., 2002; Bell and Yellon, 2003). Therefore, it was hypothesised that in the case of PTEN reduction, a lower concentration of preconditioning mimetics would be required to induce cardioprotection. Such future work would support the results from this thesis and further validate PTEN reduction for treating ischaemia-reperfusion injury.

Atorvastatin is cardioprotective, Mensah *et al.,* 2005 showed that treatment in rats for 3 days can protect the myocardium from ischaemia-reperfusion injury (Mensah et al., 2005). However, chronic treatment for 2 weeks abolished this protection, these results were attributed to an enhanced level of PTEN (Mensah et al., 2005). Many patients with CVD are prescribed statins (Ferdinandy et al., 2007) and therefore may be at risk of increased PTEN levels. Potentially, any therapy which increases the PI3K/AKT pathway may not be sufficient to confer protection against ischaemia-reperfusion injury in these patients. If this became

evident, we hypothesise that the reduction of PTEN levels may prevent the potential ablation of cardioprotection as a consequence of chronic atorvastatin treatment. To investigate this idea future work may involve studying the effects of chronic atorvastatin therapy in the presence of a PTEN inhibitor or in the $PTEN^{+/-}$ myocardium. For example, it may be predicted that myocardium from $PTEN^{+/-}$ mice subjected to chronic atorvastatin treatment may confer cardioprotection against ischaemia-reperfusion injury.

Cardioprotection and AKT activity

In this thesis the effects of reducing myocardial PTEN level was studied using a variety of models, and was associated with an increased level of phosphorylated AKT. However, these changes were not sufficient to confer protection against ischaemia-reperfusion injury. Firstly, the perfusion of mouse hearts on Langendorff apparatus, in the presence of an intraventricular balloon (as used in our studies) has been linked to inadvertent increases in phosphorylation of AKT (Stenslokken et al., 2009). The authors of this work suggest that this may be responsible for false positive results. This indicates that use of an alternative model of ischaemia-reperfusion, such as an in vivo model may be required.

Secondly, three AKT isofoms AKT exist, however, it is not clear what the significance of each isoform has on cardioprotection (Sasaoka et al., 2004). In 3T3-L1 cells insulin stimulates an increase in the phosphorylation of AKT1 and AKT2. Data suggests that SHIP2 may preferentially dephosphorylate and diminish AKT2 activity (not AKT1) in these cells (Sasaoka et al., 2004). There does appear to be different roles for different isofoms, and this may be tissue specific. It is unknown if there is any isoform of AKT that is preferentially affected by PTEN reduction and future work may include investigating this.

If AKT is activated and a down stream signalling factor is *inhibited*, reduced or mutated cardioprotection can be lost (Bell and Yellon, 2003). In isolated mouse hearts the activation of

the PI3K/AKT pathway with bradykinin conferred protection against ischaemia-reperfusion injury. This protection was associated with an increase in AKT and eNOS activity which was abolished in the presence of the PI3K inhibitor wortmanin. The authors of this work showed that in eNOS knockout mice bradykinin failed to confer protection even in the presence of enhanced phosphorylation of AKT (Bell and Yellon, 2003). This indicates that eNOS is required to confer protection downstream of the PI3K/AKT pathway. Future work may include investigating the expression and activity of other signalling pathways down stream of AKT in the $PTEN^{+/-}$ myocardium.

Finally, Nogueira *et al.,* 2008 discovered an 'Achilles' heel of AKT and show that the presence of AKT can be detrimental to the cell, in some situations. The authors of this work suggest that AKT activity increases the level of ROS by inhibiting ROS scavengers and therefore the survival is effected following ROS mediated apoptosis. Additionally, they show that cells lacking PTEN undergo an enhanced level of apoptosis (as measured by DAPI staining, in response to H_2O_2 (Nogueira et al., 2008). This work may have major implications when studying ischaemia-reperfusion injury and may explain why in our studies we were unable to show protection when the activation of AKT was enhanced. Future work using our models of PTEN knockdown may involve assessing cell death in response to increasing concentrations of H_2O_2.

<u>The role of PINK1 in cardioprotection</u>

The results from these studies indicate that the myocardium from $PTEN^{+/-}$ mice and H9c2 cells silenced for PTEN expression, have reduced expression of the mitochondrial pro survival kinase, PINK1. We did not have time to further validate PINK1 as a cardioprotective protein. Further work may include investigating PINK1 in ischaemia-reperfusion injury.

8.2 Conclusions

In this thesis, the hypothesis that PTEN inhibition would be cardioprotective against ischaemia-reperfusion injury, by reducing cell death, was investigated. A variety of experimental models were used (isolated hearts, isolated cardiomyocytes and cell lines) in which the PTEN level was reduced using different methods (using chemical inhibitors, PTEN haploinsufficient mouse and siRNA). Overall, in spite of AKT phosphorylation, PTEN reduction was not associated with an increased survival in any of our models. We attempted to investigate the reason for this but were unable to attain any conclusive explanations. Nonetheless, PTEN down regulation may favour a reduction in the threshold for cardioprotection (induced by other protective methods), which we demonstrated using ischaemic preconditioning. In conclusion, the data from the literature and this thesis indicate that PTEN inhibition may have implications for treating apoptotic related diseases such as ischaemia-reperfusion injury.

9 Publications

Research papers

- Siddall,H.K., Warrell,C.E., Davidson,S.M., Mocanu,M.M., and Yellon,D.M. (2008). Mitochondrial PINK1-A Novel Cardioprotective Kinase? Cardiovasc Drugs Ther.

- Siddall,H.K., Warrell,C.E., Yellon,D.M., and Mocanu,M.M. (2008). Ischaemia-reperfusion injury and cardioprotection: investigating PTEN, the phosphatase that negatively regulates PI3K, using a congenital model of PTEN haploinsufficiency. Basic Res Cardiol.

Abstracts

British Society for Cardiovascular Research - Autumn meeting – Bristol 15-16th September 2008

- Mitochondrial PINK1 (PTEN Induced Kinase1): a novel cardioprotective kinase?

XXVIII European section of the International Society for Heart Research, Athens, Greece, 28th-31st May 2008

- Siddall,H.K., Davidson,S.M., Mocanu,M.M., and Yellon,D.M. (2008c). Silencing PTEN, a negative regulator of the PI3K/AKT pathway, is not sufficient to confer protection against simulated ischaemia and reperfusion. Journal of Molecular and Cellular Cardiology *44*, 756.

- Siddall,H.K., Mocanu,M.M., and Yellon,D.M. (2008d). Cardioprotection from ischaemia-reperfusion injury: Dissecting the PI3K/AKT pathway with chemical inhibition of PTEN. Journal of Molecular and Cellular Cardiology *44*, 755-756.

Cold Spring Harbor meeting – PTEN/PI3K pathways in health and disease – NY USA – 5th-9th March 2008

- Title = Strategies to confer cardioprotection from ischaemia-reperfusion injury: Dissecting the PI3K/AKT pathway with genetic silencing and chemical inhibition of PTEN

XIX World Congress – International Society for Heart research 2007 - Italy 22nd-25th June 2007

- Siddall,H.K., Mocanu,M.M., and Yellon,D.M. (2007). Pten haploinsufficiency is not able to protect the myocardium against ischaemia reperfusion injury. Journal of Molecular and Cellular Cardiology *42*, S207-S208.

10 References

Reference List

1. Adrain,C., Creagh,E.M., and Martin,S.J. (2001). Apoptosis-associated release of Smac/DIABLO from mitochondria requires active caspases and is blocked by Bcl-2. EMBO J *20*, 6627-6636.

2. Al Khouri,A.M., Ma,Y., Togo,S.H., Williams,S., and Mustelin,T. (2005). Cooperative phosphorylation of the tumor suppressor phosphatase and tensin homologue (PTEN) by casein kinases and glycogen synthase kinase 3beta. J Biol. Chem. *280*, 35195-35202.

3. Alessi,D.R., Andjelkovic,M., Caudwell,B., Cron,P., Morrice,N., Cohen,P., and Hemmings,B.A. (1996). Mechanism of activation of protein kinase B by insulin and IGF-1. EMBO J *15*, 6541-6551.

4. Allender,S., Foster,C., Scarborough,P., and Rayner,M. (2007). The burden of physical activity-related ill health in the UK. J Epidemiol. Community Health *61*, 344-348.

5. Arbustini,E., Brega,A., and Narula,J. (2008). Ultrastructural definition of apoptosis in heart failure. Heart Fail. Rev. *13*, 121-135.

6. Arevalo,M.A. and Rodriguez-Tebar,A. (2006). Activation of casein kinase II and inhibition of phosphatase and tensin homologue deleted on chromosome 10 phosphatase by nerve growth factor/p75NTR inhibit glycogen synthase kinase-3beta and stimulate axonal growth. Mol. Biol. Cell *17*, 3369-3377.

7. Argaud,L., Gateau-Roesch,O., Augeul,L., Couture-Lepetit,E., Loufouat,J., Gomez,L., Robert,D., and Ovize,M. (2008). Increased mitochondrial calcium coexists with decreased reperfusion injury in postconditioned (but not preconditioned) hearts. Am J Physiol Heart Circ Physiol *294*, H386-H391.

8. Argaud,L., Gateau-Roesch,O., Chalabreysse,L., Gomez,L., Loufouat,J., Thivolet-Bejui,F., Robert,D., and Ovize,M. (2004). Preconditioning delays Ca2+-induced mitochondrial permeability transition. Cardiovasc Res *61*, 115-122.

9. Argaud,L., Gateau-Roesch,O., Muntean,D., Chalabreysse,L., Loufouat,J., Robert,D., and Ovize,M. (2005a). Specific inhibition of the mitochondrial permeability transition prevents lethal reperfusion injury. J Mol. Cell Cardiol. *38*, 367-374.

10. Argaud,L., Gateau-Roesch,O., Raisky,O., Loufouat,J., Robert,D., and Ovize,M. (2005b). Postconditioning inhibits mitochondrial permeability transition. Circulation *111*, 194-197.

11. Ashkenazi,A. (2002). Targeting death and decoy receptors of the tumour-necrosis factor superfamily. Nat Rev Cancer *2*, 420-430.

12. Auchampach,J.A., Grover,G.J., and Gross,G.J. (1992). Blockade of ischaemic preconditioning in dogs by the novel ATP dependent potassium channel antagonist sodium 5-hydroxydecanoate. Cardiovasc Res *26*, 1054-1062.

13. Baines,C.P., Goto,M., and Downey,J.M. (1997). Oxygen radicals released during ischemic preconditioning contribute to cardioprotection in the rabbit myocardium. J Mol. Cell Cardiol. *29*, 207-216.

14. Baines,C.P., Kaiser,R.A., Purcell,N.H., Blair,N.S., Osinska,H., Hambleton,M.A., Brunskill,E.W., Sayen,M.R., Gottlieb,R.A., Dorn,G.W., Robbins,J., and Molkentin,J.D. (2005). Loss of cyclophilin D reveals a critical role for mitochondrial permeability transition in cell death. Nature *434*, 658-662.

15. Baines,C.P., Kaiser,R.A., Sheiko,T., Craigen,W.J., and Molkentin,J.D. (2007). Voltage-dependent anion channels are dispensable for mitochondrial-dependent cell death. Nat Cell Biol. *9*, 550-555.

16. Baines,C.P., Wang,L., Cohen,M.V., and Downey,J.M. (1999). Myocardial protection by insulin is dependent on phospatidylinositol 3-kinase but not protein kinase C or KATP channels in the isolated rabbit heart. Basic Res Cardiol. *94*, 188-198.

17. Baker,S.J. (2007). PTEN enters the nuclear age. Cell *128*, 25-28.

18. Banga,N.R., Homer-Vanniasinkam,S., Graham,A., Al Mukhtar,A., White,S.A., and Prasad,K.R. (2005). Ischaemic preconditioning in transplantation and major resection of the liver. Br J Surg. *92*, 528-538.

19. Bao,W., Hu,E., Tao,L., Boyce,R., Mirabile,R., Thudium,D.T., Ma,X.L., Willette,R.N., and Yue,T.L. (2004). Inhibition of Rho-kinase protects the heart against ischemia/reperfusion injury. Cardiovasc Res *61*, 548-558.

20. Bayascas,J.R., Leslie,N.R., Parsons,R., Fleming,S., and Alessi,D.R. (2005). Hypomorphic mutation of PDK1 suppresses tumorigenesis in PTEN(+/-) mice. Curr. Biol. *15*, 1839-1846.

21. Becker,L.B. (2004). New concepts in reactive oxygen species and cardiovascular reperfusion physiology. Cardiovasc Res *61*, 461-470.

22. Bell,R.M., Maddock,H.L., and Yellon,D.M. (2003). The cardioprotective and mitochondrial depolarising properties of exogenous nitric oxide in mouse heart. Cardiovasc Res *57*, 405-415.

23. Bell,R.M. and Yellon,D.M. (2001). The contribution of endothelial nitric oxide synthase to early ischaemic preconditioning: the lowering of the preconditioning threshold. An investigation in eNOS knockout mice. Cardiovasc. Res. *52*, 274-280.

24. Bell,R.M. and Yellon,D.M. (2003). Bradykinin limits infarction when administered as an adjunct to reperfusion in mouse heart: the role of PI3K, Akt and eNOS. J. Mol. Cell Cardiol. *35*, 185-193.

25. Borchard,U., Greeff,K., Hafner,D., Noack,E., and Rojsathaporn,K. (1981). Effects of vanadate on heart and circulation. J Cardiovasc. Pharmacol. *3*, 510-521.

26. Brognard,J., Sierecki,E., Gao,T., and Newton,A.C. (2007). PHLPP and a second isoform, PHLPP2, differentially attenuate the amplitude of Akt signaling by regulating distinct Akt isoforms. Mol. Cell *25*, 917-931.

27. Burnette,W.N. (1981). "Western blotting": electrophoretic transfer of proteins from sodium dodecyl sulfate--polyacrylamide gels to unmodified nitrocellulose and radiographic detection with antibody and radioiodinated protein A. Anal. Biochem. *112*, 195-203.

28. Butler,M., McKay,R.A., Popoff,I.J., Gaarde,W.A., Witchell,D., Murray,S.F., Dean,N.M., Bhanot,S., and Monia,B.P. (2002). Specific inhibition of PTEN expression reverses hyperglycemia in diabetic mice. Diabetes *51*, 1028-1034.

29. Cai,Z. and Semenza,G.L. (2005). PTEN activity is modulated during ischemia and reperfusion: involvement in the induction and decay of preconditioning. Circ. Res. *97*, 1351-1359.

30. Cai,Z., Zhong,H., Bosch-Marce,M., Fox-Talbot,K., Wang,L., Wei,C., Trush,M.A., and Semenza,G.L. (2008a). Complete loss of ischaemic preconditioning-induced cardioprotection in mice with partial deficiency of HIF-1 alpha. Cardiovasc Res *77*, 463-470.

31. Cai,Z.P., Shen,Z., Van Kaer,L., and Becker,L.C. (2008b). Ischemic preconditioning-induced cardioprotection is lost in mice with immunoproteasome subunit low molecular mass polypeptide-2 deficiency. FASEB J.

32. Campbell,R.B., Liu,F., and Ross,A.H. (2003). Allosteric activation of PTEN phosphatase by phosphatidylinositol 4,5-bisphosphate. J Biol. Chem. *278*, 33617-33620.

33. Cao,J., Schulte,J., Knight,A., Leslie,N.R., Zagozdzon,A., Bronson,R., Manevich,Y., Beeson,C., and Neumann,C.A. (2009). Prdx1 inhibits tumorigenesis via regulating PTEN/AKT activity. EMBO J *28*, 1505-1517.

34. Caplen,N.J., Parrish,S., Imani,F., Fire,A., and Morgan,R.A. (2001). Specific inhibition of gene expression by small double-stranded RNAs in invertebrate and vertebrate systems. Proc. Natl. Acad. Sci U. S. A *98*, 9742-9747.

35. Carpten,J.D., Faber,A.L., Horn,C., Donoho,G.P., Briggs,S.L., Robbins,C.M., Hostetter,G., Boguslawski,S., Moses,T.Y., Savage,S., Uhlik,M., Lin,A., Du,J., Qian,Y.W., Zeckner,D.J., Tucker-Kellogg,G., Touchman,J., Patel,K., Mousses,S., Bittner,M., Schevitz,R., Lai,M.H., Blanchard,K.L., and Thomas,J.E. (2007). A transforming mutation in the pleckstrin homology domain of AKT1 in cancer. Nature *448*, 439-444.

36. Chang,J., Xie,M., Shah,V.R., Schneider,M.D., Entman,M.L., Wei,L., and Schwartz,R.J. (2006). Activation of Rho-associated coiled-coil protein kinase 1 (ROCK-1) by caspase-3 cleavage plays an essential role in cardiac myocyte apoptosis. Proc. Natl. Acad. Sci. U. S. A.

37. Chappell,W.H., Green,T.D., Spengeman,J.D., McCubrey,J.A., Akula,S.M., and Bertrand,F.E. (2005). Increased protein expression of the PTEN tumor suppressor in the presence of constitutively active Notch-1. Cell Cycle *4*, 1389-1395.

38. Chen,H., Ishii,A., Wong,W.K., Chen,L.B., and Lo,S.H. (2000). Molecular characterization of human tensin. Biochem. J *351 Pt 2*, 403-411.

39. Chen,H.W., Chien,C.T., Yu,S.L., Lee,Y.T., and Chen,W.J. (2002). Cyclosporine A regulate oxidative stress-induced apoptosis in cardiomyocytes: mechanisms via ROS generation, iNOS and Hsp70. Br J Pharmacol *137*, 771-781.

40. Chen,Z., Chua,C.C., Ho,Y.S., Hamdy,R.C., and Chua,B.H. (2001). Overexpression of Bcl-2 attenuates apoptosis and protects against myocardial I/R injury in transgenic mice. Am J Physiol Heart Circ Physiol *280*, H2313-H2320.

41. Chi,Y., Zhou,B., Wang,W.Q., Chung,S.K., Kwon,Y.U., Ahn,Y.H., Chang,Y.T., Tsujishita,Y., Hurley,J.H., and Zhang,Z.Y. (2004). Comparative mechanistic and substrate specificity study of inositol polyphosphate 5-phosphatase Schizosaccharomyces pombe Synaptojanin and SHIP2. J. Biol. Chem. *279*, 44987-44995.

42. Chipuk,J.E., Kuwana,T., Bouchier-Hayes,L., Droin,N.M., Newmeyer,D.D., Schuler,M., and Green,D.R. (2004). Direct activation of Bax by p53 mediates mitochondrial membrane permeabilization and apoptosis. Science *303*, 1010-1014.

43. Chung,J.H., Ginn-Pease,M.E., and Eng,C. (2005). Phosphatase and Tensin Homologue Deleted on Chromosome 10 (PTEN) Has Nuclear Localization Signal-Like Sequences for Nuclear Import Mediated by Major Vault Protein. Cancer Res *65*, 4108-4116.

44. Clark,I.E., Dodson,M.W., Jiang,C., Cao,J.H., Huh,J.R., Seol,J.H., Yoo,S.J., Hay,B.A., and Guo,M. (2006). Drosophila pink1 is required for mitochondrial function and interacts genetically with parkin. Nature *441*, 1162-1166.

45. Clarke,S.J., McStay,G.P., and Halestrap,A.P. (2002). Sanglifehrin A acts as a potent inhibitor of the mitochondrial permeability transition and reperfusion injury of the heart by binding to cyclophilin-D at a different site from cyclosporin A. J Biol. Chem. *277*, 34793-34799.

46. Claycomb,W.C., Lanson,N.A., Jr., Stallworth,B.S., Egeland,D.B., Delcarpio,J.B., Bahinski,A., and Izzo,N.J., Jr. (1998). HL-1 cells: a cardiac muscle cell line that contracts and retains phenotypic characteristics of the adult cardiomyocyte. Proc. Natl. Acad. Sci U. S. A *95*, 2979-2984.

47. Cleveland,J.C., Jr., Meldrum,D.R., Rowland,R.T., Cain,B.S., Meng,X., Gamboni-Robertson,F., Banerjee,A., and Harken,A.H. (1997). Ischemic preconditioning of human myocardium: protein kinase C mediates a permissive role for alpha 1-adrenoceptors. Am J Physiol Heart Circ Physiol *273*, H902-H908.

48. Climent,F., Bartrons,R., Pons,G., and Carreras,J. (1981). Effect of vanadate on phosphoryl transfer enzymes involved in glucose metabolism. Biochem. Biophys. Res Commun. *101*, 570-576.

49. Cohen,M.V. and Downey,J.M. (2008). Adenosine: trigger and mediator of cardioprotection. Basic Res Cardiol. *103*, 203-215.

50. Communal,C., Sumandea,M., de Tombe,P., Narula,J., Solaro,R.J., and Hajjar,R.J. (2002). Functional consequences of caspase activation in cardiac myocytes. Proc. Natl. Acad. Sci U. S. A *99*, 6252-6256.

51. Connor,K.M., Subbaram,S., Regan,K.J., Nelson,K.K., Mazurkiewicz,J.E., Bartholomew,P.J., Aplin,A.E., Tai,Y.T., Aguirre-Ghiso,J., Flores,S.C., and Melendez,J.A. (2005). Mitochondrial H2O2 regulates the angiogenic phenotype via PTEN oxidation. J. Biol. Chem. *280*, 16916-16924.

52. Corvera,J.S., Zhao,Z.Q., Schmarkey,L.S., Katzmark,S.L., Budde,J.M., Morris,C.D., Ehring,T., Guyton,R.A., and Vinten-Johansen,J. (2003). Optimal dose and mode of delivery of Na+/H+ exchange-1 inhibitor are critical for reducing postsurgical ischemia-reperfusion injury. Ann. Thorac. Surg. *76*, 1614-1622.

53. Couzin,J. (2006). Nobel Prize in Physiology or Medicine. Method to silence genes earns loud praise. Science *314*, 34.

54. Crackower,M.A., Oudit,G.Y., Kozieradzki,I., Sarao,R., Sun,H., Sasaki,T., Hirsch,E., Suzuki,A., Shioi,T., Irie-Sasaki,J., Sah,R., Cheng,H.Y., Rybin,V.O., Lembo,G., Fratta,L., Oliveira-dos-Santos,A.J., Benovic,J.L., Kahn,C.R., Izumo,S., Steinberg,S.F., Wymann,M.P., Backx,P.H., and Penninger,J.M. (2002). Regulation of myocardial contractility and cell size by distinct PI3K-PTEN signaling pathways. Cell *110*, 737-749.

55. Crompton,M. (1999). The mitochondrial permeability transition pore and its role in cell death. Biochem. J. *341*, 233-249.

56. Crompton,M., Costi,A., and Hayat,L. (1987). Evidence for the presence of a reversible Ca2+-dependent pore activated by oxidative stress in heart mitochondria. Biochem. J *245*, 915-918.

57. Danial,N.N. and Korsmeyer,S.J. (2004). Cell death: critical control points. Cell *116*, 205-219.

58. Dauterman,K. and Topol,E. (2002). Optimal treatment and current situation in reperfusion after thrombolysis for acute myocardial infarction. Ann. Med. *34*, 514-522.

59. Davidson,S.M., Hausenloy,D., Duchen,M.R., and Yellon,D.M. (2006). Signalling via the reperfusion injury signalling kinase (RISK) pathway links closure of the mitochondrial permeability transition pore to cardioprotection. Int. J. Biochem. Cell Biol. *38*, 414-419.

60. Davidson,S.M., Yellon,D., and Duchen,M.R. (2007). Assessing mitochondrial potential, calcium, and redox state in isolated mammalian cells using confocal microscopy. Methods Mol. Biol. *372*, 421-430.

61. DeKroon,R., Robinette,J.B., Hjelmeland,A.B., Wiggins,E., Blackwell,M., Mihovilovic,M., Fujii,M., York,J., Hart,J., Kontos,C., Rich,J., and Strittmatter,W.J. (2006). APOE4-VLDL Inhibits the HDL-Activated Phosphatidylinositol 3-Kinase/Akt Pathway via the Phosphoinositol Phosphatase SHIP2. Circ Res *99*, 829-836.

62. Deng,H., Jankovic,J., Guo,Y., Xie,W., and Le,W. (2005). Small interfering RNA targeting the PINK1 induces apoptosis in dopaminergic cells SH-SY5Y. Biochem. Biophys. Res Commun. *337*, 1133-1138.

63. Du,C., Fang,M., Li,Y., Li,L., and Wang,X. (2000). Smac, a mitochondrial protein that promotes cytochrome c-dependent caspase activation by eliminating IAP inhibition. Cell *102*, 33-42.

64. Duchen,M.R., Verkhratsky,A., and Muallem,S. (2008). Mitochondria and calcium in health and disease. Cell Calcium *44*, 1-5.

65. Eckle,T., Grenz,A., Kohler,D., Redel,A., Falk,M., Rolauffs,B., Osswald,H., Kehl,F., and Eltzschig,H.K. (2006). Systematic evaluation of a novel model for cardiac ischemic preconditioning in mice. Am. J. Physiol Heart Circ. Physiol.

66. Efthymiou,C.A., Mocanu,M.M., and Yellon,D.M. (2005). Atorvastatin and myocardial reperfusion injury: new pleiotropic effect implicating multiple prosurvival signaling. J. Cardiovasc. Pharmacol. *45*, 247-252.

67. Eickholt,B.J., Ahmed,A.I., Davies,M., Papakonstanti,E.A., Pearce,W., Starkey,M.L., Bilancio,A., Need,A.C., Smith,A.J., Hall,S.M., Hamers,F.P., Giese,K.P., Bradbury,E.J., and Vanhaesebroeck,B. (2007). Control of axonal growth and regeneration of sensory neurons by the p110delta PI 3-kinase. PLoS ONE. *2*, e869.

68. Eipel,C., Schuett,H., Glawe,C., Bordel,R., Menger,M.D., and Vollmar,B. (2005). Pifithrin-alpha induced p53 inhibition does not affect liver regeneration after partial hepatectomy in mice. J. Hepatol. *43*, 829-835.

69. Ek,R.O., Yildiz,Y., Cecen,S., Yenisey,C., and Kavak,T. (2008). Effects of tamoxifen on myocardial ischemia-reperfusion injury model in ovariectomized rats. Mol. Cell Biochem. *308*, 227-235.

70. Feng,J., Schaus,B.J., Fallavollita,J.A., Lee,T.C., and Canty,J.M., Jr. (2001). Preload induces troponin I degradation independently of myocardial ischemia. Circulation *103*, 2035-2037.

71. Fenton,R.A., Dickson,E.W., and Dobson,J.G., Jr. (2005). Inhibition of phosphatase activity enhances preconditioning and limits cell death in the ischemic/reperfused aged rat heart. Life Sci *77*, 3375-3388.

72. Ferdinandy,P., Schulz,R., and Baxter,G.F. (2007). Interaction of cardiovascular risk factors with myocardial ischemia/reperfusion injury, preconditioning, and postconditioning. Pharmacol Rev. *59*, 418-458.

73. Ferrandi,C., Ballerio,R., Gaillard,P., Giachetti,C., Carboni,S., Vitte,P.A., Gotteland,J.P., and Cirillo,R. (2004). Inhibition of c-Jun N-terminal kinase decreases cardiomyocyte apoptosis and infarct size after myocardial ischemia and reperfusion in anaesthetized rats. Br J Pharmacol *142*, 953-960.

74. Fliss,H. and Gattinger,D. (1996). Apoptosis in ischemic and reperfused rat myocardium. Circ Res *79*, 949-956.

75. Fuller,J.H., Stevens,L.K., and Wang,S.L. (2001). Risk factors for cardiovascular mortality and morbidity: the WHO Mutinational Study of Vascular Disease in Diabetes. Diabetologia *44 Suppl 2*, S54-S64.

76. Gao,L., Laude,K., and Cai,H. (2008a). Mitochondrial pathophysiology, reactive oxygen species, and cardiovascular diseases. Vet. Clin. North Am Small Anim Pract. *38*, 137-55, vi.

77. Gao,Q., Pan,H.Y., Qiu,S., Lu,Y., Bruce,I.C., Luo,J.H., and Xia,Q. (2006). Atractyloside and 5-hydroxydecanoate block the protective effect of puerarin in isolated rat heart. Life Sci *79*, 217-224.

78. Gao,T., Brognard,J., and Newton,A.C. (2008b). The phosphatase PHLPP controls the cellular levels of protein kinase C. J Biol. Chem. *283*, 6300-6311.

79. Gao,T., Furnari,F., and Newton,A.C. (2005a). PHLPP: a phosphatase that directly dephosphorylates Akt, promotes apoptosis, and suppresses tumor growth. Mol. Cell *18*, 13-24.

80. Gao,T., Furnari,F., and Newton,A.C. (2005b). PHLPP: a phosphatase that directly dephosphorylates Akt, promotes apoptosis, and suppresses tumor growth. Mol. Cell *18*, 13-24.

81. Gil,A., Andres-Pons,A., Fernandez,E., Valiente,M., Torres,J., Cervera,J., and Pulido,R. (2006). Nuclear Localization of PTEN by a Ran-dependent Mechanism Enhances Apoptosis: Involvement of an N-Terminal Nuclear Localization Domain and Multiple Nuclear Exclusion Motifs. Mol. Biol. Cell.

82. Gimm,O., Perren,A., Weng,L.P., Marsh,D.J., Yeh,J.J., Ziebold,U., Gil,E., Hinze,R., Delbridge,L., Lees,J.A., Mutter,G.L., Robinson,B.G., Komminoth,P., Dralle,H., and Eng,C. (2000). Differential nuclear and cytoplasmic expression of PTEN in normal thyroid tissue, and benign and malignant epithelial thyroid tumors. Am J Pathol. *156*, 1693-1700.

83. Griffiths,E.J. and Halestrap,A.P. (1995). Mitochondrial non-specific pores remain closed during cardiac ischaemia, but open upon reperfusion. Biochem. J *307 (Pt 1)*, 93-98.

84. Gross,E.R., Hsu,A.K., and Gross,G.J. (2008). Delayed cardioprotection afforded by the glycogen synthase kinase 3 inhibitor SB-216763 occurs via a. Am J Physiol Heart Circ Physiol *294*, H1497-H1500.

85. Gross,E.R. and Gross,G.J. (2006). Ligand triggers of classical preconditioning and postconditioning. Cardiovascular Research *70*, 212-221.

86. Gross,E.R., Hsu,A.K., and Gross,G.J. (2006). The JAK/STAT pathway is essential for opioid-induced cardioprotection: JAK2 as a mediator of STAT3, Akt, and GSK-3beta. Am J Physiol Heart Circ Physiol *291*, H827-H834.

87. Gurusamy,N., Lekli,I., Gherghiceanu,M., Popescu,L.M., and Das,D.K. (2009). BAG-1 induces autophagy for cardiac cell survival. Autophagy. *5*.

88. Haghikia,A. and Hilfiker-Kleiner,D. (2009). MiRNA-21: a key to controlling the cardiac fibroblast compartment? Cardiovasc Res *82*, 1-3.

89. Halestrap,A.P. (2009). What is the mitochondrial permeability transition pore? J Mol. Cell Cardiol.

90. Halestrap,A.P., Clarke,S.J., and Javadov,S.A. (2004). Mitochondrial permeability transition pore opening during myocardial reperfusion--a target for cardioprotection. Cardiovasc Res *61*, 372-385.

91. Halestrap,A.P., Woodfield,K.Y., and Connern,C.P. (1997). Oxidative stress, thiol reagents, and membrane potential modulate the mitochondrial permeability transition by affecting nucleotide binding to the adenine nucleotide translocase. J Biol. Chem. *272*, 3346-3354.

92. Hamacher-Brady,A., Brady,N.R., and Gottlieb,R.A. (2006a). Enhancing macroautophagy protects against ischemia/reperfusion injury in cardiac myocytes. J Biol. Chem. *281*, 29776-29787.

93. Hamacher-Brady,A., Brady,N.R., and Gottlieb,R.A. (2006b). The interplay between pro-death and pro-survival signaling pathways in myocardial ischemia/reperfusion injury: apoptosis meets autophagy. Cardiovasc Drugs Ther. *20*, 445-462.

94. Hamacher-Brady,A., Brady,N.R., Logue,S.E., Sayen,M.R., Jinno,M., Kirshenbaum,L.A., Gottlieb,R.A., and Gustafsson,A.B. (2007). Response to myocardial ischemia/reperfusion injury involves Bnip3 and autophagy. Cell Death Differ. *14*, 146-157.

95. Hamada,K., Sasaki,T., Koni,P.A., Natsui,M., Kishimoto,H., Sasaki,J., Yajima,N., Horie,Y., Hasegawa,G., Naito,M., Miyazaki,J., Suda,T., Itoh,H., Nakao,K., Mak,T.W., Nakano,T., and Suzuki,A. (2005). The PTEN/PI3K pathway governs normal vascular development and tumor angiogenesis. Genes Dev. *19*, 2054-2065.

96. Hamid,S.A., Bower,H.S., and Baxter,G.F. (2007). Rho kinase activation plays a major role as a mediator of irreversible injury in reperfused myocardium. Am J Physiol Heart Circ Physiol *292*, H2598-H2606.

97. Hansson,G.K. and Schwartz,S.M. (1983). Evidence for cell death in the vascular endothelium in vivo and in vitro. Am J Pathol. *112*, 278-286.

98. Hausenloy,D., Wynne,A., Duchen,M., and Yellon,D. (2004a). Transient mitochondrial permeability transition pore opening mediates preconditioning-induced protection. Circulation *109*, 1714-1717.

99. Hausenloy,D.J., Duchen,M.R., and Yellon,D.M. (2003). Inhibiting mitochondrial permeability transition pore opening at reperfusion protects against ischaemia-reperfusion injury. Cardiovasc Res *60*, 617-625.

100. Hausenloy,D.J., Maddock,H.L., Baxter,G.F., and Yellon,D.M. (2002). Inhibiting mitochondrial permeability transition pore opening: a new paradigm for myocardial preconditioning? Cardiovasc Res *55*, 534-543.

101. Hausenloy,D.J., Mocanu,M.M., and Yellon,D.M. (2004b). Cross-talk between the survival kinases during early reperfusion: its contribution to ischemic preconditioning. Cardiovasc. Res. *63*, 305-312.

102. Hausenloy,D.J., Tsang,A., and Yellon,D.M. (2005). The reperfusion injury salvage kinase pathway: a common target for both ischemic preconditioning and postconditioning. Trends Cardiovasc. Med. *15*, 69-75.

103. Hausenloy,D.J. and Yellon,D.M. (2004a). New directions for protecting the heart against ischaemia-reperfusion injury: targeting the Reperfusion Injury Salvage Kinase (RISK)-pathway. Cardiovasc Res *61*, 448-460.

104. Hausenloy,D.J. and Yellon,D.M. (2004b). New directions for protecting the heart against ischaemia-reperfusion injury: targeting the Reperfusion Injury Salvage Kinase (RISK)-pathway. Cardiovascular Research *61*, 448-460.

105. Hawkins,P.T. and Stephens,L.R. (2007). PI3Kgamma is a key regulator of inflammatory responses and cardiovascular homeostasis. Science *318*, 64-66.

106. Headrick,J.P., Peart,J., Hack,B., Flood,A., and Matherne,G.P. (2001). Functional properties and responses to ischaemia-reperfusion in Langendorff perfused mouse heart. Exp. Physiol *86*, 703-716.

107. Hennessy,B.T., Smith,D.L., Ram,P.T., Lu,Y., and Mills,G.B. (2005). Exploiting the PI3K/AKT pathway for cancer drug discovery. Nat. Rev. Drug Discov. *4*, 988-1004.

108. Heron-Milhavet,L., Franckhauser,C., Rana,V., Berthenet,C., Fisher,D., Hemmings,B.A., Fernandez,A., and Lamb,N.J. (2006). Only Akt1 is required for proliferation, while Akt2 promotes cell cycle exit through p21 binding. Mol. Cell Biol. *26*, 8267-8280.

109. Hoffmann,J., Haendeler,J., Aicher,A., Rossig,L., Vasa,M., Zeiher,A.M., and Dimmeler,S. (2001). Aging enhances the sensitivity of endothelial cells toward apoptotic stimuli: important role of nitric oxide. Circ Res *89*, 709-715.

110. Hori,H., Sasaoka,T., Ishihara,H., Wada,T., Murakami,S., Ishiki,M., and Kobayashi,M. (2002). Association of SH2-containing inositol phosphatase 2 with the insulin resistance of diabetic db/db mice. Diabetes *51*, 2387-2394.

111. Hou,Q. and Hsu,Y.T. (2005). Bax translocates from cytosol to mitochondria in cardiac cells during apoptosis: development of a GFP-Bax-stable H9c2 cell line for apoptosis analysis. Am J Physiol Heart Circ Physiol *289*, H477-H487.

112. Huang,X., Wullschleger,S., Shpiro,N., McGuire,V.A., Sakamoto,K., Woods,Y.L., McBurnie,W., Fleming,S., and Alessi,D.R. (2008). Important role of the LKB1-AMPK pathway in suppressing tumorigenesis in PTEN-deficient mice. Biochem. J *412*, 211-221.

113. Hui,S.T., Andres,A.M., Miller,A.K., Spann,N.J., Potter,D.W., Post,N.M., Chen,A.Z., Sachithanantham,S., Jung,D.Y., Kim,J.K., and Davis,R.A. (2008). Txnip balances metabolic and growth signaling via PTEN disulfide reduction. Proc. Natl. Acad. Sci U. S. A *105*, 3921-3926.

114. Huisamen,B. (2003). Protein kinase B in the diabetic heart. Mol. Cell Biochem. *249*, 31-38.

115. Hunter,D.R. and Haworth,R.A. (1979). The Ca2+-induced membrane transition in mitochondria. I. The protective mechanisms. Arch. Biochem. Biophys. *195*, 453-459.

116. Ijuin,T. and Takenawa,T. (2003). SKIP Negatively Regulates Insulin-Induced GLUT4 Translocation and Membrane Ruffle Formation. Mol. Cell. Biol. *23*, 1209-1220.

117. Ishihara,H., Sasaoka,T., Kagawa,S., Murakami,S., Fukui,K., Kawagishi,Y., Yamazaki,K., Sato,A., Iwata,M., Urakaze,M., Ishiki,M., Wada,T., Yaguchi,S., Tsuneki,H., Kimura,I., and Kobayashi,M. (2003). Association of the polymorphisms in

the 5'-untranslated region of PTEN gene with type 2 diabetes in a Japanese population. FEBS Lett. *554*, 450-454.

118. Jenkins,D.P., Pugsley,W.B., Alkhulaifi,A.M., Kemp,M., Hooper,J., and Yellon,D.M. (1997). Ischaemic preconditioning reduces troponin T release in patients undergoing coronary artery bypass surgery. Heart *77*, 314-318.

119. Jeremias,I., Kupatt,C., Martin-Villalba,A., Habazettl,H., Schenkel,J., Boekstegers,P., and Debatin,K.M. (2000). Involvement of CD95/Apo1/Fas in cell death after myocardial ischemia. Circulation *102*, 915-920.

120. Jonassen,A.K., Mjos,O.D., and Sack,M.N. (2004). p70s6 kinase is a functional target of insulin activated Akt cell-survival signaling. Biochem. Biophys. Res Commun. *315*, 160-165.

121. Jonassen,A.K., Sack,M.N., Mjos,O.D., and Yellon,D.M. (2001). Myocardial protection by insulin at reperfusion requires early administration and is mediated via Akt and p70s6 kinase cell-survival signaling. Circ Res *89*, 1191-1198.

122. Kajstura,J., Cheng,W., Reiss,K., Clark,W.A., Sonnenblick,E.H., Krajewski,S., Reed,J.C., Olivetti,G., and Anversa,P. (1996). Apoptotic and necrotic myocyte cell deaths are independent contributing variables of infarct size in rats. Lab Invest *74*, 86-107.

123. Kane,L.P. and Weiss,A. (2003). The PI-3 kinase/Akt pathway and T cell activation: pleiotropic pathways downstream of PIP3. Immunol. Rev. *192*, 7-20.

124. Katayose,D., Wersto,R., Cowan,K., and Seth,P. (1995). Consequences of p53 gene expression by adenovirus vector on cell cycle arrest and apoptosis in human aortic vascular smooth muscle cells. Biochem. Biophys. Res Commun. *215*, 446-451.

125. Kelly,K.J., Plotkin,Z., Vulgamott,S.L., and Dagher,P.C. (2003). P53 mediates the apoptotic response to GTP depletion after renal ischemia-reperfusion: protective role of a p53 inhibitor. J. Am. Soc. Nephrol. *14*, 128-138.

126. Kerr,J.F., Wyllie,A.H., and Currie,A.R. (1972). Apoptosis: a basic biological phenomenon with wide-ranging implications in tissue kinetics. Br J Cancer *26*, 239-257.

127. Kim,J.S., He,L., Qian,T., and Lemasters,J.J. (2003). Role of the mitochondrial permeability transition in apoptotic and necrotic death after ischemia/reperfusion injury to hepatocytes. Curr. Mol. Med. *3*, 527-535.

128. Kim,J.S., Jin,Y., and Lemasters,J.J. (2006a). Reactive oxygen species, but not Ca2+ overloading, trigger pH- and mitochondrial permeability transition-dependent death of adult rat myocytes after ischemia-reperfusion. Am J Physiol Heart Circ Physiol *290*, H2024-H2034.

129. Kim,M.Y., Kim,M.J., Yoon,I.S., Ahn,J.H., Lee,S.H., Baik,E.J., Moon,C.H., and Jung,Y.S. (2006b). Diazoxide acts more as a PKC-epsilon activator, and indirectly activates the mitochondrial K(ATP) channel conferring cardioprotection against hypoxic injury. Br J Pharmacol *149*, 1059-1070.

130. Kim,R.H., Peters,M., Jang,Y., Shi,W., Pintilie,M., Fletcher,G.C., DeLuca,C., Liepa,J., Zhou,L., Snow,B., Binari,R.C., Manoukian,A.S., Bray,M.R., Liu,F.F., Tsao,M.S., and Mak,T.W. (2005). DJ-1, a novel regulator of the tumor suppressor PTEN. Cancer Cell *7*, 263-273.

131. Kim,S., Domon-Dell,C., Kang,J., Chung,D.H., Freund,J.N., and Evers,B.M. (2004). Down-regulation of the tumor suppressor PTEN by the tumor necrosis factor-alpha/nuclear factor-kappaB (NF-kappaB)-inducing kinase/NF-kappaB pathway is linked to a default IkappaB-alpha autoregulatory loop. J Biol. Chem. *279*, 4285-4291.

132. Kimes,B.W. and Brandt,B.L. (1976). Properties of a clonal muscle cell line from rat heart. Exp. Cell Res *98*, 367-381.

133. Klein,H.H., Puschmann,S., Schaper,J., and Schaper,W. (1981). The mechanism of the tetrazolium reaction in identifying experimental myocardial infarction. Virchows Archiv A Pathological Anatomy and Histology *393*, 287-297.

134. Kok,K., Geering,B., and Vanhaesebroeck,B. (2009). Regulation of phosphoinositide 3-kinase expression in health and disease. Trends Biochem. Sci *34*, 115-127.

135. Kokoszka,J.E., Waymire,K.G., Levy,S.E., Sligh,J.E., Cai,J., Jones,D.P., MacGregor,G.R., and Wallace,D.C. (2004). The ADP/ATP translocator is not essential for the mitochondrial permeability transition pore. Nature *427*, 461-465.

136. Komarov,P.G., Komarova,E.A., Kondratov,R.V., Christov-Tselkov,K., Coon,J.S., Chernov,M.V., and Gudkov,A.V. (1999). A chemical inhibitor of p53 that protects mice from the side effects of cancer therapy. Science *285*, 1733-1737.

137. Kothakota,S., Azuma,T., Reinhard,C., Klippel,A., Tang,J., Chu,K., McGarry,T.J., Kirschner,M.W., Koths,K., Kwiatkowski,D.J., and Williams,L.T. (1997). Caspase-3-generated fragment of gelsolin: effector of morphological change in apoptosis. Science *278*, 294-298.

138. Krauskopf,A., Eriksson,O., Craigen,W.J., Forte,M.A., and Bernardi,P. (2006). Properties of the permeability transition in VDAC1(-/-) mitochondria. Biochim. Biophys. Acta *1757*, 590-595.

139. Kushner,J.A., Simpson,L., Wartschow,L.M., Guo,S., Rankin,M.M., Parsons,R., and White,M.F. (2005). Phosphatase and tensin homolog regulation of islet growth and glucose homeostasis. J Biol. Chem. *280*, 39388-39393.

140. Kuwahara,K., Saito,Y., Kishimoto,I., Miyamoto,Y., Harada,M., Ogawa,E., Hamanaka,I., Kajiyama,N., Takahashi,N., Izumi,T., Kawakami,R., and Nakao,K. (2000). Cardiotrophin-1 Phosphorylates Akt and BAD, and Prolongs Cell Survival via a PI3K-dependent Pathway in Cardiac Myocytes. Journal of Molecular and Cellular Cardiology *32*, 1385-1394.

141. Kuwana,T., Mackey,M.R., Perkins,G., Ellisman,M.H., Latterich,M., Schneiter,R., Green,D.R., and Newmeyer,D.D. (2002). Bid, Bax, and lipids cooperate to form supramolecular openings in the outer mitochondrial membrane. Cell *111*, 331-342.

142. Kwon,J., Lee,S.R., Yang,K.S., Ahn,Y., Kim,Y.J., Stadtman,E.R., and Rhee,S.G. (2004). Reversible oxidation and inactivation of the tumor suppressor PTEN in cells

stimulated with peptide growth factors. Proc. Natl. Acad. Sci. U. S. A *101*, 16419-16424.

143. Lai,J.P., Dalton,J.T., and Knoell,D.L. (2007). Phosphatase and tensin homologue deleted on chromosome ten (PTEN) as a molecular target in lung epithelial wound repair. Br J Pharmacol *152*, 1172-1184.

144. Lange,S.A., Wolf,B., Schober,K., Wunderlich,C., Marquetant,R., Weinbrenner,C., and Strasser,R.H. (2007). Chronic angiotensin II receptor blockade induces cardioprotection during ischemia by increased PKC-epsilon expression in the mouse heart. J Cardiovasc. Pharmacol. *49*, 46-55.

145. Latronico,M.V., Costinean,S., Lavitrano,M.L., Peschle,C., and Condorelli,G. (2004). Regulation of cell size and contractile function by AKT in cardiomyocytes. Ann. N. Y. Acad. Sci *1015*, 250-260.

146. Lawrence,K.M., Townsend,P.A., Davidson,S.M., Carroll,C.J., Eaton,S., Hubank,M., Knight,R.A., Stephanou,A., and Latchman,D.S. (2004). The cardioprotective effect of urocortin during ischaemia/reperfusion involves the prevention of mitochondrial damage. Biochem. Biophys. Res Commun. *321*, 479-486.

147. Lazar,D.F. and Saltiel,A.R. (2006). Lipid phosphatases as drug discovery targets for type 2 diabetes. Nat. Rev. Drug Discov. *5*, 333-342.

148. Lee,J.O., Yang,H., Georgescu,M.M., Di Cristofano,A., Maehama,T., Shi,Y., Dixon,J.E., Pandolfi,P., and Pavletich,N.P. (1999). Crystal structure of the PTEN tumor suppressor: implications for its phosphoinositide phosphatase activity and membrane association. Cell *99*, 323-334.

149. Lee,P., Sata,M., Lefer,D.J., Factor,S.M., Walsh,K., and Kitsis,R.N. (2003). Fas pathway is a critical mediator of cardiac myocyte death and MI during ischemia-reperfusion in vivo. Am J Physiol Heart Circ Physiol *284*, H456-H463.

150. Lee,S.R., Yang,K.S., Kwon,J., Lee,C., Jeong,W., and Rhee,S.G. (2002). Reversible inactivation of the tumor suppressor PTEN by H2O2. J. Biol. Chem. *277*, 20336-20342.

151. Lee,Y.R., Shim,H.J., Yu,H.N., Song,E.K., Park,J., Kwon,K.B., Park,J.W., Rho,H.W., Park,B.H., Han,M.K., and Kim,J.S. (2005). Dimethylsulfoxide induces upregulation of tumor suppressor protein PTEN through nuclear factor-kappaB activation in HL-60 cells. Leuk. Res. *29*, 401-405.

152. Lemasters,J.J., Nieminen,A.L., Qian,T., Trost,L.C., Elmore,S.P., Nishimura,Y., Crowe,R.A., Cascio,W.E., Bradham,C.A., Brenner,D.A., and Herman,B. (1998). The mitochondrial permeability transition in cell death: a common mechanism in necrosis, apoptosis and autophagy. Biochim. Biophys. Acta *1366*, 177-196.

153. Lemasters,J.J., Qian,T., He,L., Kim,J.S., Elmore,S.P., Cascio,W.E., and Brenner,D.A. (2002). Role of mitochondrial inner membrane permeabilization in necrotic cell death, apoptosis, and autophagy. Antioxid. Redox. Signal. *4*, 769-781.

154. Leung,A.W., Varanyuwatana,P., and Halestrap,A.P. (2008). The mitochondrial phosphate carrier interacts with cyclophilin d and may play a key role in the permeability transition. J Biol. Chem. *283*, 26312-26323.

155. Li,G., Whittaker,P., Yao,M., Kloner,R.A., and Przyklenk,K. (2002). The gap junction uncoupler heptanol abrogates infarct size reduction with preconditioning in mouse hearts. Cardiovasc. Pathol. *11*, 158-165.

156. Li,H., Zhu,H., Xu,C.J., and Yuan,J. (1998). Cleavage of BID by caspase 8 mediates the mitochondrial damage in the Fas pathway of apoptosis. Cell *94*, 491-501.

157. Li,J., Yen,C., Liaw,D., Podsypanina,K., Bose,S., Wang,S.I., Puc,J., Miliaresis,C., Rodgers,L., McCombie,R., Bigner,S.H., Giovanella,B.C., Ittmann,M., Tycko,B., Hibshoosh,H., Wigler,M.H., and Parsons,R. (1997a). PTEN, a putative protein tyrosine phosphatase gene mutated in human brain, breast, and prostate cancer. Science *275*, 1943-1947.

158. Li,P., Nijhawan,D., Budihardjo,I., Srinivasula,S.M., Ahmad,M., Alnemri,E.S., and Wang,X. (1997b). Cytochrome c and dATP-dependent formation of Apaf-1/caspase-9 complex initiates an apoptotic protease cascade. Cell *91*, 479-489.

159. Li,Y. and Sato,T. (2001). Dual Signaling via Protein Kinase C and Phosphatidylinositol 3'-Kinase/Akt Contributes to Bradykinin B2Receptor-induced Cardioprotection in Guinea Pig Hearts. Journal of Molecular and Cellular Cardiology *33*, 2047-2053.

160. Li,Z., Dong,X., Wang,Z., Liu,W., Deng,N., Ding,Y., Tang,L., Hla,T., Zeng,R., Li,L., and Wu,D. (2005). Regulation of PTEN by Rho small GTPases. Nat. Cell Biol. *7*, 399-404.

161. Liaw,D., Marsh,D.J., Li,J., Dahia,P.L.M., Wang,S.I., Zheng,Z., Bose,S., Call,K.M., Tsou,H.C., Peacoke,M., Eng,C., and Parsons,R. (1997). Germline mutations of the PTEN gene in Cowden disease, an inherited breast and thyroid cancer syndrome. Nat Genet *16*, 64-67.

162. Liem,D.A., Gho,C.C., Gho,B.C., Kazim,S., Manintveld,O.C., Verdouw,P.D., and Duncker,D.J. (2004). The tyrosine phosphatase inhibitor bis(maltolato)oxovanadium attenuates myocardial reperfusion injury by opening ATP-sensitive potassium channels. J Pharmacol. Exp. Ther. *309*, 1256-1262.

163. Lim,S.Y., Davidson,S.M., Hausenloy,D.J., and Yellon,D.M. (2007). Preconditioning and postconditioning: The essential role of the mitochondrial permeability transition pore. Cardiovasc. Res.

164. Lim,S.Y., Davidson,S.M., Paramanathan,A.J., Smith,C.C., Yellon,D.M., and Hausenloy,D.J. (2008). The novel adipocytokine visfatin exerts direct cardioprotective effects. J Cell Mol. Med. *12*, 1395-1403.

165. Lin,W. and Kang,U.J. (2008b). Characterization of PINK1 processing, stability, and subcellular localization. J Neurochem. *106*, 464-474.

166. Lin,W. and Kang,U.J. (2008a). Characterization of PINK1 processing, stability, and subcellular localization. J Neurochem. *106*, 464-474.

167. Lindquist,R.N., Lynn,J.L., Jr., and Lienhard,G.E. (1973). Possible transition-state analogs for ribonuclease. The complexes of uridine with oxovanadium(IV) ion and vanadium(V) ion. J Am Chem. Soc. *95*, 8762-8768.

168. Lindsay,Y., McCoull,D., Davidson,L., Leslie,N.R., Fairservice,A., Gray,A., Lucocq,J., and Downes,C.P. (2006). Localization of agonist-sensitive PtdIns(3,4,5)P3 reveals a nuclear pool that is insensitive to PTEN expression. J Cell Sci *119*, 5160-5168.

169. Liu,G.S., Thornton,J., Van Winkle,D.M., Stanley,A.W., Olsson,R.A., and Downey,J.M. (1991). Protection against infarction afforded by preconditioning is mediated by A1 adenosine receptors in rabbit heart. Circulation *84*, 350-356.

170. Liu,P., Xu,B., Cavalieri,T.A., and Hock,C.E. (2006). Pifithrin-alpha attenuates p53-mediated apoptosis and improves cardiac function in response to myocardial ischemia/reperfusion in aged rats. Shock *26*, 608-614.

171. Liu,W., Akhand,A.A., Takeda,K., Kawamoto,Y., Itoigawa,M., Kato,M., Suzuki,H., Ishikawa,N., and Nakashima,I. (2003). Protein phosphatase 2A-linked and -unlinked caspase-dependent pathways for downregulation of Akt kinase triggered by 4-hydroxynonenal. Cell Death Differ. *10*, 772-781.

172. Lobo,G.P., Waite,K.A., Planchon,S.M., Romigh,T., Houghton,J.A., and Eng,C. (2008). ATP modulates PTEN subcellular localization in multiple cancer cell lines. Hum. Mol. Genet *17*, 2877-2885.

173. Loukogeorgakis,S.P., Panagiotidou,A.T., Yellon,D.M., Deanfield,J.E., and MacAllister,R.J. (2006). Postconditioning protects against endothelial ischemia-reperfusion injury in the human forearm. Circulation *113*, 1015-1019.

174. Luo,X., Budihardjo,I., Zou,H., Slaughter,C., and Wang,X. (1998). Bid, a Bcl2 interacting protein, mediates cytochrome c release from mitochondria in response to activation of cell surface death receptors. Cell *94*, 481-490.

175. Ma,K., Cheung,S.M., Marshall,A.J., and Duronio,V. (2008). PI(3,4,5)P3 and PI(3,4)P2 levels correlate with PKB/akt phosphorylation at Thr308 and Ser473, respectively; PI(3,4)P2 levels determine PKB activity. Cell Signal. *20*, 684-694.

176. Maccario,H., Perera,N.M., Davidson,L., Downes,C.P., and Leslie,N.R. (2007). PTEN is destabilized by phosphorylation on Thr366. Biochem. J *405*, 439-444.

177. Maddock,H.L., Mocanu,M.M., and Yellon,D.M. (2002). Adenosine A(3) receptor activation protects the myocardium from reperfusion/reoxygenation injury. Am J Physiol Heart Circ Physiol *283*, H1307-H1313.

178. Maehama,T. and Dixon,J.E. (1998b). The tumor suppressor, PTEN/MMAC1, dephosphorylates the lipid second messenger, phosphatidylinositol 3,4,5-trisphosphate. J Biol. Chem. *273*, 13375-13378.

179. Maehama,T. and Dixon,J.E. (1998a). The tumor suppressor, PTEN/MMAC1, dephosphorylates the lipid second messenger, phosphatidylinositol 3,4,5-trisphosphate. J. Biol. Chem. *273*, 13375-13378.

180. Maehama,T., Taylor,G.S., and Dixon,J.E. (2001). PTEN and myotubularin: novel phosphoinositide phosphatases. Annu. Rev. Biochem. *70*, 247-279.

181. Manning,B.D. and Cantley,L.C. (2007). AKT/PKB signaling: navigating downstream. Cell *129*, 1261-1274.

182. Mao,K., Kobayashi,S., Jaffer,Z.M., Huang,Y., Volden,P., Chernoff,J., and Liang,Q. (2008). Regulation of Akt/PKB activity by P21-activated kinase in cardiomyocytes. J Mol. Cell Cardiol. *44*, 429-434.

183. Marion,E., Kaisaki,P.J., Pouillon,V., Gueydan,C., Levy,J.C., Bodson,A., Krzentowski,G., Daubresse,J.C., Mockel,J., Behrends,J., Servais,G., Szpirer,C., Kruys,V., Gauguier,D., and Schurmans,S. (2002). The gene INPPL1, encoding the lipid phosphatase SHIP2, is a candidate for type 2 diabetes in rat and man. Diabetes *51*, 2012-2017.

184. Matsusaka,H., Ide,T., Matsushima,S., Ikeuchi,M., Kubota,T., Sunagawa,K., Kinugawa,S., and Tsutsui,H. (2006). Targeted deletion of p53 prevents cardiac rupture after myocardial infarction in mice. Cardiovasc Res *70*, 457-465.

185. Mehenni,H., Lin-Marq,N., Buchet-Poyau,K., Reymond,A., Collart,M.A., Picard,D., and Antonarakis,S.E. (2005). LKB1 interacts with and phosphorylates PTEN: a functional link between two proteins involved in cancer predisposing syndromes. Hum. Mol. Genet. *14*, 2209-2219.

186. Mensah,K., Mocanu,M.M., and Yellon,D.M. (2005). Failure to protect the myocardium against ischemia/reperfusion injury after chronic atorvastatin treatment is recaptured by acute atorvastatin treatment: A potential role for phosphatase and tensin homolog deleted on chromosome ten? Journal of the American College of Cardiology *45*, 1287-1291.

187. Meuillet,E.J., Mahadevan,D., Berggren,M., Coon,A., and Powis,G. (2004). Thioredoxin-1 binds to the C2 domain of PTEN inhibiting PTEN's lipid phosphatase activity and membrane binding: a mechanism for the functional loss of PTEN's tumor suppressor activity. Arch. Biochem. Biophys. *429*, 123-133.

188. Mills,R.D., Sim,C.H., Mok,S.S., Mulhern,T.D., Culvenor,J.G., and Cheng,H.C. (2008). Biochemical aspects of the neuroprotective mechanism of PTEN-induced kinase-1 (PINK1). J Neurochem. *105*, 18-33.

189. Mise-Omata,S., Obata,Y., Iwase,S., Mise,N., and Doi,T.S. (2005). Transient strong reduction of PTEN expression by specific RNAi induces loss of adhesion of the cells. Biochem. Biophys. Res. Commun. *328*, 1034-1042.

190. Mocanu,M.M., Baxter,G.F., Yue,Y., Critz,S.D., and Yellon,D.M. (2000). The p38 MAPK inhibitor, SB203580, abrogates ischaemic preconditioning in rat heart but timing of administration is critical. Basic Res Cardiol. *95*, 472-478.

191. Mocanu,M.M., Bell,R.M., and Yellon,D.M. (2002). PI3 kinase and not p42/p44 appears to be implicated in the protection conferred by ischemic preconditioning. J. Mol. Cell Cardiol. *34*, 661-668.

192. Mocanu,M.M., Field,D.C., and Yellon,D.M. (2006). A Potential Role for Pten in the Diabetic Heart. Cardiovasc. Drugs Ther.

193. Mocanu,M.M. and Yellon,D.M. (2003). p53 down-regulation: a new molecular mechanism involved in ischaemic preconditioning. FEBS Lett. *555*, 302-306.

194. Mocanu,M.M. and Yellon,D.M. (2007). PTEN, the Achilles' heel of myocardial ischaemia/reperfusion injury? Br J Pharmacol *150*, 833-838.

195. Mosser,V.A., Li,Y., and Quon,M.J. (2001). PTEN does not modulate GLUT4 translocation in rat adipose cells under physiological conditions. Biochem. Biophys. Res Commun. *288*, 1011-1017.

196. Murry,C.E., Jennings,R.B., and Reimer,K.A. (1986). Preconditioning with ischemia: a delay of lethal cell injury in ischemic myocardium. Circulation *74*, 1124-1136.

197. Myers,M.P., Stolarov,J.P., Eng,C., Li,J., Wang,S.I., Wigler,M.H., Parsons,R., and Tonks,N.K. (1997). P-TEN, the tumor suppressor from human chromosome 10q23, is a dual-specificity phosphatase. Proc. Natl. Acad. Sci U. S. A *94*, 9052-9057.

198. Nakashima,N., Sharma,P.M., Imamura,T., Bookstein,R., and Olefsky,J.M. (2000). The tumor suppressor PTEN negatively regulates insulin signaling in 3T3-L1 adipocytes. J. Biol. Chem. *275*, 12889-12895.

199. Nemenoff,R.A., Simpson,P.A., Furgeson,S.B., Kaplan-Albuquerque,N., Crossno,J., Garl,P.J., Cooper,J., and Weiser-Evans,M.C. (2008). Targeted deletion of PTEN in smooth muscle cells results in vascular remodeling and recruitment of progenitor cells through induction of stromal cell-derived factor-1alpha. Circ Res *102*, 1036-1045.

200. Nicholson,D.W., Ali,A., Thornberry,N.A., Vaillancourt,J.P., Ding,C.K., Gallant,M., Gareau,Y., Griffin,P.R., Labelle,M., Lazebnik,Y.A., and . (1995). Identification and inhibition of the ICE/CED-3 protease necessary for mammalian apoptosis. Nature *376*, 37-43.

201. Nigorikawa,K., Yoshikawa,K., Sasaki,T., Iida,E., Tsukamoto,M., Murakami,H., Maehama,T., Hazeki,K., and Hazeki,O. (2006). A naphthoquinone derivative, shikonin, has insulin-like actions by inhibiting both phosphatase and tensin homolog deleted on chromosome 10 and tyrosine phosphatases. Mol. Pharmacol *70*, 1143-1149.

202. Ning,K., Miller,L.C., Laidlaw,H.A., Burgess,L.A., Perera,N.M., Downes,C.P., Leslie,N.R., and Ashford,M.L. (2006). A novel leptin signalling pathway via PTEN inhibition in hypothalamic cell lines and pancreatic beta-cells. EMBO J. *25*, 2377-2387.

203. Nogueira,V., Park,Y., Chen,C.C., Xu,P.Z., Chen,M.L., Tonic,I., Unterman,T., and Hay,N. (2008). Akt determines replicative senescence and oxidative or oncogenic premature senescence and sensitizes cells to oxidative apoptosis. Cancer Cell *14*, 458-470.

204. Ohno,M., Takemura,G., Ohno,A., Misao,J., Hayakawa,Y., Minatoguchi,S., Fujiwara,T., and Fujiwara,H. (1998). "Apoptotic" myocytes in infarct area in rabbit hearts may be oncotic myocytes with DNA fragmentation: analysis by immunogold electron microscopy combined with In situ nick end-labeling. Circulation *98*, 1422-1430.

205. Okumura,K., Mendoza,M., Bachoo,R.M., Depinho,R.A., Cavenee,W.K., and Furnari,F.B. (2006). PCAF modulates PTEN activity. J Biol. Chem. *281*, 26562-26568.

206. Oudit,G.Y., Kassiri,Z., Zhou,J., Liu,Q.C., Liu,P.P., Backx,P.H., Dawood,F., Crackower,M.A., Scholey,J.W., and Penninger,J.M. (2008). Loss of PTEN attenuates the development of pathological hypertrophy and heart failure in response to biomechanical stress. Cardiovasc Res *78*, 505-514.

207. Oudit,G.Y., Sun,H., Kerfant,B.G., Crackower,M.A., Penninger,J.M., and Backx,P.H. (2004). The role of phosphoinositide-3 kinase and PTEN in cardiovascular physiology and disease. J. Mol. Cell Cardiol. *37*, 449-471.

208. Paddock,S.W. (2000). Principles and practices of laser scanning confocal microscopy. Mol. Biotechnol. *16*, 127-149.

209. Palomero,T., Dominguez,M., and Ferrando,A.A. (2008). The role of the PTEN/AKT Pathway in NOTCH1-induced leukemia. Cell Cycle *7*, 965-970.

210. Papakonstanti,E.A., Ridley,A.J., and Vanhaesebroeck,B. (2007). The p110delta isoform of PI 3-kinase negatively controls RhoA and PTEN. EMBO J *26*, 3050-3061.

211. Pei,D.S., Sun,Y.F., and Song,Y.J. (2009). S-nitrosylation of PTEN Invovled in ischemic brain injury in rat hippocampal CA1 region. Neurochem. Res *34*, 1507-1512.

212. Pesesse,X., Deleu,S., De Smedt,F., Drayer,L., and Erneux,C. (1997). Identification of a second SH2-domain-containing protein closely related to the phosphatidylinositol polyphosphate 5-phosphatase SHIP. Biochem. Biophys. Res. Commun. *239*, 697-700.

213. Petit,A., Kawarai,T., Paitel,E., Sanjo,N., Maj,M., Scheid,M., Chen,F., Gu,Y., Hasegawa,H., Salehi-Rad,S., Wang,L., Rogaeva,E., Fraser,P., Robinson,B., George-Hyslop,P., and Tandon,A. (2005). Wild-type PINK1 prevents basal and induced neuronal apoptosis, a protective effect abrogated by Parkinson disease-related mutations. J Biol. Chem. *280*, 34025-34032.

214. Pilarski,R. and Eng,C. (2004). Will the real Cowden syndrome please stand up (again)? Expanding mutational and clinical spectra of the PTEN hamartoma tumour syndrome. J. Med. Genet. *41*, 323-326.

215. Ping,P., Zhang,J., Cao,X., Li,R.C., Kong,D., Tang,X.L., Qiu,Y., Manchikalapudi,S., Auchampach,J.A., Black,R.G., and Bolli,R. (1999a). PKC-dependent activation of p44/p42 MAPKs during myocardial ischemia-reperfusion in conscious rabbits. Am J Physiol *276*, H1468-H1481.

216. Ping,P., Zhang,J., Huang,S., Cao,X., Tang,X.L., Li,R.C., Zheng,Y.T., Qiu,Y., Clerk,A., Sugden,P., Han,J., and Bolli,R. (1999b). PKC-dependent activation of p46/p54 JNKs during ischemic preconditioning in conscious rabbits. Am J Physiol *277*, H1771-H1785.

217. Podsypanina,K., Ellenson,L.H., Nemes,A., Gu,J., Tamura,M., Yamada,K.M., Cordon-Cardo,C., Catoretti,G., Fisher,P.E., and Parsons,R. (1999). Mutation of Pten/Mmac1 in mice causes neoplasia in multiple organ systems. Proc. Natl. Acad. Sci. U. S. A *96*, 1563-1568.

218. Posner,B.I., Faure,R., Burgess,J.W., Bevan,A.P., Lachance,D., Zhang-Sun,G., Fantus,I.G., Ng,J.B., Hall,D.A., Lum,B.S., and . (1994). Peroxovanadium compounds. A new class of potent phosphotyrosine phosphatase inhibitors which are insulin mimetics. J. Biol. Chem. *269*, 4596-4604.

219. Potts,M.B., Vaughn,A.E., McDonough,H., Patterson,C., and Deshmukh,M. (2005). Reduced Apaf-1 levels in cardiomyocytes engage strict regulation of apoptosis by endogenous XIAP. J Cell Biol. *171*, 925-930.

220. Pridgeon,J.W., Olzmann,J.A., Chin,L.S., and Li,L. (2007). PINK1 Protects against Oxidative Stress by Phosphorylating Mitochondrial Chaperone TRAP1. PLoS Biol. *5*, e172.

221. Puc,J. and Parsons,R. (2005). PTEN loss inhibits CHK1 to cause double stranded-DNA breaks in cells. Cell Cycle *4*, 927-929.

222. Puri,V., Chakladar,A., Virbasius,J.V., Konda,S., Powelka,A.M., Chouinard,M., Hagan,G.N., Perugini,R., and Czech,M.P. (2007). RNAi-based gene silencing in primary mouse and human adipose tissues. J Lipid Res *48*, 465-471.

223. Rakhit,R.D., Mojet,M.H., Marber,M.S., and Duchen,M.R. (2001). Mitochondria as targets for nitric oxide-induced protection during simulated ischemia and reoxygenation in isolated neonatal cardiomyocytes. Circulation *103*, 2617-2623.

224. Resjo,S., Goransson,O., Harndahl,L., Zolnierowicz,S., Manganiello,V., and Degerman,E. (2002). Protein phosphatase 2A is the main phosphatase involved in the regulation of protein kinase B in rat adipocytes. Cell Signal. *14*, 231-238.

225. Rodriguez-Sinovas,A., Boengler,K., Cabestrero,A., Gres,P., Morente,M., Ruiz-Meana,M., Konietzka,I., Miro,E., Totzeck,A., Heusch,G., Schulz,R., and Garcia-Dorado,D. (2006). Translocation of connexin 43 to the inner mitochondrial membrane of cardiomyocytes through the heat shock protein 90-dependent TOM pathway and its importance for cardioprotection. Circ Res *99*, 93-101.

226. Rosivatz,E., Matthews,J.G., McDonald,N.Q., Mulet,X., Ho,K.K., Lossi,N., Schmid,A.C., Mirabelli,M., Pomeranz,K.M., Erneux,C., Lam,E.W., Vilar,R., and Woscholski,R. (2006). A small molecule inhibitor for phosphatase and tensin homologue deleted on chromosome 10 (PTEN). ACS Chem. Biol. *1*, 780-790.

227. Roy,S., Khanna,S., Hussain,S.R., Biswas,S., Azad,A., Rink,C., Gnyawali,S., Shilo,S., Nuovo,G.J., and Sen,C.K. (2009). MicroRNA expression in response to murine myocardial infarction: miR-21 regulates fibroblast metalloprotease-2 via phosphatase and tensin homologue. Cardiovasc Res *82*, 21-29.

228. Ruan,H., Li,J., Ren,S., Gao,J., Li,G., Kim,R., Wu,H., and Wang,Y. (2009). Inducible and cardiac specific PTEN inactivation protects ischemia/reperfusion injury. J Mol. Cell Cardiol. *46*, 193-200.

229. Sadoshima,J. (2008). The role of autophagy during ischemia/reperfusion. Autophagy. *4*, 402-403.

230. Saotome,M., Katoh,H., Yaguchi,Y., Tanaka,T., Urushida,T., Satoh,H., and Hayashi,H. (2009). Transient opening of mitochondrial permeability transition pore by reactive oxygen species protects myocardium from ischemia-reperfusion injury. Am J Physiol Heart Circ Physiol *296*, H1125-H1132.

231. Sasaoka,T., Wada,T., Fukui,K., Murakami,S., Ishihara,H., Suzuki,R., Tobe,K., Kadowaki,T., and Kobayashi,M. (2004). SH2-containing inositol phosphatase 2 predominantly regulates Akt2, and not Akt1, phosphorylation at the plasma membrane in response to insulin in 3T3-L1 adipocytes. J. Biol. Chem. *279*, 14835-14843.

232. Schmid,A.C., Byrne,R.D., Vilar,R., and Woscholski,R. (2004). Bisperoxovanadium compounds are potent PTEN inhibitors. FEBS Lett. *566*, 35-38.

233. Schwanke,U., Konietzka,I., Duschin,A., Li,X., Schulz,R., and Heusch,G. (2002). No ischemic preconditioning in heterozygous connexin43-deficient mice. Am J Physiol Heart Circ Physiol *283*, H1740-H1742.

234. Seo,J.H., Ahn,Y., Lee,S.R., Yeol,Y.C., and Chung,H.K. (2005). The major target of the endogenously generated reactive oxygen species in response to insulin stimulation is phosphatase and tensin homolog and not phosphoinositide-3 kinase (PI-3 kinase) in the PI-3 kinase/Akt pathway. Mol. Biol. Cell *16*, 348-357.

235. Sharrard,R.M. and Maitland,N.J. (2006). Regulation of Protein Kinase B activity by PTEN and SHIP2 in human prostate-derived cell lines. Cell Signal.

236. Shaw,R.J., Lamia,K.A., Vasquez,D., Koo,S.H., Bardeesy,N., Depinho,R.A., Montminy,M., and Cantley,L.C. (2005). The kinase LKB1 mediates glucose homeostasis in liver and therapeutic effects of metformin. Science *310*, 1642-1646.

237. Shen,W.H., Balajee,A.S., Wang,J., Wu,H., Eng,C., Pandolfi,P.P., and Yin,Y. (2007). Essential role for nuclear PTEN in maintaining chromosomal integrity. Cell *128*, 157-170.

238. Shen,Y.H., Zhang,L., Utama,B., Wang,J., Gan,Y., Wang,X., Wang,J., Chen,L., Vercellotti,G.M., Coselli,J.S., Mehta,J.L., and Wang,X.L. (2006). Human cytomegalovirus inhibits Akt-mediated eNOS activation through upregulating PTEN (phosphatase and tensin homolog deleted on chromosome 10). Cardiovasc Res *69*, 502-511.

239. Simpkin,J.C., Yellon,D.M., Davidson,S.M., Lim,S.Y., Wynne,A.M., and Smith,C.C. (2007). Apelin-13 and apelin-36 exhibit direct cardioprotective activity against ischemiareperfusion injury. Basic Res Cardiol. *102*, 518-528.

240. Skrzypiec-Spring,M., Grotthus,B., Szelag,A., and Schulz,R. (2007). Isolated heart perfusion according to Langendorff--Still viable in the new millennium. Journal of Pharmacological and Toxicological Methods *55*, 113-126.

241. Smith,C.C., Davidson,S.M., Lim,S.Y., Simpkin,J.C., Hothersall,J.S., and Yellon,D.M. (2007). Necrostatin: a potentially novel cardioprotective agent? Cardiovasc Drugs Ther. *21*, 227-233.

242. Smith,C.C.T., Mocanu,M.M., Davidson,S.M., Wynne,A.M., Simpkin,J.C., and Yellon,D.M. (2006). Leptin, the obesity-associated hormone, exhibits direct cardioprotective effects. Br J Pharmacol *149*, 5-13.

243. Smith,J. and Kampine,J.P. (1990). Circulatory physiology the essentials. (Baltimore: Williams & Wilkins).

244. Staat,P., Rioufol,G., Piot,C., Cottin,Y., Cung,T.T., L'Huillier,I., Aupetit,J.F., Bonnefoy,E., Finet,G., Andre-Fouet,X., and Ovize,M. (2005). Postconditioning the human heart. Circulation *112*, 2143-2148.

245. Stambolic,V., MacPherson,D., Sas,D., Lin,Y., Snow,B., Jang,Y., Benchimol,S., and Mak,T.W. (2001). Regulation of PTEN transcription by p53. Mol. Cell *8*, 317-325.

246. Stambolic,V., Suzuki,A., de la Pompa,J.L., Brothers,G.M., Mirtsos,C., Sasaki,T., Ruland,J., Penninger,J.M., Siderovski,D.P., and Mak,T.W. (1998). Negative regulation of PKB/Akt-dependent cell survival by the tumor suppressor PTEN. Cell *95*, 29-39.

247. Steck,P.A., Pershouse,M.A., Jasser,S.A., Yung,W.K., Lin,H., Ligon,A.H., Langford,L.A., Baumgard,M.L., Hattier,T., Davis,T., Frye,C., Hu,R., Swedlund,B., Teng,D.H., and Tavtigian,S.V. (1997). Identification of a candidate tumour suppressor gene, MMAC1, at chromosome 10q23.3 that is mutated in multiple advanced cancers. Nat Genet *15*, 356-362.

248. Stenslokken,K.O., Rutkovskiy,A., Kaljusto,M.L., Hafstad,A.D., Larsen,T.S., and Vaage,J. (2009). Inadvertent phosphorylation of survival kinases in isolated perfused hearts: a word of caution. Basic Res Cardiol.

249. Stephanou,A., Brar,B.K., Scarabelli,T.M., Jonassen,A.K., Yellon,D.M., Marber,M.S., Knight,R.A., and Latchman,D.S. (2000). Ischemia-induced STAT-1 expression and activation play a critical role in cardiomyocyte apoptosis. J Biol. Chem. *275*, 10002-10008.

250. Stephens,L., Eguinoa,A., Corey,S., Jackson,T., and Hawkins,P.T. (1993). Receptor stimulated accumulation of phosphatidylinositol (3,4,5)-trisphosphate by G-protein mediated pathways in human myeloid derived cells. EMBO J *12*, 2265-2273.

251. Sugano,M., Tsuchida,K., Hata,T., and Makino,N. (2005). RNA interference targeting SHP-1 attenuates myocardial infarction in rats. FASEB J. *19*, 2054-2056.

252. Sumeray,M.S., Rees,D.D., and Yellon,D.M. (2000). Infarct size and nitric oxide synthase in murine myocardium. J Mol. Cell Cardiol. *32*, 35-42.

253. Sun,H., Kerfant,B.G., Zhao,D., Trivieri,M.G., Oudit,G.Y., Penninger,J.M., and Backx,P.H. (2006). Insulin-like growth factor-1 and PTEN deletion enhance cardiac L-type Ca2+ currents via increased PI3Kalpha/PKB signaling. Circ. Res. *98*, 1390-1397.

254. Svoboda,P., Teisinger,J., Pilar,J., and Vyskocil,F. (1984). Vanadyl (VO2+) and vanadate (VO-3) ions inhibit the brain microsomal Na,K-ATPase with similar affinities. Protection by transferrin and noradrenaline. Biochem. Pharmacol *33*, 2485-2491.

255. Taimor,G., Lorenz,H., Hofstaetter,B., Schluter,K.D., and Piper,H.M. (1999). Induction of necrosis but not apoptosis after anoxia and reoxygenation in isolated adult cardiomyocytes of rat. Cardiovasc Res *41*, 147-156.

256. Tang,Y. and Eng,C. (2006). p53 down-regulates phosphatase and tensin homologue deleted on chromosome 10 protein stability partially through caspase-mediated degradation in cells with proteasome dysfunction. Cancer Res *66*, 6139-6148.

257. Tekin,D., Xi,L., and Kukreja,R.C. (2006). Genetic deletion of fas receptors or Fas ligands does not reduce infarct size after acute global ischemia-reperfusion in isolated mouse heart. Cell Biochem. Biophys. *44*, 111-117.

258. Teresi,R.E., Shaiu,C.W., Chen,C.S., Chatterjee,V.K., Waite,K.A., and Eng,C. (2006). Increased PTEN expression due to transcriptional activation of PPARgamma by Lovastatin and Rosiglitazone. Int. J. Cancer *118*, 2390-2398.

259. Torres,J. and Pulido,R. (2001). The tumor suppressor PTEN is phosphorylated by the protein kinase CK2 at its C terminus. Implications for PTEN stability to proteasome-mediated degradation. J. Biol. Chem. *276*, 993-998.

260. Torres,J., Rodriguez,J., Myers,M.P., Valiente,M., Graves,J.D., Tonks,N.K., and Pulido,R. (2003). Phosphorylation-regulated cleavage of the tumor suppressor PTEN by caspase-3: implications for the control of protein stability and PTEN-protein interactions. J. Biol. Chem. *278*, 30652-30660.

261. Toth,A., Jeffers,J.R., Nickson,P., Min,J.Y., Morgan,J.P., Zambetti,G.P., and Erhardt,P. (2006). Targeted deletion of Puma attenuates cardiomyocyte death and improves cardiac function during ischemia-reperfusion. Am J Physiol Heart Circ Physiol *291*, H52-H60.

262. Trotman,L.C., Wang,X., Alimonti,A., Chen,Z., Teruya-Feldstein,J., Yang,H., Pavletich,N.P., Carver,B.S., Cordon-Cardo,C., Erdjument-Bromage,H., Tempst,P., Chi,S.G., Kim,H.J., Misteli,T., Jiang,X., and Pandolfi,P.P. (2007). Ubiquitination Regulates PTEN Nuclear Import and Tumor Suppression. Cell *128*, 141-156.

263. Tsang,A., Hausenloy,D.J., Mocanu,M.M., and Yellon,D.M. (2004). Postconditioning: a form of "modified reperfusion" protects the myocardium by activating the phosphatidylinositol 3-kinase-Akt pathway. Circ Res *95*, 230-232.

264. Tsang,A., Hausenloy,D.J., Mocanu,M.M., Carr,R.D., and Yellon,D.M. (2005). Preconditioning the Diabetic Heart: The Importance of Akt Phosphorylation. Diabetes *54*, 2360-2364.

265. Turcato,S., Turnbull,L., Wang,G.Y., Honbo,N., Simpson,P.C., Karliner,J.S., and Baker,A.J. (2006). Ischemic preconditioning depends on age and gender. Basic Res. Cardiol. *101*, 235-243.

266. Unoki,M. and Nakamura,Y. (2001). Growth-suppressive effects of BPOZ and EGR2, two genes involved in the PTEN signaling pathway. Oncogene *20*, 4457-4465.

267. Valente,E.M., Abou-Sleiman,P.M., Caputo,V., Muqit,M.M., Harvey,K., Gispert,S., Ali,Z., Del Turco,D., Bentivoglio,A.R., Healy,D.G., Albanese,A., Nussbaum,R., Gonzalez-Maldonado,R., Deller,T., Salvi,S., Cortelli,P., Gilks,W.P., Latchman,D.S., Harvey,R.J., Dallapiccola,B., Auburger,G., and Wood,N.W. (2004). Hereditary early-onset Parkinson's disease caused by mutations in PINK1. Science *304*, 1158-1160.

268. Valiente,M., Andres-Pons,A., Gomar,B., Torres,J., Gil,A., Tapparel,C., Antonarakis,S.E., and Pulido,R. (2005). Binding of PTEN to specific PDZ domains contributes to PTEN protein stability and phosphorylation by microtubule-associated serine/threonine kinases. J. Biol. Chem. *280*, 28936-28943.

269. van Nieuwenhoven,F.A., Musters,R.J., Post,J.A., Verkleij,A.J., van der Vusse,G.J., and Glatz,J.F. (1996). Release of proteins from isolated neonatal rat cardiomyocytes subjected to simulated ischemia or metabolic inhibition is independent of molecular mass. J Mol. Cell Cardiol. *28*, 1429-1434.

270. Van Themsche,C., Leblanc,V., Parent,S., and Asselin,E. (2009). X-linked Inhibitor of Apoptosis Protein (XIAP) Regulates PTEN Ubiquitination, Content, and Compartmentalization. J Biol. Chem. *284*, 20462-20466.

271. Vanhaesebroeck,B. and Alessi,D.R. (2000). The PI3K-PDK1 connection: more than just a road to PKB. Biochem. J *346 Pt 3*, 561-576.

272. Walker,S.M., Downes,C.P., and Leslie,N.R. (2001). TPIP: a novel phosphoinositide 3-phosphatase. Biochem. J. *360*, 277-283.

273. Wang,H.L., Chou,A.H., Yeh,T.H., Li,A.H., Chen,Y.L., Kuo,Y.L., Tsai,S.R., and Yu,S.T. (2007a). PINK1 mutants associated with recessive Parkinson's disease are defective in inhibiting mitochondrial release of cytochrome c. Neurobiol. Dis. *28*, 216-226.

274. Wang,J., Ouyang,W., Li,J., Wei,L., Ma,Q., Zhang,Z., Tong,Q., He,J., and Huang,C. (2005). Loss of tumor suppressor p53 decreases PTEN expression and enhances signaling pathways leading to activation of activator protein 1 and nuclear factor kappaB induced by UV radiation. Cancer Res. *65*, 6601-6611.

275. Wang,X., Trotman,L.C., Koppie,T., Alimonti,A., Chen,Z., Gao,Z., Wang,J., Erdjument-Bromage,H., Tempst,P., Cordon-Cardo,C., Pandolfi,P.P., and Jiang,X. (2007b). NEDD4-1 Is a Proto-Oncogenic Ubiquitin Ligase for PTEN. Cell *128*, 129-139.

276. Whelan,J.T., Forbes,S.L., and Bertrand,F.E. (2007). CBF-1 (RBP-J kappa) binds to the PTEN promoter and regulates PTEN gene expression. Cell Cycle *6*, 80-84.

277. Wijesekara,N., Konrad,D., Eweida,M., Jefferies,C., Liadis,N., Giacca,A., Crackower,M., Suzuki,A., Mak,T.W., Kahn,C.R., Klip,A., and Woo,M. (2005). Muscle-specific Pten deletion protects against insulin resistance and diabetes. Mol. Cell Biol. *25*, 1135-1145.

278. Wong,J.T., Kim,P.T., Peacock,J.W., Yau,T.Y., Mui,A.L., Chung,S.W., Sossi,V., Doudet,D., Green,D., Ruth,T.J., Parsons,R., Verchere,C.B., and Ong,C.J. (2007). Pten (phosphatase and tensin homologue gene) haploinsufficiency promotes insulin hypersensitivity. Diabetologia *50*, 395-403.

279. Wood-Kaczmar,A., Gandhi,S., Yao,Z., Abramov,A.S., Miljan,E.A., Keen,G., Stanyer,L., Hargreaves,I., Klupsch,K., Deas,E., Downward,J., Mansfield,L., Jat,P., Taylor,J., Heales,S., Duchen,M.R., Latchman,D., Tabrizi,S.J., and Wood,N.W. (2008). PINK1 is necessary for long term survival and mitochondrial function in human dopaminergic neurons. PLoS ONE. *3*, e2455.

280. Woodfield,K., Ruck,A., Brdiczka,D., and Halestrap,A.P. (1998). Direct demonstration of a specific interaction between cyclophilin-D and the adenine nucleotide translocase confirms their role in the mitochondrial permeability transition. Biochem. J *336 (Pt 2)*, 287-290.

281. WROBLEWSKI,F. and LADUE,J.S. (1955). Lactic dehydrogenase activity in blood. Proc. Soc. Exp. Biol. Med. *90*, 210-213.

282. Wu,D.N., Pei,D.S., Wang,Q., and Zhang,G.Y. (2006). Down-regulation of PTEN by sodium orthovanadate inhibits ASK1 activation via PI3-K/Akt during cerebral ischemia in rat hippocampus. Neurosci. Lett.

283. Wu,W., Wang,X., Zhang,W., Reed,W., Samet,J.M., Whang,Y.E., and Ghio,A.J. (2003). Zinc-induced PTEN protein degradation through the proteasome pathway in human airway epithelial cells. J. Biol. Chem. *278*, 28258-28263.

284. Wu,X., Hepner,K., Castelino-Prabhu,S., Do,D., Kaye,M.B., Yuan,X.J., Wood,J., Ross,C., Sawyers,C.L., and Whang,Y.E. (2000a). Evidence for regulation of the PTEN tumor suppressor by a membrane-localized multi-PDZ domain containing scaffold protein MAGI-2. Proc. Natl. Acad. Sci U. S. A *97*, 4233-4238.

285. Wu,Y., Dowbenko,D., Spencer,S., Laura,R., Lee,J., Gu,Q., and Lasky,L.A. (2000b). Interaction of the Tumor Suppressor PTEN/MMAC with a PDZ Domain of MAGI3, a Novel Membrane-associated Guanylate Kinase. J. Biol. Chem. *275*, 21477-21485.

286. Wyllie,A.H., Kerr,J.F., and Currie,A.R. (1980). Cell death: the significance of apoptosis. Int. Rev. Cytol. *68*, 251-306.

287. Xi,L., Hess,M.L., and Kukreja,R.C. (1998). Ischemic preconditioning in isolated perfused mouse heart: reduction in infarct size without improvement of post-ischemic ventricular function. Mol. Cell Biochem. *186*, 69-77.

288. Yao,Z., Cavero,I., and Gross,G.J. (1993). Activation of cardiac KATP channels: an endogenous protective mechanism during repetitive ischemia. Am J Physiol *264*, H495-H504.

289. Yellon,D.M. and Baxter,G.F. (2000). Sodium-hydrogen exchange in myocardial reperfusion injury. Lancet *356*, 522-523.

290. Yellon,D.M. and Downey,J.M. (2003). Preconditioning the myocardium: from cellular physiology to clinical cardiology. Physiol Rev *83*, 1113-1151.

291. Yellon,D.M. and Hausenloy,D.J. (2005). Realizing the clinical potential of ischemic preconditioning and postconditioning. Nat. Clin. Pract. Cardiovasc. Med. *2*, 568-575.

292. Yitzhaki,S., Huang,C., Liu,W., Lee,Y., Gustafsson,A.B., Mentzer,R.M., Jr., and Gottlieb,R.A. (2009). Autophagy is required for preconditioning by the adenosine A1 receptor-selective agonist CCPA. Basic Res Cardiol. *104*, 157-167.

293. Yoshikawa,K., Nigorikawa,K., Tsukamoto,M., Tamura,N., Hazeki,K., and Hazeki,O. (2007). Inhibition of PTEN and activation of Akt by menadione. Biochim. Biophys. Acta *1770*, 687-693.

294. Zhang,Q.G., Wu,D.N., Han,D., and Zhang,G.Y. (2007). Critical role of PTEN in the coupling between PI3K/Akt and JNK1/2 signaling in ischemic brain injury. FEBS Lett. *581*, 495-505.

295. Zhao,Z.Q. (2004). Oxidative stress-elicited myocardial apoptosis during reperfusion. Curr. Opin. Pharmacol *4*, 159-165.

296. Zhao,Z.Q., Corvera,J.S., Halkos,M.E., Kerendi,F., Wang,N.P., Guyton,R.A., and Vinten-Johansen,J. (2003). Inhibition of myocardial injury by ischemic postconditioning during reperfusion: comparison with ischemic preconditioning. Am J Physiol Heart Circ Physiol *285*, H579-H588.

297. Zhao,Z.Q., Velez,D.A., Wang,N.P., Hewan-Lowe,K.O., Nakamura,M., Guyton,R.A., and Vinten-Johansen,J. (2001). Progressively developed myocardial apoptotic cell death during late phase of reperfusion. Apoptosis. *6*, 279-290.

298. Zimmer,H.G. (1998). The Isolated Perfused Heart and Its Pioneers. News Physiol Sci *13*, 203-210.

299. Zito,C.I., Qin,H., Blenis,J., and Bennett,A.M. (2007). SHP-2 regulates cell growth by controlling the mTOR/S6 kinase 1 pathway. J Biol. Chem. *282*, 6946-6953.

300. Zorov,D.B., Filburn,C.R., Klotz,L.O., Zweier,J.L., and Sollott,S.J. (2000). Reactive oxygen species (ROS)-induced ROS release: a new phenomenon accompanying induction of the mitochondrial permeability transition in cardiac myocytes. J Exp. Med. *192*, 1001-1014.

301. Zuluaga,S., Alvarez-Barrientos,A., Gutierrez-Uzquiza,A., Benito,M., Nebreda,A.R., and Porras,A. (2007). Negative regulation of Akt activity by p38[alpha] MAP kinase in cardiomyocytes involves membrane localization of PP2A through interaction with caveolin-1. Cellular Signalling *19*, 62-74.